Environmental Effects Monitoring Program
Quarterly Report: April-June 2021

June 30, 2021

Executive Summary

Tidal stream energy devices are an emerging renewable energy technology that use the ebb and flow of the tides to generate electricity. These devices are in various stages of research, development, operation and testing in countries around the world.

FORCE was established in 2009 after undergoing a joint federal-provincial environmental assessment with the mandate to enable the testing and demonstration of tidal stream devices. Since that time, more than 100 related research studies have been completed or are underway with funding from FORCE, the Offshore Energy Research Association of Nova Scotia (OERA), and others. These studies have considered physical, biological, socioeconomic and other research areas.

The current suite of monitoring programs implemented by FORCE build off those initiated during 2016-2020 that were conducted in anticipation of turbine deployments at FORCE's tidal demonstration site. These efforts are divided into two components: mid-field monitoring activities led by FORCE (>100 metres from a turbine), and near-field or 'turbine-specific' monitoring led by project developers (≤100 metres from a turbine) at the FORCE site. All plans are reviewed by FORCE's independent Environmental Monitoring Advisory Committee (EMAC) and federal and provincial regulators prior to implementation.

Mid-field monitoring at the FORCE site presently consists of monitoring for fish, marine mammals, seabirds, lobster, and marine sound. During monitoring from 2016 through 2020, FORCE completed:

- ~564 hours of hydroacoustic fish surveys;
- more than 5,083 'C-POD' marine mammal monitoring days;
- bi-weekly shoreline observations;
- 49 observational seabird surveys;
- four drifting marine sound surveys and additional sound monitoring; and
- 11 days of lobster surveys

In the first quarter of 2021, Sea Mammal Research Unit (SMRU) Consulting Ltd. provided their 4th year final report of harbour porpoise monitoring at the FORCE test site using C-PODs. The report describes the results of C-POD deployments #11-12 (August 2019 – September 2020), and places the results in the broader context of the overall marine mammal monitoring program implemented as part of FORCE's multiyear Environmental Effects Monitoring Program (EEMP). This ongoing monitoring program continues to show the prevalence of harbour porpoise at FORCE, with the species being detected on approximately 99% of the 1,888 calendar days since monitoring with C-PODs commenced in 2011. Harbour porpoise detections at FORCE vary seasonally, with peak activity occurring during May – August, and lowest detections during December – March. Harbour porpoise detections also vary spatially, with C-PODs deployed at locations W2 and S2 recording the greatest detection rates, and D1 values typically low. Mean lost time across C-PODs, due to ambient flow noise saturating the detection buffer on the C-POD, averages 22.6%. The report by SMRU is included here as Appendix I, and supports the findings of previous monitoring activities that harbour porpoise are prevalent at the FORCE test site. The report also reiterates that a sufficient amount of baseline data has been collected to meet the goals of the EEMP, and that future C-POD deployments could be suspended until an operational turbine is deployed at the FORCE site.

FORCE submitted its 2021-2023 proposed EEMP to regulators earlier this year and is awaiting feedback. The 2021-2023 EEMP is designed to prepare for effects testing with the deployment of operational turbines, and adheres to the principles of adaptive management by evaluating existing datasets to ensure appropriate monitoring approaches are being implemented. Moreover, the plan adopts internationally accepted standards for monitoring where possible, including feasibility assessments for new monitoring approaches that are planned to be implemented.

FORCE is working collaboratively with the OERA to advance 'The Pathway Program' to identify effective and regulator approved monitoring solutions for the tidal energy industry in Nova Scotia. Phase I of the program consisted of a 'Global Capability Assessment' that involved comprehensive literature reviews about the use of different classes of environmental monitoring technologies for monitoring tidal energy devices around the world. While this element of Phase I was completed in 2019, ongoing international engagement and knowledge exchange was fostered through a series of workshops that generated international collaborations that have assisted with other phases of the program. Phase II, 'Advancing Data Processing and Analysis', is nearly completed. Work to automate the post-processing of hydroacoustic data with DeepSense (Dalhousie University) generated a new processing tool called 'Echofilter'. Work was recently completed to develop a hydroacoustic data analysis pipeline that will generate quarterly reports to provide information on three metrics of interest to regulators: i) frequency of target detections, ii) abundance of targets detected, and iii) vertical distribution of targets in the water column. Automation of PAM data has also been completed with partners at Oregon State University that generated a harbour porpoise click detector and classification tool for application to Minas Passage called 'FindPorpoises'. The Pathway Program team is working with Sustainable Oceans Applied Research (SOAR) to pursue automated detection, tracking and classification of targets from multibeam imaging sonars with partners in Washington state and the United Kingdom. Phase III, 'Technology Validation', is nearing completion. Sustainable Oceans Applied Research (SOAR) recently completed a performance assessment for imaging sonars (Blueview and Gemini) in both surface and bottom-mounted deployments using a series of known targets. While entrained air from turbulence made tracking targets difficult in surface deployments, both sonars were useful for target detection, although the Gemini performed better for average target detection and target tracking at greater distances (10-50 m) (Appendix II). While insufficient data was collected by the Blueview imaging sonar during the bottom-mounted tests (due to its relatively small ensonified area), the Gemini performed well for target detection, identification and tracking (Appendix III). Importantly, there was not significant relationship between flow speed and the ability of the Gemini to tack targets during bottom-mounted deployments. FORCE recently completed collaborative work with Sustainable Marine Energy Canada (Sustainable Marine) to assess the efficacy of upward and downward facing echosounders for monitoring fish, and surface-deployed and bottom-mounted PAM instruments for monitoring harbour porpoise. The results of the echosounder comparison highlight the important role of localized hydrodynamics and turbulence for effective monitoring, and indicate that upward facing echosounders are needed for generating quantitative data about fish density and distribution in tidal channels (Appendix IV). The PAM comparison revealed that while both surface and bottom mounted hydrophones could detect harbour porpoise echolocation clicks, the data from the surface hydrophone contained interference from bubbles that was difficult to distinguish from echolocations. This interference negatively impacts automated porpoise click detectors, potentially leading to false-positive detections and a reduced detection range for surface deployed hydrophones (Appendix V). However, the choice of hydrophone deployment location depends on the monitoring question(s) being asked, and the results of this study did not provide sufficient evidence to strongly prefer one deployment location over the other. DP Energy

completed a 'wet test' of their integrated monitoring platform in Halifax Harbour during fall 2020 and is preparing for deployment at the FORCE test site in July 2021.

FORCE is also working with academic and First Nations partners to advance the Risk Assessment Program (RAP) for tidal stream energy. This program seeks to develop credible and statistically robust encounter rate models for migratory and resident fish species in Minas Passage with tidal turbines. This will be accomplished by combining physical oceanographic data related to flow and turbulence in the Minas Passage with hydroacoustic tagging information for various fish species in the region curated by the Ocean Tracking Network at Dalhousie University. Since the start of the project, FORCE has established a high-resolution radar network in Minas Passage and has started to quantify hydrodynamic features in the region and build the tidal flow atlas required for the program. FORCE has also started modelling the spatiotemporal distributions for the nine species for which sufficient acoustic tracking data is available, and is developing species distribution maps for each species. In partnership with FORCE, the Mi'kmaw Conservation Group (MCG) has commenced the fish tagging component of the program that is required for encounter rate model validation. To share the results of the modelling work, FORCE is currently exploring the development of a user-friendly graphical user interface as a science-based decision support tool that would be accessible by regulators, rights holders, stakeholders, industry, and academia. Ultimately, this work will contribute towards understanding the risk of instream tidal power development for fishes in the Bay of Fundy and will assist in the development of future environmental effects monitoring programs.

This report provides a summary of monitoring activities and data analyses completed at the FORCE site up to the end of the second quarter of 2021. In addition, it also highlights findings from international research efforts, previous data collection periods at the FORCE site, and additional research work that is being conducted by FORCE and its partners. This includes supporting fish tagging efforts with Acadia University and the Ocean Tracking Network, radar research projects, and subsea instrumentation platform deployments through the Fundy Advanced Sensor Technology (FAST) Program. Finally, the report presents details regarding future research and monitoring efforts at the FORCE test site. Due to the ongoing risk of COVID-19 transmission, marine operations are being conducted following guidelines with respect to social distancing and the use of face masks that were developed in consultation with information provided by NS public health. This includes work in support of the 2021 EEMP and the RAP program.

All reports, including quarterly monitoring summaries, are available online at www.fundyforce.ca/document-collection.

Contents

Appendices

Appendix I   FORCE marine mammal EEMP – Year 4 Final Report

Appendix II   Pathway Program – Performance of imaging sonars in surface deployments

Appendix III   Pathway Program – Performance of imaging sonars in bottom-mounted deployments

Appendix IV   Pathway Program – Performance of echosounders in surface and bottom-mounted deployments

Appendix V   Pathway Program – Performance of hydrophones in surface and bottom-mounted deployments

Acronyms

AAM	Active Acoustic Monitoring
ADCP	Acoustic Doppler Current Profiler
AMAR	Autonomous Multichannel Acoustic Recorder
BACI	Before/After, Control/Impact
BC	British Columbia
BoFEP	Bay of Fundy Ecosystem Partnership
CFI	Canadian Foundation for Innovation
CLA	Crown Lease Area
cm	Centimetre(s)
CPUE	Catch Per Unit Effort
CSTV	Cape Sharp Tidal Venture
DFO	Department of Fisheries and Oceans (Canada)
DEM	Department of Energy and Mines (Nova Scotia)
EA	Environmental Assessment
EEMP	Environmental Effects Monitoring Program
EMAC	Environmental Monitoring Advisory Committee
EMP	Environmental Management Plan
FAD	Fish Aggregation Device
FAST	Fundy Advanced Sensor Technology
FAST-EMS	Fundy Advanced Sensor Technology – Environmental Monitoring System
FERN	Fundy Energy Research Network
FORCE	Fundy Ocean Research Center for Energy
GPS	Global Positioning System
hr	Hour(s)
IEA	International Energy Agency
kg	Kilogram(s)
km	Kilometre(s)
kW	Kilowatt(s)
m	Metre(s)
MET	Meteorological
MRE	Marine Renewable Energy
MREA	Marine Renewable-electricity Area
NL	Newfoundland and Labrador
NRCan	Natural Resources Canada
NS	Nova Scotia
NSDEM	Nova Scotia Department of Energy and Mines
NSE	Nova Scotia Department of Environment
NSERC	Natural Sciences and Engineering Research Council
NSPI	Nova Scotia Power Inc.
OERA	Offshore Energy Research Association of Nova Scotia
OES	Ocean Energy Systems
ONC	Ocean Networks Canada
ORJIP	Offshore Renewables Joint Industry Programme
OSC	Ocean Supercluster
OTN	Ocean Tracking Network
PAM	Passive Acoustic Monitoring
Q1/2/3	Quarter (1, 2, 3), based on a quarterly reporting schedule
R&D	Research and Development
TC114	Technical Committee 114

TISEC   Tidal In-Stream Energy Converter
SUBS   Streamlined Underwater Buoyancy System
SME   Sustainable Marine Energy (Canada)
UAV   Unmanned Aerial Vehicle
UK   United Kingdom
VEC(s)   Valuable Ecosystem Component(s)

Introduction

This report outlines monitoring activities occurring at the Fundy Ocean Research Center for Energy test site in the Minas Passage, Bay of Fundy during April-June 2021. Specifically, this report highlights results of environmental monitoring activities conducted in the mid-field zone and other research and development activities conducted at the FORCE site. This report also provides a summary of international research activities around tidal stream energy devices.

About FORCE

FORCE was created in 2009 to lead research, demonstration, and testing for high flow, industrial-scale tidal stream energy devices. FORCE is a not-for-profit entity that has received funding support from the Government of Canada, the Province of Nova Scotia, Encana Corporation, and participating developers.

FORCE has two central roles in relation to the demonstration of tidal stream energy converters in the Minas Passage:

1. Host: providing the technical infrastructure to allow demonstration devices to connect to the transmission grid; and
2. Steward: research and monitoring to better understand the interaction between devices and the environment.

The FORCE project currently consists of five undersea berths for subsea turbine generators, four subsea power cables to connect the turbines to land-based infrastructure, an onshore substation and power lines connected to the Nova Scotia Power transmission system, and a Visitor Centre that is free and open to the public from May to November annually. These onshore facilities are located approximately 10 km west of Parrsboro, Nova Scotia.

The marine portion of the project is located in a 1.6 km x 1.0 km Crown Lease Area in the Minas Passage. It is also identified as a Marine Renewable-electricity Area under the Province's Marine Renewable-energy Act. This area consists of five subsea berths that are leased to tidal energy companies[1] selected by the Nova Scotia Department of Energy and Mines. Current berth holders at FORCE are:

> Berth A: Minas Tidal Limited Partnership
> Berth B: Rio Fundo Operations Canada Limited[2]
> Berth C: Sustainable Marine Energy (Canada)[3]
> Berth D: Big Moon Power Canada
> Berth E: Halagonia Tidal Energy Limited[4]

Research, monitoring, and associated reporting is central to FORCE's steward role, to assess whether tidal stream energy devices can operate in the Minas Passage without causing significant adverse effects on the environment, electricity rates, and other users of the Bay.

---

[1] Further information about each company may be found at: fundyforce.ca/partners

[2] On April 30, 2019 the Department of Energy and Mines approved the transfer of the Project Agreement and FIT approvals from Atlantis Operations (Canada) Ltd. to Rio Fundo Operations Canada Ltd.

[3] On May 15, 2019 the Department of Energy and Mines issued an approval for Black Rock Tidal Power to change its name to Sustainable Marine Energy (Canada) Ltd. with the transfer of assets from SCHOTTEL to Sustainable Marine Energy. Learn more: sustainablemarine.com/news/schottel

[4] Berth E does not have a subsea electrical cable provided to it.

As part of this mandate FORCE has a role to play in supporting informed, evidence-based decisions by regulators, industry, the scientific community, and the public. As deployments of different technologies are expected to be phased in over the next several years, FORCE and regulators will have the opportunity to learn and adapt environmental monitoring approaches as lessons are learned.

Background

The FORCE demonstration project received its environmental assessment (EA) approval on September 15, 2009 from the Nova Scotia Minister of Environment. The conditions of its EA approval[5] provide for comprehensive, ongoing, and adaptive environmental management. The EA approval has been amended since it was issued to accommodate changes in technologies and inclusion of more berths to facilitate provincial demonstration goals.

In accordance with this EA approval, FORCE has been conducting an Environmental Effects Monitoring Program (EEMP) to better understand the natural environment of the Minas Passage and the potential effects of turbines as related to fish, seabirds, marine mammals, lobster, marine sound, benthic habitat, and other environmental variables. All reports on site monitoring are available online at: www.fundyforce.ca/document-collection.

Since 2009, more than 100 related research studies have been completed or are underway with funding from FORCE, the Offshore Energy Research Association (OERA) and others. These studies have considered socioeconomics, biological, and other research areas.[6]

Monitoring at the FORCE site is currently focused on lobster, fish, marine mammals, seabirds, and marine sound and is divided into 'near-field' (≤ 100 m from a turbine) and 'mid-field' or 'site-level' (> 100 m from a turbine) monitoring. As approved by regulators, individual berth holders are responsible for leading near-field monitoring in direct vicinity of their turbine(s), in recognition of the unique design and operational requirements of different turbine technologies. FORCE completes 'mid-field' monitoring activities as well as supporting integration of data analysis between these monitoring zones, where applicable.

All near-field and mid-field monitoring programs are reviewed by FORCE's Environmental Monitoring Advisory Committee (EMAC), which includes representatives from scientific, First Nations, and local fishing communities.[7] These programs are also reviewed by federal and provincial regulators prior to turbine installation. In addition, FORCE and berth holders also submit an Environmental Management Plan (EMP) to regulators for review prior to turbine installation. EMP's include: environmental management roles and responsibilities and commitments, environmental protection plans, maintenance and inspection requirements, training and education requirements, reporting protocols, and more.

Turbine Deployments

Since FORCE's establishment in 2009, turbines have been installed at the FORCE site three times: once in 2009/2010, November 2016 – June 2017, and July 2018 – present. Given the limited timescales in which a tidal turbine has been present and operating at the FORCE site,

---

[5] FORCE's Environmental Assessment Registration Document and conditions of approval are found online at: www.fundyforce.ca/document-collection.

[6] OERA's Tidal Energy Research Portal (http://tidalportal.oera.ca/) includes studies pertaining to infrastructure, marine life, seabed characteristics, socio-economics and traditional use, technology, and site characterization.

[7] Information about EMAC may be found online at: www.fundyforce.ca/about-us

environmental studies to-date have largely focused on the collection of baseline data and developing an understanding of the capabilities of monitoring devices in high flow tidal environments.

On July 22, 2018, CSTV installed a two-megawatt OpenHydro turbine at Berth D of the FORCE site and successfully connected the subsea cable to the turbine. CSTV confirmed establishment of communication with the turbine systems on July 24. On July 26, 2018, Naval Energies unexpectedly filed a petition with the High Court of Ireland for the liquidation of OpenHydro Group Limited and OpenHydro Technologies Limited.[8] For safety purposes, the turbine was isolated from the power grid that same day. On September 4, 2018, work began to re-energize the turbine, but soon afterwards it was confirmed that the turbine's rotor was not turning. It is believed that an internal component failure in the generator caused sufficient damage to the rotor to prevent its operation. Environmental sensors located on the turbine and subsea base continued to function at that time with the exception of one hydrophone.

As a result of the status of the turbine, the monitoring requirements and reporting timelines set out in CSTV's environmental effects monitoring program were subsequently modified under CSTV's Authorization from Fisheries and Oceans Canada. The modification requires that CSTV provide written confirmation to regulators on a monthly basis that the turbine is not spinning by monitoring its status during the peak tidal flow of each month. This began October 1, 2018 and was expected to continue until the removal of the turbine; however, as a result of the insolvency of OpenHydro Technology Ltd., all near-field reporting activities by CSTV ceased as of March 1, 2019. FORCE subsequently provided monthly reports to regulators confirming the continued non-operational status of the CSTV turbine from March 2019 – May 2020, and received authorization from the Nova Scotia Department of Environment on June 2, 2020 to conclude these monthly reports.

In September 2020, Big Moon Canada Corporation (Big Moon) was announced as the successful applicant to fill berth D at the FORCE test site following a procurement procedure administered by Power Advisory LLC. As part of the agreement, Big Moon has provided a $4.5 million security deposit to remove the non-operational CSTV turbine currently deployed at berth D, and has until December 31, 2024 to raise the turbine. The project start date for BigMoon is largely dependent on the economic recovery from the COVID-19 pandemic and the potential impact to Big Moon's supply chain. As such, the project start date is not known at this time.

Additional turbines are expected to be deployed at the FORCE site in the coming years. In 2018, Sustainable Marine Energy (formerly Black Rock Tidal Power) installed a PLAT-I system in Grand Passage, Nova Scotia under a Demonstration Permit.[9] This permit allows for a demonstration of the 280 kW system to help SME and its partners learn about how the device operates in the marine environment of the Bay of Fundy. Also in 2018, Natural Resources Canada announced a $29.8 million contribution to Halagonia Tidal Energy's project at the FORCE site through its Emerging Renewable Power Program.[10] The project consists of submerged turbines for a total of nine megawatts – enough capacity to provide electricity to an estimated 2,500 homes.

---

[8] See original news report: https://www.irishexaminer.com/breakingnews/business/renewable-energy-firms-with-more-than-100-employees-to-be-wound-up-857995.html.

[9] To learn more about this project, see: https://novascotia.ca/news/release/?id=20180919002.

[10] To learn more about this announcement, see: https://www.canada.ca/en/natural-resources-canada/news/2018/09/minister-sohi-announces-major-investment-in-renewable-tidal-energy-that-will-power-2500-homes-in-nova-scotia.html.

Each berth holder project will be required to develop a turbine-specific monitoring program, which will be reviewed by FORCE's EMAC and federal and provincial regulators including Fisheries and Oceans Canada, the Nova Scotia Department of Environment, and the Nova Scotia Department of Energy and Mines prior to turbine installation.

Overall, the risks associated with single device or small array projects are anticipated to be low given the relative size/scale of devices (Copping 2018). For example, at the FORCE site a single two-megawatt OpenHydro turbine occupies ~ 1/1,000th of the cross-sectional area in the Minas Passage (Figure 1). A full evaluation of the risks of tidal stream energy devices, however, will not be possible until more are tested over a longer-term period with monitoring that documents local impacts, considers far-field and cumulative effects, and adds to the growing global knowledge base.
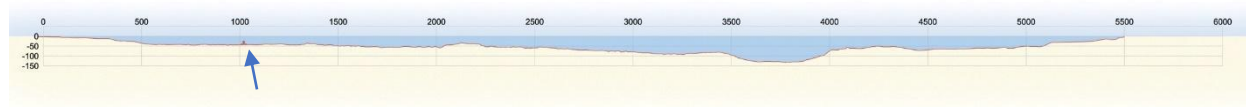
Figure 1: The scale of a single turbine (based on the dimensions of the OpenHydro turbine deployed by CSTV, indicated by the red dot and above the blue arrow) in relation to the cross-sectional area of the Minas Passage. The Passage reaches a width of ~ 5.4 km and a depth of 130 m.

International Experience & Cooperation

The research and monitoring being conducted at the FORCE test site is part of an international effort to evaluate the risks tidal energy poses to marine life (Copping 2018; Copping and Hemery 2020). Presently, countries such as China, France, Italy, the Netherlands, South Korea, the United Kingdom, and the United States (Marine Renewables Canada 2018) are exploring tidal energy, supporting environmental monitoring and innovative R&D projects. Tidal energy and other marine renewable energy (MRE) technologies such as tidal range, tidal current, wave, and ocean thermal energy offer significant opportunities to replace carbon fuel sources in a meaningful and permanent manner. Some estimates place MRE's potential as exceeding current human energy needs (Lewis et al. 2011; Gattuso et al. 2018). Recent research includes assessments of operational sounds on marine fauna (Schramm et al. 2017; Lossent et al. 2018; Robertson et al. 2018; Pine et al. 2019), the utility of PAM sensors for monitoring marine mammal interactions with turbines (Malinka et al. 2018) and collision risk (Joy et al. 2018b), and the influence of tidal turbines on fish behavior (Fraser et al. 2018).

Through connections to groups supporting tidal energy demonstration and R&D, FORCE is working to inform the global body of knowledge pertaining to environmental effects associated with tidal power projects. This includes participation in the Fundy Energy Research Network[11],

---

[11] FERN is a research network designed to" coordinate and foster research collaborations, capacity building and information exchange" (Source: fern.acadiau.ca/about.html). FORCE participates in the Natural Sciences, Engineering, and Socio-Economic Subcommittees of FERN.

the Bay of Fundy Ecosystem Partnership[12], TC114[13], the Atlantic Canadian-based Ocean Supercluster[14], and OES-Environmental[15].

On February 25th, Dr. Daniel Hasselman, FORCE's science director, participated in a virtual workshop hosted by 'International Waters' – a group whose aim is to foster international collaborations among MRE test centers. Following updates from each test center, Dr. Hasselman co-moderated a session on 'Environmental Monitoring and Consenting' that centered around environmental monitoring instrumentation, data collection practices and challenges. Discussions focused on i) identifying opportunities for collaboration where MRE development is a concern for marine animals that are common to multiple test centers, ii) identifying novel monitoring technologies that may be better suited for monitoring in dynamic marine environments, and iii) identifying opportunities for combining physical oceanographic and biological data to provide a more holistic approach for understanding the risk of MRE devices to marine animals. Participants agreed that there are some marine animals (e.g., harbour porpoise) that are common to multiple test centers and of similar concern to regulators where collaborations towards developing standardized approaches to data collection, analyses and reporting are warranted. However, the transferability of monitoring results between test centers remains an issue, and participants identified the need to build trust with regulators through transparency in methodologies and interpretation of results. Recent technological advances (i.e., Passive Acoustic Monitoring array, acoustic tracking), ongoing development of standards for acquisition of monitoring data (International Electrotechnical Commission 2019), and advances in data processing and analyses for imaging sonars and echosounders were identified by participants as important advancements. Participants were intrigued by the notion of combining physical oceanographic and biological data for informing risk, and were particularly interested in the influence of hydrodynamics on the spatial distributions of marine animals.

Dr. Hasselman also participated in two collision risk workshops (fish – March 16; marine mammals – March 18) jointly hosted by OES-Environmental and ORJIP. The purpose of the workshops was to review the elements of collision risk models, including a discussion about how collision risk models have been used to date, and progress being made in the application of collision risk models for understanding the potential impacts of MRE devices on marine animals.

FORCE will continue to work closely with OES-Environmental and its members to document and improve the state of knowledge about the interactions of MRE devices interactions with the marine environment. To that end, Dr. Hasselman has agreed to serve as a guest editor alongside Dr. Huidong Li (Pacific Northwest National Laboratory), Dr. Emma Cotter (Woods Hole Oceanographic Institute) and Dr. James Joslin (University of Washington) for a special issue of Frontiers in Marine Science entitled 'Novel Technologies for Assessing the Environmental and Ecological Impacts of Marine Renewable Energy Systems'. The editorial team advertised the special issue on the Tethys website and received nine abstracts from researchers developing cutting-edge technologies for monitoring around marine renewable energy devices. Full manuscript submissions are due by November 26, 2021, and the editorial

---

[12] BoFEP is a 'virtual institute' interested in the well-being of the Bay of Fundy. To learn more, see www.bofep.org.

[13] TC114 is the Canadian Subcommittee created by the International Electrotechnical Commission (IEC) to prepare international standards for marine energy conversion systems. Learn more: tc114.oreg.ca.

[14] The OSC was established with a mandate to "better leverage science and technology in Canada's ocean sectors and to build a digitally-powered, knowledge-based ocean economy." Learn more: www.oceansupercluster.ca.

[15] OES Environmental was established by the International Energy Agency (IEA) Ocean Energy Systems (OES) in January 2010 to examine environmental effects of marine renewable energy development. Member nations include: Australia, China, Canada, Denmark, France, India, Ireland, Japan, Norway, Portugal, South Africa, Spain, Sweden, United Kingdom, and United States. Further information is available at https://tethys.pnnl.gov.

team is aiming for publication of the special issue in 2022. Additionally, OES-Environmental is pursuing the development of new research topics for the 2024 State of the Science Report related to i) knowledge of environmental effects as the tidal energy industry scales up from single devices to arrays, ii) understanding the cumulative impacts of marine renewable energy with other anthropogenic effects, and iii) an ecosystem approach for understanding environmental effects, including interactions between trophic levels, between ecosystems and between ecosystem services. Dr. Hasselman is involved in the development of all three of these topics, but is leading the effort to understand the environmental effects of 'scaling up'.

Mid-Field Monitoring Activities

FORCE has been leading 'mid-field area' or 'site-level' monitoring for a number of years, focusing on a variety of environmental variables. FORCE's previous environmental effects monitoring program (2016-2020) was developed in consultation with SLR Consulting (Canada)[16] and was strengthened by review and contributions by national and international experts and scientists, DFO, NSE, and FORCE's EMAC. The most recent version of the EEMP (2021-2023) was developed in consultation with Atlantis Watershed Consultants Ltd. with input from national and international experts, including FORCE's EMAC, and has been submitted to regulators for approval. The 2021-2023 EEMP has been modified from the 2016-2020 EEMP based results of previous monitoring activities, experience and lessons learned. This is consistent with the adaptive management approach inherent to FORCE EEMP – the process of monitoring, evaluating and learning, and adapting (AECOM 2009) that has been used at the FORCE site since its establishment in 2009.[17]

FORCE's EEMP currently focuses on the impacts of operational turbines on lobster, fish, marine mammals, and seabirds as well as the impact of turbine-produced sound. Overall, these research and monitoring efforts, detailed below, were designed to test the predictions made in the FORCE EA. As mentioned in the Executive Summary, since the beginning of the 2016-2020 EEMP, FORCE has completed approximately:

- 564 hours of hydroacoustic fish surveys;
- more than 5,083'C-POD' (marine mammal monitoring) days;
- bi-weekly shoreline observations;
- 49 observational seabird surveys;
- four drifting marine sound surveys and additional bottom-mounted instrument sound data collection; and
- 11 days of lobster surveys.

The following pages provide a summary of the mid-field monitoring activities conducted at the FORCE site up to the end of June 2021, including data collection, data analyses performed, initial results, and lessons learned; building on activities and analyses from previous years. Where applicable, this report also presents analyses that have integrated data collected through the near-field and mid-field monitoring programs to provide a more complete understanding of turbine-marine life interactions.

---

[16] This document is available online at: www.fundyforce.ca/document-collection.

[17] The adaptive management approach is necessary due to the unknowns and difficulties inherent with gathering data in tidal environments such as the Minas Passage and allows for adjustments and constant improvements to be made as knowledge about the system and environmental interactions become known. This approach has been accepted by scientists and regulators.

Monitoring Objectives

The overarching purpose of environmental monitoring is to test the accuracy of the environmental effect predictions made in the original EA. These predictions were generated through an evaluation of existing physical, biological, and socioeconomic conditions of the study area, and an assessment of the risks the tidal energy demonstration project poses to components of the ecosystem.

A comprehensive understanding of turbine-marine life interactions will not be possible until turbine-specific and site-level monitoring efforts are integrated, and additional data is collected in relation to operating turbines. Further, multi-year data collection will be required to consider seasonal variability at the FORCE test site and appropriate statistical analyses of this data will help to obtain a more complete understanding of marine life-turbine interactions.

Table 1 outlines the objectives of the mid-field monitoring activities conducted at the FORCE demonstration site. Near-field monitoring summaries will be updated as turbines are scheduled for deployment at FORCE. At this time, and considering the scale of turbine deployments in the near-term at FORCE, it is unlikely that significant effects in the far-field will be measurable (SLR Consulting 2015). Far-field studies such as sediment dynamics will be deferred until such time they are required. However, recent discussions with scientists serving on FORCE's EMAC suggests that the natural variability inherent to the upper Bay of Fundy ecosystem far exceeds what could be measured by far-field monitoring efforts. Moreover, the scale of tidal power development would need to surpass what is possible at the FORCE tidal demonstration site to extract sufficient energy from the system to have any measurable effects. In short, far-field monitoring would be futile unless tidal power development transitions from demonstration scale to commercial arrays. As more devices are scheduled for deployment at the FORCE site and as monitoring techniques are improved, monitoring protocols will be revised in keeping with the adaptive management approach. These studies will be developed in consultation with FORCE's EMAC, regulators, and key stakeholders.

Table 1: The objectives of each of the 'mid-field' environmental effects monitoring activity, which consider various Valued Ecosystem Components (VECs), led by FORCE.

Mid-Field Environmental Effects Monitoring VEC	Objectives
Lobster	● to determine if the presence of a tidal stream energy turbine affects commercial lobster catches
Fish	● to test for indirect effects of tidal stream energy turbines on water column fish density and fish vertical distribution ● to estimate probability of fish encountering a device based on fish density proportions in the water column relative to turbine depth in the water column
Marine Mammals	● to determine if there is permanent avoidance of the mid-field study area during turbine operations ● to determine if there is a change in the distribution of a portion of the population across the mid-field study area
Marine Sound (Acoustics)	● to conduct ambient sound measurements to characterize the soundscape prior to and following deployment of the in-stream turbines

| Seabirds | ● to understand the occurrence and movement of bird species in the vicinity of tidal stream energy turbines |
| | ● to confirm FORCE's Environmental Assessment predictions relating to the avoidance and/or attraction of birds to tidal stream energy turbines |

Lobster

FORCE conducted a baseline lobster catchability survey in fall 2017 (NEXUS Coastal Resource Management Ltd. 2017). This catch-and-release survey design was conducted over 11 days and consisted of commercial traps deployed at varying distances around the future location of the CSTV turbine deployment planned for 2018. Captured lobsters were measured (carapace length), had their sex and reproductive stage determined (male, female, and berried female), and shell condition evaluated. This baseline survey captured 351 lobsters and reported a high catchability rate (> 2.7 kg/trap).[18] Preliminary qualitative analyses indicated that catch rates declined during the survey and were associated with increasing tidal velocities; a statistically significant negative relationship was detected between catch rates and maximum tidal range. No significant difference in catch rates was detected across separate locations from the proposed turbine deployment site. Cumulatively, these results suggested that the impact of turbines may be higher on lobster catchability than anticipated in the EA (AECOM 2009), but a repeat of the study in the presence of an operational turbine is required to verify this prediction.

Indeed, a repeat of this catchability survey was planned for fall 2018 in the presence of an operational turbine to test the EA prediction (with pre-installation and operating turbine collection periods) that tidal stream turbines will have minimal have impacts on lobster populations within the FORCE test site (AECOM 2009). However, given the non-operational status of the CSTV turbine, the objectives of the 2018 survey effort could not be achieved, and the survey has been postponed until an operational turbine is present at the site.

In 2019, FORCE commissioned TriNav Fisheries Consultants Ltd. to redesign FORCE's lobster monitoring program based on feedback from regulators to include a more statistically robust study design for monitoring lobster at the FORCE test site. TriNav Fisheries Consultants evaluated the efficacy of using a variety of methods including divers and hydroacoustic tags to track lobster movements. However, given the strong tidal flows and brief window available during periods of slack tide, divers are not a viable option due to safety concerns. Ultimately, TriNav Fisheries Consultants identified the combination of a modified catchability survey design and a mark-recapture study using conventional tags as the best approach for monitoring lobster at the FORCE site. Given the operational restrictions generated from the COVID-19 pandemic in 2020-2021, this new study design is intended to be implemented in late summer 2022 in partnership with the Fishermen and Scientists Research Society (FSRS).

---

[18] This is classified as 'high' according to DFO's Catch Per Unit Effort (CPUE) index (Serdynska and Coffen-Smout, 2017).

Fish

FORCE has been conducting mobile fish surveys since May 2016 to test the EA prediction that tidal stream turbines are unlikely to cause substantial impacts to fishes at the test site (AECOM 2009). To that end, the surveys are designed to:

- test for indirect effects of tidal stream energy turbines on water column fish density and fish vertical distribution; and
- estimate the probability of fish encountering a device based on any 'co-occurrence' relative to turbine depth in the water column.

Moreover, these surveys follow a 'BACI' (Before/After, Control/Impact) design to permit a comparison of data collected before a turbine is installed with data collected while a turbine is operational at the FORCE site, and in relation to a reference site along the south side of the Minas Passage. These 24-hour mobile surveys encompass two tidal cycles and day/night periods using a scientific echosounder, the Simrad EK80, mounted on a vessel, the Nova Endeavor (Huntley's Sub-Aqua Construction, Wolfville, NS). This instrument is an active acoustic monitoring device and uses sonar technology to detect fish by recording reflections of a fish's swim bladder.

Analyses of hydroacoustic fish surveys completed during baseline studies in 2011 and 2012 (Melvin and Cochrane 2014) and surveys during May 2016 – August 2017 (Daroux and Zydlewski 2017) evaluated changes in fish densities in association with diel stage (day/night), tidal stage (ebb/flood), and turbine presence or absence (an OpenHydro turbine was present November 2016 – June 2017). Results support the EA prediction that tidal stream devices have minimal impact on marine fishes. However, additional surveys in relation to an operating turbine are required to fully test this prediction.

In 2019, the University of Maine conducted a thorough analysis for 15 fish surveys conducted by FORCE from 2011-2017. The hydroacoustic data set included six 'historical' surveys conducted between August 2011 and May 2012, and nine 'contemporary' surveys conducted between May 2016 and August 2017. The analyses included comparisons of fish presence/absence and relative fish density with respect to a series of temporal (historical vs. contemporary, or by survey), spatial (CLA vs. reference study area, or by transect) and environmental (tide phase, diel state, or with/against predicted tidal flow) explanatory variables. The report identified a statistically significant difference in fish presence/absence and relative fish density between the historical and contemporary data sets that may be attributable to differences in the survey design/execution between the time periods, or could reflect changes in fish usage of the site. As such, remaining analyses were restricted to the contemporary data sets. The results revealed that: i) data collection during the ebb tide and at night are important for understanding fish presence in the CLA, ii) various explanatory variables and their additive effects should be explored further, and iii) increasing the frequency of surveys during migratory periods (consecutive days in spring/fall) may be required to understand patterns and variability of fish presence and density in Minas Passage. Importantly, the report suggested a statistically significant difference in fish presence/absence and relative density between the CL and reference site, suggesting that the reference site may not be sufficiently representative to serve as a control for the CLA, and for testing the effects of an operational turbine on fish density and distribution in Minas Passage. Additional work is underway using data from eight additional contemporary fish surveys (2017-2018) to determine whether this finding is biologically meaningful, or whether it is simply a statistical artefact of how the data was aggregated in the original analysis.

Because complex hydrodynamic features of the Minas Passage introduce turbulence and bubbles into the water column that interfere with the use of hydroacoustics, FORCE's mobile fish surveys have been optimized for collecting data during the best neap tidal cycle per month when turbulence is greatly reduced. However, this approach limits the number of surveys that can be conducted, and regulators have suggested that the scope of the program be expanded so that survey results are more representative of how fish use the Minas Passage. To that end, FORCE conducted multiple fish surveys during each of three neap tidal cycles in fall 2020 (i.e., September 25, 27, 29; October 7, 9, 13; and October 24, 26, 29) to determine whether variation in fish density and distribution for any given survey within a neap cycle was representative of the other surveys conducted during that same time frame. Previous work comparing stationary and mobile hydroacoustic surveys in Minas Passage found that the temporal representative range of a 24-hr mobile was approximately three days (Viehman et al. 2019). Post-processing and analyses of the data will commence in 2021 and will provide additional information about the temporal representativeness of FORCE's mobile fish surveys, and will help determine how frequently these surveys are required to understand fish usage of the Minas Passage.

Marine Mammals

Since 2016, FORCE has been conducting two main activities to test the EA prediction that project activities are not likely to cause significant adverse residual effects on marine mammals within the FORCE test site (AECOM 2009):

- passive acoustic monitoring (PAM) using 'click recorders' known as C-PODs; and
- an observation program that includes shoreline, stationary, and vessel-based observations.

Passive Acoustic Monitoring

The first component of FORCE's marine mammal monitoring program involves the use of PAM mammal detectors known as C-PODs, which record the vocalizations of toothed whales, porpoises, and dolphins.[19] The program focuses mainly on harbour porpoise – the key marine mammal species in the Minas Passage that is known to have a small population that inhabits the inner Bay of Fundy (Gaskin 1992). The goal of this program is to understand if there is a change in marine mammal presence in proximity to a deployed tidal stream energy device and builds upon baseline C-POD data collection within the Minas Passage since 2011.

From 2011 to early 2018, more than 4,845 'C-POD days'[20] of data were collected in the Minas Passage. Over the study period, it was found that harbour porpoise use and movement varies over long (i.e., seasonal peaks and lunar cycles) and short (i.e., nocturnal preference and tide stage) timescales. This analysis, completed by Sea Mammal Research Unit (Canada) (Vancouver, BC), showed some evidence to suggest marine mammal exclusion within the near-field of CSTV turbine when it was operational (November 2016 – June 2017) (Joy et al. 2018a). This analysis revealed that the C-PODs in closest proximity to the turbine (230 m and 210 m distance) had reduced frequency of detections, but no evidence of mid-field avoidance with a turbine present and operating. These findings also revealed a decrease in detections during

---

[19] The C-PODs, purchased from Chelonia Limited, are designed to passively detect marine mammal 'clicks' from toothed whales, dolphins, and porpoises.

[20] A 'C-POD day' refers to the number of total days each C-POD was deployed times the number of C-PODs deployed.

turbine installation activities, consistent with previous findings (Joy et al. 2017), but requiring additional data during an operational turbine to permit a full assessment of the EA predictions.

This monitoring program demonstrates the prevalence of harbour porpoise at FORCE, with the species being detected on 98.8% of the 1,888 calendar days since monitoring with C-PODs commenced in 2011. Harbour porpoise detections at FORCE varies seasonally, with peak activity occurring during May – August, and lowest detections during December – March. Harbour porpoise detections also vary spatially, with C-PODs deployed at locations W2 and S2 recording the greatest detection rates, and D1 values typically low. Mean lost time across C-PODs, due to ambient flow noise saturating the detection buffer on the C-POD, averaged 22.6%. Interestingly, an analysis against past datasets that controlled for time of year, indicated that the effects of the non-operational CSTV turbine structure had no detectable effect on the rate of harbour porpoise detection.

SMRU provided their 4th year final report of harbour porpoise monitoring using C-PODs at the FORCE test site (Palmer et al. 2021). The report describes the results of C-POD deployments #11-12 (i.e., 1,043 days of monitoring from August 2019 – September 2020), and places the results in the broader context of the overall marine mammal monitoring program at FORCE. The final report (see Appendix I) includes summary data that revealed that harbour porpoise was detected on a least one C-POD every day, with a median value of 11 and 17 minutes of porpoise detections per day during deployments 11 and 12, respectively. The mean percent lost time due to ambient flow and sediment noise was 19.5% and 23.8%, respectively; comparable to previous deployments. Overall, the final report supports previous findings of monitoring activities that harbour porpoise are prevalent at the FORCE test site.

The final report also reiterates that sufficient baseline data has been collected to meet the goals of the EEMP. As such, FORCE has recommended in its 2021-2023 EEMP proposal that the collection of additional baseline harbour porpoise data using C-PODs be suspended until an operational turbine is deployed at the FORCE site. As a result of the damage that the SUBs package experience at the FORCE site, the C-PODs were shipped back to the manufacturer in February for refurbishment and were not available for deployment during the first quarter of 2021. They were returned to FORCE in April 2021 and are available for deployment once operational turbines are installed at the tidal demonstration site.

Harbor porpoise (Phocoena phocoena) monitoring at the FORCE Test Site, Canada featured on Tethys (by FORCE and SMRU): https://tethys.pnnl.gov/tethys-stories/harbor-porpoise-phocoena-phocoena-monitoring-force-test-site-canada

Observation Program

FORCE's marine mammal observation program in 2021 includes observations made during bi-weekly shoreline surveys, stationary observations at the FORCE Visitor Centre, and marine-based observations during marine operations. All observations and sightings are recorded, along with weather data, tide state, and other environmental data. Any marine mammal observations are shared with SMRU Consulting to support validation efforts of PAM activities.

FORCE has begun using an Unmanned Aerial Vehicle (UAV) for collecting observational data along the shoreline and over the FORCE site using transects by programming GPS waypoints in the UAV to standardize flight paths. Several FORCE staff including *Science Director* Dr.

Daniel Hasselman, *Facility Manager* Sandra Currie, and *Ocean Technologist* Jessica Douglas received training to operate FORCE's UAV, and have acquired UAV pilot certification by successfully passing the 2019 Canadian Drone Pilot Basic Operations Examination, administered by Transport Canada. These staff are now licensed to safely operate the UAV at the FORCE site. FORCE also hosts a public reporting tool that allows members of the public to report observations of marine life: mmo.fundyforce.ca

Marine Sound (Acoustics)

Marine sound – often referred to as 'acoustics' or 'noise' – monitoring efforts are designed to characterize the soundscape of the FORCE test site. Data collected from these monitoring efforts will be used to test the EA predictions that operational sounds produced from functioning tidal stream turbines are unlikely to cause mortality, physical injury or hearing impairment to marine animals (AECOM 2009).

Results from previous acoustic analyses completed at the FORCE site indicate that the CSTV turbine was audible to marine life at varying distances from the turbine, but only exceeded the threshold for behavioural disturbance at very short ranges and during particular tide conditions (Martin et al. 2018). This is consistent with findings at the Paimpol-Bréhat site in France where an OpenHydro turbine was also deployed – data suggests that physiological trauma associated with a tidal turbine is improbable, but that behavioural disturbance may occur within 400 m of a turbine for marine mammals and at closer distances for some fish species (Lossent et al. 2018).

In previous years, regulators have encouraged FORCE to pursue integration of results from multiple PAM instruments deployed in and around the FORCE test site. To that end, FORCE and its partner JASCO Applied Sciences (Canada) Ltd. pursued a comparative integrated analysis of sound data collected by various hydrophones (i.e., underwater sound recorders) deployed autonomously and mounted on the CSTV turbine. That work revealed that flow noise increased with the height of the hydrophone off the seabed but had little effect on hydrophones deployed closer to the sea floor. The comparative integrated analysis provided valuable information about future marine sound monitoring technologies and protocols while building on previous acoustics analyses at the FORCE site.

In its 2021-2023 EEMP proposal, FORCE has recommended conducting a test survey in the presence of an operational turbine using an internationally recognized standard methodology for monitoring sound (International Electrotechnical Commission 2019). This would permit the feasibility of the approach to be tested in the Minas Passage to ensure the method can be implemented as described.

Seabirds

FORCE's seabird monitoring program is designed to test the EA prediction that project activities are not likely to cause adverse residual effects on marine birds within the FORCE test area (AECOM 2009). However, there has been limited opportunity to determine potential effects of an operational turbine on seabirds at the FORCE test site and to test the EA predictions.

Since 2011, FORCE and Envirosphere Consultants Ltd. (Windsor, NS) have collected observational data from the deck of the FORCE Visitor Centre, documenting seabird species presence, distribution, behaviour, and seasonality throughout the FORCE site (Envirosphere Consultants Ltd. 2017). In 2019, FORCE commissioned Envirosphere Consultants Ltd. and Dr.

Phil Taylor (Acadia University) to synthesize the results of its observational seabird surveys (2011-2018) at the FORCE test site, and to evaluate advanced statistical techniques for analysing seabird count data in relation to environmental predictor variables. The seabird count data were examined using Generalized Additive Models (GAMs) to characterize seabird abundance and to better understand the potential impacts of tidal turbines on seabirds at the FORCE test site. The results of the analyses revealed that overall model fit is suitable to characterize count data for some species, and that there are clear patterns of effects of time of year, wind speed and direction, tide height and time of day on the number of seabirds observed. However, the analyses also revealed that not all species reported at FORCE have been observed frequently enough to be modelled effectively using the GAM approach. This is due in part to the variability in count data that is particularly relevant for modelling abundance of migratory species that are only present at the FORCE site for brief periods during annual migrations. This is consistent with observational data collected over the course of these surveys that have demonstrated that the FORCE site has a lower abundance of seabirds in relation to other areas of the Bay of Fundy, and even other regions of Atlantic Canada. Given these results, the report recommends that future monitoring and analyses focus on locally resident species (i.e., great black-backed gull, herring gull, black guillemot and common eider) so that the EA predictions can be tested most effectively. This work contributes to the development of appropriate analytical methods for assessing the impacts of tidal power development in the Minas Passage on relevant seabird populations and supports the continued responsible development of tidal energy at FORCE. For 2021-2023, FORCE plans to collaborate with Dr. Phil Taylor to test radar-based seabird monitoring capabilities and to adapt existing data processing algorithms and statistical analysis tools for quantifying seabird use of the FORCE site.

FORCE recently worked with Atlantis Watershed Consultants Ltd. to develop its 2021-2023 EEMP for the five VECs listed above. As in the past, the 2021-2023 EEMP adheres to the principles of adaptive management, and is designed to prepare for effects testing with the deployment of operational turbines. The plan evaluates existing datasets to ensure appropriate monitoring approaches are being implemented, and adopts internationally accepted standards for monitoring where possible, including feasibility assessments for new monitoring approaches that are planned to be implemented.

Near-field Monitoring Activities

While FORCE completes site-level or 'mid-field' monitoring activities at the FORCE site, near-field monitoring is led by individual berth holders. Like the mid-field monitoring programs, the near-field monitoring plans and reports undergo review by FORCE's EMAC and regulators..

In September 2018, it was confirmed that that CSTV turbine rotor was not spinning. Since that time, CSTV had been providing written confirmation to regulators on a monthly basis that the turbine is not operational by monitoring its status during the peak tidal flow of each month. However, as a result of the insolvency of OpenHydro Technology Ltd., all reporting activities by CSTV ceased as of March 1, 2019. Data collection from the turbine-mounted ADCPs to confirm the turbine is no longer spinning was managed and reported by FORCE to regulators on a monthly basis from March 2019 – May 2020, but was discontinued following an amendment to this requirement.

As additional near-field, device-specific environmental effects monitoring programs are required and implemented for deployed tidal stream devices, berth holder updates will be included as appendices to this report.

Other FORCE Research Activities

The Pathway Program

The Pathway Program is a collaborative effort between FORCE and OERA to identify an effective and regulator approved monitoring solution for the tidal energy industry in Nova Scotia. The Pathway Program involves several phases, including i) Global Capability Assessment, ii) Advancing Data Processing and Analytics, and iii) Technology Validation.

The first phase of this program, a Global Capability Assessment, involved a comprehensive literature review about the use of different classes of environmental monitoring technologies (i.e., PAM, imaging sonars, echosounders) for monitoring tidal energy devices around the world. Subject matter experts were commissioned to provide reports on these instrument classes, and these reports are publicly available.[21]

Phase II of the program ('Advancing Data Processing and Analytics') involved the development of automation tools for expediting post-processing and reporting of monitoring data. To that end, the Pathway Program partnered with DeepSense (Dr. Scott Lowe) in the Computer Science Department at Dalhousie University and used machine learning methods to develop a new tool (i.e., 'Echofilter') for post-processing raw hydroacoustic data. This new tool accurately (Jaccard Index >94%) identifies the boundary between turbulence and biological targets on raw echograms and reduces the time required for manual post-processing by 45-59%. This tool was recently paired with a streamlined analysis and reporting pipeline developed by FORCE's hydroacoustician, Dr. Louise McGarry, that generates standardized figures and tables for inclusion in quarterly and annual reports for regulators. The analysis pipelines provides standardized information about the i) frequency of fish detections, ii) abundance of fish, and iii) fish vertical distribution in the water column and how those metrics vary with environmental variables like tide stage and diel state. Cumulatively, this work reduces the time between data collection and reporting and allows regulators to see the results of monitoring activities more quickly.

The Pathway Program also partnered with Dr. Dave Mellinger at Oregon State University to develop a harbour porpoise click detector and classifier algorithm that would be suitable for use in Minas Passage. That effort has generated a new python-based tool (i.e., 'FindPorpoises'; Figure 1) which recently underwent beta-testing and proved to be a valuable method for detecting harbour porpoise echolocation clicks in tidal channels dominated by noise contamination from flow and ambient noise. This new tool is also being paired with a streamlined analysis pipeline to generate standardized figures and tables for inclusion in quarterly and annual reports for regulators.

---

[21] These are available online at: https://oera.ca/research/pathway-program-towards-regulatory-certainty-instream-tidal-energy-projects
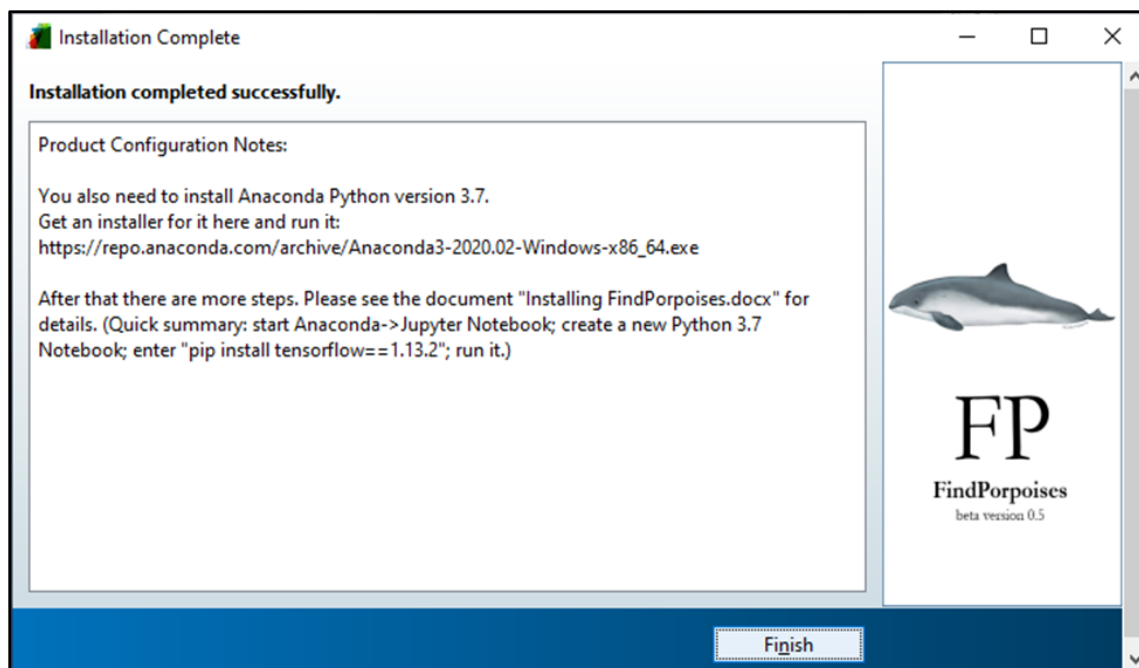
Figure 1: Screenshot from beta testing of the 'FindPorpoises' click detector and classifier tool.

Several projects were developed under Phase III (Technology Validation) of the Pathway Program, including a study to evaluate the performance of surface deployed and bottom-mounted multibeam imaging sonars (Gemini and Blueview). These were recently completed in Grand Passage by SOAR (Sustainable Oceans Applied Research), and the reports are available online[22]. For the surface deployment (see Appendix II), SOAR pole-mounted both imaging sonars from the side of a moored vessel and suspended a series of targets (i.e., tungsten carbide sphere, lead fishing weight, basalt rock and a V-wing glider) 2 metres below a surfboard. The targets were initially held in a fixed position but were also allowed to passively drift across the field of view to assess the ability of the imaging sonars to detect targets at increasing range. The V-wing glider was the largest target and was easiest for the Gemini and Blueview to detect, identify and track. Entrained air from turbulence, waves and the wake generated by the vessel and the pole-mount made tracking targets difficult. While both the Gemini and Blueview were useful for detecting targets, the Gemini performed better for average target detection and tracking at greater distances (10-50 m).

For the bottom-mounted assessment (see Appendix III), SOAR integrated the Gemini and Blueview imaging sonars into an autonomous subsea platform that was deployed at 25 m depth (at low water) in Grand Passage. Three targets (i.e., lead fishing weight, basalt rock and a V-wing glider) were suspended below a vessel that passively drifted through the ensonified areas of the imaging sonars. While insufficient data was collected by the Blueview due to its small ensonified area, the Gemini performed well for target detection, identification and tracking.

---

[22] These are available online at: https://oera.ca/research/pathway-program-towards-regulatory-certainty-instream-tidal-energy-projects

Moreover, there was no significant relationship between flow speed and the ability to track targets that were observed.

FORCE collaborated with Sustainable Marine and used the floating tidal energy platform (PLAT-I) deployed in Grand Passage, NS, to conduct four projects outlined in Phase III of the Pathway Program. Three of those projects focused on evaluating the utility of upwards and downward facing echosounders for quantifying biological targets in high flow environments (Figure 2). Those projects evaluated the performance of echosounders in bottom-mounted (upward facing) and surface (downward facing) deployments and used a suite of complementary technologies (optical cameras and imaging sonars) to investigate target detections. The report is provided herein at Appendix IV. While the upward facing echosounder detected targets that were consistent with the presence of fish in the upper water column, the optical camera failed to detect these targets, and the imaging sonar provided insufficient resolution to classify targets beyond ambiguous categories (e.g., 'single fish/debris' and 'turbulence/fish/fish school'). However, non-overlapping sample volumes likely contributed to the inability to cross-reference targets between the upward facing echosounder and the optical camera/imaging sonar, and these results should not be interpreted as an indication that cameras and imaging sonars are not useful monitoring tools; they have been used to good effect elsewhere.

Comparisons between the upward-facing and downward facing echosounder and the extent of signal interference from entrained air suggested a strong difference in the hydrodynamic regimes at the deployment locations of the instruments. Signal interference from turbulence and local hydrodynamics manifested in multiple ways: i) tide phase symmetry in the proportion of data excluded from analyses due to the persistence and depth penetration of entrained air, ii) a pronounced negative relationship between tidal flow speed and the proportion of useable data, and iii) a reduction in the proportion of useable observation periods with increasingly restrictive minimum acceptable proportions of useable water column. This interference had a direct influence on the proportion of useable data for hydroacoustic data analysis, and suggests that understanding the hydrodynamics of the deployment location for active acoustic instruments is an important component of establishing monitoring plans. However, the most relevant finding of this study is that the collection of *quantitative* (emphasis added) hydroacoustic data in tidal channels that is needed for estimating fish density, abundance and vertical distribution requires the use of a bottom-mounted, upward facing echosounder so that the acoustic signal does not get scattered by entrained air before encountering fish.

The fourth collaborative project with Sustainable Marine involved an assessment of the relative performance of PAM instruments for detecting synthetic harbour porpoise clicks in high flow environments using similar bottom mounted and surface deployed icListen hydrophones (Figure 3). The report is provided herein as Appendix V. While both hydrophones could detect synthetic harbour porpoise clicks, data from the surface deployed hydrophone contained audible interference from waves and the broadband, impulsive, bursting of bubbles associated with wave action that is difficult to distinguish from echolocation clicks. This ambient noise will negatively affect the use of automated harbour porpoise click detectors, could lead to increased false-positive detections, and could reduce the detection range of surface deployed hydrophones. Ultimately, the choice of which hydrophone to use and its deployment location depends on the monitoring question(s) being asked, and the results of this study did not provide sufficient evidence to strongly prefer one deployment location over the other.
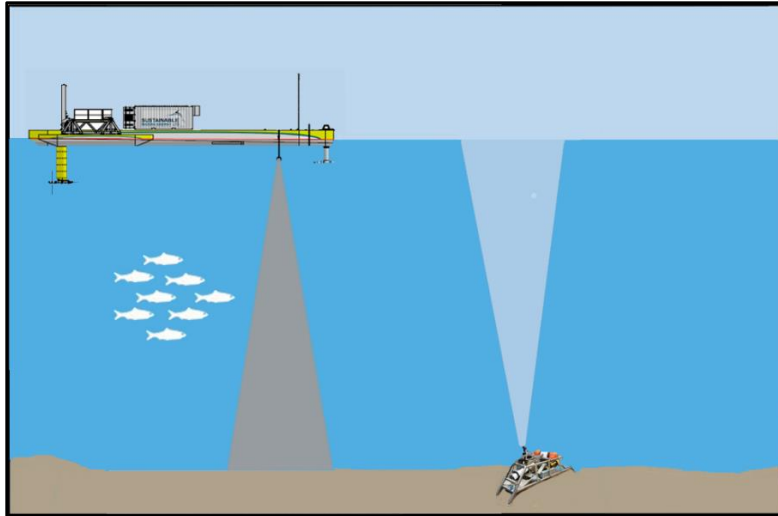
Figure 2: Schematic of the conceptual study design for an assessment of the relative performance of echosounders in bottom-deployments (FAST platform) surface deployments (PLAT-I). Shaded areas are intended for visualization purposes only, and do not accurately represent sample volumes.

Figure 3: Deployment of the FAST platform in Grand Passage for an assessment of PAM instrument performance.

The sensors being evaluated under the Pathway Program are being integrated onto a cabled FAST platform by DP Energy (Figure 4). The integrated sensor platform underwent a successful 'wet test' in Halifax Harbour in October 2020 and is planned to be deployed at the FORCE site in July 2021. The deployment is planned for two months, during which time

monitoring data will stream live to the FORCE visitor center, and provide data needed to validate new methods being developed to automate the detection, classification and tracking of targets observed using the Gemini imaging sonar. This effort is being led by SOAR under Phase II of the Pathway Program.

Figure 4: The integrated sensor platform developed by DP Energy under the Pathway Program.

Risk Assessment Program

The Risk Assessment Program (RAP) for instream tidal energy is a collaborative effort between FORCE, academic partners, First Nations, and industry to advance our understanding of the environmental risks of tidal stream development in Minas Passage. The greatest potential risk of tidal turbine operations continues to be perceived by regulators and stakeholders as collisions between marine animals and turbines blades (Copping and Hemery 2020). However, these types of interactions are difficult to observe directly due to the environmental conditions under which they would occur (i.e., fast flowing, turbid waters) and using the suite of environmental monitoring instrumentation currently available (i.e., standard oceanographic and remote sensing instruments intended for use in more benign marine conditions) (Hasselman et al. 2020), but can be modeled using appropriate baseline data. The objective of the RAP program is to develop statistically robust encounter rate models for migratory and resident fishes with tidal turbines in the Bay of Fundy using a combination of physical oceanographic data related to flow and turbulence in the Minas Passage and hydroacoustic tagging data for various fish species curated by the Ocean Tracking Network (OTN) at Dalhousie University.

Recent research has revealed how hydrodynamics (flow and turbulence-related features) in tidal stream environments can influence the distribution of marine animals, including fish (Lieber et al. 2018, 2019; McInturf et al. 2019). The Minas Passage is characterized by a series of turbulent hydrodynamics features (i.e., vortices, eddies, whirlpools, wakes, and shear currents) that could impact the spatiotemporal distribution of various fishes. The RAP will use a series of mobile ADCP transects combined with a high-resolution radar network to create the first spatiotemporal flow atlas of the Minas Passage to understand these hydrodynamic features. Concurrently, hydroacoustic data for various migratory and resident fish species in the Bay of Fundy that is curated by OTN will be compiled and analysed to understand their spatiotemporal distributions. The hydrodynamic and hydroacoustic data will then be combined with information

about turbine specific parameters (e.g., turbine blade length, swept area, turbine height off the seabed) to develop encounter rate models for various fish species. These models will then be refined and validated through a series of hydroacoustic tagging efforts, ultimately leading to the development of a user-friendly Graphical User Interface (GUI) similar to what is available for the offshore wind energy industry in the United Kingdom (McGregor et al. 2018). Ultimately, the RAP will contribute towards improving our understanding of the risks of instream tidal power development for fishes of commercial, cultural, and conservation importance in the Bay of Fundy, and will assist in the development of future environmental effects monitoring programs.

Since the program commenced in April 2020, OTN has acquired acoustic tag data from 22 contributors, covering nine species of fish in the Bay of Fundy (i.e., alewife (*Alosa pseudoharengus*), American shad (*A. sapidissima*), American eel (*Anguilla rostrata*), Atlantic salmon (*Salmo salar*), Atlantic sturgeon (*Acipenser oxyrhinchus oxyrhinchus*), Atlantic tomcod (*Microgadus tomcod*), spiny dogfish (*Squalus acanthias*), striped bass (*Morone saxatilis*), and white shark (*Carcharodon carcharias*)). FORCE has also established a high-resolution radar network in Minas Passage and has begun quantifying hydrodynamic features (turbulence, flow etc.) of Minas passage (Figure 5). The integration of physical habitat variables with acoustic tag data has commenced, model development for each species has begun, and species distribution maps are being created. The number of individuals per species to be tagged for validating model predictions has been determined, and the tagging program has commenced, with alewife and American shad already tagged and Atlantic sturgeon and spiny dogfish to be tagged later this summer (Figure 6). The acoustic receiver array (Figure 7) for detecting tagged fish was deployed in early June and will be recovered in late August to download data and replace receiver batteries and will then be redeployed to collect additional data.

Figure 5: One of two high-resolution radars constructed near the FORCE site to be used for the RAP program.

Figure 6: Acoustic tagging of alewife from the Avon River by RAP partner organization Mi'kmaw Conservation Group.
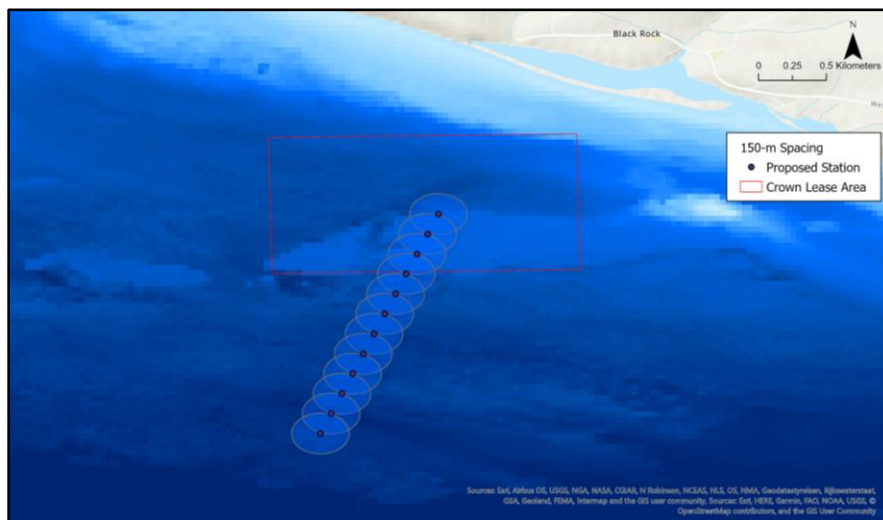
Figure 7: Acoustic receiver array deployment configuration in Minas Passage.

Fundy Advanced Sensor Technology (FAST) Activities

FORCE's Fundy Advanced Sensor Technology Program is designed to advance capabilities to monitor and characterize the FORCE site. Specifically, the FAST Program was designed to achieve the following objectives:

1) To advance capabilities of site characterization;
2) To develop and refine environmental monitoring standards and technologies; and
3) To enhance marine operating methodologies.

FAST combines both onshore and offshore monitoring assets. Onshore assets include a meteorological station, video cameras, an X-band radar system, and tide gauge. Offshore assets include modular subsea platforms for both autonomous and cabled data collection and a suite of instrumentation for a variety of research purposes. Real-time data collected through FAST assets is broadcasted live on the Ocean Networks Canada's (ONC; Victoria, BC) website.[23]

Platform Projects

The first and largest of the FAST platforms houses an instrument called the Vectron. Developed in partnership with Nortek Scientific (Halifax, NS), Memorial University (St. John's, NL), and Dalhousie University (Halifax, NS), the Vectron is the world's first stand-alone instrument to remotely measure, in high resolution, turbulence in the mid-water column. Measurements and analysis from the Vectron will help tidal energy companies to better design devices, plan marine operations, and characterize the tidal energy resource.

A smaller platform called FAST-3 was equipped with an upward looking echosounder and deployed during 2017-2018 to monitor fish densities at the FORCE site. FORCE and its partners, including Echoview Software completed data processing and analysis in 2019. This data was integrated with the mobile hydroacoustic surveys that FORCE conducts as part of its EEMP to evaluate the temporal and spatial representativeness of each method and to determine the degree to which results were corroborative (Figure 8). Although the spatial representative range of the stationary results could not be determined from the mobile data, it did reveal strong tidal and diel periods in fish density estimates at the site, with greater variation over shorter time frames than over the course of a year. These findings reinforce the importance of 24-hr data collection periods in ongoing monitoring efforts. The report reveals that collecting 24 hours of data allows the tidal and diel variability to be quantified and isolated from the longer-term trends in fish density and distribution that need to be monitored for testing the EA predictions. This project was funded by Natural Resources Canada (NRCan), the NSDEM, and the OERA.
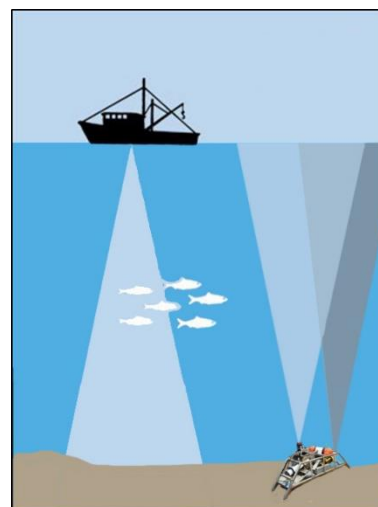
Figure 8: A representation of the data collection methods of the FORCE mid-field fish EEMP and the FAST-3 platform.

Fish Tracking

To enhance fish monitoring and to expand its data collection capacity, FORCE partnered with the Ocean Tracking Network (OTN)[24] and attached one VEMCO[25] fish tag receiver (a VR2 receiver) to each C-POD mooring/SUBS (Streamlined Underwater Buoyancy System) package (see above). These receivers are used to supplement OTN's ongoing data collection program within the Minas Passage and are referred to as 'Buoys of Opportunity.' Upon retrieval of the C-PODs and receivers, instruments are shared with OTN where data is offloaded prior to

---

[23] This is available online at: www.oceannetworks.ca/observatories/atlantic/bay-fundy

[24] Ocean Tracking Network's website: www.oceantrackingnetwork.org.

[25] VEMCO is "the world leader in the design and manufacture of acoustic telemetry equipment used by researchers worldwide to study behaviour and migration patterns of a wide variety of aquatic animals." Learn more: www.vemco.com.

redeployment. This effort will support increased knowledge of fish movement within the Minas Passage, which has applicability beyond tidal energy demonstration, as well as complement FORCE's hydroacoustic data collection efforts that do not allow for species identification.

OTN data managers are in the process of acquiring information, including species identification, and sharing this with FORCE. Initial results show that the OTN receivers deployed by FORCE have detected tags from the following projects:

- Maritimes Region Atlantic salmon marine survival and migration (Hardie, D.C., 2017);
- Quebec MDDEFP Atlantic Sturgeon Tagging (Verreault, G., Dussureault, J., 2013);
- Gulf of Maine Sturgeon (Zydlewski, G., Wippelhauser, G. Sulikowski, J., Kieffer, M., Kinnison, M., 2006);
- OTN Canada Atlantic Sturgeon Tracking (Dadswell, M., Litvak, M., Stokesbury, M., Bradford, R., Karsten, R., Redden, A., Sheng, J., Smith, P.C., 2010);
- Darren Porter Bay of Fundy Weir Fishing (Porter, D., Whoriskey, F., 2017);
- Movement patterns of American lobsters in the Minas Basin, Minas Passage, and Bay of Fundy Canada (2017);
- Shubenacadie River Monitoring Project: Tomcod (Marshall, J., Fleming, C., Hunt, A., and Beland, J., 2017);
- MA Marine Fisheries Shark Research Program (Skomal, G.B., Chisholm, J., 2009);
- UNB Atlantic Sturgeon and Striped Bass tracking (Curry, A., Linnansaari, T., Gautreau, M., 2010); and
- Inner Bay of Fundy Striped Bass (Bradford, R., LeBlanc, P., 2012).

- Minas Basin Salmon Kelt (McLean, M., Hardie, D., Reader, J., Stokesbury, M.J.W., 2019)

- New York Juvenile White Shark Study (Tobey Curtis)

Further information about these Buoys of Opportunity, and the projects listed above, can be found on OTN's website: https://members.oceantrack.org/project?ccode=BOOFORCE

Starting in 2018, FORCE has worked in collaboration with Dr. Mike Stokesbury at Acadia University to install additional VEMCO receivers of a new design on FORCE's C-POD moorings/SUBS packages. These new receivers are expected to be even more effective in picking up acoustic detections in high flow environments, where tag signals can be obscured by noise. This partnership will contribute additional information regarding movement patterns of Atlantic salmon, sturgeon, striped bass, and alewife in Minas Passage and Basin. This work is sponsored by the OERA, NRCan, NSDEM, the Natural Sciences and Engineering Research Council of Canada (NSERC), and the Canadian Foundation for Innovation (CFI).[26]

---

[26] Information about this project, and others funded through this program, is available online at: www.oera.ca/press-release-research-investments-in-nova-scotia-in-stream-tidal-technology-research/

Discussion

The year 2021 represents a strategic opportunity for FORCE and its partners to learn from previous experiences, incorporate regulatory advice, and to re-evaluate approaches to research and monitoring in the high flows of the Minas Passage. FORCE recently submitted its 2021-2023 proposed EEMP to regulators for review. The 2021-2023 EEMP is designed to prepare for effects testing with the deployment of operational turbines, and adheres to the principles of adaptive management by evaluating existing datasets to ensure appropriate monitoring approaches are being implemented. Moreover, the plan adopts internationally accepted standards for monitoring where possible, including feasibility assessments for new monitoring approaches that are planned to be implemented.

FORCE has also invested the development of its internal scientific capacity by hiring a PhD level hydroacoustician (Dr. Louise McGarry). This will assist FORCE with tackling the high volume of monitoring data that requires processing, analyses and integration with other data sets. Dr. McGarry will also assist with the development of study designs to help advance our understanding of how fish utilize the Minas Passage, and in transferring knowledge about hydroacoustics to less experienced staff.

While the 2020 COVID19 outbreak initially impacted our ability to gather data at our site and conduct marine operations – all of which require multiple people working in close proximity – our operations and monitoring data collection activities have resumed, and are following health guidelines to maintain social distancing and the wearing of face masks. As such, FORCE and its partners have resumed conducting monitoring, engaging in meaningful assessments of monitoring technology capabilities, and providing data analyses and interpretation that advance our ability to effectively monitor the effects of tidal turbines in high flow environments, and specifically at the FORCE test site. Reports from FORCE's partners and updates are routinely subjected to review by FORCE's EMAC and regulators, along with continued results from FORCE's ongoing monitoring efforts.

FORCE continues to implement lessons learned from the experiences of local and international partners, build local capacity and enhance skills development, test new sensor capabilities, and integrate results from various instruments. Cumulatively, these efforts provide an opportunity for adaptive management and the advancement and refinement of scientific approaches, tools, and techniques required for effectively monitoring the near- and mid-field areas of tidal stream energy devices in dynamic, high-flow marine environments.

Ongoing monitoring efforts will continue to build on the present body of knowledge of marine life-turbine interactions. While it is still early to draw conclusions, initial findings internationally and at the FORCE test site have documented some disturbance of marine mammals primarily during marine operations associated with turbine installation/removal activities, but otherwise have not observed significant effects.

FORCE will continue to conduct environmental research and monitoring to increase our understanding of the natural conditions within the Minas Passage and, when the next turbine(s) are deployed and operating, test the EA prediction that tidal energy is unlikely to cause significant harm to marine life. In the longer-term, monitoring will need to be conducted over the full seasonal cycle and in association with multiple different turbine technologies in order to understand if tidal energy can be a safe and responsibly produced energy source. FORCE will

continue to report on progress and release results and lessons learned in keeping with its mandate to inform decisions regarding future tidal energy projects.

References

AECOM. 2009. Environmental Assessment Registration Document - Fundy Tidal Energy Demonstration Project Volume I: Environmental Assessment. Available from Available at www.fundyforce.ca.

Copping, A.E. 2018. The State of knowledge for environmental effects - driving consenting/permitting for the marine renewable energy industry. Available from https://tethys.pnnl.gov/sites/default/files/publications/The State of Knowledge Driving Consenting Permiting for the MRE.pdf.

Copping, A.E., Hemery, L.G., and editors. 2020. OES-Environmental 2020 State of the Science Report: Environmental Effects of Marine Renewable Energy Development Around the World. Report for Ocean Energy Systems (OES). *In* State Sci. Rep. doi:10.2172/1632878.

Daroux, A., and Zydlewski, G. 2017. Marine fish monitoring program tidal energy demonstration site – Minas Passage. : 34. Orono, ME.

Envirosphere Consultants Ltd. 2017. Marine seabirds monitoring program – tidal energy demonstration site – Minas Passage, 2016-2017.

Fraser, S., Williamson, B.J., Nikora, V., and Scott, B.E. 2018. Fish distributions in a tidal channel indicate the behavioural impact of a marine renewable energy installation. Energy Reports **4**: 65–69. Elsevier Ltd. doi:10.1016/j.egyr.2018.01.008.

Gaskin, D.E. 1992. Status of the harbour porpoise, Phocoena phocoena, in Canada. Can. F. Nat. **106**(1): 36–54.

Gattuso, J.P., Magnan, A.K., Bopp, L., Cheung, W.W.L., Duarte, C.M., Hinkel, J., Mcleod, E., Micheli, F., Oschlies, A., Williamson, P., Billé, R., Chalastani, V.I., Gates, R.D., Irisson, J.O., Middelburg, J.J., Pörtner, H.O., and Rau, G.H. 2018. Ocean solutions to address climate change and its effects on marine ecosystems. Front. Mar. Sci. **5**(OCT). doi:10.3389/fmars.2018.00337.

Hasselman, D.J., Barclay, D.R., Cavagnaro, R., Chandler, C., Cotter, E., Gillespie, D.M., Hastie, G.D., Horne, J.K., Joslin, J., Long, C., McGarry, L.P., Mueller, R.P., Sparling, C.E., Williamson, B.J., and Staines, G.J. 2020. Environmental monitoring technologies and techniques for detecting interactions of marine animals with turbines. *In* Report for Ocean Energy Systems (OES).

International Electrotechnical Commission. 2019. Marine Energy - Wave, tidal and other water current converters - Part 40: Acoustic characterization of marine energy converter.

Joy, R., Robertson, F., and Tollit, D. 2017. FORCE Marine Mammal Environmental Effects Monitoing Program - 1st Year (2017) Monitoring Report.

Joy, R., Wood, J., and Tollit, D. 2018a. FORCE echolocating marine mammal environmental effects monitoring program - 2nd year (2018) monitoring report.

Joy, R., Wood, J.D., Sparling, C.E., Tollit, D.J., Copping, A.E., and McConnell, B.J. 2018b. Empirical measures of harbor seal behavior and avoidance of an operational tidal turbine. Mar. Pollut. Bull. **136**(July): 92–106. Elsevier. doi:10.1016/j.marpolbul.2018.08.052.

Lewis, A., Estefen, S., Huckerby, J., Musial, W., Pontes, T., and Torres-Martinez, J. 2011. Ocean Energy. *In* Renewable Energy Sources and Climate Change Mitigation: Special Report of the Intergovernmental Panel on Climate Change. *Edited by* O. Edenhofer, R. Pichs-Madruga, Y. Sokona, K. Seyboth, P. Matschoss, and S. Kadner. Cambridge University Press, Cambridge, Massachusetts. pp. 497–534.

Lieber, L., Nimmo-Smith, W.A.M., Waggitt, J.J., and Kregting, L. 2018. Fine-scale hydrodynamic metrics underlying predator occupancy patterns in tidal stream environments. Ecol. Indic. **94**(June): 397–408. Elsevier. doi:10.1016/j.ecolind.2018.06.071.

Lieber, L., Nimmo-Smith, W.A.M., Waggitt, J.J., and Kregting, L. 2019. Localised anthropogenic wake generates a predictable foraging hotspot for top predators. Commun. Biol. **2**(1): 12–

13. Springer US. doi:10.1038/s42003-019-0364-z.

Lossent, J., Lejart, M., Folegot, T., Clorennec, D., Di Iorio, L., and Gervaise, C. 2018. Underwater operational noise level emitted by a tidal current turbine and its potential impact on marine fauna. Mar. Pollut. Bull. **131**(May 2017): 323–334. Elsevier. doi:10.1016/j.marpolbul.2018.03.024.

Malinka, C.E., Gillespie, D.M., Macaulay, J.D.J., Joy, R., and Sparling, C.E. 2018. First in situ passive acoustic monitoring for marine mammals during operation of a tidal turbine in Ramsey Sound, Wales. Mar. Ecol. Prog. Ser. **590**: 247–266. doi:10.3354/meps12467.

Marine Renewables Canada. 2018. State of the Sector Report: Marine Renewable Energy in Canada.

Martin, B., Whitt, C., and Horwich, L. 2018. Acoustic data analysis of the OpenHydro opencentre turbine at FORCE: final report.

McGregor, R.M., King, S., Donovan, C.R., Caneco, B., and Webb, A. 2018. A Stochastic Collision Risk Model for Seabirds in Flight. Available from https://www2.gov.scot/Resource/0053/00536606.pdf.

McInturf, A.G., Steel, A.E., Buckhorn, M., Sandstrom, P., Slager, C.J., Fangue, N.A., Klimley, A.P., and Caillaud, D. 2019. Use of a hydrodynamic model to examine behavioral response of broadnose sevengill sharks (Notorynchus cepedianus) to estuarine tidal flow. Environ. Biol. Fishes **102**(9): 1149–1159. Environmental Biology of Fishes. doi:10.1007/s10641-019-00894-3.

Melvin, G.D., and Cochrane, N.A. 2014. Investigation of the vertical distribution, movement and abundance of fish in the vicinity of proposed tidal power energy conversion devices. Final Report for the Offshore Energy Research Association. Research Project 300-170-09-12.

NEXUS Coastal Resource Management Ltd. 2017. Lobster Catchability Study Report.

Palmer, K.J., Wood, J., and Tollit, D.J. 2021. FORCE Marine Mammal EEMP - Yer 4 Final Report.

Pine, M.K., Schmitt, P., Culloch, R.M., Lieber, L., and Kregting, L.T. 2019. Providing ecological context to anthropogenic subsea noise: Assessing listening space reductions of marine mammals from tidal energy devices. Renew. Sustain. Energy Rev. **103**(July 2018): 49–57. Elsevier Ltd. doi:10.1016/j.rser.2018.12.024.

Robertson, F., Wood, J., Joslin, J., Joy, R., and Polagye, B. 2018. Marine Mammal Behavioral Response to Tidal Turbine Sound. (206). doi:10.2172/1458457.

Schramm, M.P., Bevelhimer, M., and Scherelis, C. 2017. Effects of hydrokinetic turbine sound on the behavior of four species of fish within an experimental mesocosm. Fish. Res. **190**: 1–14. Elsevier B.V. doi:10.1016/j.fishres.2017.01.012.

SLR Consulting. 2015. Proposed Environmental Effects Monitoring Programs 2015-2020 for Fundy Ocean Research Center for Energy (FORCE).

Viehman, H., Hasselman, D., Boucher, T., Douglas, J., and Bennett, L. 2019. Integrating hydroacoustic approaches to predict fish interactions with in-stream tidal turbines.

Appendix I

FORCE Marine Mammal EEMP – Year 4
Final Report

Prepared for FORCE

[February 2021]

FORCE Marine Mammal EEMP – Year 4 Final Report

February 2021

Prepared by SMRU Consulting NA

Authors:
Kaitlin Palmer, PhD
Senior Acoustician

Jason Wood, PhD
Senior Research Scientist

Dominic Tollit, PhD
Senior Research Scientist

Executive Summary

The main objectives of FORCE's marine mammal Environental Effects Monitoring Program (EEMP) are to assess long-term effects of direct and indirect stressors on harbour porpoise (*Phocoena phocoena*) by monitoring their activity and site use, with the primary objectives to assess firstly, permanent avoidance of the mid field study area during turbine installation and operation and secondly, large magnitude (~50%) change in the distribution (echolocation activity levels) of a portion of the population in the study mid-field area (see SLR Consulting Ltd. 2015).

This final report provides summary data for the eleventh and twelfth deployment of C-PODs of FORCE's ongoing multi-year EEMP, representing the deployments of the fourth year of the EEMP. Data cover the period between August 2019 through September 2020. Results include data collected from five C-PODs representing a total of 1,043 days of monitoring of the FORCE site. There was at least one porpoise detection on all survey days throughout both deployments. The median number of porpoise positive minutes for the first deployment was 11, and 17 minutes for the second deployment. Both deployments experienced equipment malfunction with E1 failing to return data in October and November 2019 and D1 failing to return any incontestable data for the second deployment. Mean lost time due to sediment noise was 19.5% for the first deployment and 23.8% for the second deployment.

Table of Contents

List of Figures

List of Tables

1. Introduction and EEMP Objectives

Tidal energy is an excellent potential renewable energy source. Worldwide, only a small number of in-stream tidal turbines have been deployed to date. The Fundy Ocean Research Center for Energy (FORCE) is a Canadian non-profit institute that owns and operates a facility in the Bay of Fundy, Nova Scotia (Figure 1), where grid-connected tidal energy turbines can be tested and demonstrated. It enables developers, regulators and scientists to study the performance and interaction of tidal energy turbines with the environment. The offshore test site is in the Minas Passage area of the Bay of Fundy (Figure 2).
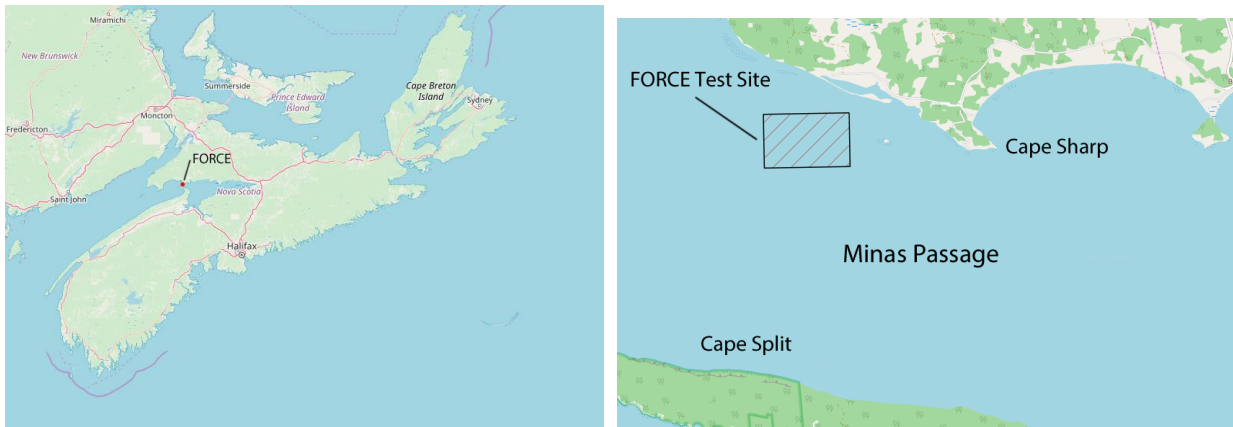

Figure 1: Regional location of FORCE test site. Figure 2: Detailed location in Minas Passage.

Harbour porpoise (*Phocoena phocoena*), the key marine mammal species in Minas Passage (Tollit et al. 2011; Wood et al. 2013; Porskamp et al. 2015), use high frequency echolocation clicks to hunt and communicate and are known to be very susceptible to pulsed noise disturbance (Tougaard et al. 2009), but few studies have focused on exposure to continuous low frequency noise sources, such as those emitted by tidal turbines.

This Year 4 Final Report describes the results of the overall Marine Mammal C-POD Monitoring Program. The program was put in place as part of FORCE's multi-year Environmental Effects Monitoring Program (EEMP) at its marine demonstration and testing facility in Minas Passage. Baseline C-POD monitoring has been ongoing since 2011 (see references above) and year 1, 2 and 3 EEMP results are documented in Joy et al. (2017, 2018) and Tollit et al. (2020).

The main objectives of the marine mammal EEMP are to assess long-term effects of direct and indirect stressors on harbour porpoise by monitoring porpoise activity and site use, with the primary objectives to assess: 1) Permanent avoidance of the mid field study area during turbine installation and operation. 2) Large magnitude (~50%) change in the distribution (echolocation activity levels) of a portion of the population in the study mid-field area (see SLR Consulting Ltd. (2015).

The location of the five C-POD monitoring sites relative to the turbine are found in Figure 3. This final report provides summary data for August 2019 to September 2020 deployment of 5 C-PODs as part of FORCE's continued EEMP.
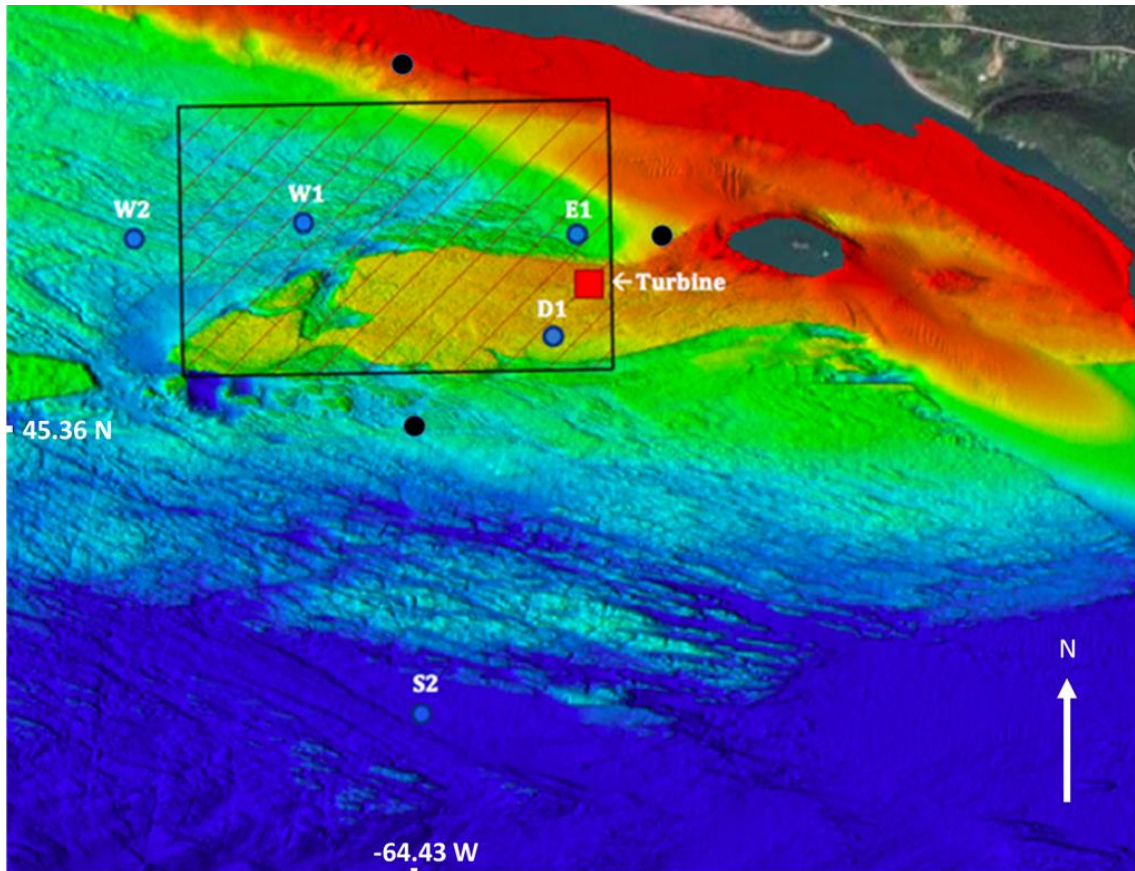
Figure 3: Locations of five monitoring C-PODs and CSTV turbine installed at Berth D. The hatched box denotes the FORCE demonstration area. Shallow water is depicted by warmer colours. C-POD locations are marked and labelled as E1 = East 1, D1 = Berth D, W1 = West1, W2 = West2 and S2 = South2. Locations of three previously used C-POD locations (N1, E2, S1; black circles) are provided.

2. Methods and Results

2.1. C-POD deployment and recovery information (conducted by FORCE field scientists)

Five C-PODS and associated moorings and buoys were deployed between June and August 2020. Each torpedo-shaped C-POD is approximately 1.21 m (4 ft.) long and approximately 40 cm (16") in diameter. Each C-POD is assembled into a "subs package" containing the acoustic release mechanism and recovery buoy. This is connected by a 2.5 m long chain to an anchor made of several lengths of chain (Figure 4).

Deployment of the C-PODs was completed by assembling each individual mooring on board the *Nova Endeavour*. The mooring was placed in the water over the stern, the anchor then raised with the capstan via the A-frame mounted on the stern, lifted clear of the deck, and pushed forward away from the vessel and deployed using a quick release when safe to do so, allowing the C-POD and mooring to free fall to the sea bottom. Five deployment locations were selected (Table 1) and are depicted in Figure 3 above. Depths ranged from 32-70 m. These locations were similar to previous deployments varying from the last reported by ~60m.

Where possible, the same C-POD units were deployed at the same locations. The exception being units 2790 and 2793 that were deployed at locations W1 and D1 respectively for the first data period and reversed for the second (Table 2)
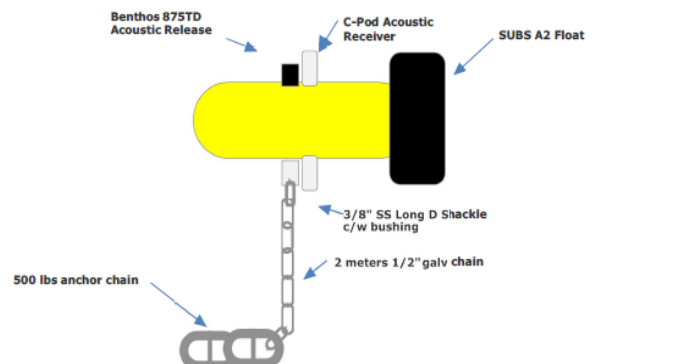

Figure 4: Diagram of FORCE C-POD mooring.

Table 1: Data summary for the two deployments during the year 4 EEMP. Gray shading for ease of use only. All dates and times are presented in UTC.

Location	Lat	Lon	Deployment Date		Retrieval Date		Data Start Date		Data Stop Date	
			Deployment 1	Deployment 2	Deployment 1	Deployment 2	Deployment 1	Deployment 2	Deployment 1	Deployment 2
W1	45' 21.973	-64' 26.074	2019-08-14	2020-06-12	2020-01-14	2020-11-06	2019-08-15	2020-06-13	2020-01-14	2020-09-05
E1	45' 21.984	-64' 25.988	2019-08-14	2020-06-12	2019-12-13	2020-11-06	2019-08-15	2020-06-13	2019-12-13	2020-09-13
W2	45' 21.960	-64' 26.596	2019-08-14	2020-06-12	2020-01-14	2020-11-08	2019-08-15	2020-06-13	2020-01-14	2020-09-30
D1	45' 21.765	-64' 25.424	2019-08-14	2020-06-12	2019-12-13	2020-09-23	2019-08-15	2020-08-13	2019-12-13	2020-09-23
S2	45' 21.008	-64' 25.777	2019-08-14	2020-06-12	2019-12-13	2020-11-06	2019-08-15	2020-06-13	2019-12-13	2020-09-29

Table 2: C-POD instrument number and data duration. Gray cells highlight locations where the instruments were switched between deployments.

Location	C-POD number		Data Duration (Days)	
	Deployment 1	Deployment 2	Deployment 1	Deployment 2
W1	2790	2793	151	85
E1	2765	2765	77	93
W2	2792	2792	152	110
D1	2793	2790	121	29
S2	2931	2931	116	109

2.2. C-POD Data QA

C-POD.exe V2.044 was used to process the data and extract narrow bandwith high frequency (NBHF) click trains representative of porpoises. Custom Matlab R2020b code was used to calculate statistical outputs and create data plots using detection positive minutes (DPM) per day and DPM per 10-minute period (DPMp10M) as the key metrics for comparison. Data were excluded from each C-POD for the first 12 hours after the reported deployment time and one hour prior to the recovery time. This pruning procedure reduced any disturbance or artifacts in the data resulting from deploying and recovering the instruments.

The QA assessment specifically targets if non-biological interference has occurred, confirms that the porpoise click detector is operational and assesses the scale of % time lost due to click maximum buffer exceedance. Buffer exceedance occurs when noise generated from sediment movement and moorings exceeds internal memory of the C-POD and results in periods of lost recording time in each minute.

The instrument deployed at D1 ostensibly collected data from the deployment on June 12 until recovery on September 23, 2020. At around 02:30, the instrument appears to have become lodged in a horizontal position and ceased collecting data. The C-PODs have an on/off switch that can be controlled by their internal tilt meter. If the unit were stuck on its side or upside down, it would have stopped recording until the unit was upright again. The unit deployed at D1 was recovered September 23rd and the remainder of the instruments recorded continuously until either internal storage or battery capacity was exhausted. The data that were collected at D1 do not match up with known deployment dates and appear to show no time lost due to sediment interference which is unlikely. For this reason, we recommend that any statistical modeling of trends in porpoise detections (e.g. Wood et al. 2013) exclude data from the second the D1 deployment. For consistency with previous reports, we report the number the number of days this instrument was in the water but exclude it from any statistical calculations .

2.3. Porpoise click detection rates

2.3.1. Overall summary of detection rates

Across all years of the Minas Passage C-POD monitoring study, there have been a total of 7,581 C-POD days over 1,888 calendar days, with a total of over one million 10-minute periods (Table 3). This final report covers 110 calendar days, 426 C-POD days with a total of 60,842 10-minute periods (Table 3).

Porpoises were detected on 100% of days across all pods combined, with an overall average median of 17 minutes per day, and with the probability of presence detected in 5.64% of all 10-minute periods across this monitoring period. This later statistic (termed 'PBinDPM=1' within Joy et al. 2018) is considered the optimal comparative metric to assess potential effects, as mean values are skewed by the number of periods without detection. Across individual C-PODs, detection rates averaged 93.4% of days with a C-POD median DPM per day of 17 minutes (IQR =

10-24) when presence occurred (Table 4). The DPM value is similar to the previous recording period but the average detection rate across C-PODs was lower.

No dolphin clicks were detected in Minas Passage during this C-POD monitoring period, as also found during previous deployments (Wood et al. 2013; Joy et al. 2017, 2018).

Table 3: Definitions of deployment scenarios and associated summary of C-POD monitoring effort, turbine status, and EEMP details. The turbine operational period is highlighted in bold.

Deployment Scenario and Turbine Status	Deployment Dates	# of Days Monitored	# of Pod-Days	# 10-Min Intervals
2011 Deployment: Absent	2011-05-05 - 2012-01-17	258	958	136,446
2012 Deployment: Absent	2012-05-31 - 2012-12-03	137	391	56,795
2014 Deployment: Absent	2013-12-06 - 2014-07-01	208	689	99,108
2016 Deployment 1: Absent	2016-06-08 - 2016-08-30	84	252	35,775
2016 Deployment 2: Absent	2016-09-23 - 2016-11-06	45	225	32,065
*2016 Deployment 2: Turbine 1 Operational	**2016-11-07 - 2017-01-18**	**73**	**332**	**47,403**
*2017 Deployment 3: Turbine 1 Operational	**2017-02-24 - 2017-04-21**	**57**	**262**	**37,229**
2017 Deployment 3: Turbine 1 Free-spinning	*2017-04-22 - 2017-06-01*	41	146	20,756
2017 Deployment 4: Turbine 1 Free-spinning	*2017-06-03 - 2017-06-15*	13	39	5,382
2017 Deployment 4: Turbine 1 Absent	*2017-06-16 - 2017-09-14*	91	357	51,009
2017 Deployment 5: Turbine 1 Absent	*2017-09-27 - 2018-01-08*	104	520	74,135
2018 Deployment 6: Turbine 1 Absent	*2018-01-23 - 2018-05-18*	99	480	68,094
*2018 Deployment 7: **Turbine 2 operational or free-spinning 07-22 to 08-09**, then present (non-operational/non-free-spinning)	2018-05-05 - 2018-08-23	111	542	77,419
2018 Deployment 8: Turbine 2 Present, non-operational/non-free-spinning	2018-09-07 - 2018-11-30	85	367	51,722
2018 Deployment 9: Turbine 2 Present, non-operational/non-free-spinning	2018-12-07 - 2019-04-02	117	453	64,418

2019 Deployment 10: Turbine 2 Present, non-operational/non-free-spinning	2019-05-04 - 2019-08-14	103	506	72,090
2019 Deployment 11: Turbine 2 Present, non-operational/non-free-spinning	2019-08-14 - 2019-12-13	152	636	90,600
2020 Deployment 12: Turbine 2 Present, non-operational/non-free-spinning	2020-06-12- 2020-09-05	111	426	62,392
All Deployment data		**1,888**	**7,581**	**1,082,838**

Table 4: FORCE site monitoring summary: Percent of days (across all deployment locations) with high or moderate quality porpoise detections present. Mean percent of days (between deployment locations) with 'NBHF' detections. Number of days without porpoise detection and the median number of detection-positive minutes for days/units with detections.

Deployment Scenario and Turbine Status	Overall % Days Porpoise Present	% Days Across C-PODs Porpoise present	Days Without Porpoise (Days Monitored)	Median (IQR) of Minutes of Detection if Present
2011 Deployment: Absent	99.2	83.2	2 (258)	7 (2, 17)
2012 Deployment: Absent	95.6	82.9	6 (137)	5 (1, 13)
2014 Deployment: Absent	99.0	87.5	2 (208)	9 (3, 16)
2016 Deployment 1: Absent	98.8	92.5	1 (84)	7 (3.75, 14)
2016 Deployment 2: Absent	100.0	76.4	0 (45)	4 (1, 10)
2016 Deployment 2: Operational	**97.3**	**73.8**	**2 (73)**	**3 (0, 7)**
2017 Deployment 3: Operational	**100.0**	**92.4**	**0 (57)**	**7 (3, 14.75)**
2017 Deployment 3: Free-spinning	100.0	95.2	0 (41)	7 (4, 12)
2017 Deployment 4: Free-spinning	100.0	100	0 (13)	12 (7, 18.5)
2017 Deployment 4: Absent	100.0	96.9	0 (91)	12 (6, 21)
2017 Deployment 5: Absent	100.0	88.3	0 (104)	8 (2.75, 20)
2018 Deployment 6: Absent	100.0	88.3	0 (99)	7 (2, 16)
2018 Deployment 7: Present from 2018-07-22, unknown status	100.0	98.0	0(111)	12 (6, 20)
2018 Deployment 8: Turbine 2 Present, non-operational/non-free-spinning	98.8	84.7	1(85)	5 (1.5, 11)
2018 Deployment 9: Turbine 2 Present, non-operational/non-free-spinning	94.9	88.1	6(117)	7 (3, 19)
2019 Deployment 10: Turbine 2 Present, non-operational/non-free-spinning	100.0	99.8	0(103)	15 (8, 24)

2019 Deployment 11: Turbine 2 Present, non-operational/non-free-spinning	100.0	91.04	0(152)	11(5, 19.5)
2020 Deployment 12: Turbine 2 Present, non-operational/non-free-spinning	100.0	93.4	0(110)	17(10,24)
All Deployment data	**99.08**	**89.6**	**20(1888)**	**7(3, 16.5)**

2.3.2. C-POD location detection rates

Porpoise detections rates varied across locations. Table 5 provides summary of percent probability of detecting a porpoise in a 10-minute interval for both deployments. For the second deployment, E1 and S2 sites had the highest detection rates. The sum of daily detection positive minutes averaged below five minutes for W2 and D1 sites, however, D1 did not produce data for the majority of the study and the data it did produce appear to be spurious.

Table 5: Descriptive statistics for the 5 C-POD locations for the 4th year of EEMP. Percent probability (95% CI) of detecting a porpoise in a 10-minute Interval (P(BinDPM=1). Orange highlighted cells indicate non or inconsistent data recovery.

Location number	Deployment 1		Deployment 2	
	Means (95%.C.I.)	# 10-minute Intervals	Means (95%.C.I.)	# 10-minute Intervals
W1	3.87 (2.24 - 14.83)	10,760	6.8 (6.16 – 16.23)	12,139
E1	4.74 (3.47 - 14.58)	21,750	8.12(7.41 – 20.95)	13,369
W2	9.02 (6.25 - 25.56)	16,558	4.86 (4.16 – 11.11)	15,751
D1	3.3 (2.78 - 8.66)	17,241	0.47 (0 – 7.07)	4,032
S2	4.25 (3.47 - 12.64)	21,518	7.87 (7.63 – 13.73)	15,551

Data inspection indicated mid-June through October for the four functioning deployment locations (excepting D1). For the final deployment mean % time lost was 23.9%, with median of 0% and interquartile range of 0-52% (Figure 5).
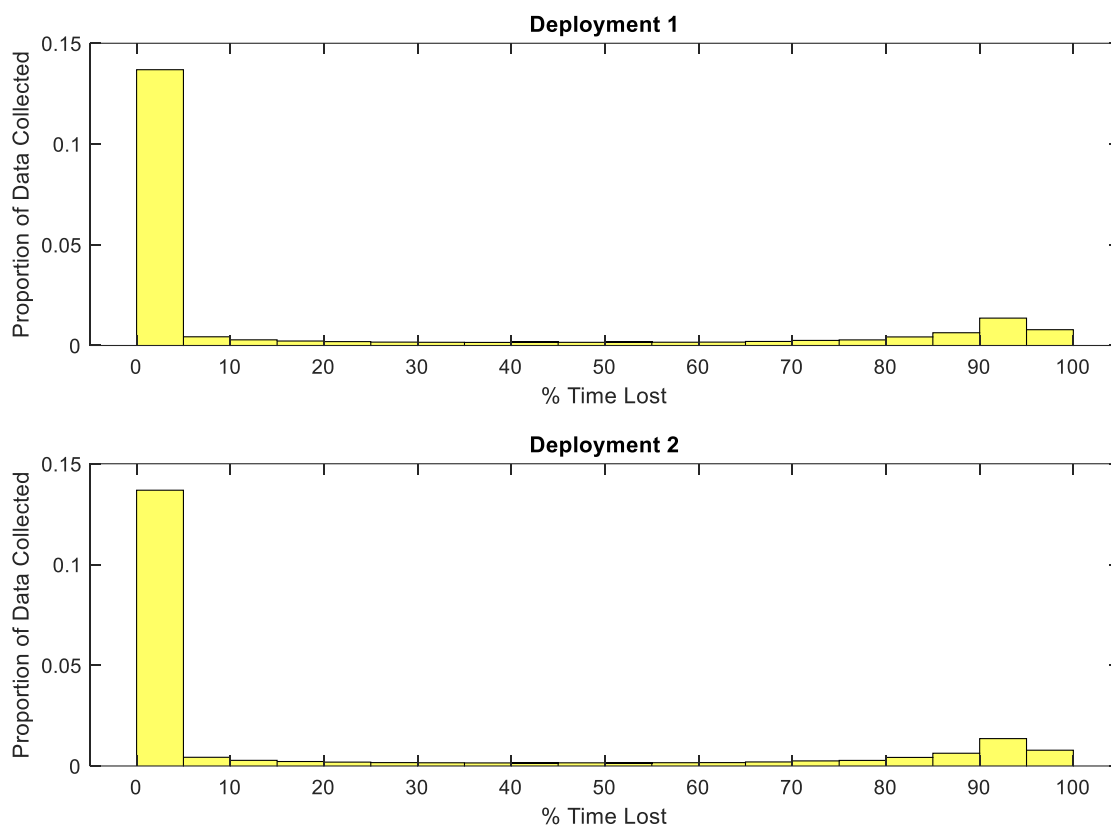
Figure 5: Distribution of time lost across the two year 5 deployments.

2.3.3. Temporal Trends in Detections

As with previous years, there was a seasonal trend in detections. However, the data gap between January and July across all sites and site-specific data failures preclude robust statistical analysis of seasonal trends. At the W2 deployment location there was considerably less variation in the average number of detection positive minutes per day in the second deployment than the first. There similarly appeared to be fluctuations in total detection positive 10 minute periods per day consistent with lunar cycles with peaks occurring every 30 days (Figure 6). This is most evident in W1 and W2 locations during the first deployment. The same trend was visible in the daily average proportion of time lost (Figure 7).
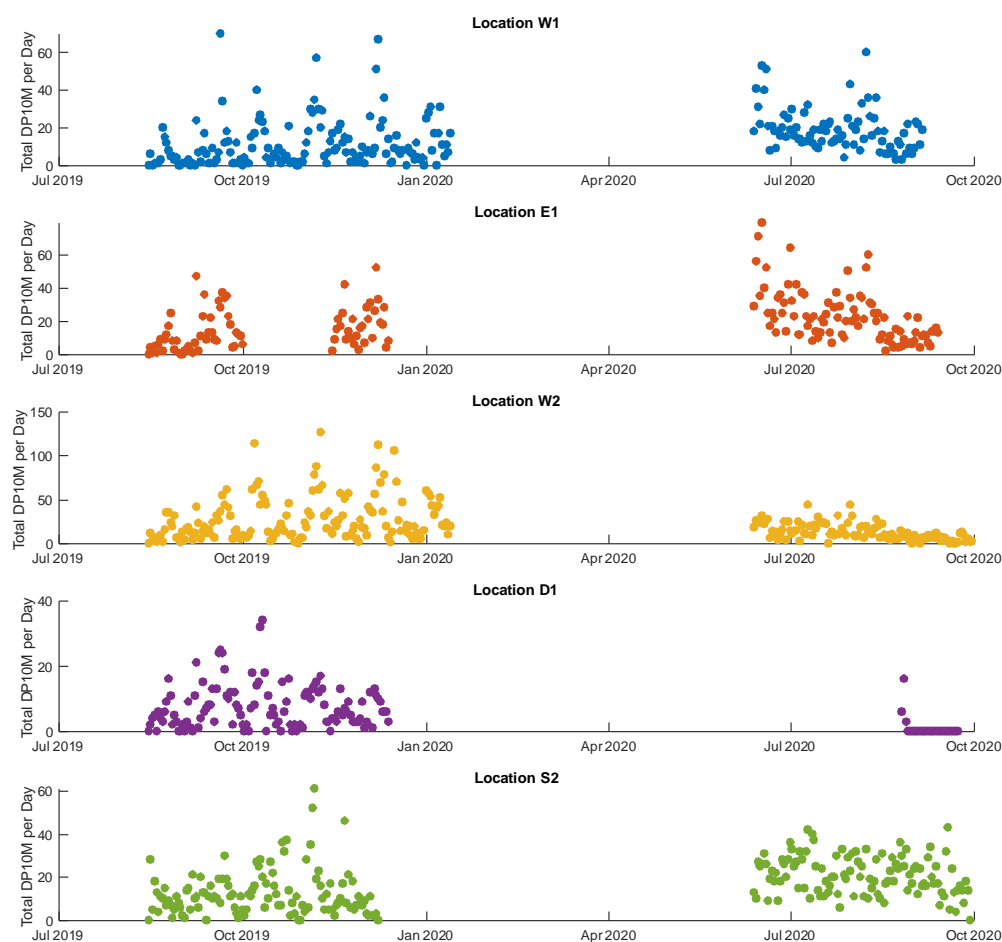
Figure 6: Total detection positive 10 minute periods throughout the year 4 EEMP. Data points prior to January represent the first deployment and data points after June 2020 represent the second deployment. C-PODS were not deployed between these periods due to the impact of COVID-19 on marine operations during winter and spring 2020.
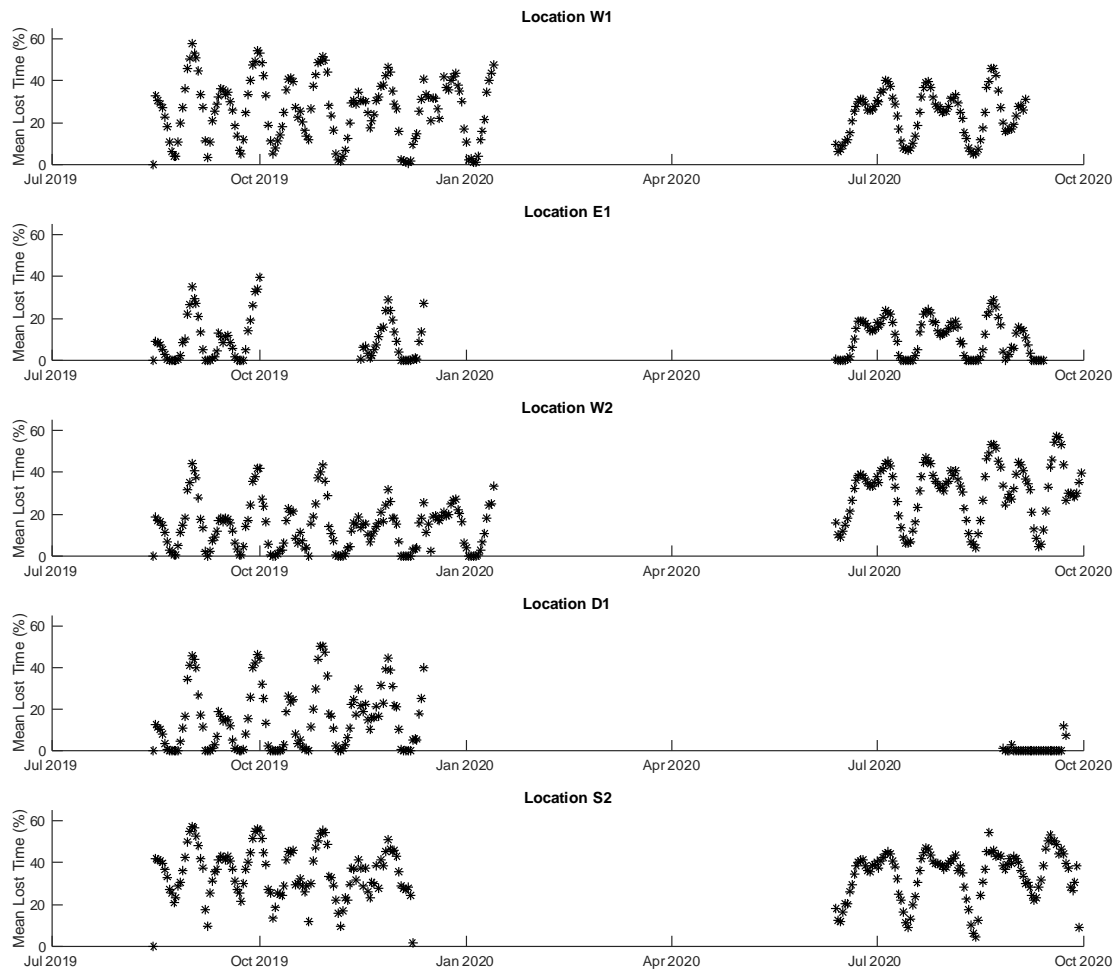
Figure 7: Average time lost per day for the fourth year of the EEMP. Tidal cycles are evident at all locations.

There was some evidence of diel trends in detection at the W1 and E1 sites and to a lesser degree the W2 site. At these locations there were fewer detection positive minutes during daylight hours (between 0500 and 1800) than in the evening hours (Figure 8). This trend was not present in the winter nor at the remaining three sites.

Deployment 1
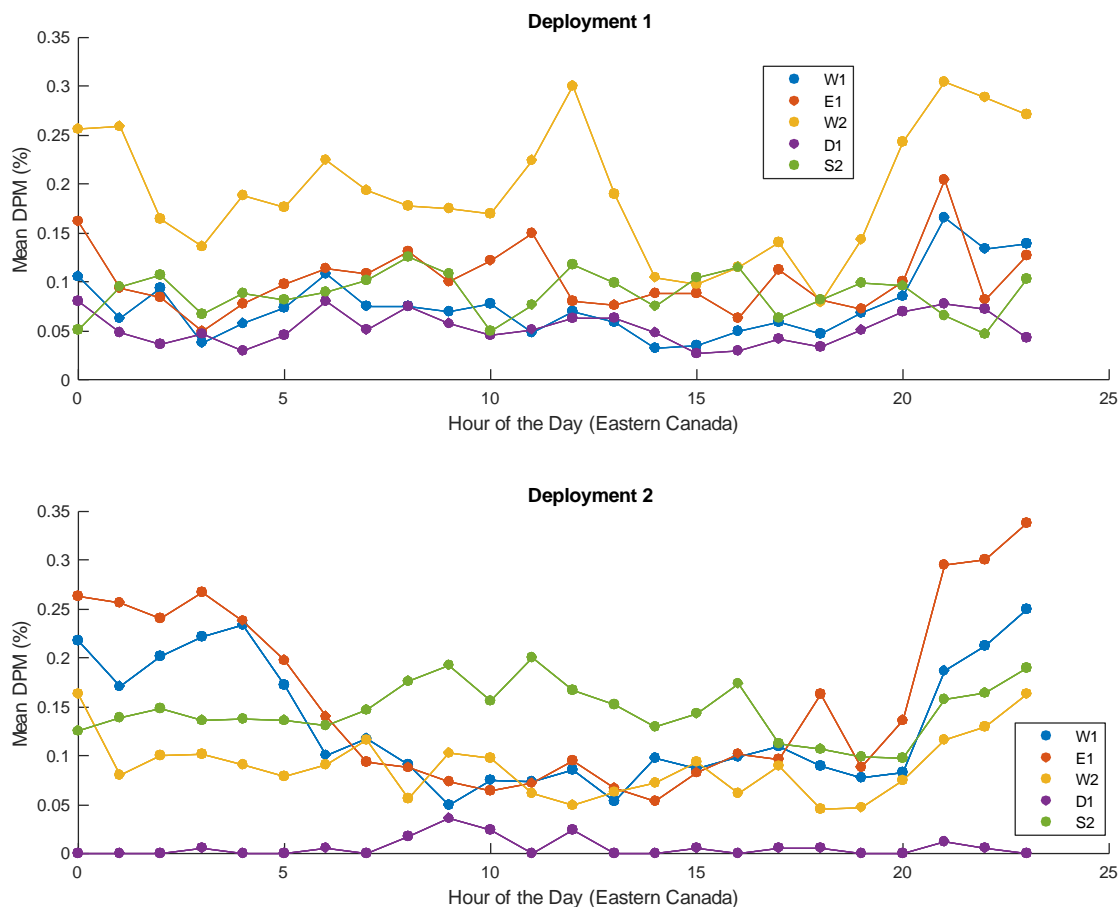
Deployment 2

Figure 8: Relationship between the daily mean precent of time lost and the total detection positive 10-minute periods per day.

2.3.4 Comparison of year 4 EEMP porpoise detection rates with previous C-POD deployments

In year four of the monitoring effort there were no operational turbines deployed at the FORCE site. The percent probability of detecting a harbour porpoise in a 10-minute interval (P(BinDPM=1) at each C-POD deployment location was calculated for each period (Figure 9, top panel). Seasonal and site-specific trends in the detection probabilities are visible. The probability of detecting potential porpoise clicks was highest at the W2 site in the first deployment. In the second deployment, average detection rates were similar to previous deployments and years with the exception of 2016 where detection positive days for were considerably lower for the entirety of the survey period than subsequent years.
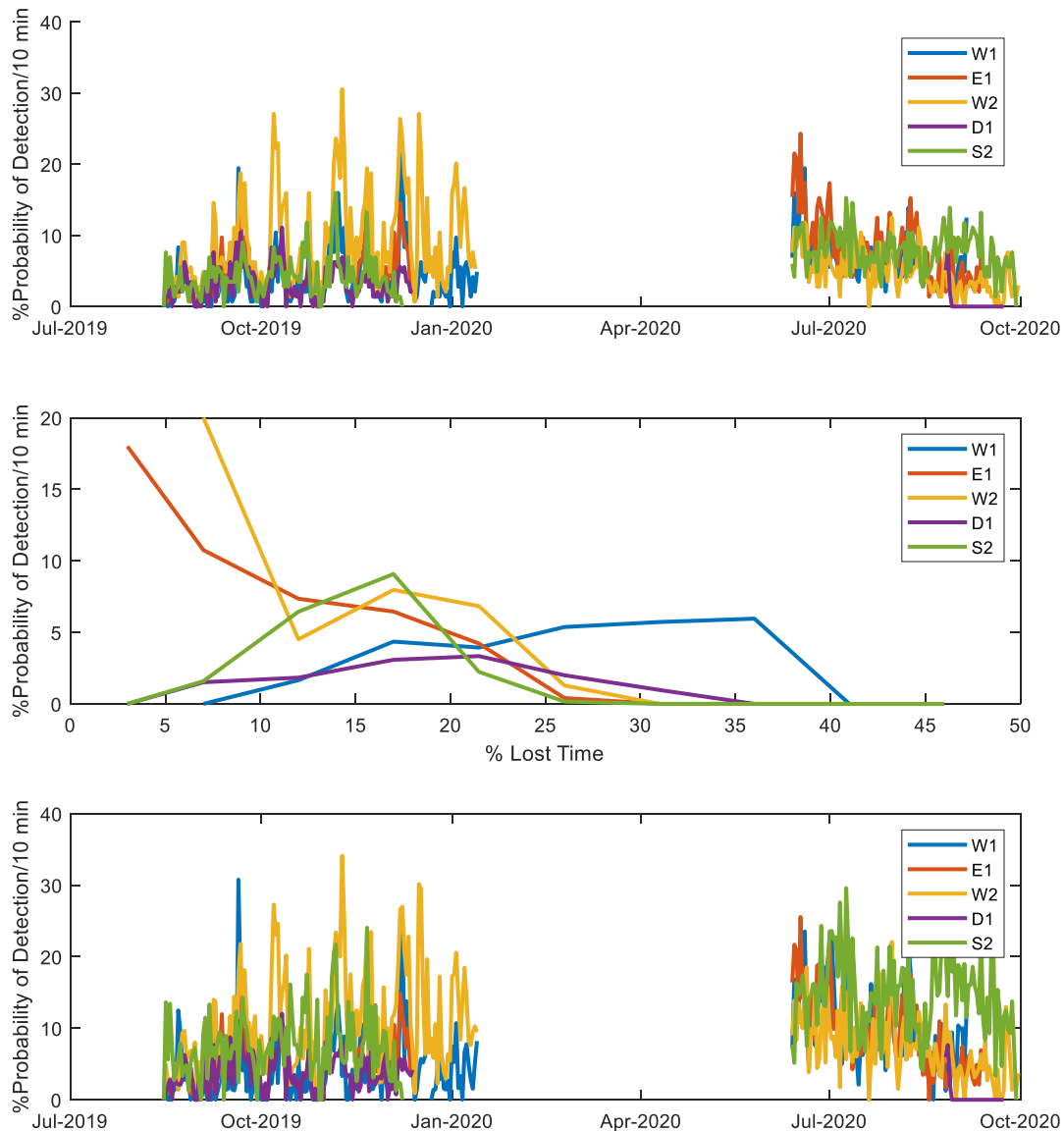
Figure 9: Percent probability of detecting a porpoise in a 10-minute Interval (P(BinDPM=1) at each C-POD monitoring location for year 4 of the EEMP. Top panel; probability of detection at each location throughout the season. Middle panel: the relationship between detection probability and time lost. Bottom panel: Probability of detection for only data where no time was lost.

The relationship between detection probability and time lost was also calculated and is shown in the middle panel of Figure 10. Again, there were site specific trends across the five survey locations. W2 had the strongest relationship between detection probability and the proportion of time lost. W1 showed a likely spurious positive relationship between detection probability and time lost, with more detections occurring with 35% of time lost than 15%. The third panel shows the probability of detection for each site through the deployments, excluding any periods where any time was lost. The general trends shown in the bottom panel are relatively consistent with those from the raw data (top panel).

3. Discussion

Five C-PODs were successfully deployed and recovered in Minas Passage as part of FORCE's marine mammal EEMP. Four C-PODs returned good quality and continuous data in each deployment while two instruments failed to return data (D1 in the first deployment and E1 in the second deployment). For the D1 instrument, inspection of the vertical angle data exceeded 90° for at least 300 minutes but this is insufficient to explain the duration of the data gap. We recommend that both instruments 2765 and 2790 be refurbished by the manufacturer.

Average percent time lost due to sediment noise interference (23.9%) was similar to previous studies at these locations. Across all years of the Minas Passage C-POD monitoring study, there have been a total of 7,581 C-POD days across 1,888 calendar days, with a total of 1,082,838 10-minute periods.

In this last period, across all C-PODs, harbour porpoise were detected across 93.4% of monitored days, and at higher rates than have previously been observed (17 min/day). No dolphins were detected as per previous baseline studies. Differences across deployment locations mirrored previous results.

The relationship between detection probability and the proportion of lost time was also investigated. The trend was again, location dependent but on average no porpoise click trains were detected in each 10-minute monitoring period where the proportion of lost time was greater than 50%.

As with previous studies the fairly convincing diel trend was found in the second deployment of the FORCE array (Tollit, Joy et al. 2019). Such trends can be indicative of animal behavior by providing insights beyond presence-absence. In Scotland, differing diel trends in porpoise detections have been linked to sediment type and tentatively linked to different foraging strategies. Ongoing evaluation of these trends, when operational turbines are deployed may also yield information regarding behavioral changes associated with turbine operations. Such analyses have the potential to be more informative and robust than simple presence-absence given the complexities in processing C-POD data in a tidal environment. Trend analysis allows for variation in measuring efficacy between instruments by considering only the relative probabilities between time and locations. For instance, if a diurnal trend is observed in one location prior to the turbine activation and detection rates remain constant but the diel trend

changes, it could be indicative of a change in behavior (e.g., more or less foraging activity) during turbine operation. Furthermore, if the C-PODs are replaced with F-PODs, direct 1:1 comparison of DPM may not be possible. However, trends in small scale tidal and diel-linked patterns should be comparable between the instruments.

To date, we consider a sufficiently long timeline of C-POD baseline data has been collected to meet the goals of the FORCE EEMP. Optimally, additional baseline data collection would allow an improved understanding of natural variability and/or detect changing regional trends. However, until operational turbines are deployed at the FORCE tidal demonstration site, an adaptive management approach might be adopted, whereby baseline studies are curtailed, scaled back to every other year or potentially (to meet DFO expectations) continued at one single long-term monitoring site such as at W1.

References

Joy, R., Wood, J., Robertson, F. and Tollit D. (2017). Force Marine Mammal Environmental Effects Monitoring Program – 1st Year (2017) Monitoring Report. Prepared by SMRU Consulting (Canada) on behalf of FORCE, May 1, 2017.

Joy, R., Wood, J., and Tollit D. (2018). FORCE Echolocating Marine Mammal Environmental Effects Monitoring Program – 2nd Year (2018) Monitoring Report. Prepared by SMRU Consulting (Canada) on behalf of FORCE, December 9, 2018.

Porskamp, P, A. Redden, J. Broome, B. Sanderson and J. Wood. (2015). Assessing marine mammal presence in and near the FORCE Lease Area during winter and early spring – addressing baseline data gaps and sensor performance. Final Report to the Offshore Energy Research Association and Fundy Ocean Research Center for Energy.

SLR Consulting Ltd. (2015). Proposed Environmental Effects Monitoring Program for 2015 -2020 Fundy Ocean Research Center for Energy (FORCE).

Tollit, D., J. Wood, J. Broome and A. Redden (2011). Detection of Marine Mammals and Effects Monitoring at the NSPI (OpenHydro) Turbine Site in the Minas Passage during 2010. Publication No. 101 of the Acadia Centre for Estuarine Research (ACER) Acadia University, Wolfville, NS, Canada prepared for Fundy Ocean Research Centre for Energy (FORCE). FORCE: Fundy Ocean Research Center for Energy. 2011. Environmental Effects Monitoring Report, September 2009 to January 2011. Appendix D.

Tollit, D., et al. (2019). "Baseline Presence of and Effects of Tidal Turbine Installation and Operations on Harbor Porpoise in Minas Passage, Bay of Fundy, Canada." Journal of Ocean Technology 14.

Tougaard, J., Carstensen, J., Teilmann, J., Skov, H., & Rasmussen, P. (2009). Pile driving zone of responsiveness extends beyond 20 km for harbor porpoises (Phocoena phocoena (L.)). The Journal of the Acoustical Society of America, 126(1), 11–14. doi:10.1121/1.3132523.

Wood, J., D. Tollit, A. Redden, P. Porskamp, J. Broome, L. Fogarty, C. Booth and R. Karsten (2013). Passive Acoustic Monitoring of Cetacean Activity Patterns and Movements in Minas Passage: Pre-Turbine Baseline Conditions (2011-2012). SMRU Consulting and ACER collaborative report prepared for Fundy Ocean Research Center for Energy (FORCE) and the Offshore Energy Research Association of Nova Scotia (OERANS). FORCE: Fundy Ocean Research Center for Energy. 2015. Environmental Effects Monitoring Report, 2011 to 2013. Appendix C.

Appendix II

OERA Pathway 2020 Program

Field Assessment of Multi-beam Sonar Performance in Surface Deployments

OERA Project number: 200-216

February 1, 2021

Project Lead: SOAR – Sustainable Oceans Applied Research Ltd.

By: Greg Trowse, Dr. Tristan Guest, Gavin Feiel, Richard Cheel, and Dr. Alex Hay

Executive Summary

Multibeam imaging sonars have application to monitoring fish and marine mammal presence and behaviours in the near field of tidal turbine installations, including evaluating avoidance, evasion, and potential blade strikes.   SOAR conducted field experiments to help reduce uncertainty in performance of the Tritech Gemini 720is and Teledyne Blueview M900-2250 multibeam imaging sonars for identifying and tracking discrete targets in high-flow environments.   This information will help inform the Department of Fisheries and Oceans Canada, tidal energy developers, and other stakeholders in the design and implementation of effective monitoring systems for tidal energy projects in the Bay of Fundy and beyond.   These two imaging sonars were the technologies recommended for testing by the subject matter expert for imaging sonars during the first phase (Global Capability Assessment) of the Pathway Program. The Tritech Gemini 720is operates at 720 kHz and has a maximum effective sampling range of approximately 50 m. The Teledyne Blueview M900-2250 has operating frequencies of 900 or 2250 kHz, with a 10 m range for the high frequency transducer head.   As per the recommendation from the Global Capability Assessment, this report focuses on the Blueview's capabilities while operating at 2250 kHz, for which the effective sampling range is 10 m.

Field trials were conducted in Grand Passage aboard research vessel Grand Adventure.   The two sonars and a camera were mounted on a pole which could be lowered over the vessel's port side and fixed in position.   The deployed sonars were oriented such that the top of their ensonified areas extended behind the boat approximately parallel with the water surface and extended downward at a 20 degree angle.   The Grand Adventure was anchored in mid-channel during ebb and flood tide flow conditions, such that current velocities ranged from approximately 1 to 2.5 m/s with the instruments oriented downstream.   Targets were suspended approximately 2 m beneath a 3 m long surfboard (SciBoard) and included a 2.54 cm (1 inch) diameter tungsten carbide sphere, 0.45 kg (1 lb.) (9.5 cm long x 3.8 cm max diameter) lead fishing weight, approx. 12 cm diameter basalt rock in a lobster bait bag, and a V-Wing glider (approx. 52 cm wing tip to tip and 46 cm nose to tail) from Dartmouth Ocean Technologies.   During data collection the SciBoard and suspended target were held at constant ranges from the sonars along the port side and downstream of the Grand Adventure, and also released to freely drift downstream with increasing range.

The visualization and organization of the data was conducted using the industry standard software for each sonar: Gemini SeaTec and Teledyne ProViewer.   Data were exported to

video and organized into training and test data sets, which were shared with 9 sonar observers who conducted the manual analysis for target detection, identification, and tracking. Links to the training and test data sets for each sonar are provided below. The data are best viewed in video form. As such, readers of this report are encouraged to watch these data videos for better understanding of the results and conclusions discussed in this report.

Gemini training data	https://vimeo.com/473580369
Gemini test data with 50m range	https://vimeo.com/473665614
Gemini test data with 10m range	https://vimeo.com/473688042
Blueview training data	https://vimeo.com/473964794
Blueview test data	https://vimeo.com/474025663

The Gemini 720is and Blueview M900-2250 multibeam imaging sonars were both found to be useful for detection and tracking of all target sizes used in our experimentation. However, differentiation of similar targets such as the 2.54 cm (1 inch) tungsten carbide sphere (Target 1) and 0.45 kg (1 lb.) lead fishing weight (Target 2) proved difficult. The sonars performed best for detecting, identifying, and tracking the V-Wing. This is an expected result as it was the largest target and had the most recognizable backscatter signature due to its characteristic shape. Entrained air from turbulence, waves, and the vessel/pole wake made tracking targets more difficult, but target persistence allowed them to be effectively detected and tracked by eye for all target types tested.

SOAR recommends use of the Tritech Gemini 720is for application to monitoring interactions between marine animals and tidal turbines.   With the 10 m range setting, the Gemini demonstrated comparable ability to the Blueview to identify targets and outperformed the Blueview in average target detection and tracking scores. At 50 m range, the Gemini still demonstrated a high level of utility for target detection, tracking, and presence/absence, though was less effective (ca. 50%) for target identification.   It is likely that this technology will contribute significantly to effective monitoring and advancing knowledge of importance to regulators and other stakeholders. The Blueview M900-2250 was included in testing due to its higher frequency output, which is better suited for close range target detection and tracking. The Blueview is an impressive technology and offered the ability to resolve finer scale features of the targets and their movements in some cases. However, the MKI model of the Blueview M900-2250 has a hardware limitation which results in multiple high-noise bands in the output

data, which limited our ability to detect and track targets considerably. We conclude that data from the Blueview did not add substantial value or insight to the target analysis when used in conjunction with the Gemini. This should not rule out potential use of other MHz frequency multibeam sonars for monitoring the 10 m range in a combined sonar approach, including MKII of the Blueview.

We evaluated the effects of acoustic interference (cross talk) between the Gemini and Blueview based on the ability of manual observers to detect, track, and identify targets through repeat collections of data with the sonars running both concurrently and independently. In general, the acoustic interference can be described as distracting, but tolerable. We observed no relationship between flow speed and observers' abilities to detect and track targets with testing up to approximately 2.5 m/s. Tidal flows are faster at the FORCE site in the Minas Passage, with flow speeds exceeding 2.5 m/s 30 to 40% of the time.

The project addressed the objective of assessing the performance of surface deployed multibeam imaging sonars for target detections, including the extent of signal interference from waves/turbulence, and entrained air. Further testing of and research into multibeam sonar usage from a vessel mounted (near surface) position would be useful in four focus areas, including:

1) fish and other marine animals in locations and seasons (times) with high levels of animal abundance and variety,
2) evaluating the most effective sonar orientations for monitoring the near field of tidal turbines,
3) flow speeds that exceed 3 m/s, and
4) increasing efficiency in data assessment, including reliable automation.

This work should build upon success in Grand Passage to conduct next steps in stronger flow conditions present in Petit Passage and Minas Passage. The report titled "Field Assessment of Multi-beam Sonar Performance in Bottom Mount Deployments" (Trowse et al. 2020) provides similar analysis for the case of seabed mounted Gemini 720is and Blueview M900-2250, including comparison of results and further recommendations for next steps.

Table of Contents

List of Figures

List of Tables

Acknowledgments

SOAR thanks the following support organizations and supply chain who helped us deliver on this work:

- Offshore Energy Research Association of Nova Scotia
- Natural Resources Canada
- Dalhousie Ocean Acoustics Laboratory
- Villages of Westport, Freeport, and Tiverton
- Clare Machine Works
- Luna Sea Solutions
- MarineSitu
- Mi'kmaw Conservation Group
- Fundy Ocean Research Centre for Energy (a.k.a. FORCE)
- Dasco Equipment Inc.
- Tritech and Teledyne technical support staff
- Canadian Hydrokinetic Turbine Test Centre

1.0   Introduction

Multibeam imaging sonars have application to monitoring fish and marine mammal presence and behaviours in the near-field of tidal turbine installations, including evaluating avoidance, evasion, and potential blade strikes (Hastie 2013; Viehman and Zydlewski 2014; Bevelhimer et al. 2016; Williamson et al. 2016, 2017; Sanderson et al. 2019). However, there is uncertainty in performance of these instruments in high-flow environments due to turbulence and associated entrained air in the water column, where a reduction in instrument efficacy may result from scattering of the transmitted acoustic signal through turbulent zones of the water column before the signal reaches potential targets, with further signal dilution on the return to the transducer (Melvin and Cochrane 2014). Some additional challenges include a) mounting sonars at sufficient depth in high-flow environments to avoid acoustic returns from the surface (horizontal sonar orientation) and reduce exposure to entrained air, and b) transferring, storing, and efficiently analyzing large amounts of data.

Several makes and models of multibeam imaging sonars are available, with a major source of difference being the frequency at which they transmit acoustic energy. Higher frequencies are associated with shorter wavelengths; this results in resolution increasing with frequency, and range decreasing with increasing frequency. The combined use of kHz and MHz frequency range multi-beam imaging sonars is of interest for monitoring marine animals because it offers potential for an instrument package to detect and track targets at ranges up to approximately 50 m with identification (and/or finer scale tracking) of targets at a range up to approximately 10 m. For environments with suitable visibility, the addition of an optical camera offers increased potential for target identification, target validation, and tracking at ranges of approximately 0.1 to 15 m in very clear waters.

As part of the Pathway Program, SOAR conducted work to help evaluate the performance of the Tritech Gemini 720is and Teledyne Blueview M900-2250 (2.25 MHz transducer head) multibeam imaging sonars for evaluating interactions between marine animals and tidal turbines. This information will help inform the Department of Fisheries and Oceans Canada (DFO), tidal energy developers, and other stakeholders in the design and implementation of effective monitoring systems for tidal energy projects in the Bay of Fundy and beyond.

The Tritech Gemini 720is multibeam imaging sonar has been used by MCT Seagen in Strangford Lough (Hastie 2013), OpenHydro at the Fundy Ocean Research Centre for Energy (FORCE) (Viehman et al. 2017), and other applications including studies commissioned by FORCE (Gnann 2017). With an operating frequency centered at 720 kHz, the Gemini has a target detection range of up to 100 m (Cotter, et al. 2017) but has reduced resolution in comparison to higher frequency systems. The dual frequency Teledyne Blueview M900-2250 has two sets of transducers, one set centered at 900 kHz (close to the Gemini) and the other set at 2250 kHz (2.25 MHz). Use of the Blueview 2.25 MHz transducer head may have application in shorter range monitoring, up to approximately 10 m (Cotter et al. 2017). These two imaging sonars are the technologies recommended for testing by the subject matter expert for imaging sonars during the first phase (Global Capability Assessment) of the Pathway Program (Joslin 2019).

SOAR's work in 2020 has included data collection and analysis from near surface (vessel mounted) and seabed deployments.   This report covers the methodology and results for the vessel mounted experiment. "Field Assessment of Multi-beam Sonar Performance in Bottom Mount Deployments" (Trowse et al. 2020) discusses the seabed deployment and a comparison of results for the two approaches.

The **objective** of the work covered in this report is to assess the performance of surface deployed multibeam imaging sonars for target detections, including the extent of signal interference from waves/turbulence, and entrained air.

The **expected outcomes** include**:**
- Primary - Report on performance of surface deployed multibeam imaging sonars for target detections, and a recommendation on whether the use of surface deployed multibeam imaging sonars is feasible for monitoring interactions between marine animals and tidal turbines.
- Secondary - Data sets to support further research (beyond the scope and timeline of this project) including potential for calibration of multibeam imaging sonars, quantification of the effects of air entrainment on target detectability, and autodetection and classification algorithms (software).

2.0   Methodology

The methodology was developed to evaluate the performance of two multibeam imaging sonars when deployed near surface on a downward-oriented vessel mounted pole, including the Tritech Gemini 720is (Gemini) and the dual frequency Teledyne Blueview M900-2250 MKI (Blueview). The Gemini has 512 beams aligned along a 120° swath width (angular resolution of 0.25°), with each beam having a 20° width perpendicular to the swath.   The Blueview has 768 beams aligned along a 130° swath width (angular resolution of 0.18°), with each beam having a 20° width perpendicular to the swath.   Multibeam sonars resolve target locations as range along each beam.   The resulting composite (by combining all beams) is used to generate a sonogram with target locations in the swath width but does not resolve target location in the beam width. For this experiment, the sonars were both aligned such that field of view had swath width on the horizontal plane (parallel to water surface) and beam width on the vertical plane (depth).   The acoustic frequency and geometry of the ensonified area for each sonar is summarized in Table 1. The Subaqua SAIS IP Cam (optical camera) was also included for target verification, and to demonstrate ability for targets to be identified optically.

Table 1: Multibeam imaging sonar frequency and ensonified area

Sonar	Frequency (kHz)	Range (m)	Swath width	Beam width
Gemini	720	120 [1]	120°	20°
Blueview	900 or 2250[2]	10	130°	20°

Notes:

- The Tritech supplied specifications for the Gemini report a max range of 120 m, however the maximum effective range for monitoring marine animals in tidal channels is 50 to 60 m.
- The Blueview is dual frequency, with two transducer heads. Our work focused on the high frequency capabilities with the 2250 kHz (2.25 MHz) transducers, and associated range of 10 m.   For brevity, ongoing reference to the Blueview in this report implies the high frequency transducer head.
- Both sonars transmit a "chirp" pulse that spans a range of frequencies, centered at the values listed above.

2.1 Data Collection

2.1.1 Method

An initial experiment was conducted in Freeport Harbour to a) evaluate potential interference between the Gemini and Blueview sonars in a controlled setting, b) test and refine the mounting arrangement and sonar angles, and c) evaluate various instrument configuration settings and how they affect the image quality. This was followed by a system test in tidal flow in Grand Passage to confirm the pole mount and anchor function, and the main field trials which were also conducted in Grand Passage.

The work was conducted aboard research vessel Grand Adventure, using a stand-alone power supply for the sonars, displays, and data acquisition computers. The Grand Adventure has an inboard diesel main propulsion system, backup outboard engine, and hydraulics for boom/winch and hauler/davit lifting systems. She is shown in Figure 1 in Westport Harbour fully outfitted for this work. The interior of the wheelhouse with sonar displays is shown in Figure 2 (photo taken during data collection in Grand Passage).

Figure 1: Research vessel Grand Adventure in Westport Harbour outfitted for work
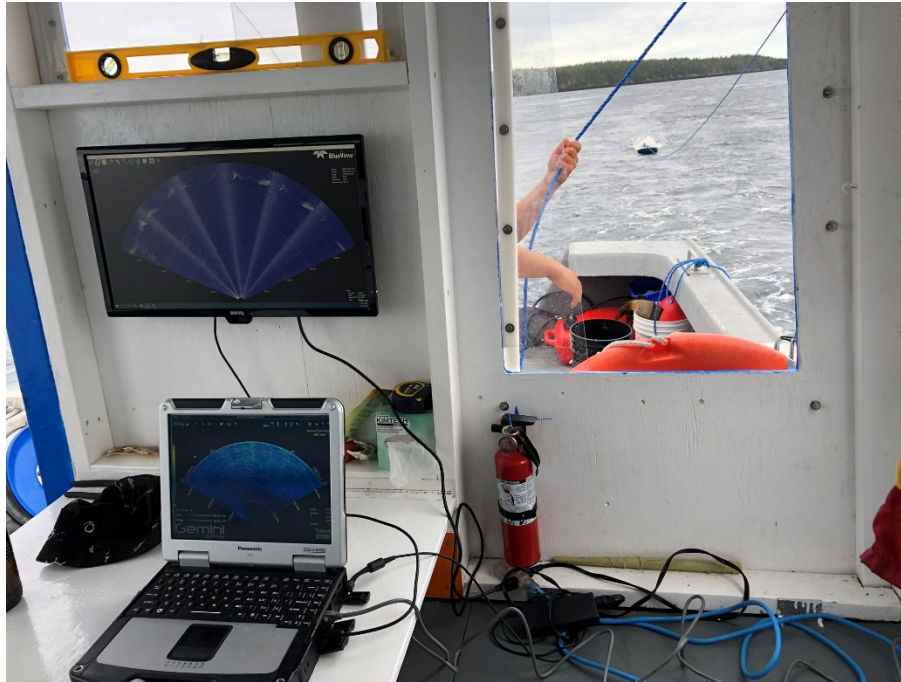
Figure 2: Data display and collection on research vessel Grand Adventure

The sonars and camera were mounted on a pole which could be lowered over the vessel's port side and fixed in position as shown in Figure 3. In the deployed position, the instruments were submerged to a depth of approximately 1 m. The deployed sonars were oriented such the that top of the ensonified area extended behind the boat approximately parallel with the water surface and extended downward at the 20 degree angle of the beam spread for both sonars. During the principle data collection periods, the Grand Adventure was anchored in mid-channel during ebb and flood tide flow conditions, such that current velocities ranged from approximately 1 to 2.5 m/s with the instruments oriented downstream. Targets were suspended approximately 2 m beneath a 3 m long surfboard (the SciBoard) outfitted with towing and instrument attachment points for use as a towed platform. The targets could then be introduced to the ensonified area by towing the SciBoard a known distance behind the Grand Adventure. This placed targets in the upper portion of the ensonified area that was also most susceptible to wake and wave related air entrainment. The targets' proximity to the sea surface was required in order for them to be ensonified while close to the sonars. The SciBoard and experiment setup are shown in Figures 4 and 5. The targets, shown in Figure 6, included a 2.54 cm (1 inch) diameter tungsten carbide sphere (Target 1), 0.45 kg (1 lb.) (9.5 cm long x 3.8 cm max diameter) lead fishing weight (Target 2), approx. 12 cm diameter basalt rock in a lobster bait bag (Target 3), and a V-Wing glider (Target 4) (approx. 52 cm wing tip to tip and 46 cm nose to tail) from Dartmouth Ocean Technologies (DOT). Targets 1, 2, and 3 were suspended from the

SciBoard using a combination of 40 pound and 200 pound test monofilament fishing line. Target 4 was suspended using 1/4 inch Polysteel fishing line due to the increased downward force, increased cost of the target (reducing risk of loss), and ease of handling. The V-Wing is designed to create downforce and maintain orientation in flow, with approximately (27 kg) 60 lbs. of downforce in 2.5 m/s flow. No metal was included in the target suspension system. Knots were used to secure the targets with no hooks, shackles, etc. below the water line.
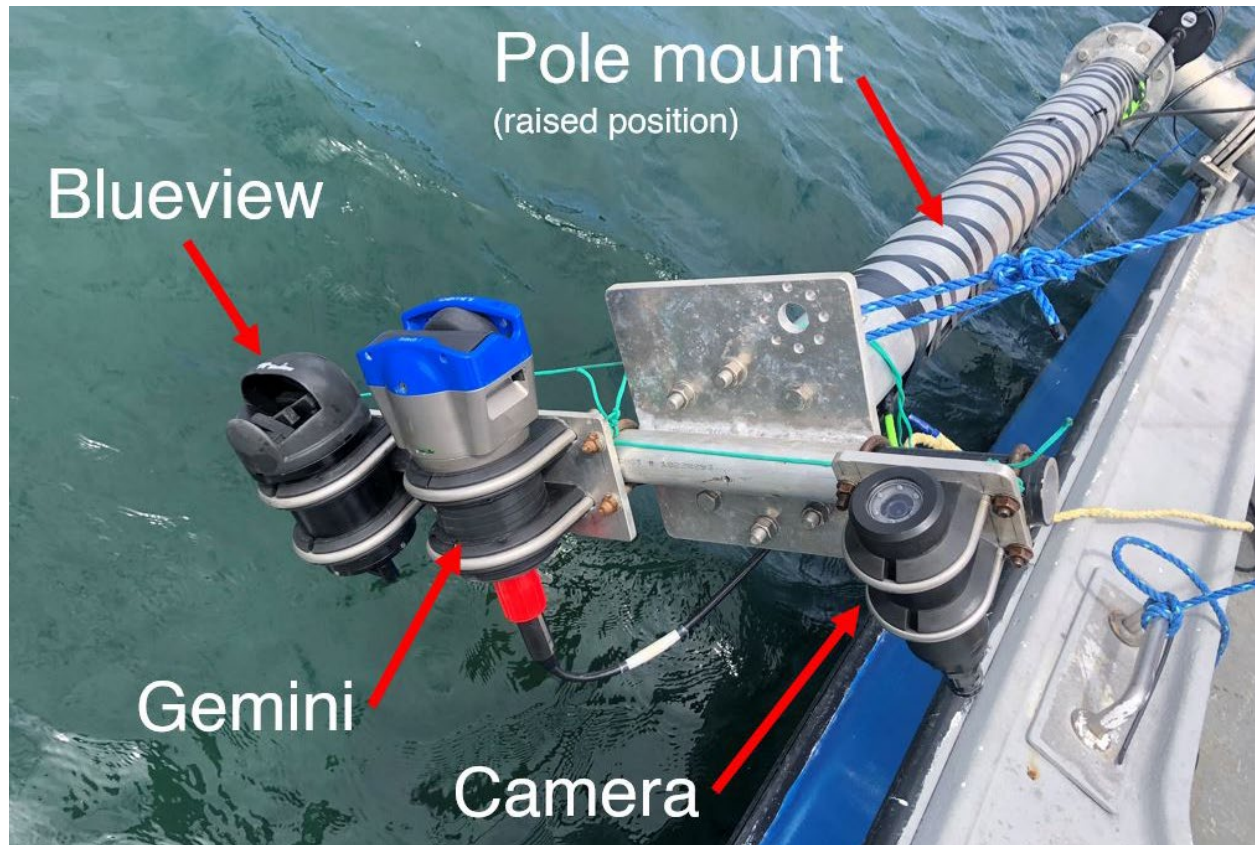
Figure 3: Pole mounted sonars and camera

Figure 4: SciBoard
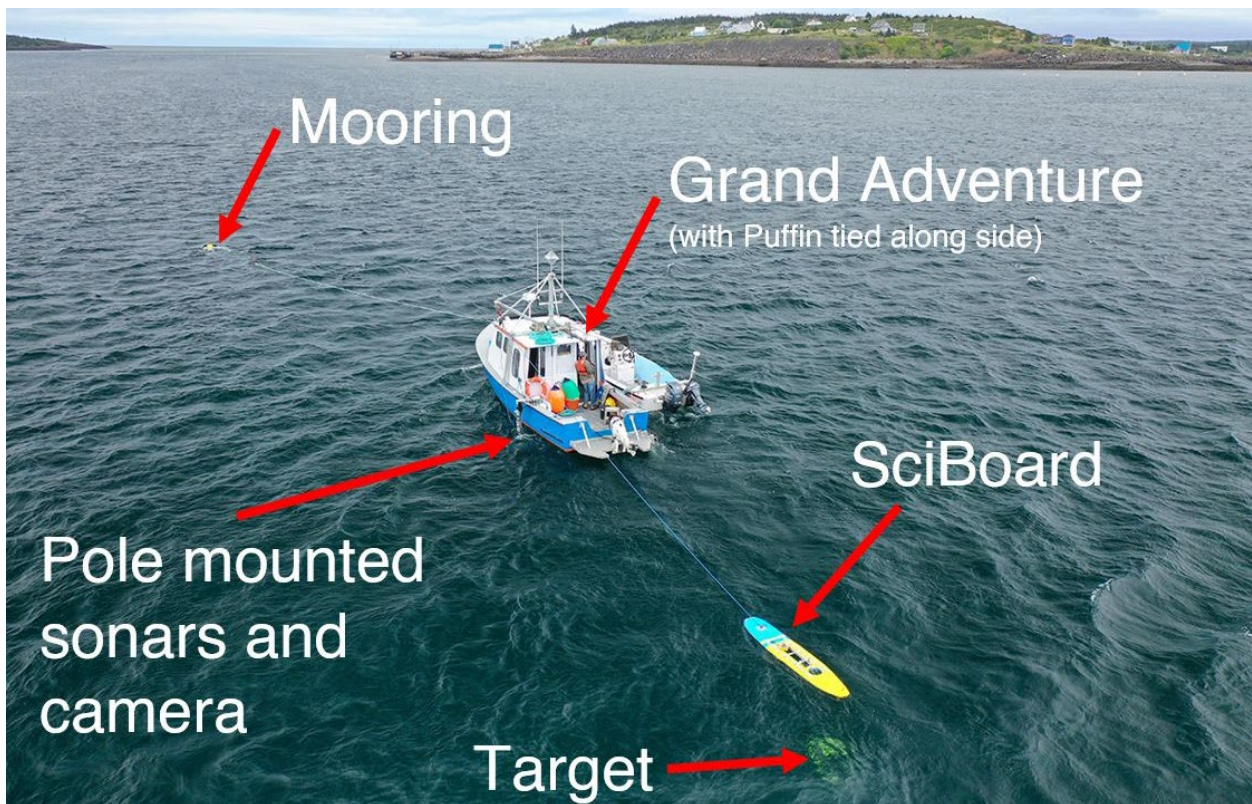
Figure 5: Aerial image of experiment layout
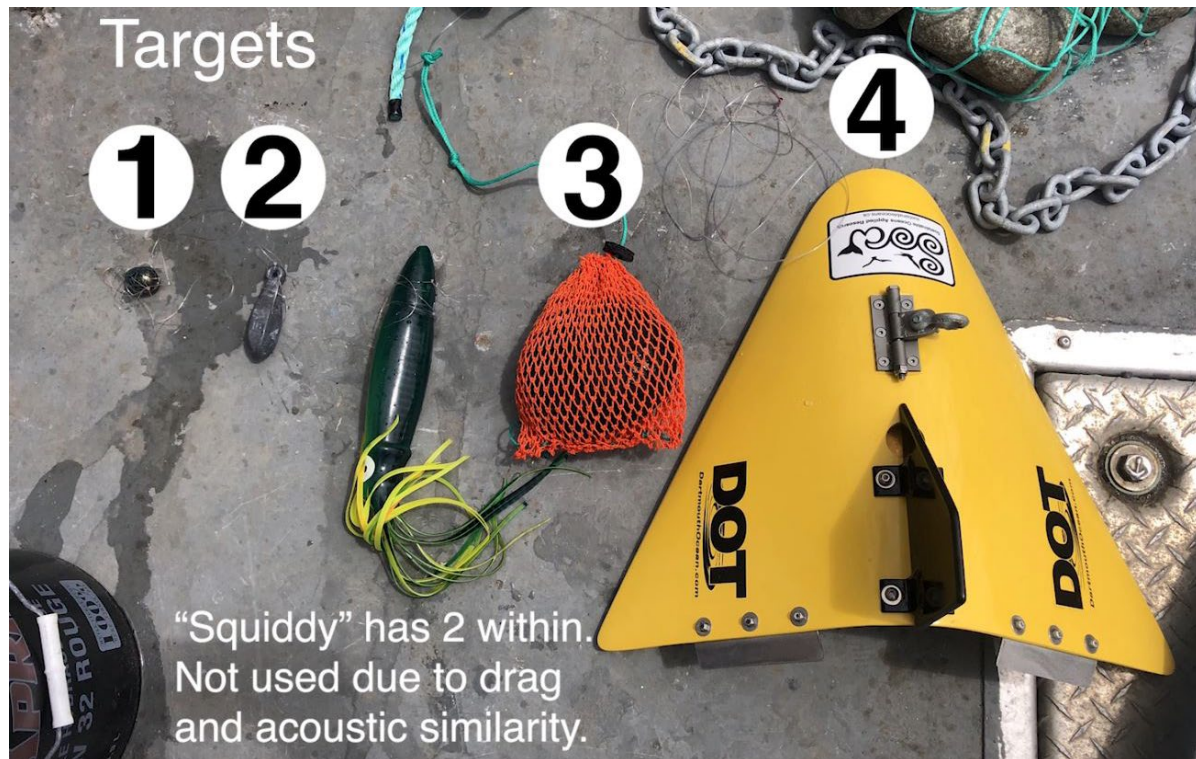
Figure 6: Targets

During data collection the SciBoard and suspended target were held at constant ranges from the sonars along the port side and downstream of the Grand Adventure, and also released to freely drift downstream with increasing range. Holding targets at a constant range had the advantage of allowing plumes of entrained air (bubbles) to pass by the targets. For each target, a series of data files were collected using: the Gemini with the sampling range set to 50 m then 10 m, and the Blueview with the range set to its maximum value of 10 m. A video of the experiment setup is available at https://vimeo.com/473592147, and a schematic showing the profile and plan views is provided in Figure 7.

Although the Grand Adventure was powered down during data collection, the wake induced by tidal flow along the hull and pole mount created significant entrained air downstream of the vessel in the focus area for data collection. This is an inherent limitation of vessel mounted systems. The experimental setup should be considered similar to deployment of a multibeam sonar from a tidal power platform, looking downstream towards turbines, with entrained air introduced from the mounting pole and tidal platform hull/structure.
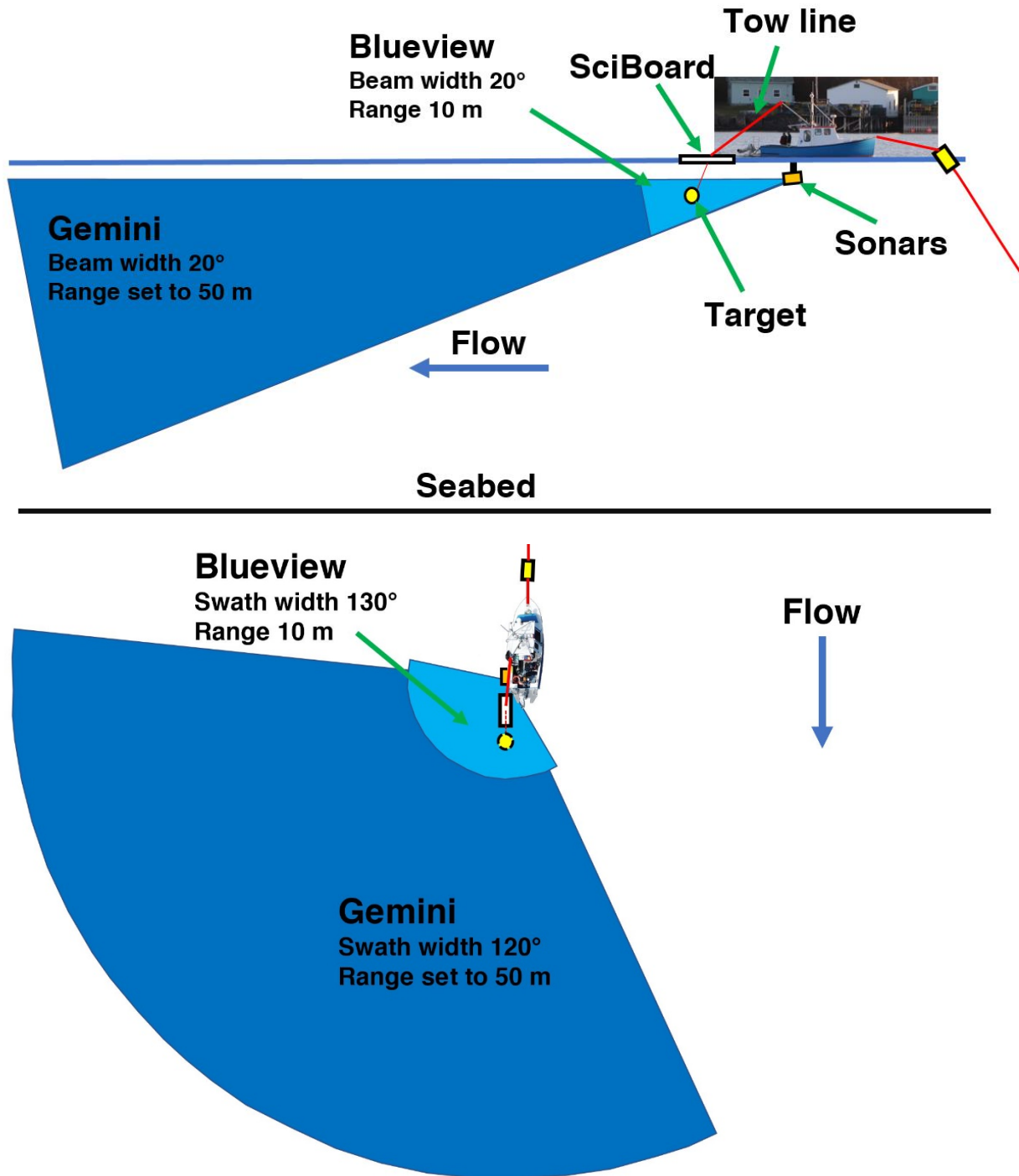
Figure 7: Schematic of experiment setup

2.1.2   Locations

The data collection locations are shown in Figure 8.   Location 1 was selected for initial trials to provide a relatively shallow depth (15 m at low tide) in order to test our ability to anchor in strong tidal flow.   The shallow depth imposed a limitation on the Gemini's ensonified area, which reached bottom at distances greater than approximately 25 to 30 m, depending on the stage of the tide.   A sample sonogram of this case is shown in Figure 9. Location 1 was used for sampling on 2020-07-16 (flood) and 2020-07-17 (ebb) and was subject to maximum current velocities of approximately 2.5 m/s during sampling. Location 2 was characterized by depths of 25 to 30 m at low tide. Here, no returns from the seabed were recorded out to the full 50 m range utilized for the experiments.   Data collection was conducted at Location 2 on 2020-07-31 (flood) and 2020-08-07 (ebb), with peak current velocities of approximately 2.5 m/s.
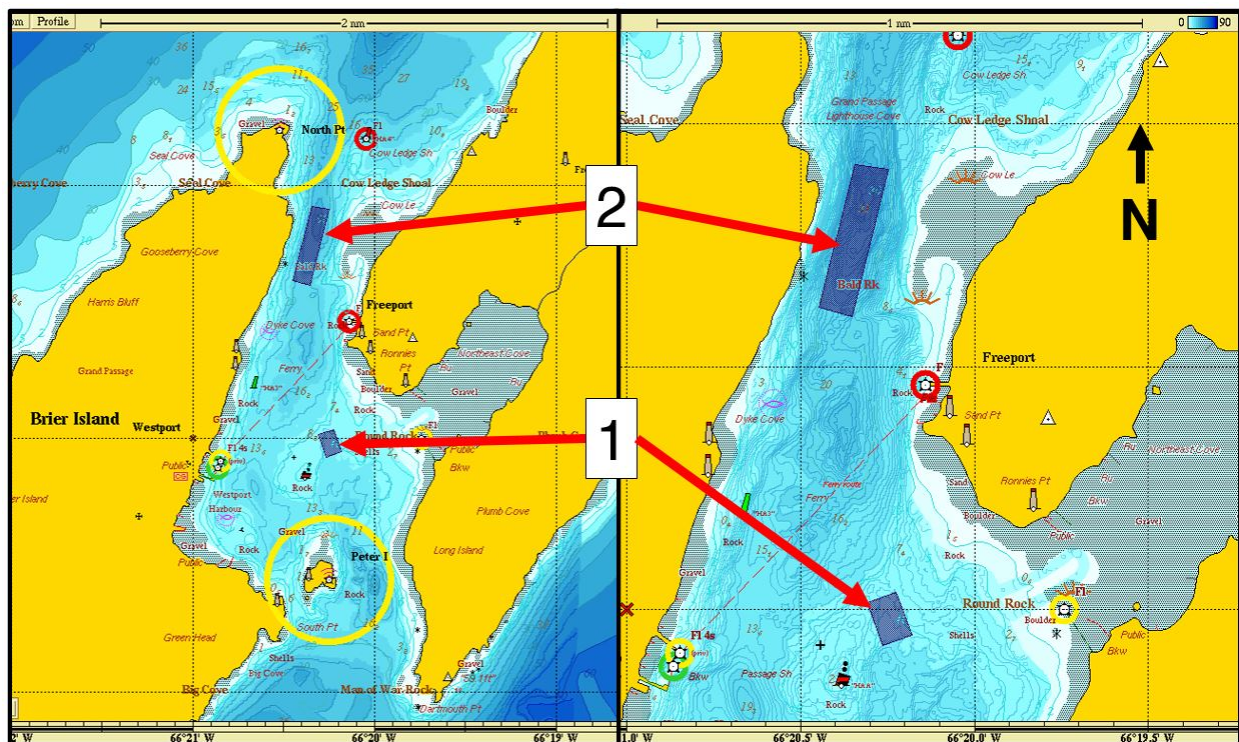

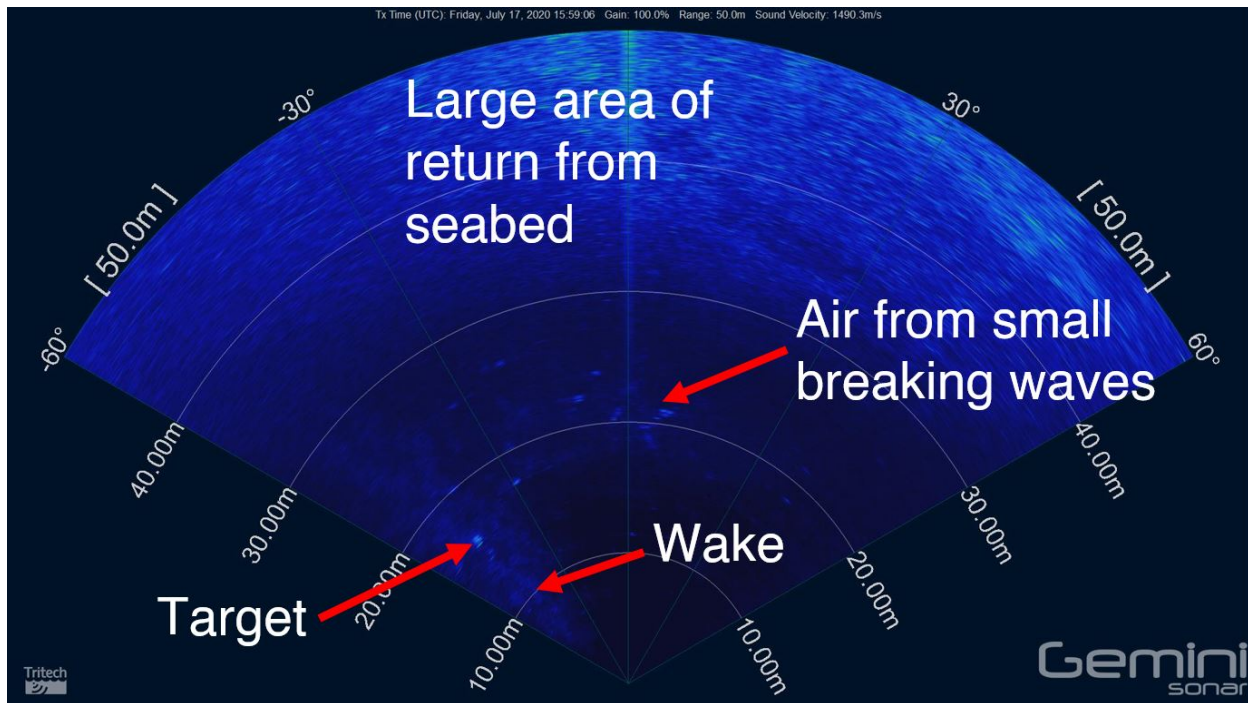*Figure 8: Data collection locations in Grand Passage*

Figure 9: Example of seabed returns, wake, and air from waves on the Gemini

2.1.3   Acoustic Interference

Acoustic interference was not present at observable levels during the initial testing in Freeport Harbour but was persistent during sampling in Grand Passage.   This may be due to an increase in sound scatterers in Grand Passage, as the water was observed to have high levels of plankton and entrained air that both produce stronger overall returns of acoustic energy to the sonars.   As a result, data were collected in Grand Passage with the sonars operating both concurrently and independently to allow evaluation of the effect of acoustic interference (or 'cross talk') between the two instruments.   Figures 10 and 11 provide examples of acoustic interference in sonogram images from each of the sonars caused by cross talk from the other. The interference pattern is consistent for both cases, appearing as radially symmetric bands on the Gemini and more localized jagged patterns on the Blueview visible in sectors 1, 2, and 6 of the sonogram in Figure 11.   The interference signatures in both instruments are not static in position nor continuous or persistent in movement.   The effects of acoustic interference are best viewed in the video files provided in the Results section of this report and are discussed further therein.
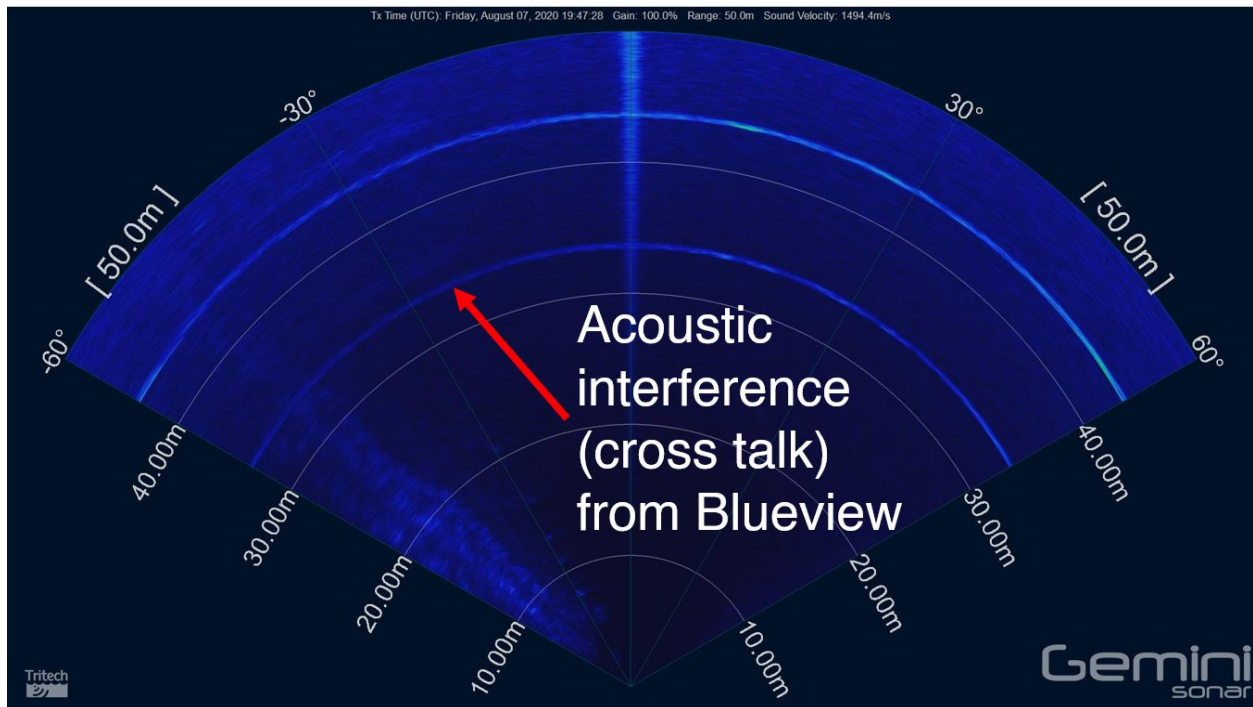
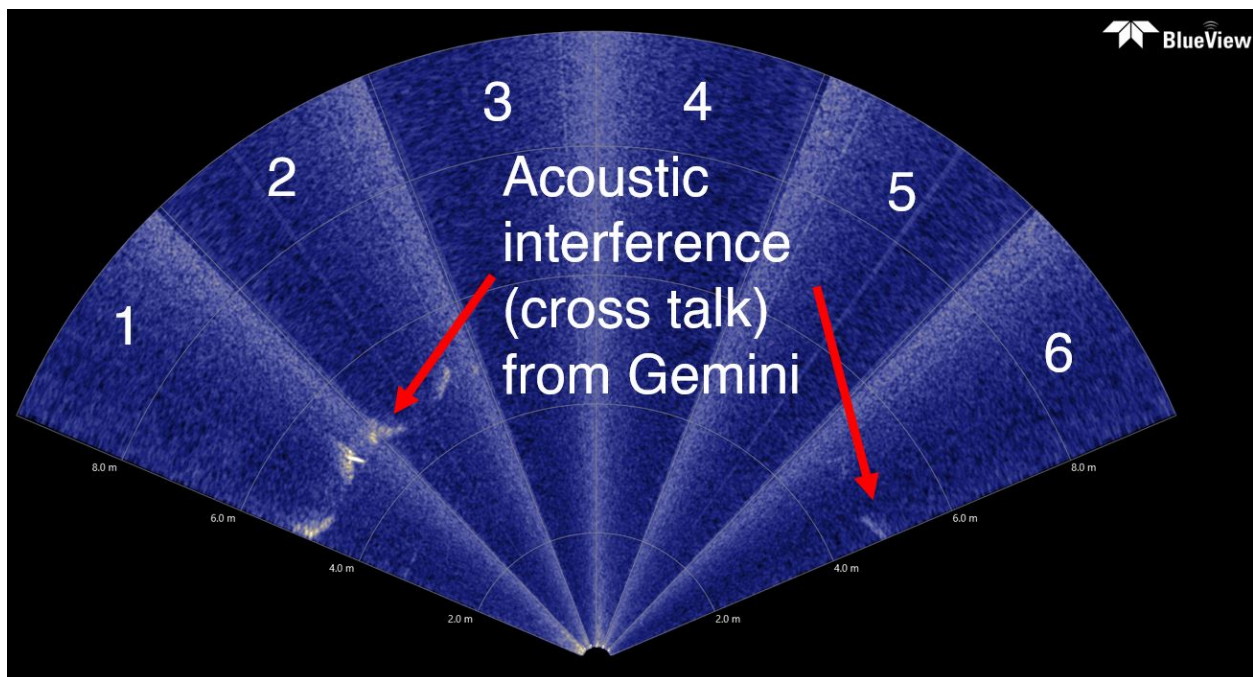*Figure 10: Example of acoustic interference for the Gemini*

Figure 11: Example of acoustic interference for the Blueview

2.2   Data analysis

The data collected in Grand Passage were manually analyzed to evaluate the performance of the Gemini and Blueview multibeam imaging sonars for detecting and tracking near surface targets in strong tidal flow with a high level of air entrainment.   The visualization and organization of the data was conducted using the industry standard software for each sonar: Gemini SeaTec and Teledyne ProViewer[1].   SOAR used these software packages for live viewing of all data as it was collected, followed by initial review and organization by target type.

The sonar images were exported to video (1920 x 1080 resolution) to facilitate ease of sharing and consistency in the manual analysis. Video framerates were set to display data at 2x real-time speed. The ability to use increased playback speed was apparent from SOAR's initial analysis of the data files and utilized to demonstrate an increase in efficiency that may be applicable to active monitoring of tidal turbines.

The video files from both sonars were organized into training and test data sets, which were shared with 9 sonar observers who conducted the manual analysis, including participants from SOAR, Luna Sea Solutions, FORCE, Mi'kmaw Conservation Group, and MarineSitu. The training data sets provide examples in which each target is detected and tracked with a red circle indicating target position and a photograph from the optical camera identifying the target. The test data sets include:

- 21 files with the Gemini set to 50 m range,
- 14 with the Gemini set to 10 m range, and
- 30 files with the Blueview set to 10 m range,
  - 14 of these 30 files were simultaneous data collection with the Gemini at 10 m for direct comparison of the sonars.

---

[1] The development of automatic data processing algorithms for multibeam imaging sonars is an active area of research. Recent publications (e.g. Cotter and Polagye, 2020) on these methods have demonstrated the ability to detect and track targets with some ability to automatically classify between biologic and non-biologic classes. This classification level of processing typically relies on information from multiple instruments for co-registration of known targets (Joslin 2019).   However, there is currently no software readily available with known ability to conduct reliable data analysis in turbulent flow with high levels of air entrainment. Therefore, data were analyzed manually to meet the primary objectives of the study.

The test data sets included additional data files, for which it was left to the observers to detect, track, and identify the targets. A standard spreadsheet was provided to each observer including columns for:

- File number (for SOAR to cross-reference the data files)
- Target present (yes/no)
- Target identification
    - Type (1 through 4)
    - Certainty (1 low to 5 high)
- Detection range (minimum and maximum)
- Ability for detection and tracking (1 low to 5 high)
- Notes describing the trajectory of the target.

The results were categorized by sonar and target type and used to evaluate the performance of each sonar including the effects of flow speed and acoustic interference. Links to the training and test data sets for each sonar are provided below. The data are best viewed in video form. As such, readers of this report are encouraged to watch these data videos for better understanding of the results and conclusions discussed in the following sections. Some example screen shots from the training data sets are also provided in Figures 12 through 15.

Gemini training data	https://vimeo.com/473580369
Gemini test data with 50m range	https://vimeo.com/473665614
Gemini test data with 10m range	https://vimeo.com/473688042
Blueview training data	https://vimeo.com/473964794
Blueview test data	https://vimeo.com/474025663

Through use of the Vimeo platform we also tested video review functionality that allowed observers to directly enter notes encoded to video in space and time. In the case of Vimeo this review functionality was created to facilitate collaboration in video editing. For our analysis it provides the ability to visually verify what the observers were identifying. It was important for each observer to work independently, so links were provided to private review pages. Vimeo or another similar collaborative video editing system may be useful for future manual analyses of video data from multibeam sonars and/or optical cameras at active tidal project sites, including facilitating communication of times and locations of interest for further investigation and analysis.
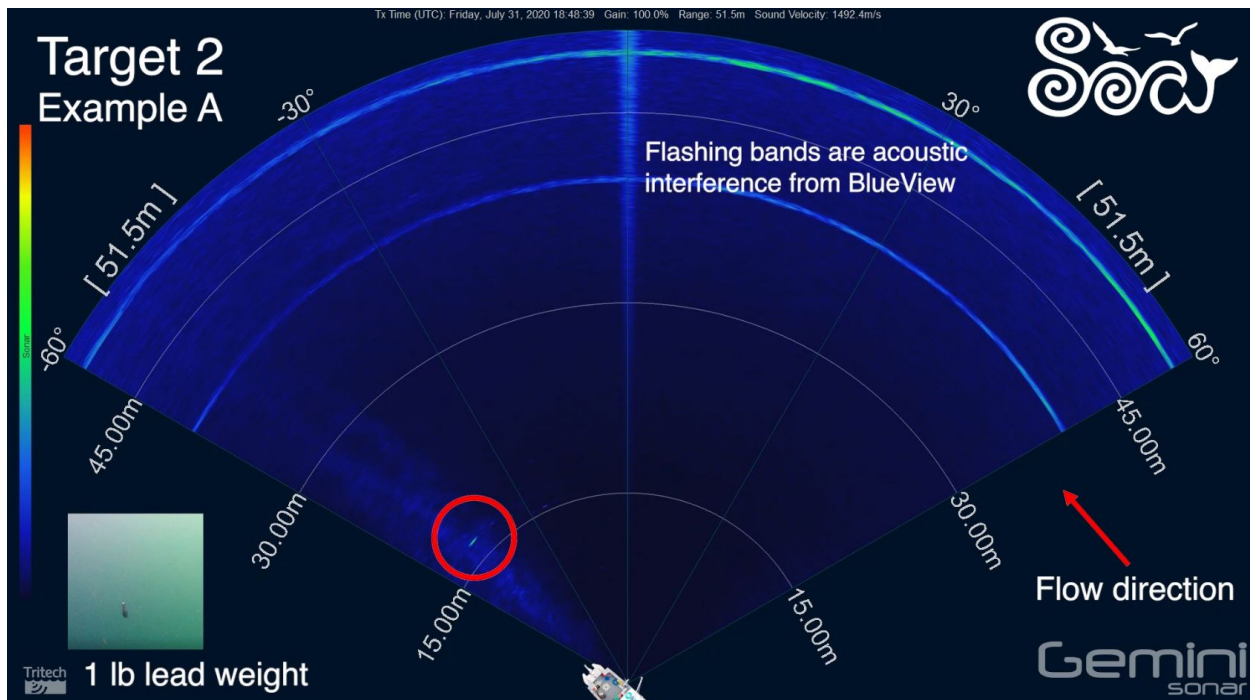
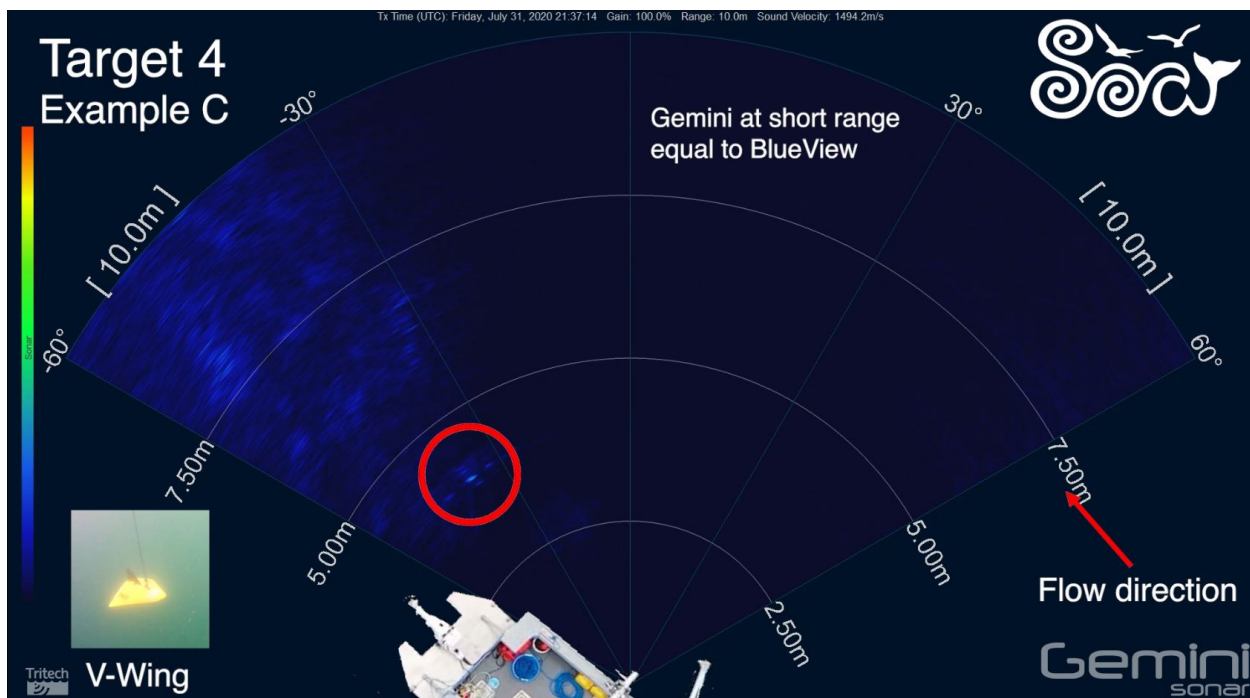*Figure 12: Example from training data - Gemini - 50m range - Target 2*

Figure 13: Example from training data - Gemini - 10m range - Target 4
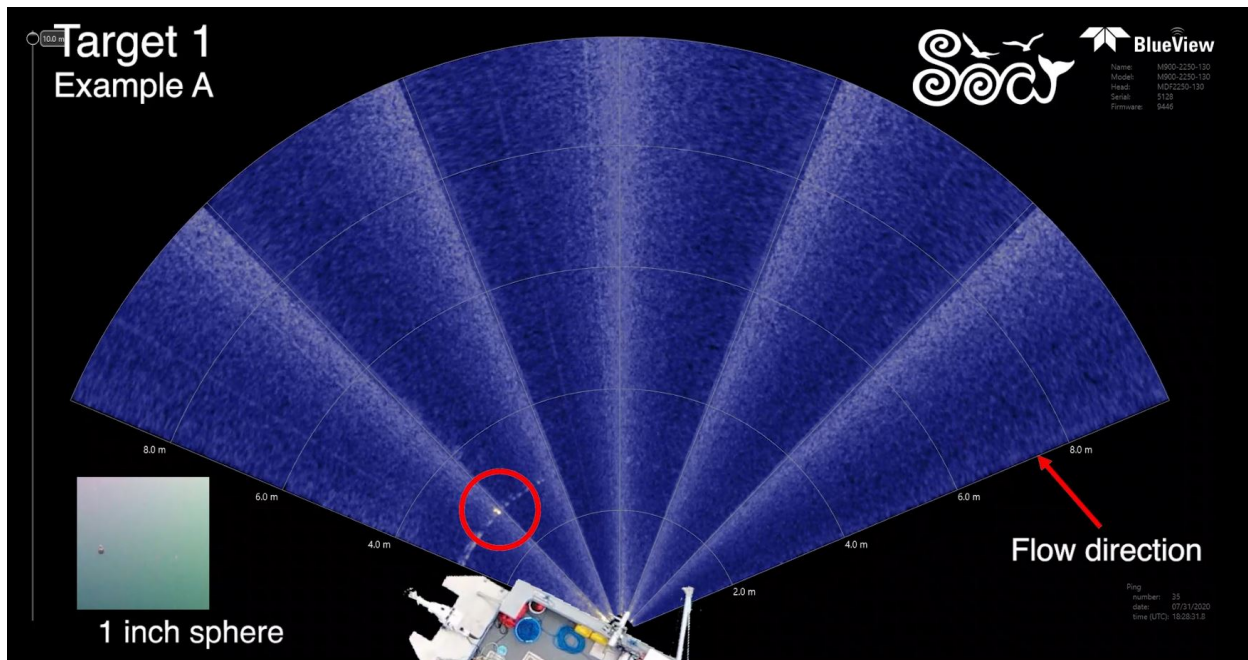
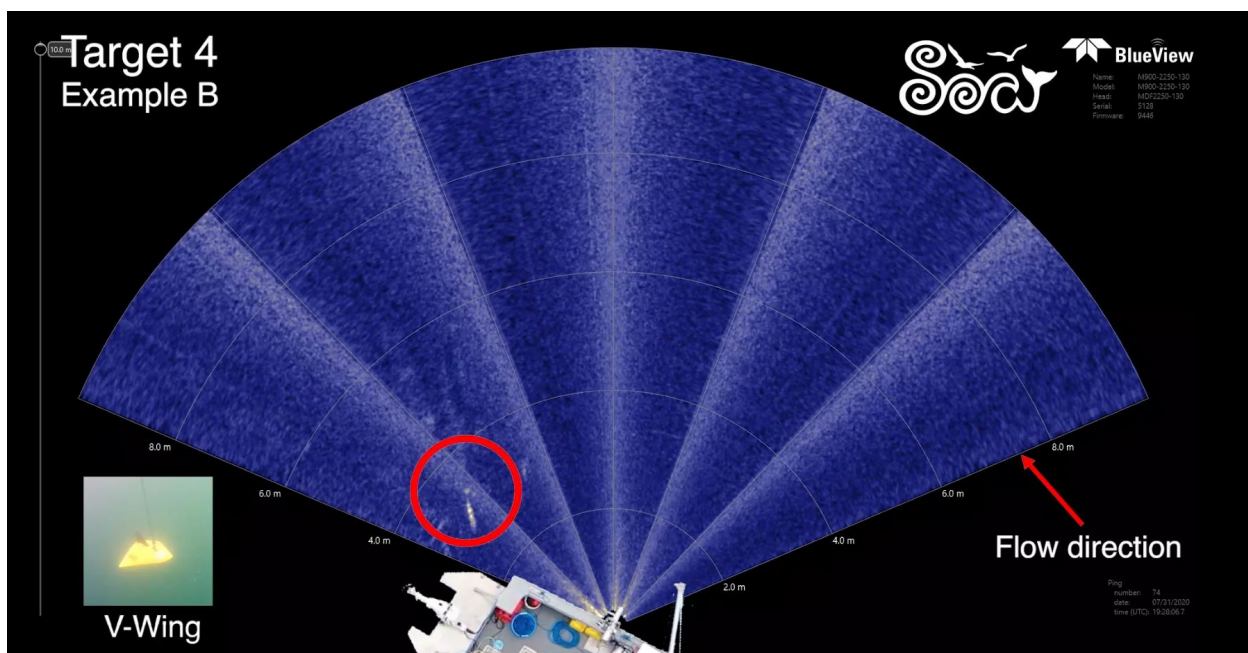*Figure 14: Example from training data - Blueview - 10m range - Target 1*

Figure 15: Example from training data - Blueview - 10m range - Target 4

3.0   Results

3.1   Detection, identification, and tracking

A summary of results from the manual analysis of test data organized by sonar type is provided in Table 2. The observers' scores for target present (detected), target identified, max range tracked, ability to detect and track targets are used to evaluate the performance of the sonars.

The Tritech Gemini with range set to 10 m preformed particularly well, with 99% of all targets detected, and 63% correctly identified. On average, the targets were tracked to 92% (9 m) of the set range, and the detection and tracking abilities scored greater than 4 out of 5. The reduced ability to detect and track targets with the Gemini range set to 50 m is an expected result, primarily due to targets occupying fewer pixels in the sonogram image and the presence of additional returns from potential targets other than our own.

Using the Blueview data, observers demonstrated the ability to resolve finer-scale differences between targets (highest average score for target type correct). However, the Blueview was limited in detection and tracking due to the areas of increased noise on the sonogram. This most significantly affected the ability to track targets as they passed into or through the high-noise areas, but also reduced ability to initially detect and identify targets depending on target location. The intensity of backscatter returned from the targets also varied depending on which sector of the sonogram it was in, potentially due to variable sensitivity of the receiving transducer elements.

Table 2: Summary of results by sonar

Sonar	Target present % correct	Target type % correct	Max range tracked % of set value	Ability to (1 to 5)	
				Detect	Track
Gemini 50m	93%	43%	85%	3.8	3.6
Gemini 10m	99%	63%	92%	4.3	4.2
Blueview 10m	98%	68%	83%	3.7	3.5

A further breakdown of the survey results by sonar and target type is provided in Table 3. As expected, the results indicate an increase in sonar performance with increasing target size. Observers had the most trouble with the 2.54 cm (1 inch) tungsten carbide sphere (Target 1) and the 0.45 kg (1 lb.) (9.5 cm long x 3.8 cm max diameter) lead fishing weight (Target 2), and

were more successful in identifying and tracking the basalt rock in a lobster bait bag (Target 3) and the DOT V-Wing (Target 4). The detection and tracking results by target type are summarized in Figures 16 and 17.

Table 3: Summary of results by sonar and target type

Target type	Target present % correct	Target type % correct	Max range tracked % of set value	Ability to (1 to 5)	
				Detect	Track
Gemini (50m range)					
1	75%	31%	51%	2.7	2.2
2	95%	23%	82%	3.4	3.1
3	96%	33%	93%	4.1	3.9
4	100%	79%	102%	4.5	4.5
All	**93%**	**43%**	**85%**	**3.8**	**3.6**
Gemini (10m range)					
1	100%	63%	96%	4.0	3.8
2	96%	25%	81%	3.3	3.0
3	100%	59%	95%	4.7	4.7
4	100%	94%	93%	4.8	4.8
All	**99%**	**63%**	**92%**	**4.3**	**4.2**
Blueview (10m range)					
1	100%	57%	70%	3.1	2.8
2	89%	50%	76%	3.0	3.0
3	100%	71%	92%	4.0	3.9
4	100%	88%	91%	4.5	4.3
All	**98%**	**68%**	**83%**	**3.7**	**3.5**

An example interpretation of the tabulated results is as follows. For the case of Target 1 with the Gemini at 50 m range, sonar observers were able to:

- correctly detect a target present 75% percent time
- correctly identify it as Target 1 31% of the time, and
- track the target to 51% of the maximum set range – in other words, track the target from 0 to approximately 25 m.

The observers' scores indicate the Gemini 50 m, Target 1, case to be the least effective of all tested for detecting and tracking, with average scores of 2.7 and 2.2 for ability to detect and track, respectively.
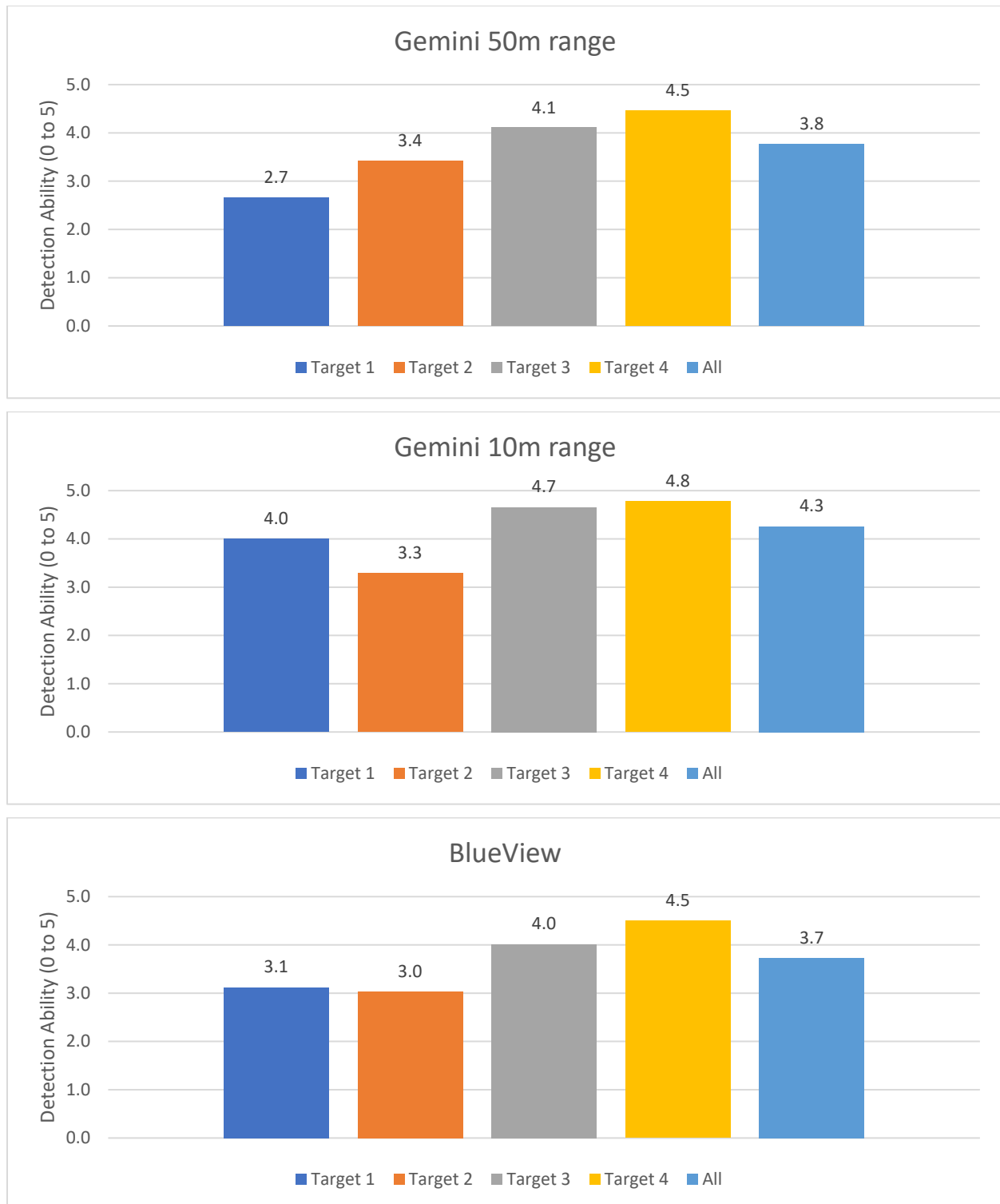
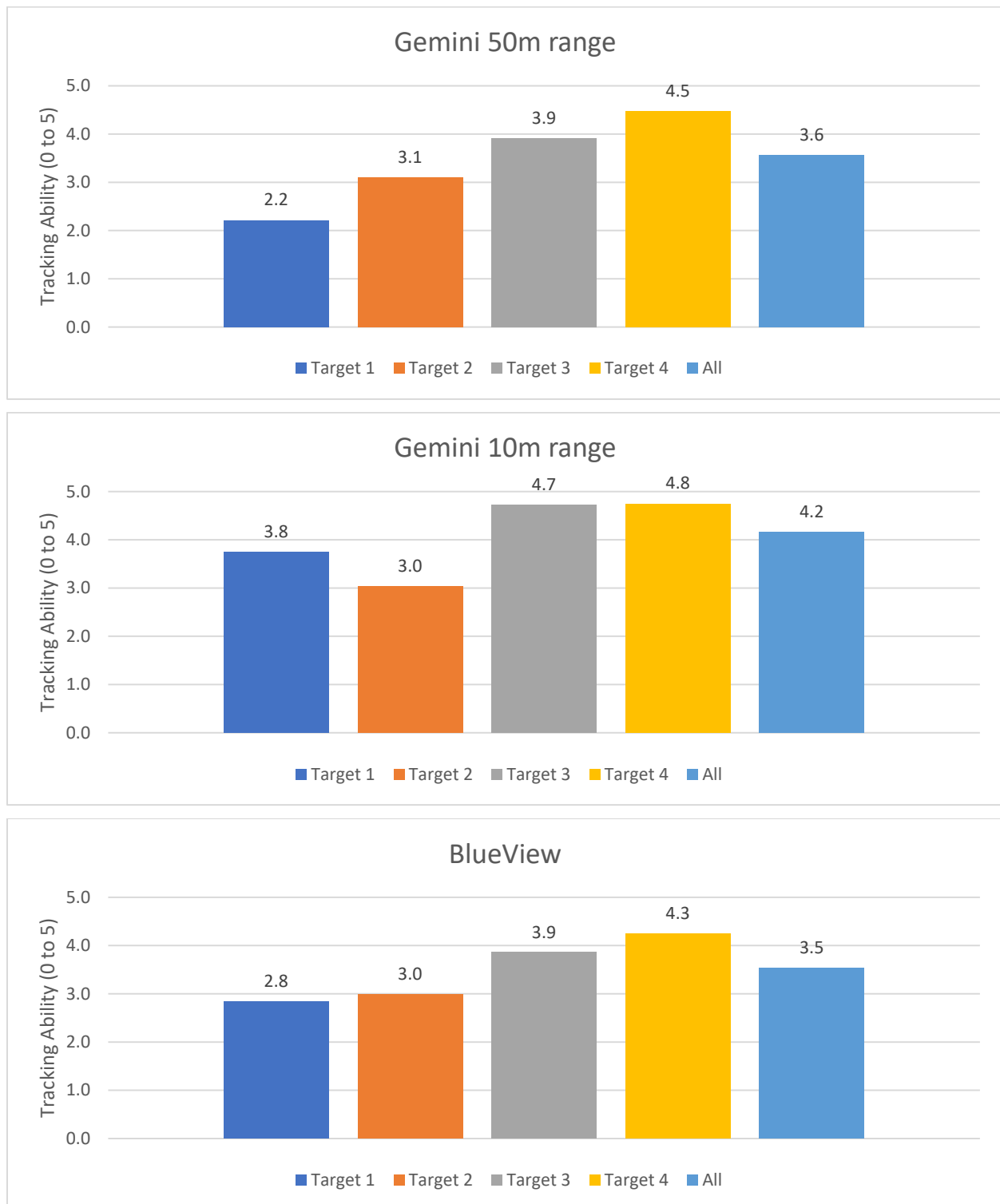*Figure 16: Detection ability for each sonar by target type*

Figure 17: Tracking ability for each sonar by target type

3.2   Effect of Flow Speed

The relationship between flow speed and sonar performance was evaluated by calculating the coefficient of determination, R^2, value between the flow speed and the detection and tracking scores. R^2 is a measure of the proportion of the variance in the dependent variable (detection and tracking scores) that can be predicted from the independent variable (flow speed). R^2 values range from 0 to 1, with 1 being one-to-one correlation. Maximum flow speeds were between 2 and 2.5 m/s, with R^2 values ranging from 0.00 to 0.05 based on 65 data points (N = 65), suggesting no significant relationship between flow speed and sonar performance. A summary of the R^2 values is provided in Table 4.

Table 4: Effect of flow speed on sonar ability to detect and track targets (R^2 with N=65)

Sonar	R^2	
	Detect	Track
Gemini 50m	0.02	0.00
Gemini 10m	0.05	0.01
Blueview 10m	0.04	0.03

3.2   Hardware Limitations

The Blueview was included in testing due to its higher frequency output, which is better suited for close range target detection and tracking. However, the MKI model of the Blueview M900-2250 has a hardware limitation resulting in several persistent high-noise bands in the data. The high-noise bands resulted in difficultly for detection and tracking when target backscatter values were similar to the background noise levels. This effect is observed in all training and test data examples (see Figures 11, 14, and 15). SOAR contacted Teledyne technical support for further information and were informed that Teledyne have now released a second version MKII of the M900-2250 sonar to help alleviate this problem, at the sacrifice of narrowing the field of view (swath width) from 130 to 45 degrees.

"The inconsistency between sectors in the MKI model is due to the BlueView FLS systems producing a Chirp signal that sweeps across frequencies, for example the 900 kHz actually sweeps from ~600 kHz to 1200 kHz across each sector. With the 3 transducer model (MKI), we had to map the sectors so that the high frequency end of a sector was adjacent to the low frequency end of the next sector. This produces imagery that is not nearly as consistent or "smooth" across all sectors. With the 4/2 transducer model (MKII), we can map sectors so that

high frequency is adjacent to high frequency and low adjacent to low for a much better image on both the 900 kHz head and 2250 kHz head. We decided to sacrifice FOV on the 2250 head to make the system more affordable and much smaller and less cumbersome." – Correspondence from Teledyne Engineer (2020-10-07)

An inconsistency in acoustic returns between sectors of the Blueview sonogram was also observed during data collection and analysis, which manifested as one or both of sudden changes in the magnitude of the acoustic return, and a discontinuity in the angular coordinate. This was most evident for natural targets (bubbles and potential fish) as they travelled with the flow (right to left) across the swath width. Numbering the sectors 1 to 6 from left to right, sector 3 seems to have the most notable decrease in returns. There is uncertainty in the cause, as at least some of the targets likely changed vertical position (and may have left the ensonified area), but the consistent nature of decreased returns in this sector suggests variability in transducer/beam sensitivity and/or difference in alignment. This effect can be observed in the training and test data set videos, with links provided in the Methods section.

The Gemini 720is has a similar technical hardware limitation that produces the single "spike" of increased return down the middle of the image which is easily viewable with range set to 50 m (see Figures 9, 10, and 12). This single and narrow spike cause minimal issues with data analysis, but correspondence from Tritech suggests that it might be reduced in a future hardware upgrade for the sonar.

3.3 Acoustic Interference

We evaluated the effects of acoustic interference (cross talk) between the Gemini and Blueview on the ability of manual observers to detect, track, and identify targets through repeat collections of data with the sonars running both concurrently and independently. The results of the comparison are shown in Table 5 and indicate a reduction on the order of 10% in ability to detect, identify, and track targets on the Gemini when the Blueview is operated concurrently. The results for the Blueview look similar with and without acoustic interference from the Gemini. In general, the acoustic interference can be described as distracting, but tolerable.

Table 5: Effect of acoustic interference

Sonar	Target present % correct	Target type % correct	Max range tracked % of set value	Ability to (1 to 5)	
				Detect	**Track**
Independent Operation					
Gemini 50m	97%	47%	88%	3.9	3.7
Blueview 10m	99%	66%	83%	3.8	3.6
Acoustic Interference					
Gemini 50m	86%	38%	77%	3.6	3.3
Blueview 10m	96%	70%	82%	3.6	3.5
Difference					
Gemini 50m	-11%	-10%	-11%	-0.3	-0.3
Blueview 10m	-4%	3%	-1%	-0.2	-0.1

4.0   Conclusions

The project addressed the objective of assessing the performance of surface deployed multibeam imaging sonars for target detections, including the extent of signal interference from waves/turbulence, and entrained air.

The Gemini 720is and Blueview M900-2250 multibeam imaging sonars were both found to be useful for detection and tracking of all target sizes used in our experimentation. However, differentiation of similar targets such as the 2.54 cm (1 inch) tungsten carbide sphere (Target 1) and 0.45 kg (1 lb.) lead fishing weight (Target 2) proved difficult. The sonars performed best for detecting, identifying, and tracking the V-Wing glider. This is an expected result as it was the largest target and had the most recognizable backscatter signature due to its characteristic shape. Entrained air from turbulence, waves, and the vessel/pole wake made tracking targets more difficult, but target persistence allowed them to be effectively detected and tracked by eye for all target types tested. We observed no relationship between flow speed and observers' abilities to detect and track targets with testing up to approximately 2.5 m/s, which is near to the maximum flow speed at Grand Passage. The Minas Passage is known to have higher flow speeds, which may result in higher levels of air entrainment. For comparison to the Minas Passage a flow speed exceedance curve is provided in Figure 18 calculated using depth averaged ADCP measured flow speeds from FORCE Berth Site A (45.3649 -64.4308). It shows maximum flow speeds of approximately 4.5 m/s and 2.5 m/s to be exceeded approximately 36% of the time, or conversely, flow speeds to be less than 2.5 m/s 64% of the time.
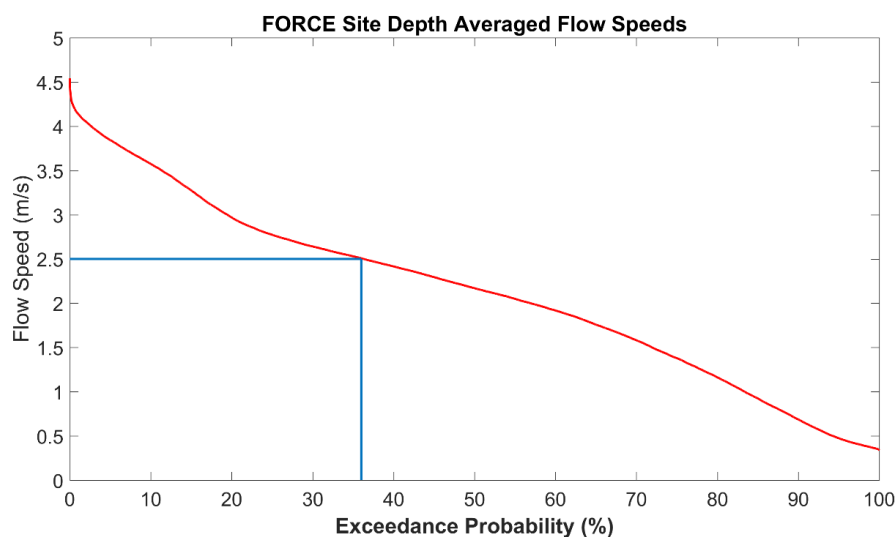

Figure 18: FORCE Site flow speed exceedance curve

SOAR recommends use of the Tritech Gemini 720is for application to monitoring interactions between marine animals and tidal turbines. With the 10 m range setting, the Gemini demonstrated comparable ability to the Blueview to identify targets and outperformed the Blueview in average target detection and tracking scores. At 50 m range, the Gemini still demonstrated a high level of utility for target detection, tracking, and presence/absence, though was less effective (ca. 50%) for target identification.   It is likely that this technology will contribute significantly to effective monitoring and advancing knowledge of importance to regulators and other stakeholders.

The Teledyne Blueview M900-2250 MKI is an impressive technology that offered the ability to resolve finer scale features of the targets and their movements in some cases. However, the persistent high-noise bands resulting from the hardware limitation discussed in Section 3.2 represented a substantial impediment to reliable target detection and tracking. We conclude that data from the Blueview did not add substantial value or insight to the target analysis when used in conjunction with the Gemini. This should not rule out potential use of other MHz frequency multibeam sonars for monitoring the 10 m range in a combined sonar approach, including MKII of the Blueview.

Data analysis was successful for manual observers viewing data played back at 2x real time speed.   Future work should consider efficiencies associated with accelerated data playback and could support use of software with variable speed playback that also allows for time and space encoded notes. Manual observer-based analyses should transition to automated feature detection and tracking, where possible, if multibeam sonar data are to be used for regular or long-term site monitoring.

For planning future data collection careful consideration of sonar orientation is critical.   In an oceanographic context, the ensonified areas are relatively small and are sensitive to returns from seabed and sea surface. Careful planning of the ensonified area is required based on the questions to be addressed by the monitoring while minimizing unwanted returns.   The ability to adjust orientation is highly beneficial, as we were able to do in this work by raising the pole and adjusting sonar pan and tilt by hand.

Another critical component for near surface deployments is the stability of the pole mount system to withstand strong flow with minimal vibrations. Upon initial tests in Grand Passage the pole mount aboard the Grand Adventure required additional strengthening prior to data collection. The image on the Acknowledgements page shows sparks flying at Meteghan Wharf as welding was being conducted by Clare Machine Works.

Some level of acoustic interference from other active sonar systems must be expected when carrying out deployments in or near active ports or passages, whether from passing pleasure or commercial craft, or from other marine operations. Data analysis methods and systems should be designed with this in mind, treating acoustic interference as an element to be anticipated and mitigated where possible through software processing.

Manufactured targets were the focus of this experiment, but marine animal targets were also observed in abundance in Grand Passage and adjacent Bay of Fundy waters. Data were collected that also show the multibeam sonars are likely to perform well in detection and tracking of fish, dolphins, and whales. These data require additional analysis, but some preliminary images are available. An example of a Humpback whale (belly up) diving into a school of fish in the Bay of Fundy (Gemini orientated downward) is shown in Figure 18. This connects with the secondary expected outcome of the project, providing data sets to support further research beyond scope/timeline of this project.

Further testing of and research into multibeam sonar usage from a vessel mounted (near surface) position would be useful in four focus areas, including:

1) fish and other marine animals in locations and seasons (times) with high levels of animal abundance and variety,
2) evaluating the most effective sonar orientations for monitoring the near field of tidal turbines,
3) flow speeds that exceed 3 m/s, and
4) increasing efficiency in data assessment, including reliable automation.

This work should build upon success in Grand Passage to conduct next steps in stronger flow conditions present in Petit Passage and Minas Passage.

The report titled "Field Assessment of Multi-beam Sonar Performance in Bottom Mount Deployments" (Trowse et al. 2020) provides similar analysis for the case of seabed mounted Gemini 720is and Blueview M900-2250, including comparison of results and further recommendations for next steps.
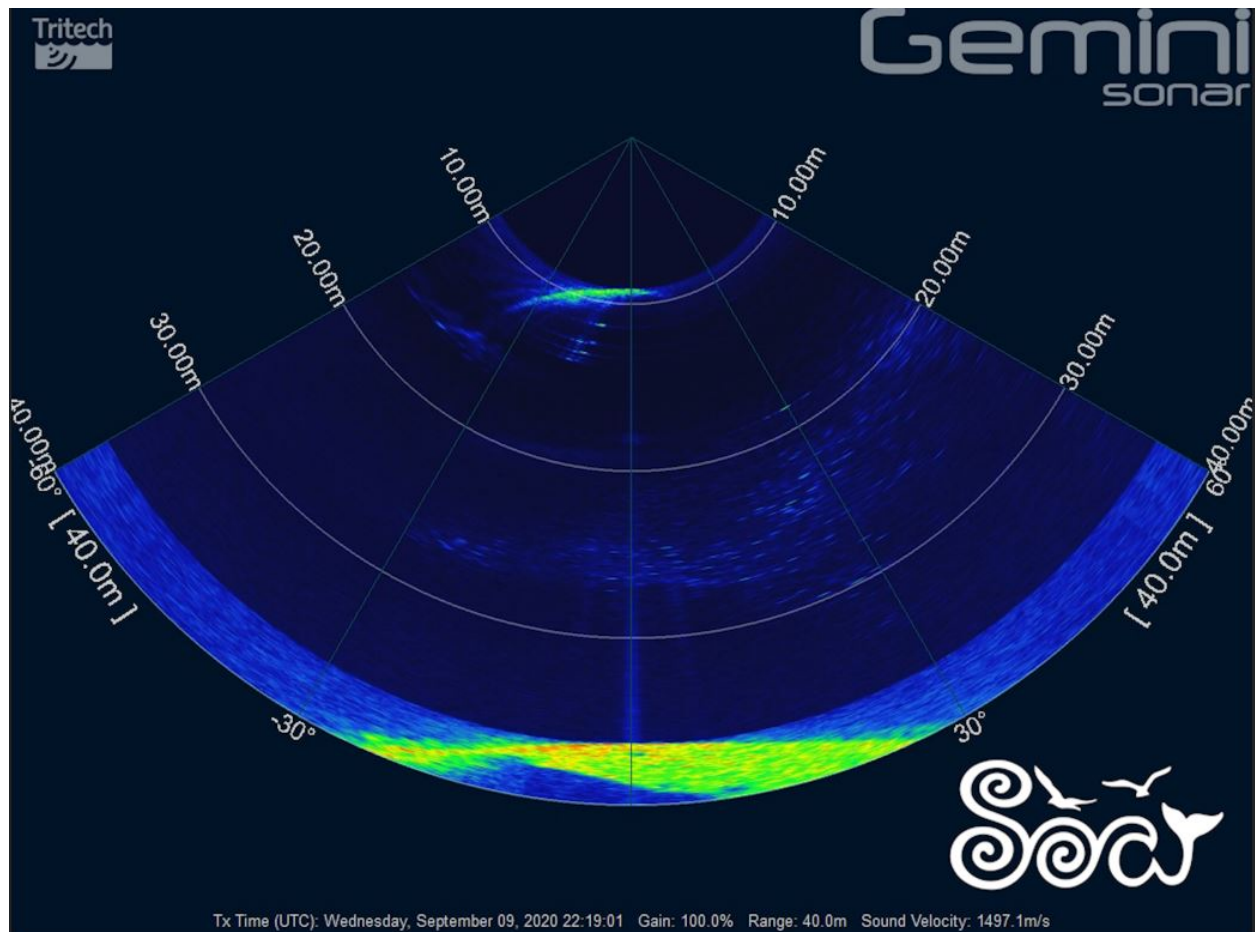

Figure 19: Gemini example of Humpback whale and school of fish

References:

Trowse, G., Guest, T., Feiel, G., Cheel, R., and Hay, A.E. 2020. Field Assessment of Multibeam Sonar Performance in Bottom Mount Deployments. Final Report to the Offshore Energy Research Association of Nova Scotia. SOAR – Sustainable Oceans Applied Research, Technical Report. Freeport, NS, Canada.

Bevelhimer, M., Colby, J., Adonizio, M.A., Tomichek, C., and Scherelis, C. 2016. Informing a tidal turbine strike probability model through characterization of fish behavioral response using multibeam sonar output. *In* Oak Ridge National Laboratory Tm-2016/219. Available from http://www.ntis.gov/help/ordermethods.aspx%5Cnhttp://www.osti.gov/contact.html.

Cotter, E., Murphy, P., and Polagye, B. 2017. Benchmarking sensor fusion capabilities of an integrated instrumentation package. Int. J. Mar. Energy **20**: 64–79. Elsevier Ltd. doi:10.1016/j.ijome.2017.09.003.

Cotter, E. and Polagye, B. (2020). Automatic Classification of Biological Targets in a Tidal Channel using a Multibeam Sonar. Journal of Atmospheric and Oceanic Technology, DOI: 10.1175/JTECH-D-19-0222.1

Foote, K.G., Chu, D., Hammar, T.R., Baldwin, K.C., Mayer, L.A., Hufnagle, L.C., and Jech, J.M. 2005. Protocols for calibrating multibeam sonar. J. Acoust. Soc. Am. **117**(4): 2013–2027. doi:10.1121/1.1869073.

Gnann, F. 2017. FAST-2 Test Deployment : Experimental low-flow test of the Gemini Sonar.

Hastie, G. 2013. Tracking marine mammals around marine renewable energy devices using active sonar. *In* SMRU Ltd report number SMRUL-DEC-2012-002 to the Department of Energy and Climate Change. doi:10.1109/CIDM.2011.5949297.

Joslin, J. 2019. Imaging sonar review for marine environmental monitoring around tidal turbines. Available from https://oera.ca/sites/default/files/2019-06/James Joslin Report - Imaging sonar review for marine mammal and fish monitoring around.pdf.

Melvin, G.D., and Cochrane, N.A. 2014. Investigation of the vertical distribution, movement and abundance of fish in the vicinity of proposed tidal power energy conversion devices.

Sanderson, BG, MJ Adams and AM Redden. 2019. Sensor Testing Research for Environmental Effects Monitoring (STREEM). Final Report to the Offshore Energy Research Association of Nova Scotia. Acadia Centre for Estuarine Research, Technical Report No. 127, 68 pp. Acadia University, Wolfville, NS, Canada.

Viehman, H., Gnann, F., and Redden, A.M. 2017. Cape Sharp Tidal Gemini Multibeam Imaging Sonar : Monitoring Report Report to Cape Sharp Tidal Prepared and submitted by. (123).

Viehman, H.A., and Zydlewski, G.B. 2014. Fish interactions with a commercial-scale tidal

energy device in the natural environment. Estuaries and Coasts **38**(Suppl. 1): S241–S252. doi:10.1007/s12237-014-9767-8.

Williamson, B., Fraser, S., … P.B.-I.J. of, and 2017, U. 2017. Multisensor acoustic tracking of fish and seabird behavior around tidal turbine structures in Scotland. IEEE J. Ocean. Eng. **42**(4): 948–965. doi:10.1109/JOE.2016.2637179.

Williamson, B.J., Blondel, P., Armstrong, E., Bell, P.S., Hall, C., Waggitt, J.J., and Scott, B.E. 2016. A self-contained subsea platform for acoustic monitoring of the environment around marine renewable energy devices-field deployments at wave and tidal energy sites in Orkney, Scotland. IEEE J. Ocean. Eng. **41**(1): 67–81. doi:10.1109/JOE.2015.2410851.

Wilson, G.W., and Hay, A.E. 2017. Short-pulse method for acoustic backscatter amplitude calibration at MHz frequencies. J. Acoust. Soc. Am. **142**(3): 1655–1662. doi:10.1121/1.5003788.
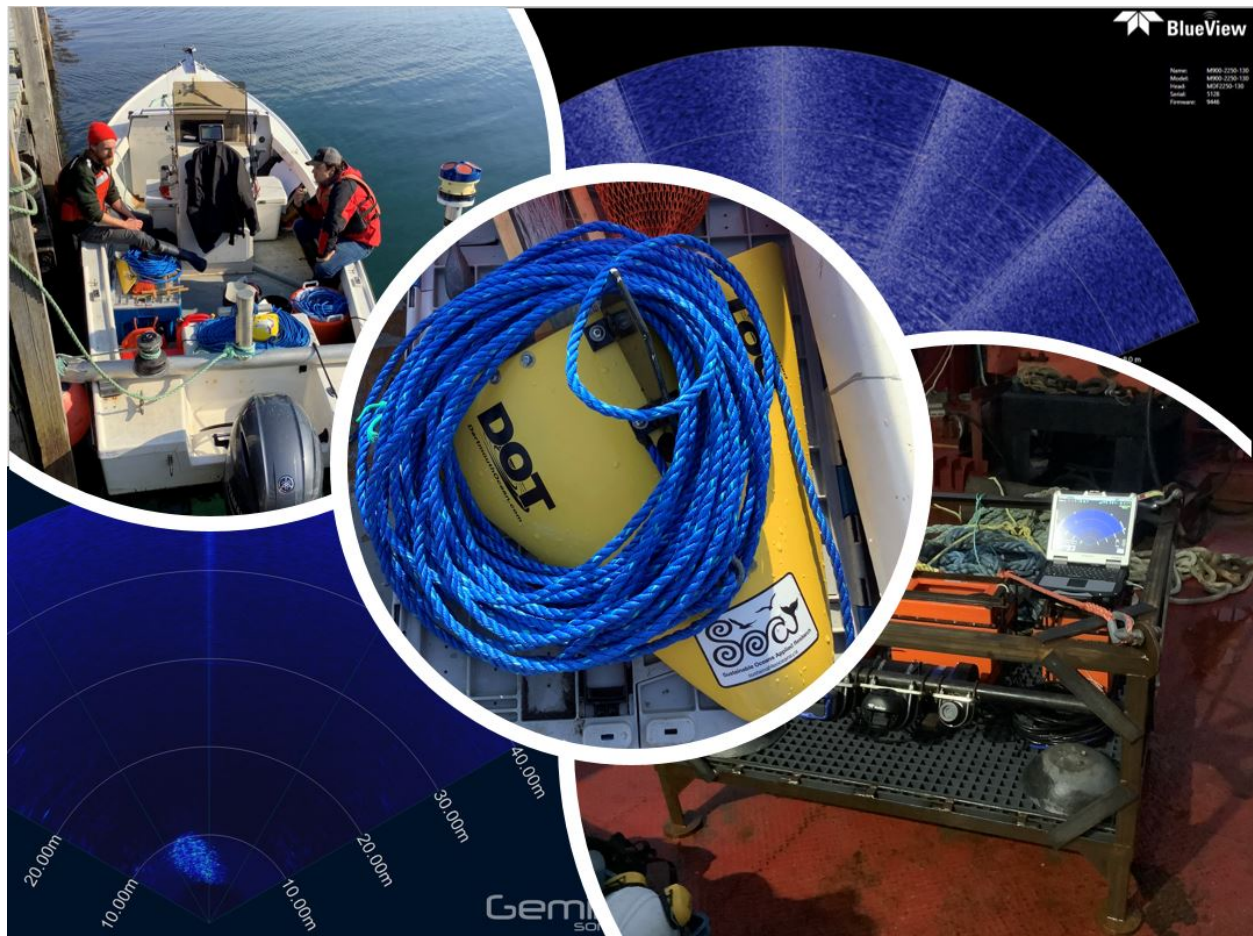
Appendix III

OERA Pathway 2020 Program

Field Assessment of Multi-beam Sonar Performance in Bottom Mount Deployments

OERA Project number: 200-219

February 1, 2021

Project Lead: SOAR – Sustainable Oceans Applied Research Ltd.

By: Greg Trowse, Dr. Tristan Guest, Gavin Feiel, Richard Cheel, and Dr. Alex Hay

Executive Summary

Multibeam imaging sonars have application to monitoring fish and marine mammal presence and behaviours in the near field of tidal turbine installations, including evaluating avoidance, evasion, and potential blade strikes. SOAR conducted field experiments to help reduce uncertainty in performance of the Tritech Gemini 720is and Teledyne Blueview M900-2250 multibeam imaging sonars for identifying and tracking discrete targets in high-flow environments. This information will help inform the Department of Fisheries and Oceans Canada, tidal energy developers, and other stakeholders in the design and implementation of effective monitoring systems for tidal energy projects in the Bay of Fundy and beyond. These two imaging sonars were the technologies recommended for testing by the subject matter expert for imaging sonars during the first phase (Global Capability Assessment) of the Pathway Program. The Tritech Gemini 720is operates at 720 kHz and has a maximum effective sampling range of approximately 50 m. The Teledyne Blueview M900-2250 has operating frequencies of 900 or 2250 kHz, with a 10 m range for the high frequency transducer head. As per the recommendation from the Global Capability Assessment, this report focuses on the Blueview's capabilities while operating at 2250 kHz.

Field trials included deployments of an Autonomous Multibeam Imaging Sonar (AMIS) monitoring system in Grand Passage. The depth at the deployment location is approximately 25 m at low water, with flow speeds up to approximately 2.5 m/s. The deployed sonars were oriented with their ensonified areas directed downstream. The instruments' horizontal fields of view oriented across-channel and vertical fields of view tilted upward from the bed.

Three targets were used during data collection: a 0.45 kg (1 lb.) (9.5 cm long x 3.8 cm max diameter) lead fishing weight, approx. 12 cm diameter basalt rock in a lobster bait bag, and a V-Wing glider (approx. 50 cm diameter) from Dartmouth Ocean Technologies. The targets were suspended beneath research vessel Puffin while drifting through the study area. The Puffin repeatedly travelled to a position upstream from the sonars, then drifted with the tidal flow such that the drift trajectory allowed the targets to pass through the sonars' ensonified areas. The AMIS system was fully autonomous, so no live view of data collection was available.

The data were manually analyzed to evaluate the performance of the Gemini and Blueview multibeam imaging sonars for detecting and tracking targets in strong tidal flow. The visualization and organization of the data were conducted using the proprietary software

packages associated with each sonar: Gemini SeaTec and Teledyne ProViewer.   Data from the Gemini were exported into video and organized into training and test data sets, which were shared with 7 sonar observers who conducted the manual analysis to detect, track, and identify the targets. Links to the training and test data sets for are provided below.

Gemini training data   https://vimeo.com/483141927

Gemini test data with 50m range   https://vimeo.com/483142328

Due to the small ensonified area of the Blueview, insufficient sightings of known targets were collected to generate training and test data sets.   A manual analysis was conducted by SOAR, with a focus of events of concurrent detection by the Blueview and Gemini including natural targets (primarily fish) and occasionally the artificial targets used in our methodology. A link to a video file with 21 comparative cases is provided below.

Concurrent Blueview and Gemini   https://vimeo.com/487808248

The Tritech Gemini 720is received high scores from the observers in the ability to identify the presence of, visually detect, and track targets in videos displaying sonogram data output. The observers correctly identified the presence of a target in 99% of cases, and gave average scores greater than 4 out of 5 describing their visual detection and tracking ability. Targets were correctly identified roughly 50% of the time.   No significant relationship between flow speed and ability to detect and track the targets was observed.

The Teledyne Blueview M900-2250 MKI is an impressive technology that offered the ability to resolve finer scale features of the targets and their movements in some cases. However, persistent high-noise bands resulting from a known hardware issue and an apparent transducer alignment issue represented substantial impediments to reliable target detection and tracking. We conclude that data from the Blueview did not add substantial value or insight to the target analysis when used in conjunction with the Gemini. This should not rule out potential use of other MHz frequency multibeam sonars for monitoring the 10 m range in a combined sonar approach, including MKII of the Blueview.

SOAR recommends use of the Tritech Gemini 720is for application to monitoring interactions between marine animals and tidal turbines.   The Gemini demonstrated a high level of utility for

detecting and tracking targets from vessel and bottom mounted orientations in tidal flows up to approximately 2.5 m/s in Grand Passage. It is likely that this technology will contribute significantly to effective monitoring and advancing knowledge of importance to regulators and other stakeholders. Tidal flows are faster at the FORCE site in the Minas Passage, with flow speeds exceeding 2.5 m/s 30 to 40% of the time.

With respect to deploying multibeam sonars from the surface (i.e., vessel) or seabed, the sonars performed well from both positions, despite increased levels of air entrainment in the vessel mount case. The selection of deployment position for monitoring tidal turbines is likely to be defined by the nature of the tidal device (floating or seabed mounted) and the questions to be addressed by the monitoring.

The project addressed the objective of assessing the performance of bottom deployed multibeam imaging sonars for target detections, including the extent of signal interference from waves/turbulence, and entrained air.

Further testing of bottom mounted multibeam sonars would be useful in four focus areas, including:

1) fish and other marine animals in locations and seasons (times) with high levels of animal abundance and variety,
2) evaluating most effective sonar orientations for monitoring the near field of tidal turbines,
3) flow speeds that exceed 3 m/s, and
4) increasing efficiency in data assessment, possibly including reliable automation.

This work should build upon success in Grand Passage to conduct next steps in stronger flows present in Petit Passage and Minas Passage. The report titled "Field Assessment of Multi-beam Sonar Performance in Surface Mount Deployments" (Trowse et al. 2020) provides similar analysis for the case of surface mounted Gemini 720is and Blueview M900-2250.

Table of Contents

List of Figures

List of Tables

Acknowledgments

SOAR thanks the following support organizations and supply chain who helped us deliver on this work:

- Offshore Energy Research Association of Nova Scotia

- Natural Resources Canada

- Dalhousie Ocean Acoustics Laboratory

- Villages of Westport, Freeport, and Tiverton

- Clare Machine Works

- Luna Sea Solutions

- MarineSitu

- Mi'kmaw Conservation Group

- Fundy Ocean Research Centre for Energy (a.k.a. FORCE)

- Dasco Equipment Inc.

- Tritech and Teledyne technical support staff

- Canadian Hydrokinetic Turbine Test Centre

1.0   Introduction

Multibeam imaging sonars have application to monitoring fish and marine mammal presence and behaviours in the near-field of tidal turbine installations, including evaluating avoidance, evasion, and potential blade strikes (Hastie 2013; Viehman and Zydlewski 2014; Bevelhimer et al. 2016; Williamson et al. 2016, 2017; Sanderson et al. 2019). However, there is uncertainty in performance of these instruments in high-flow environments due to turbulence and associated entrained air in the water column, where a reduction in instrument efficacy may result from scattering of the transmitted acoustic signal through turbulent zones of the water column before the signal reaches potential targets, with further signal dilution on the return to the transducer (Melvin and Cochrane 2014). Some specific and additional challenges include a) mounting sonars at sufficient depth in high-flow environments to reduce exposure to entrained air, b) achieving optimal orientation such that the area of interest is ensonified while minimizing acoustic returns from surface and/or seabed, and c) transferring, storing, and efficiently analyzing large amounts of data.

Several makes and models of multibeam imaging sonars are available, with a major source of difference being the frequency at which they transmit acoustic energy. Higher frequencies are associated with shorter wavelengths, which results in resolution increasing with frequency, and range decreasing with increasing frequency. The combined use of kHz and MHz frequency range multi-beam imaging sonars is of interest for monitoring marine animals because it offers potential for an instrument package to detect and track targets at ranges up to approximately 50 m with identification (and/or finer scale tracking) of targets at a range up to approximately 10 m. For environments with suitable visibility, the addition of an optical camera offers increased potential for target identification, target validation, and tracking at ranges of approximately 0.1 to 15 m in very clear waters.

As part of the Pathway Program, SOAR conducted work to help evaluate the performance of the Tritech Gemini 720is and Teledyne Blueview M900-2250 (2250 kHz transducer head) multibeam imaging sonars for evaluating interactions between marine animals and tidal turbines. This information will help inform the Department of Fisheries and Oceans Canada (DFO), tidal energy developers, and other stakeholders in the design and implementation of effective monitoring systems for tidal energy projects in the Bay of Fundy and beyond.

The Tritech Gemini 720is multibeam imaging sonar has been used by MCT Seagen in Strangford Lough (Hastie 2013), OpenHydro at the Fundy Ocean Research Centre for Energy (FORCE) (Viehman et al. 2017), and other applications including studies commissioned by FORCE (Gnann 2017). With an operating frequency centered at 720 kHz, the Gemini has a target detection range of up to 100 m (Cotter, et al. 2017) but has reduced resolution in comparison to higher frequency systems. The dual frequency Teledyne Blueview M900-2250 has two sets of transducers, one set centered at 900 kHz (close to the Gemini) and the other set at 2250 kHz (2.25 MHz). Use of the Blueview 2.25 MHz transducer head may have application in shorter range monitoring, up to approximately 10 m (Cotter et al. 2017). These two imaging sonars are the technologies recommended for testing by the subject matter expert for imaging sonars during the first phase (Global Capability Assessment) of the Pathway Program (Joslin 2019).

SOAR's work in 2020 has included data collection and analysis from near surface (vessel mounted) and seabed deployments. This report covers the methodology and results for the bottom mounted experiment. "Field Assessment of Multi-beam Sonar Performance in Surface Mount Deployments" (Trowse et al. 2020) discusses the vessel mount deployment (vessel mount project).

The **objective** of the work covered in this report is to assess the performance of seabed deployed multibeam imaging sonars for target detections, including the extent of signal interference from waves/turbulence, and entrained air.

The **expected outcomes** include:
- Primary - Report on performance of bottom deployed multibeam imaging sonars for target detections, and a recommendation on whether the use of bottom deployed multibeam imaging sonars is feasible for monitoring interactions between marine animals and tidal turbines.
- Secondary - Data sets to support further research (beyond the scope and timeline of this project) including potential for calibration of multibeam imaging sonars, quantification of the effects of air entrainment on target detectability, and autodetection and classification algorithms (software).

2.0   Methodology

The methodology was developed to evaluate the performance of two multibeam imaging sonars when deployed on the seabed, including the Tritech Gemini 720is (Gemini) and the dual frequency Teledyne Blueview M900-2250 MKI (Blueview). The Gemini has 512 beams aligned along a 120° swath width (angular resolution of 0.25°), with each beam having a 20° width perpendicular to the swath. The Blueview has 768 beams aligned along a 130° swath width (angular resolution of 0.18°), with each beam having a 20° width perpendicular to the swath. Multibeam sonars resolve target locations as range along each beam.   The resulting composite (by combining all beams) is used to generate a sonogram with target locations in the swath width but does not resolve target location in the beam width.   For this experiment, the sonars were both aligned such that field of view had swath width on the horizontal plane (parallel to water surface) and beam width on the vertical plane (depth).   The acoustic frequency and geometry of the ensonified area for each sonar are summarized in Table 1. The Subaqua SAIS IP Cam (optical camera) and a GoPro were included for target verification, and to demonstrate ability for targets to be identified optically.

Table 1: Multibeam imaging sonar frequency and ensonified area

Sonar	Frequency (kHz)	Range (m)	Swath width (degrees)	Beam width (degrees)
Gemini	720	120 m[1]	120	20
Blueview	900 or 2250[2]	10	130	20

Notes:

- The Tritech supplied specifications for the Gemini report a max range of 120m, however the maximum effective range for monitoring marine animals in tidal channels is 50 to 60 m.

- The Blueview is dual frequency, with two transducer heads. Our work focused on the high frequency capabilities with the 2250 kHz (2.25 MHz) transducers, and associated range of 10 m.   For brevity, ongoing reference to the Blueview in this report implies the high frequency transducer head.

- Both sonars transmit a "chirp" pulse that spans a range of frequencies, centered at the values listed above.

2.1 Instrument Configuration and Deployment

SOAR worked with Dalhousie Ocean Acoustics Laboratory, Clare Machine Works, and Dasco Equipment to design and build an Autonomous Multibeam Imaging Sonar (AMIS) monitoring system including the bottom lander/frame with sonar mounts, power supply (three 24 V Deepsea Power and Light SeaBattery Power Modules), subsea data acquisition system (sonar control and data storage with an Intel NUC computer and power conditioning inside a Nortek 500 m depth rated pressure case with custom end cap), and custom cables for power supply and communication.   The frame also carried 140 kg of lead ballast. The AMIS monitoring system is shown in Figure 1.
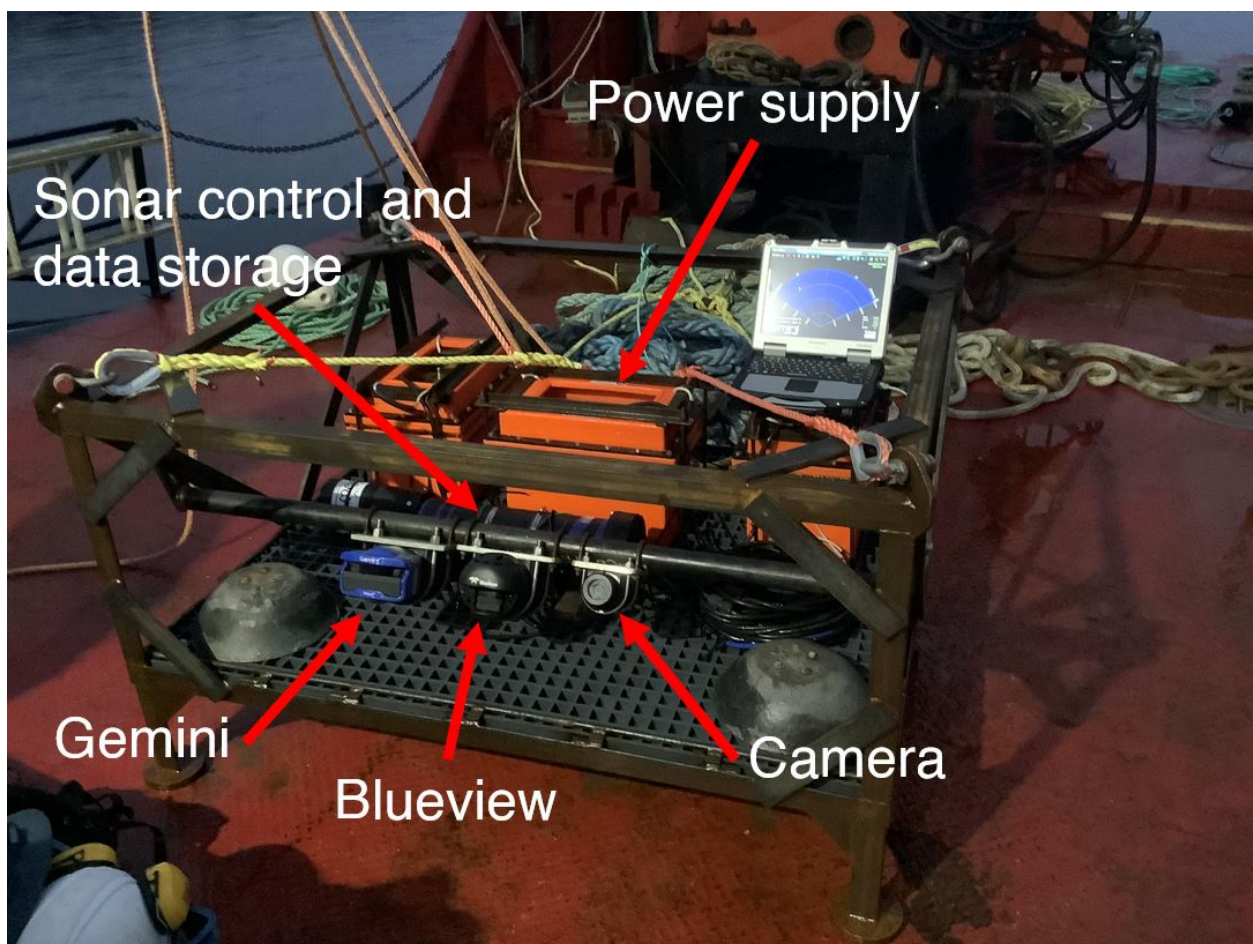

Figure 1: Autonomous Multibeam Imagining Sonar (AMIS) monitoring system

Submergence tests were conducted in Westport Harbour prior to each of two principal deployments in Grand Passage. The submergence tests allowed for a) testing and refinement of the mounting arrangement and sonar angles, b) testing the subsea data acquisition system, and

c) refinement of the deployment methodology. A time-lapse video of frame assembly and harbour testing is available at: https://vimeo.com/488171392

The vertical tilt angles of the sonars were refined to avoid or limit acoustic returns from both the seabed and the AMIS instrument frame (see the horizontal frame member above the sonars in Figure 1), which imposed lower and upper constraints on the range of possible sonar orientations, respectively. During the harbour testing, efforts were made to remove or reduce the acoustic returns from the AMIS frame by changing the tilt angles and positions of the sonars. However, returns from the frame were found to persist unless the transducer heads were positioned outside of the frame's perimeter, increasing the risk of damage to the sonars. The frame-returns do not appear to create an acoustic shadow, suggesting they may be related to the presence of acoustic sidelobes outside of the principle 20° beam width.

The principal experiment consisted of two deployments in Grand Passage, on 2020-10-20 and 2020-10-22, hereafter referred to as Deployments 1 and 2. The deployment location is shown in Figure 2. On both occasions, AMIS was deployed during low water slack and retrieved during high water slack, data being collected during the flood tide. The depth at the deployment location is approximately 25 m at low water, with flow speeds up to approximately 2.5 m/s. A video of the deployment is available at: https://vimeo.com/483103490.

The deployed sonars were oriented such that their ensonified areas were directed downstream, with the instruments' horizontal fields of view oriented across-channel. The configuration was chosen to minimize limitations of the ensonified areas by the sea surface or bottom, while maximizing the horizontal (i.e., downstream) extent over which targets would be visible if drifting downstream at a fixed depth. The horizontal alignment of the instruments was accomplished through use of a ground line and clump weight, which were attached to the AMIS frame. The weight and ground line were lowered first, upstream of the target location for the instrument frame, so that the taught ground line would ensure the correct orientation of the frame when it reached bottom. For both deployments, a diver verified the orientation of the frame and made minor adjustments, and confirmed that no boulders or other obstructions were apparent in the field of view. The diver reported the frame to be sitting well on relatively level ground (less than approximately 5° slope) in both cases.

For Deployment 1, the Gemini was tilted such that the vertical beam width spanned from 5 to 25° above the horizontal plane of the instrument frame. The vertical field of view of the Blueview spanned 20 to 40°. The sampling range of the Gemini was set to 30 m with an associated sampling rate of 13 to 14 Hz, and the range for the Blueview set to its maximum of 10 m with an associated sampling rate of 15 to 16 Hz. For Deployment 2, both sonars were tilted such that their ensonified areas spanned from 15 to 35° in the vertical. The increase in Gemini tilt for the second deployment was applied due to the presence of consistent returns from the seabed during Deployment 1. The Blueview was tilted down 5° relative to Deployment 1 to align with the Gemini. The sampling range of the Gemini was set to 50 m with an associated sampling rate of 10 to 11 Hz during Deployment 2, and the range for the Blueview set to 10 m.

Schematics of the sonar orientations are provided below, with the plan view shown in Figure 3 and profile views for the first and second deployments in Figures 4 and 5. Example sonograms for the Gemini and Blueview are provided in Figures 6 and 7.
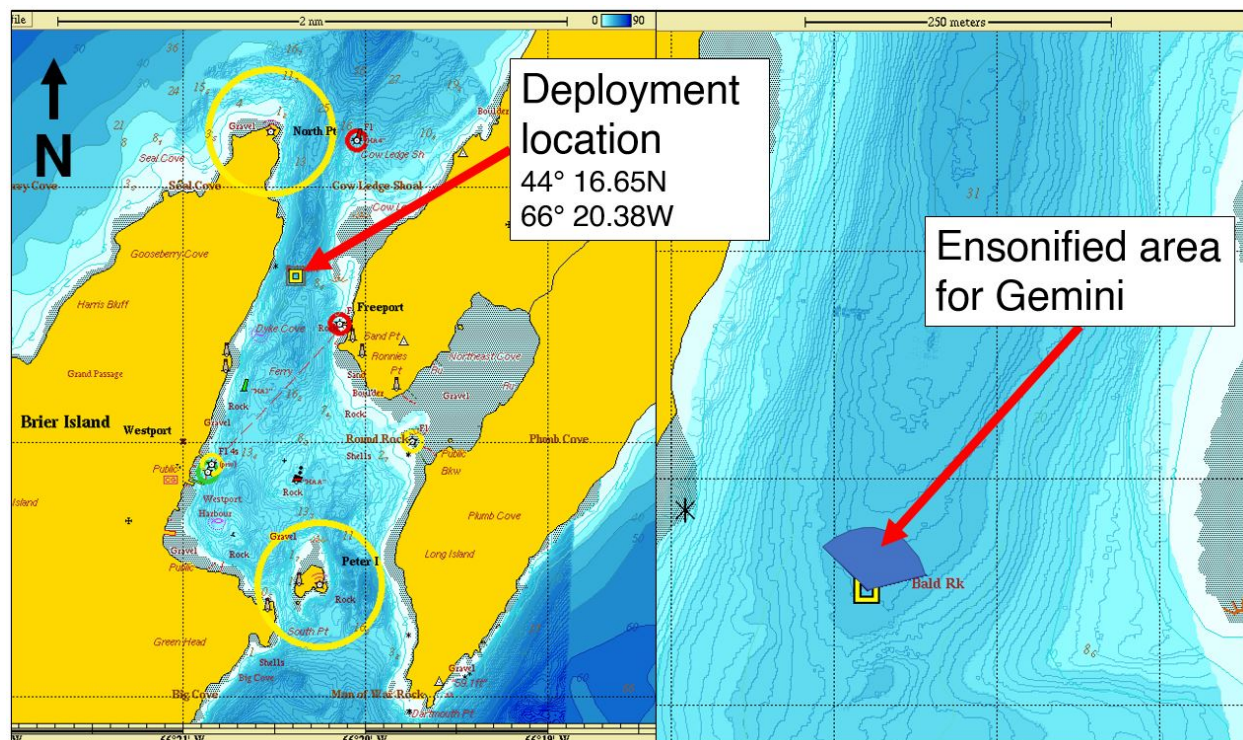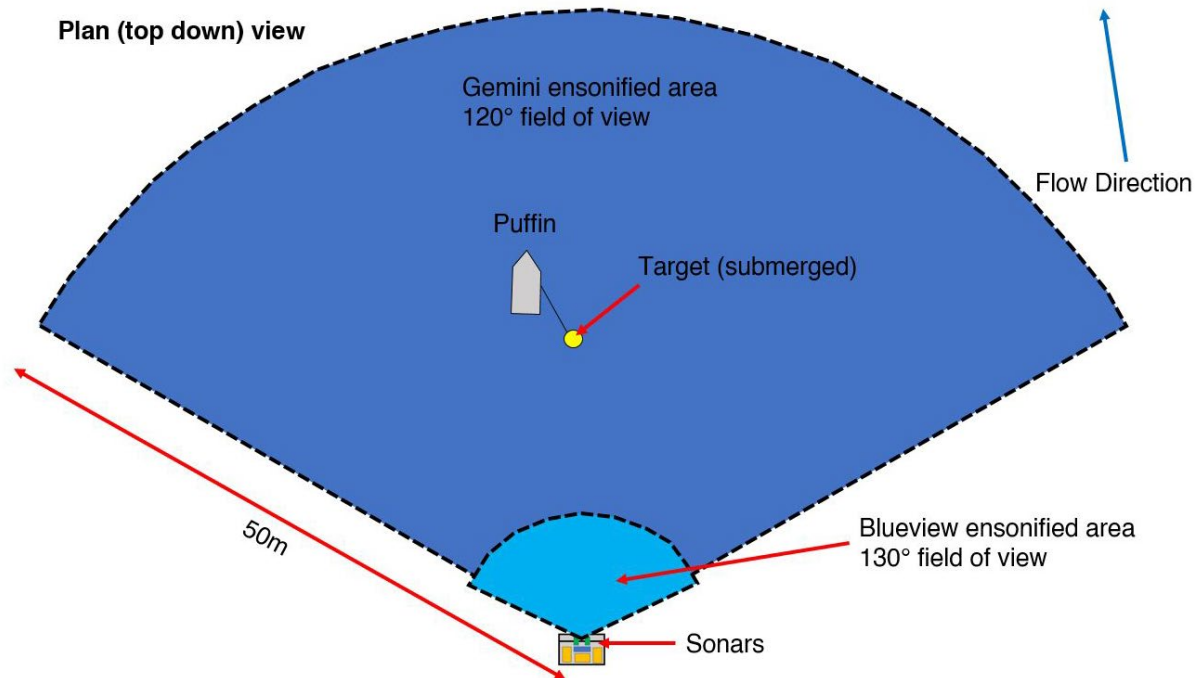

Figure 2: Deployment location

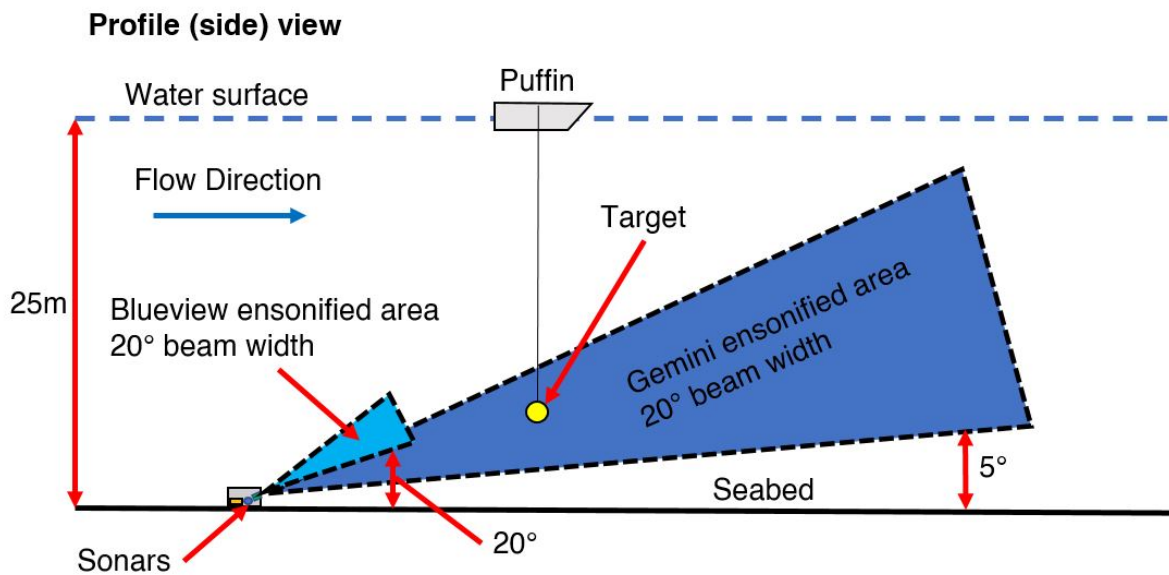*Figure 3: Experiment schematic - plan view*

Figure 4: Experiment schematic - profile view - deployment 1
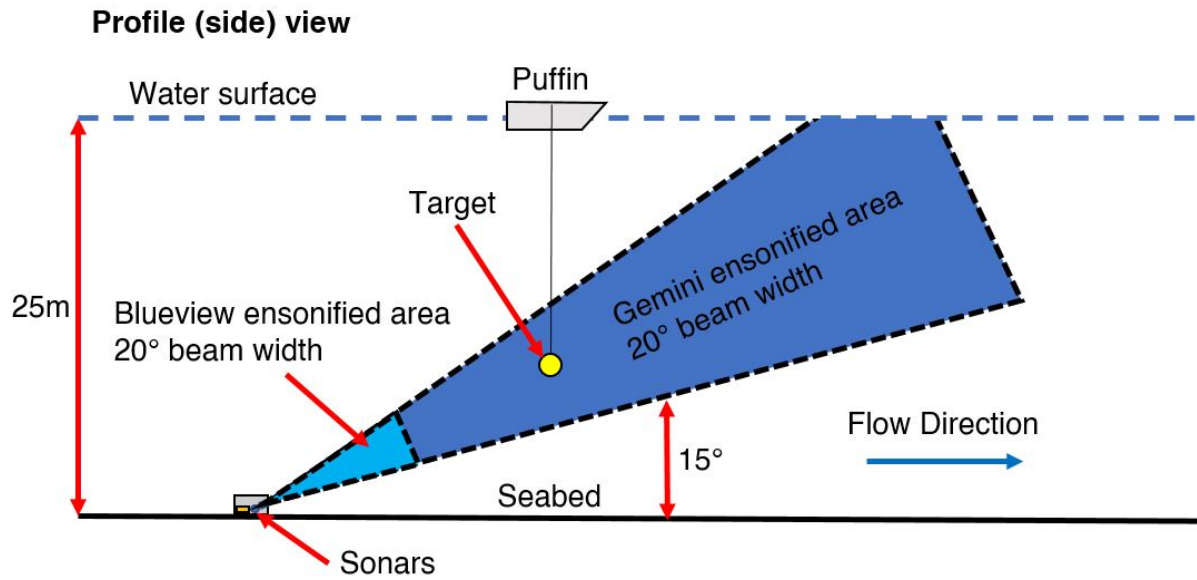
Profile (side) view

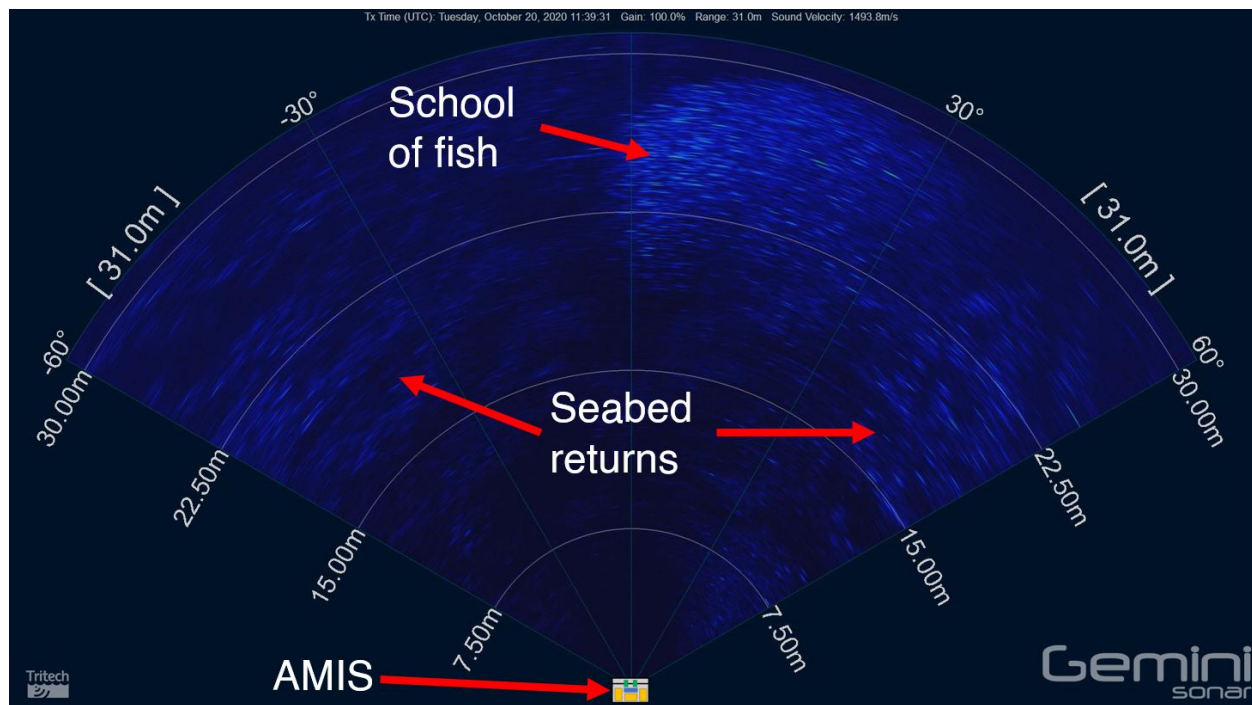*Figure 5: Experiment schematic - profile view - deployment 2*

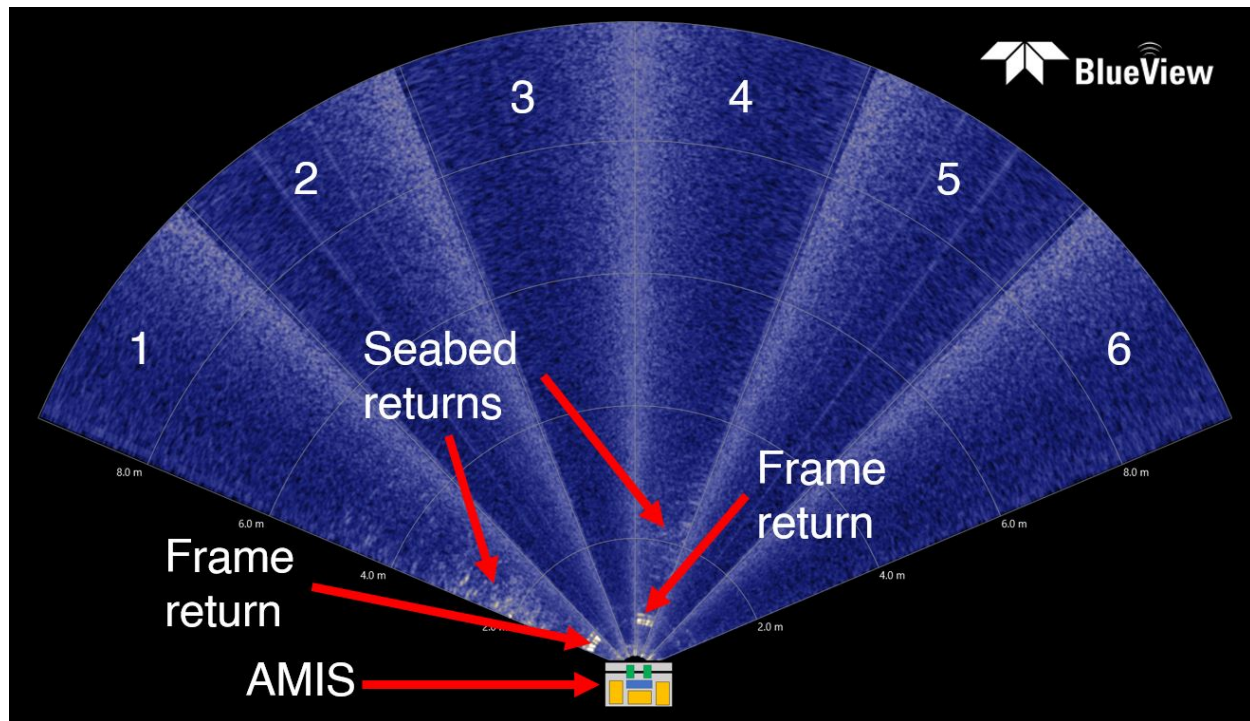*Figure 6: Example sonagram - Gemini first deployment*

Figure 7: Example sonogram – Blueview second deployment

2.2: Data Collection

Three targets were used during data collection: a 0.45 kg (1 lb.) (9.5 cm long x 3.8 cm max diameter) lead fishing weight (Target 2), approx. 12 cm diameter basalt rock in a lobster bait bag (Target 3), and a V-Wing glider (Target 4) (approx. 52 cm wing tip to tip and 46 cm nose to tail) from Dartmouth Ocean Technologies (DOT). The V-Wing is designed to create downforce and maintain orientation in flow, with approximately (27 kg) 60 lbs. of downforce in 2.5 m/s flow. The target numbers were chosen to remain consistent with the convention used in vessel mount project (Trowse et al. 2020). The 1 inch diameter tungsten carbide sphere (Target 1 in the vessel mount project) was not included due to its acoustic similarity to Target 2 and the need to reduce the number of targets based on a relatively short data collection window.

Targets were suspended beneath research vessel Puffin (shown in Figure 8) while drifting through the study area.   The Puffin repeatedly travelled to a position upstream from the sonars, then drifted with the tidal flow such that the drift trajectory allowed the targets to pass through the sonars' ensonified areas. The Puffin operated with its dual frequency Raymarine transducer (depth sounder and fish finder) turned off to avoid acoustic interference and collected flow

measurements with a RDI 600 kHz ADCP periodically when changing between target types. The ADCP was out of the water during target deployments.

Targets 2, and 3 were suspended from the Puffin using a hand line spool with 200 pound test monofilament fishing line. Target 4 was suspended using 1/4 inch Polysteel fishing line due to the increased downward force, increased cost of the target (reducing risk of loss), and ease of handling. No metal was included in the target suspension system, knots were used to secure the targets with no hooks, shackles, etc. below the water line.

A series of 5 to 15 drifts were conducted for each target, with heights above the seabed that were consecutively increased at 3.6 m (2 fathom) intervals and with minor variations in the drift trajectory to the east and west of the AMIS deployment location. More drifts were conducted for Target 4 due to the higher level of control over depth and horizontal position relative to the Puffin. The AMIS system was fully autonomous, so no live view of data collection was available.
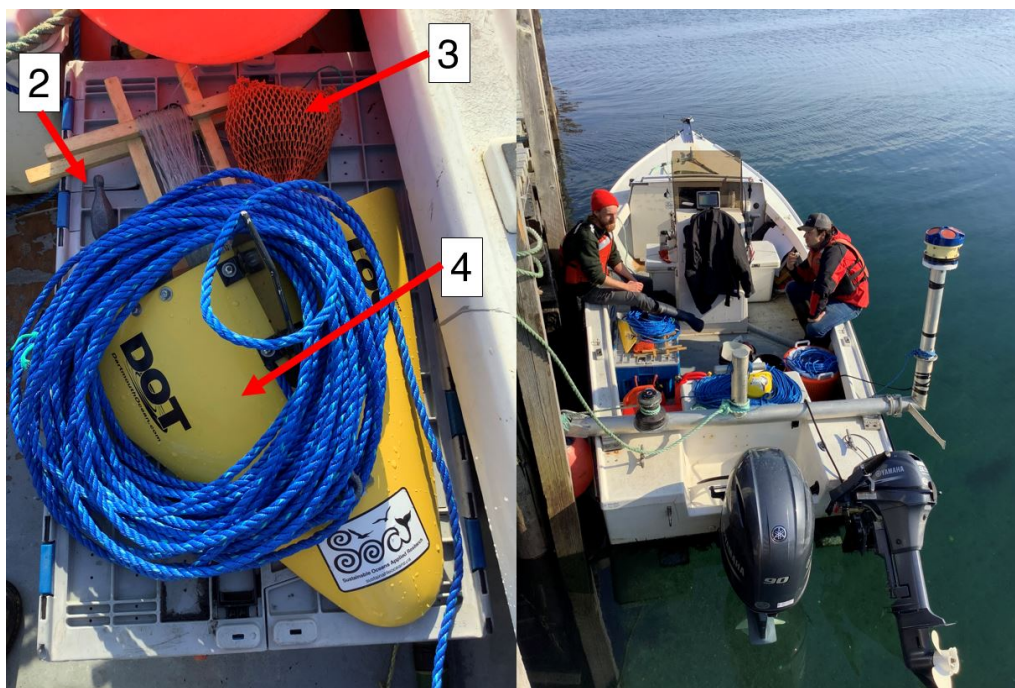

Figure 8: Targets and research vessel Puffin

2.2   Data analysis

The data collected in Grand Passage were manually analyzed to evaluate the performance of the Gemini and Blueview multibeam imaging sonars for detecting and tracking targets in strong tidal flow. The visualization and organization of the data were conducted using the proprietary software packages associated with each sonar: Gemini SeaTec and Teledyne ProViewer[1]. SOAR used these software packages for data review and organization by target type.

Consistent with the vessel mount project the sonar images were exported to video (1920 x 1080 resolution) to facilitate ease of sharing and consistency in the manual analysis.   Video framerates were set to display data at 2x real-time speed. The ability to use increased payback speed was apparent from SOAR's initial analysis of the data files and utilized to demonstrate an increase in efficiency that may be applicable to active monitoring of tidal turbines.

Based on the results of Trowse et al. (2020), acoustic interference between the Gemini and the Blueview was expected. The signatures of acoustic interference for both instruments were consistent with those observed in the Trowse et al. vessel mount study.

2.2.1   Gemini

The video files from the Gemini were organized into training and test data sets, which were shared with 7 sonar observers who conducted the manual analysis, including participants from SOAR, Luna Sea Solutions, FORCE, Mi'kmaw Conservation Group, and MarineSitu. The training data set provides examples where each target is detected and tracked with a red circle indicating target position and a photograph from the optical camera identifying the target.   The test data set included 41 data files where it was left to the observers to detect, track, and identify the targets.

---

[1] The development of automatic data processing algorithms for multibeam imaging sonars is an active area of research. Recent publications (e.g. Cotter and Polagye, 2020) on these methods have demonstrated the ability to detect and track targets with some ability to automatically classify between biologic and non-biologic classes. This classification level of processing typically relies on information from multiple instruments for co-registration of known targets (Joslin 2019).   However, there is currently no software readily available with known ability to conduct reliable data analysis in turbulent flow with high levels of air entrainment. Therefore, data were analyzed manually to meet the primary objectives of the study.

A standard spreadsheet was provided to each observer including columns for:

- File number (for SOAR to cross-reference the data files)
- Target present (yes/no)
- Target identification
  - Type (1 through 4)
  - Certainty (1 low to 5 high)
- Detection range (minimum and maximum)
- Ability for detection and tracking (1 low to 5 high)
- Notes describing the trajectory of the target.

The results were categorized by target type and used to evaluate the performance of the Gemini including the effects of flow speed.   The test data set included 3 files for Target 2, 9 files for Target 3, and 29 files for Target 4. The analysis was consistent with methodology for the vessel mount project, providing a quantitative comparison of performance for the Gemini sonar.

Links to the training and test data sets for are provided below. The data are best viewed in video form. As such, readers of this report are encouraged to watch these data videos for better understanding of the results and conclusions discussed in the following sections. A screen shot from the training data set is provided for each target in Figures 9 through 11.

Gemini training data   https://vimeo.com/483141927
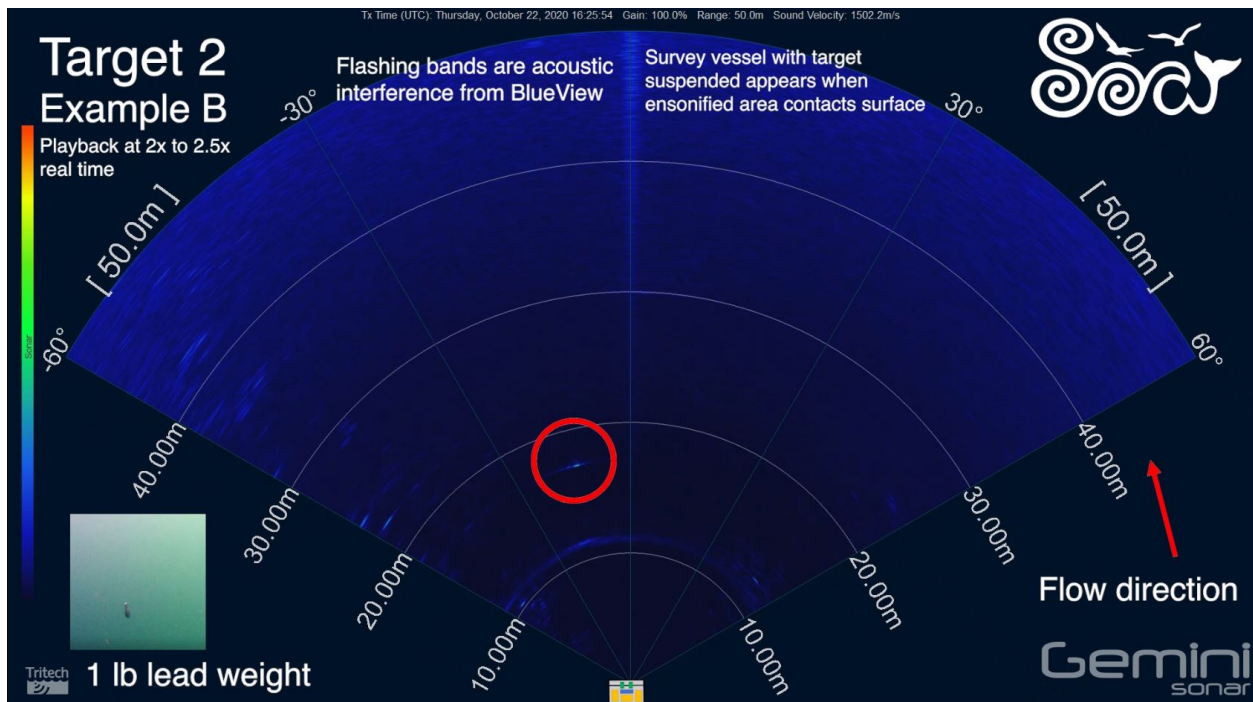Gemini test data with 50m range   https://vimeo.com/483142328

Figure 9: Example from training data - Gemini - Target 2
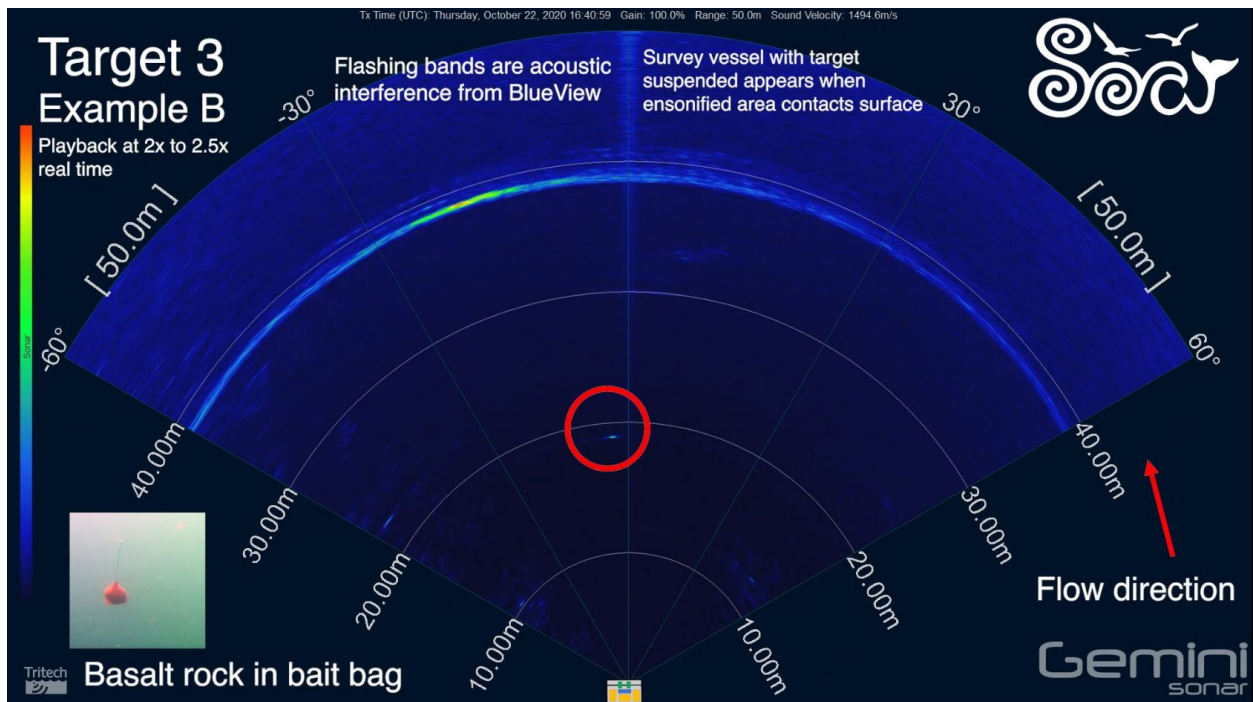
Figure 10: Example from training data - Gemini - Target 3
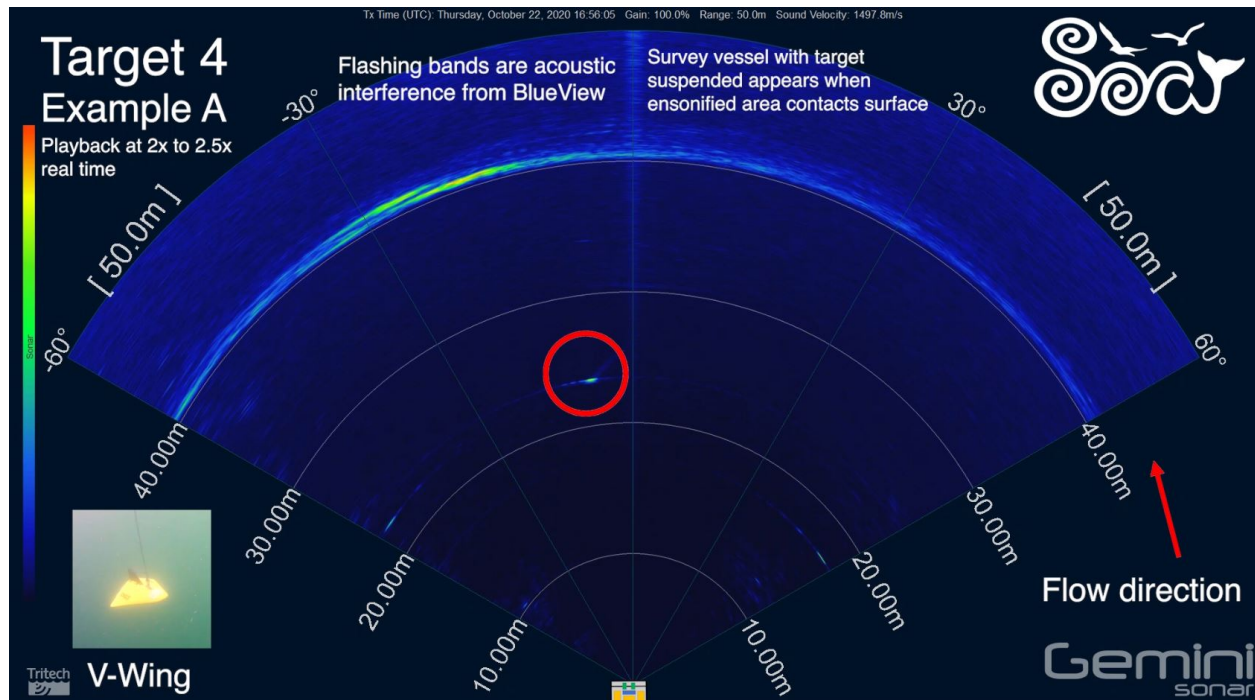
Figure 11: Example from training data - Gemini - Target 4

2.2.1 Blueview

Due to the small ensonified area of the Blueview, insufficient sightings of known targets were collected to generate training and test data sets. A manual analysis was conducted by SOAR, with a focus of events of concurrent detection by the Blueview and Gemini including natural targets (primarily fish) and occasionally the artificial targets used in our methodology. The data are discussed further in the Results section, including comparison of the two sonars.

3.0   Results and Discussion

3.1   Analysis of Gemini training and test data

A summary of results from the manual analysis of the Gemini test data is provided in Table 2, where observers' scores for target present (detected), target identified, max range tracked, and ability to detect and track targets were used to evaluate the performance of the sonar. Only data from Deployment 2 were used for consistent range (50 m) with the vessel mount project, with the comparison discussed in Section 3.4.

Table 2: Summary of results for Gemini, Deployment 2

Target type	Target present % correct	Target type % correct	Max range tracked % of set value	Ability to (1 to 5)	
				Detect	Track
Gemini (50m range)					
1					
2	95%	81%	74%	3.4	2.7
3	100%	43%	91%	4.3	3.8
4	100%	58%	99%	4.6	4.3
All	**99%**	**56%**	**95%**	**4.4**	**4.1**

The observers were able to reliably detect all targets in the majority (99%) of the test files, with tracking close to the 50 m range for Targets 3 and 4.   Tracking range was reduced for Target 2, which is significantly smaller than targets 3 and 4. However, it is not clear whether the target tracks ended due to performance of the sonar or our ability to keep the 1 lb lead weight within the ensonified area. Conversely, the smaller size of Target 2, relative to Targets 3 and 4, aided in target identification, with 81% of the instances being correctly identified. Greater difficulty differentiating between Targets 3 and Target 4 is reflected by the lower target type percent correct scores.

The relationship between flow speed and sonar performance was evaluated by calculating the coefficient of determination, R^2, value between the flow speed and the detection and tracking scores. R^2 is a measure of the proportion of the variance in the dependent variable (detection and tracking scores) that can be predicted from the independent variable (flow speed). R^2 values range from 0 to 1, with 1 being one-to-one correlation. Flow speeds ranged from 1.4 to 2.4 m/s. The R^2 values for detection and tracking are 0.07 and 0.04, respectively, suggesting no significant relationship between flow speed and ability to detect and track the targets. A wider

distribution of ability scores is apparent for the higher flow speed cases (see Figure 12). However, this may be a result of a larger number of samples at higher flow speeds as well as the distribution of target usage relative to flow speed.
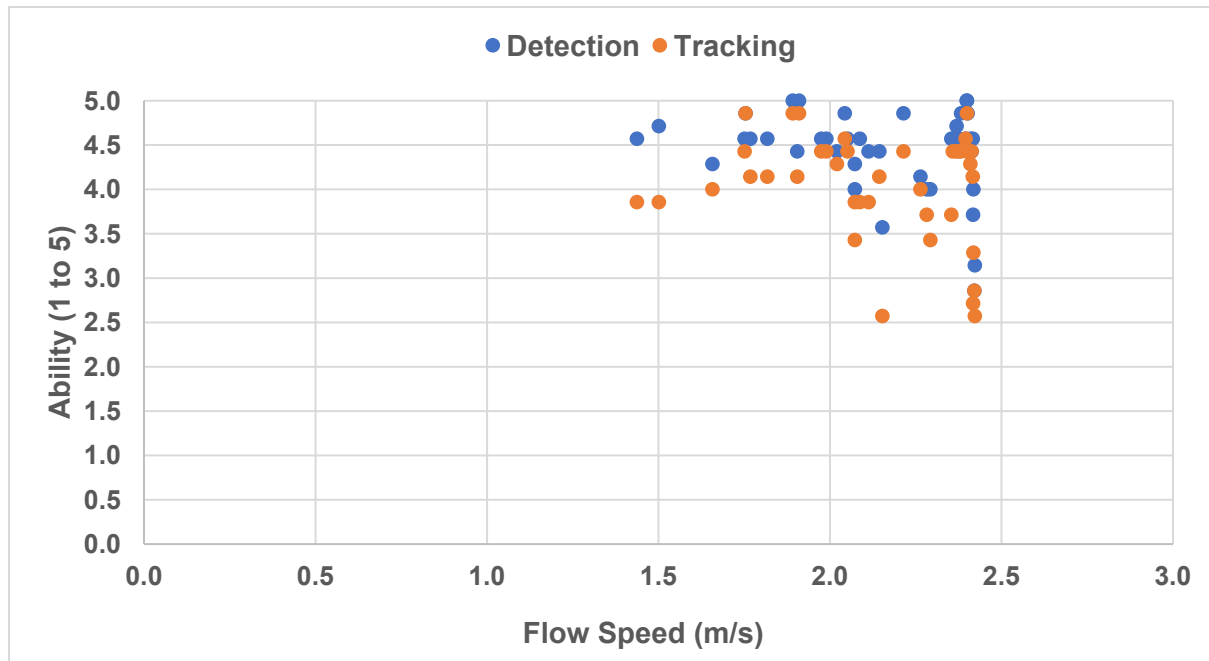

Figure 12: Effect of flow speed on Gemini target detection and tracking

3.2   Comparative analysis of Gemini and Blueview concurrent target detections

Data sets from both deployments were reviewed by SOAR to identify instances where natural targets (primarily fish) and occasionally the artificial targets used in our methodology could be identified in the data from both the Gemini and the Blueview. A link to a video file with 21 comparative cases is provided below, where cases 1 through 15 are from Deployment 1 and cases 16 through 20 are from Deployment 2.   As with the training and test data analysis, the sonar data are best viewed in video form. Screen shots from cases 1, 4, 8, and 18 are also provided in Figures 13 through 16.

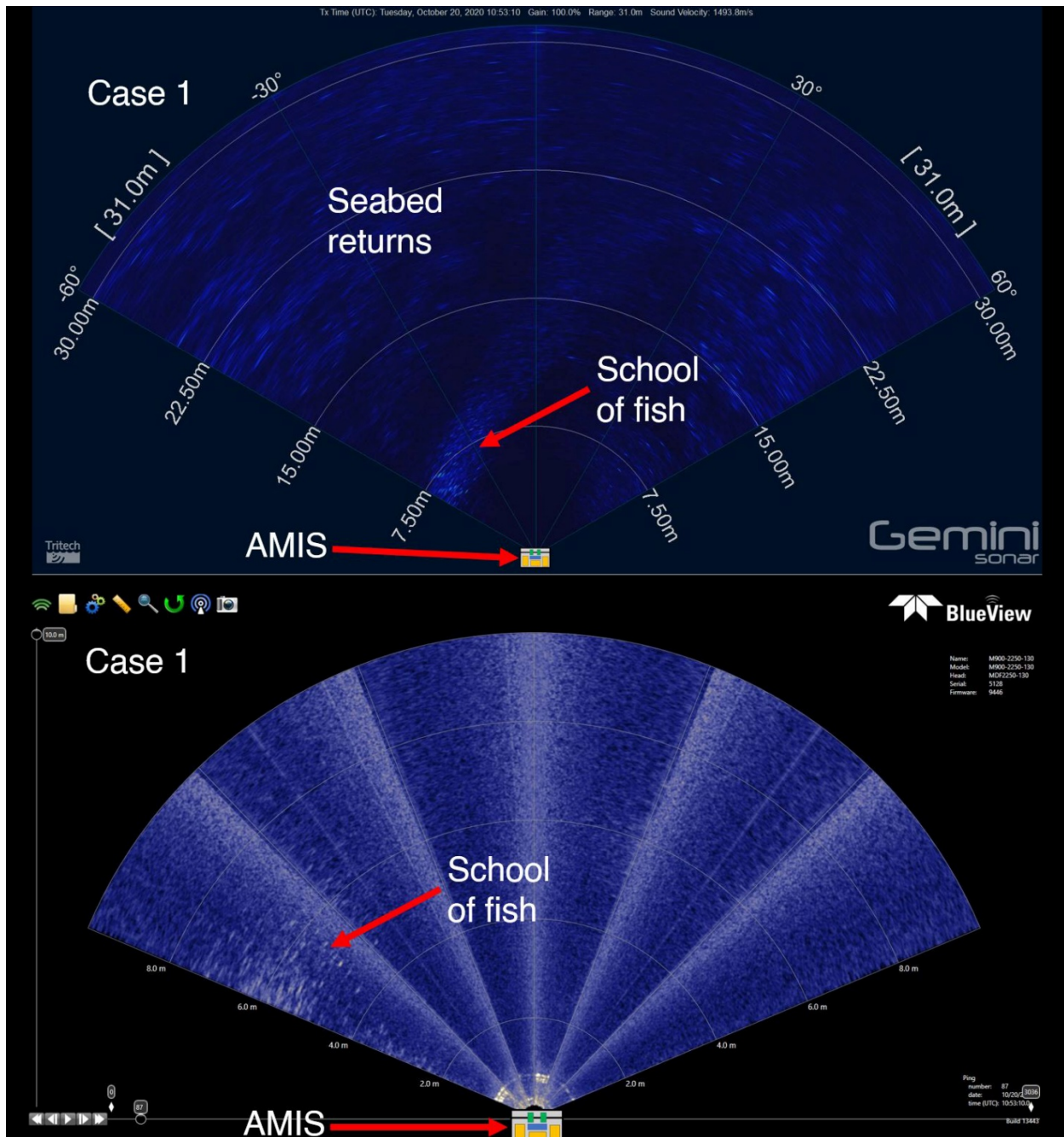Concurrent Blueview and Gemini   https://vimeo.com/487808248

Figure 13: Concurrent Gemini and Blueview target detection - Case 1
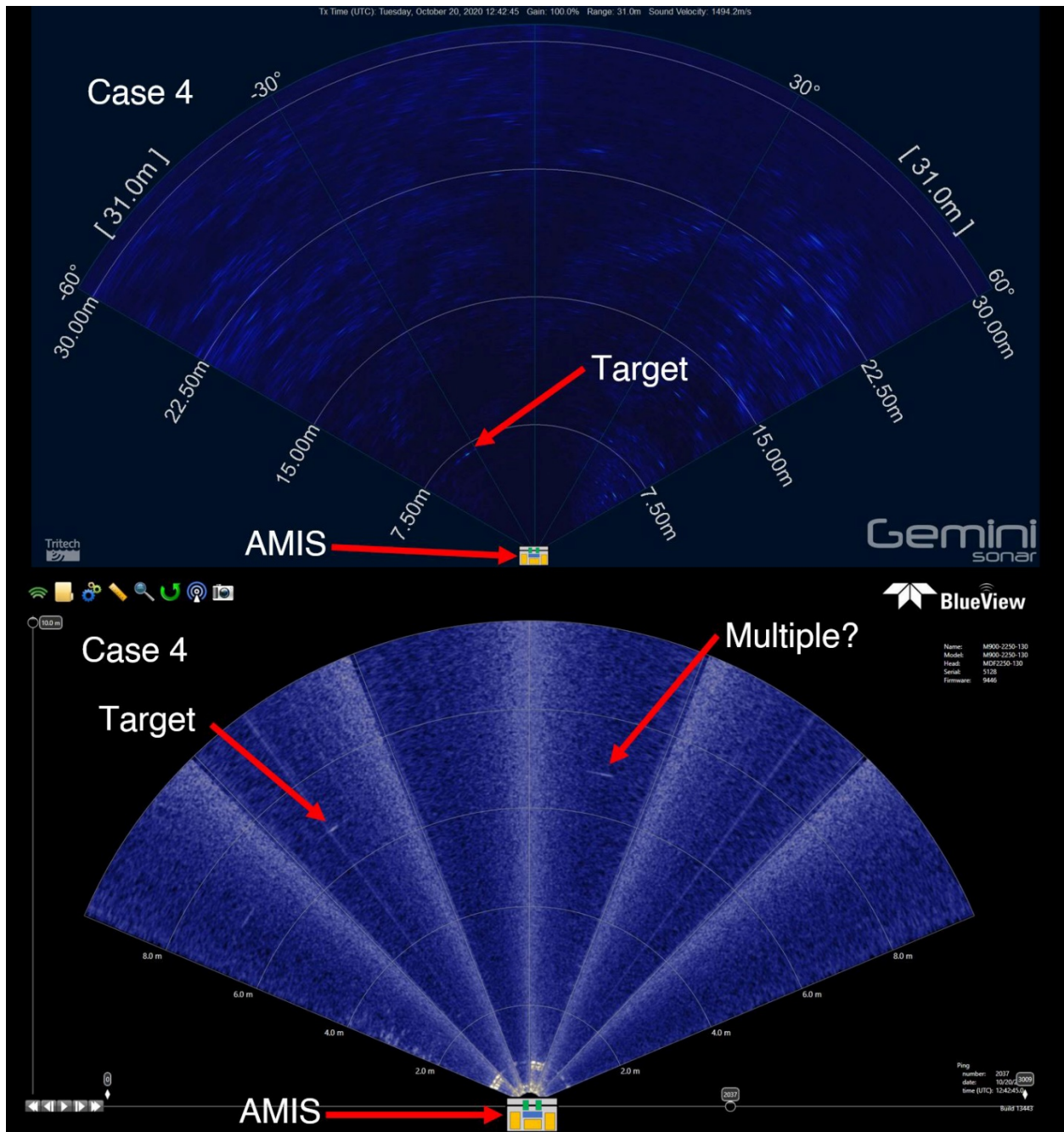
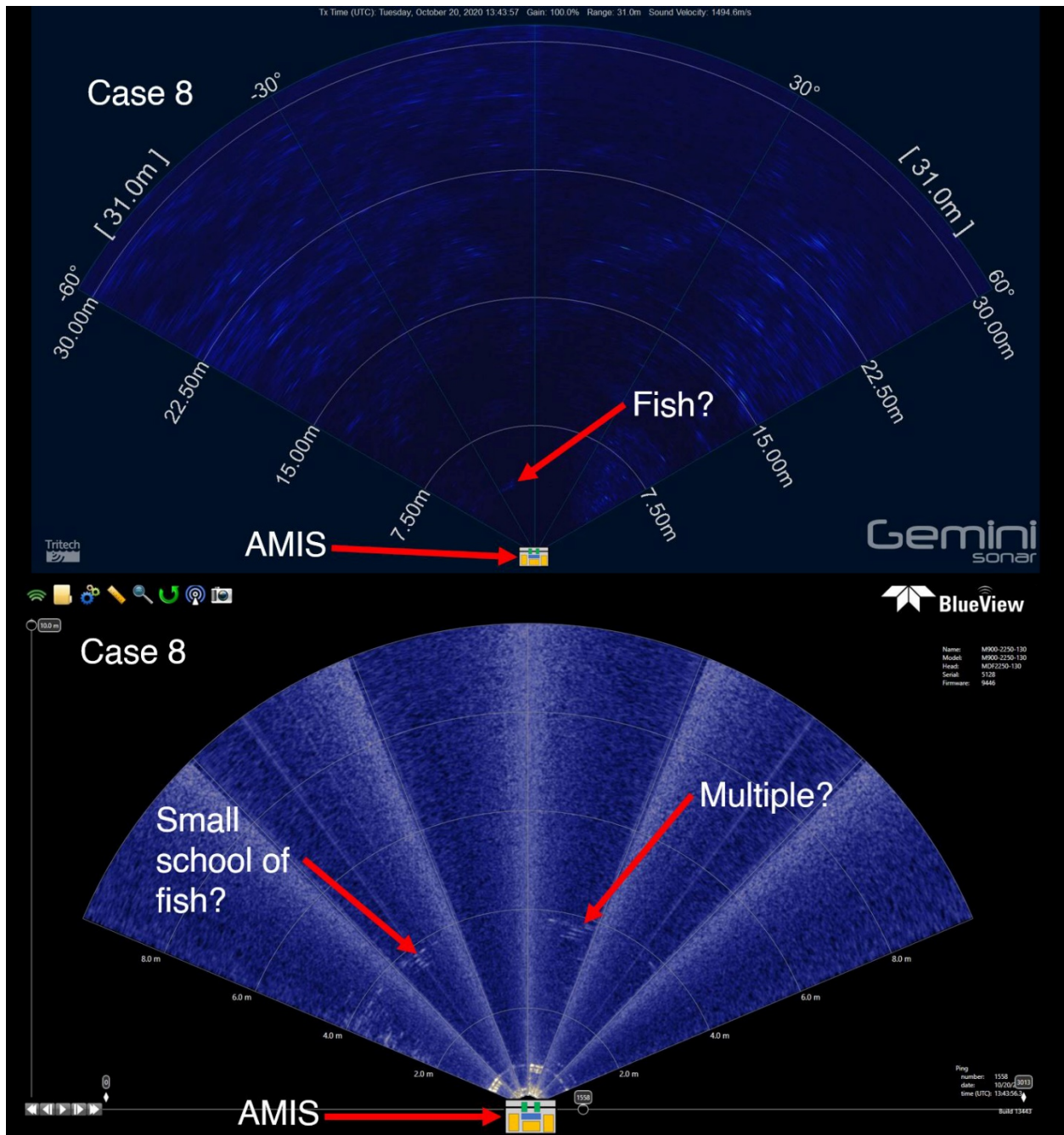*Figure 14: Concurrent Gemini and Blueview target detection - Case 4*

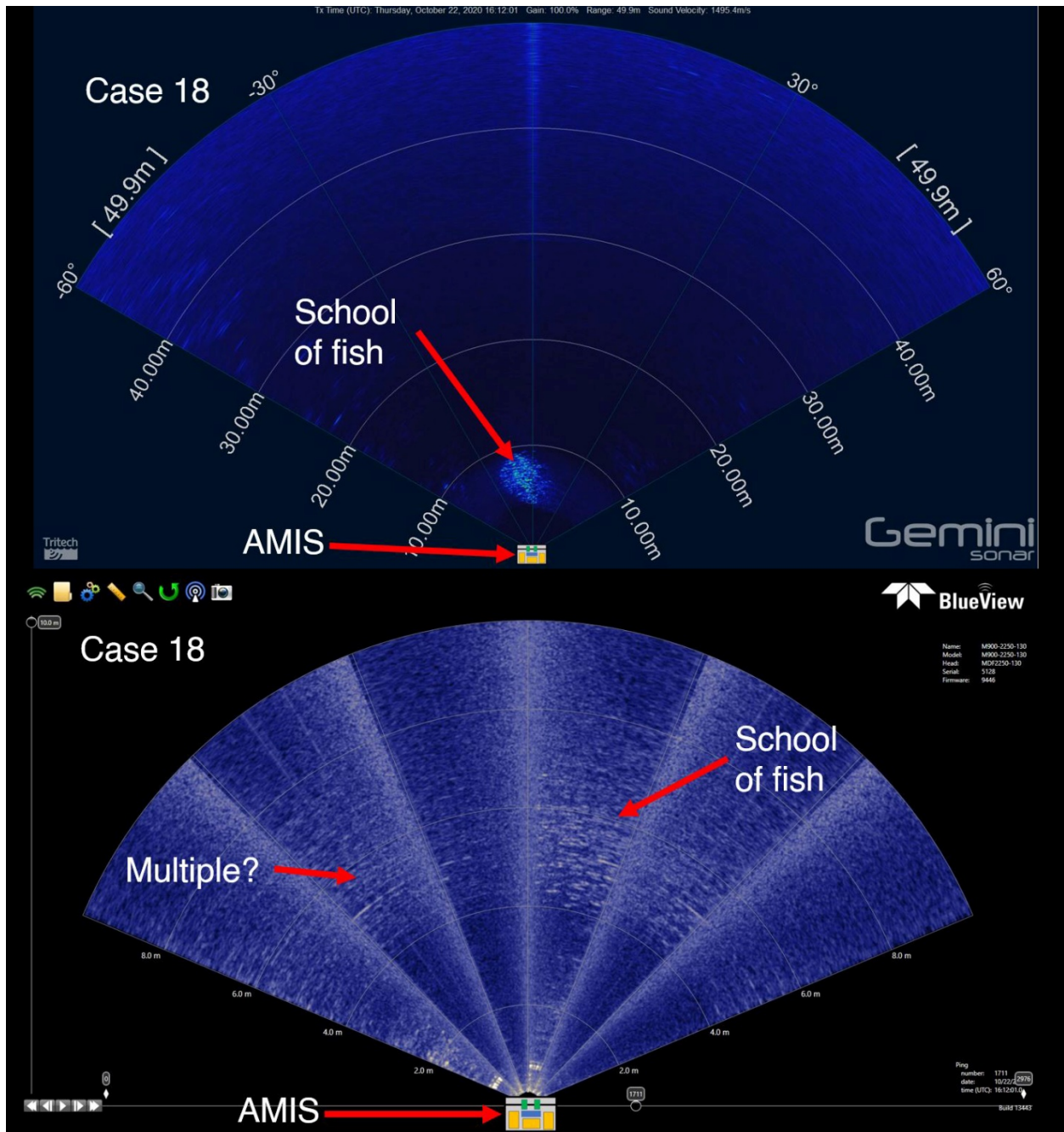*Figure 15: Concurrent Gemini and Blueview target detection - Case 8*

Figure 16: Concurrent Gemini and Blueview target detection - Case 18

Targets that were visible in the sonograms of both the Gemini and Blueview (up to 10 m range) were generally visible at larger ranges using the Gemini – often to its full sampling range of 30 m for Deployment 1 and 50 m for Deployment 2. For the first deployment with the ensonified area angled at 5 to 25° there were areas of seabed returns, but target identification and tracking were still possible due to the static nature of the seabed and continuous movement of the target.

When observing targets at close range, the Blueview demonstrated ability to provide the additional resolution expected of a higher frequency system. For example, in case 8, shown in Figure 15, individual fish in a small school are clearly identifiable. Fish in close proximity (< 2 m) to AMIS were well resolved by the Blueview. Though identifying discrete targets (i.e., individual fish in a school) was also possible with the Gemini at close range, it was subject to limitations associated with sampling frequency (range dependent), wavelength of the transmitted ping (720 kHz), and resolution of the sonogram (pixels/m).

3.3 Hardware limitations

The MKI model of the Blueview M900-2250 suffers from hardware limitations, one of which manifested in this study as multiple high-noise bands at fixed angular coordinates in the sonograms (see the lighter-coloured boundaries between numbered sectors in the Blueview sonogram shown in Figure 7). Targets generally could not be identified when they coincided with the bands, as the backscattered target signals were of comparable magnitude to the background noise level. This is consistent with observations made during the Trowse et al. (2020) vessel mount project.

SOAR contacted Teledyne technical support for further information, and were informed that Teledyne have released a second version (MKII) of the M900-2250, which mitigates this issue at the expense of a narrower swath width (reduced to from 130 to 45°). Further information is provided in the report for the vessel mounted project.

Some phenomena observed in the Blueview data suggest a transducer alignment issue. As noted in the Methodology section, despite the upward tilt of the Blueview at angles of 20° to 40° from the horizontal plane of the AMIS frame (Deployment 1) and 15° to 35° (Deployment 2), the frame and seabed are visible in sectors 1 and 4 of the sonogram. The lack of an acoustic shadow suggests that the frame and bottom returns are from sidelobes rather than the main acoustic beam. A potential transducer misalignment could explain target disappearance

observed during data collection and analysis for the vessel mount project, where target tracks were regularly lost when travelling from the area occupied by one sector to the adjacent one. In some cases the Blueview sonograms show multiple returns from targets, as shown in Figures 14 through 16, that are not visible on the Gemini. If an artifact of a hardware issue it could result in uncertainty in target position, especially relevant in application to monitoring near-field interactions between marine animals and tidal turbines. Note that we have not yet contacted Teledyne regarding these issues.

3.4   Comparison to vessel mounted multibeam sonars

A comparison of the observers' scores for the bottom and vessel mounted Gemini cases is provided in Table 3. The vessel mount data (see Trowse et al. 2020) were analysed using the same methodology outlined in this report: that is, manual review by sonar observers using training and test data sets. For the vessel mount data, the values for "All" are increased from those in Trowse et al. 2020 due to the exclusion of Target 1 (1 inch tungsten carbine sphere) from the calculation. Target 1 was the smallest of the four targets and was characterized by the lowest scores.

Table 3: Comparison of results from bottom and vessel mounted Gemini

Target type	Target present % correct	Target type % correct	Max range tracked % of set value	Ability to (1 to 5)	
				Detect	Track
Gemini Bottom Mount					
2	95%	81%	74%	3.4	2.7
3	100%	43%	91%	4.3	3.8
4	100%	58%	99%	4.6	4.3
All	99%	56%	95%	4.4	4.1
Gemini Vessel Mount					
2	95%	23%	81%	3.4	3.1
3	96%	33%	92%	4.1	3.9
4	100%	79%	100%	4.5	4.5
All	97%	46%	91%	4.0	3.9
Bottom - Vessel Mount Scores					
2	0%	58%	-7%	0.0	-0.4
3	4%	10%	0%	0.2	-0.1
4	0%	-22%	-1%	0.1	-0.2
All	2%	10%	4%	0.4	0.2

The target-averaged scores for the bottom mount data set are slightly higher in all categories relative to the vessel mount data. We had substantially greater control of target positioning during the vessel mount data collection. We were able to start tracks closer to the sonars and hold targets at a constant range. This provided observers more time to detect and identify the targets at close range. Despite this, the greater bottom mount scores may not be surprising given the reduction in data contamination by wave and wake-related entrained air.

Proximity to the sonars likely increased the observers' ability to correctly identify Target 4 from the vessel mounted sonar. The characteristic shape of Target 4 was easily recognizable when viewed at close range (i.e., within ca. 20 m), but it exhibited acoustic returns that were less easily differentiated from Target 3 at larger ranges. The omission of Target 1 from the bottom mount experiment led to Target 2 being easier to distinguish (no confusion between similar targets) and is likely the reason for greater success compared to the vessel mount case. The reduced ability to identify Target 4 in the bottom mount data is most likely related to the reduced amount of time it was present in close range to the sonars.

4.0   Conclusions

The project addressed the objective of assessing the performance of bottom deployed multibeam imaging sonars for target detections, including the extent of signal interference from waves/turbulence, and entrained air.

The Tritech Gemini 720is received high scores from the observers in the ability to identify the presence of, visually detect, and track targets in videos displaying sonogram data output. The observers correctly identified the presence of a target in 99% of cases, and gave average scores greater than 4 out of 5 describing their visual detection and tracking ability. Targets were correctly identified roughly 50% of the time.

The results indicate a slight increase in visual detection and tracking ability relative to similar data collected from a vessel mounted orientation, and a net decrease in ability to correctly identify targets. We attribute the apparent increase in efficacy in the bottom mount case to the reduced presence of entrained air from waves and vessel wake in the sonar's ensonified areas. The reduction in percentage of correctly identified targets in the bottom mount case may be attributable to the increased ranges between target and sonar, as well as faster movement of the targets through the ensonified area. In general, the range to the target within the Gemini's detection area appears to play an important role in the ability to resolve and identify targets with diameters between ca. 5 and 50 cm.

For the bottom mount experiment, we were drifting guided by the currents and the AMIS deployment location, and were highly successful in getting detectable, identifiable, and trackable targets into the Gemini's ensonified area. Due to the smaller area ensonified by the Blueview, we had difficulty getting targets into the field of view. The limited number of target sightings precluded our use of the planned training and test video methodology. SOAR instead conducted a comparative analysis for which targets of opportunity (e.g., fish) were detected in the fields of view of both sonars. The Blueview demonstrated ability to resolve close-range (less than 10 m) targets. However, the use of the Blueview data was limited by the same hardware issues described by Trowse et al. (2020), and in the Hardware Limitations section of this report.

The Teledyne Blueview M900-2250 MKI is an impressive technology that offered the ability to resolve finer scale features of the targets and their movements in some cases. However, the persistent high-noise bands resulting from a known hardware issue and an apparent transducer

alignment issue (discussed in Section 3.3) represented substantial impediments to reliable target detection and tracking. We conclude that data from the Blueview did not add substantial value or insight to the target analysis when used in conjunction with the Gemini. This should not rule out potential use of other MHz frequency multibeam sonars for monitoring the 10 m range in a combined sonar approach, including MKII of the Blueview.

SOAR recommends use of the Tritech Gemini 720is for application to monitoring interactions between marine animals and tidal turbines.   It is likely that this technology will contribute significantly to effective monitoring and advancing knowledge of importance to regulators and other stakeholders. The Gemini demonstrated a high level of utility for detecting and tracking targets from vessel and bottom mounted orientations in tidal flows up to approximately 2.5 m/s, which is near to the maximum flow speed at Grand Passage. The Minas Passage is known to have higher flow speeds, which may result in higher levels of air entrainment. For comparison to the Minas Passage a flow speed exceedance curve is provided in Figure 18 calculated using depth averaged ADCP measured flow speeds from FORCE Berth Site A (45.3649 -64.4308). It shows maximum flow speeds of approximately 4.5 m/s and 2.5 m/s to be exceeded approximately 36% of the time, or conversely, flow speeds to be less than 2.5 m/s 64% of the time.
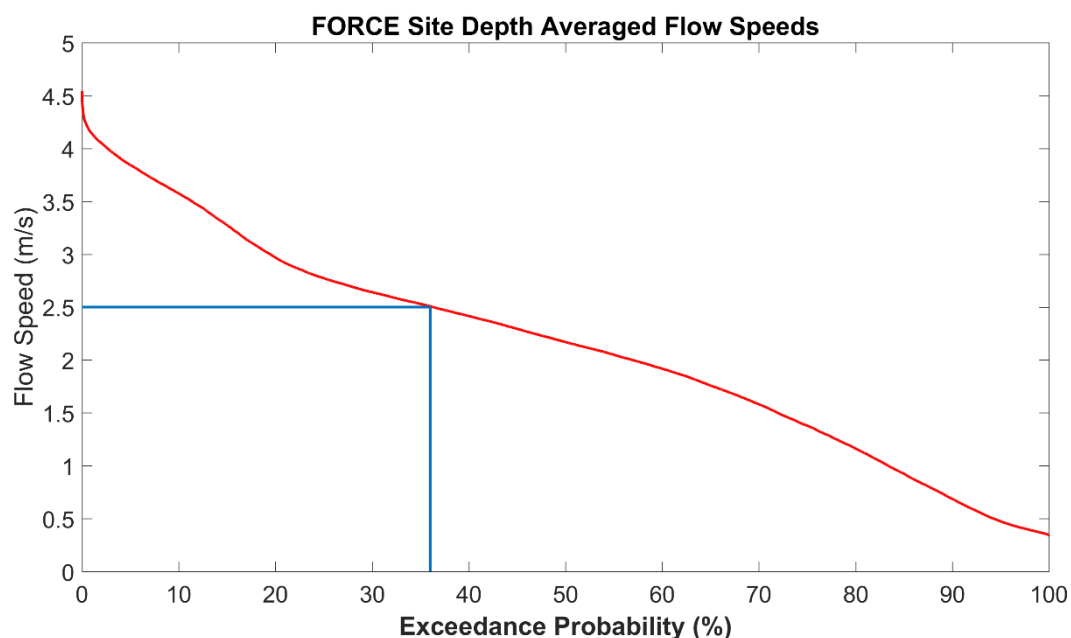

Figure 17: FORCE Site flow speed exceedance curve

Data analysis was successful for manual observers viewing data played back at 2x real time speed. Future work should consider efficiencies associated with accelerated data playback and could support use of software with variable speed playback that also allows for time and space encoded notes.

For planning future data collection careful consideration of sonar orientation is critical. In an oceanographic context, the ensonified areas are relatively small and are sensitive to returns from seabed and sea surface. Careful planning of the ensonified area is required based on the questions to be addressed by the monitoring while minimizing unwanted returns. The ability to adjust orientation is highly beneficial.

With respect to deploying multibeam sonars from the surface (i.e., vessel) or seabed, the sonars performed well from both positions, despite increased levels of air entrainment in the vessel mount case. The selection of deployment position for monitoring tidal turbines is likely to be defined by the nature of the tidal device (floating or seabed mounted) and the questions to be addressed by the monitoring.

Some level of acoustic interference from other active sonar systems must be expected when carrying out deployments in or near active ports or passages, whether from passing pleasure or commercial craft, or from other marine operations. Data analysis methods and systems should be designed with this in mind, treating acoustic interference as an element to be anticipated and mitigated where possible through software processing.

Manufactured targets were the focus of this experiment, but marine animal targets were also observed in abundance in Grand Passage. Data were collected that show the multibeam sonars to perform well in detection and tracking of fish and other targets of opportunity. These data require additional analysis, but some preliminary images are available. This connects with the secondary expected outcome of the project, providing data sets to support further research beyond the scope and timeline of this project.

Further testing of bottom mounted multibeam sonars would be useful in four focus areas, including:

1) fish and other marine animals in locations and seasons (times) with high levels of animal abundance and variety,

2) evaluating most effective sonar orientations for monitoring the near field of tidal turbines,

3) flow speeds that exceed 3 m/s, and

4) increasing efficiency in data assessment, possibly including reliable automation.

This work should build upon success in Grand Passage to conduct next steps in stronger flows present in Petit Passage and Minas Passage.

The report titled "Field Assessment of Multi-beam Sonar Performance in Surface Mount Deployments" (Trowse et al. 2020) provides similar analysis for the case of surface mounted Gemini 720is and Blueview M900-2250.

References:

Trowse, G., Guest, T., Feiel, G., Cheel, R., and Hay, A.E. 2020. Field Assessment of Multibeam Sonar Performance in Surface Mount Deployments. Final Report to the Offshore Energy Research Association of Nova Scotia. SOAR – Sustainable Oceans Applied Research, Technical Report. Freeport, NS, Canada.

Bevelhimer, M., Colby, J., Adonizio, M.A., Tomichek, C., and Scherelis, C. 2016. Informing a tidal turbine strike probability model through characterization of fish behavioral response using multibeam sonar output. *In* Oak Ridge National Laboratory Tm-2016/219. Available from http://www.ntis.gov/help/ordermethods.aspx%5Cnhttp://www.osti.gov/contact.html.

Cotter, E., Murphy, P., and Polagye, B. 2017. Benchmarking sensor fusion capabilities of an integrated instrumentation package. Int. J. Mar. Energy **20**: 64–79. Elsevier Ltd. doi:10.1016/j.ijome.2017.09.003.

Cotter, E. and Polagye, B. (2020). Automatic Classification of Biological Targets in a Tidal Channel using a Multibeam Sonar. Journal of Atmospheric and Oceanic Technology, DOI: 10.1175/JTECH-D-19-0222.1

Foote, K.G., Chu, D., Hammar, T.R., Baldwin, K.C., Mayer, L.A., Hufnagle, L.C., and Jech, J.M. 2005. Protocols for calibrating multibeam sonar. J. Acoust. Soc. Am. **117**(4): 2013–2027. doi:10.1121/1.1869073.

Gnann, F. 2017. FAST-2 Test Deployment : Experimental low-flow test of the Gemini Sonar.

Hastie, G. 2013. Tracking marine mammals around marine renewable energy devices using active sonar. *In* SMRU Ltd report number SMRUL-DEC-2012-002 to the Department of Energy and Climate Change. doi:10.1109/CIDM.2011.5949297.

Joslin, J. 2019. Imaging sonar review for marine environmental monitoring around tidal turbines. Available from https://oera.ca/sites/default/files/2019-06/James Joslin Report - Imaging sonar review for marine mammal and fish monitoring around.pdf.

Melvin, G.D., and Cochrane, N.A. 2014. Investigation of the vertical distribution, movement and abundance of fish in the vicinity of proposed tidal power energy conversion devices.

Sanderson, BG, MJ Adams and AM Redden. 2019. Sensor Testing Research for Environmental Effects Monitoring (STREEM). Final Report to the Offshore Energy Research Association of Nova Scotia. Acadia Centre for Estuarine Research, Technical Report No. 127, 68 pp. Acadia University, Wolfville, NS, Canada.

Viehman, H., Gnann, F., and Redden, A.M. 2017. Cape Sharp Tidal Gemini Multibeam Imaging Sonar : Monitoring Report Report to Cape Sharp Tidal Prepared and submitted by. (123).

Viehman, H.A., and Zydlewski, G.B. 2014. Fish interactions with a commercial-scale tidal

energy device in the natural environment. Estuaries and Coasts **38**(Suppl. 1): S241–S252. doi:10.1007/s12237-014-9767-8.

Williamson, B., Fraser, S., … P.B.-I.J. of, and 2017, U. 2017. Multisensor acoustic tracking of fish and seabird behavior around tidal turbine structures in Scotland. IEEE J. Ocean. Eng. **42**(4): 948–965. doi:10.1109/JOE.2016.2637179.

Williamson, B.J., Blondel, P., Armstrong, E., Bell, P.S., Hall, C., Waggitt, J.J., and Scott, B.E. 2016. A self-contained subsea platform for acoustic monitoring of the environment around marine renewable energy devices-field deployments at wave and tidal energy sites in Orkney, Scotland. IEEE J. Ocean. Eng. **41**(1): 67–81. doi:10.1109/JOE.2015.2410851.

Wilson, G.W., and Hay, A.E. 2017. Short-pulse method for acoustic backscatter amplitude calibration at MHz frequencies. J. Acoust. Soc. Am. **142**(3): 1655–1662. doi:10.1121/1.5003788.

Appendix IV

Study 2 – Relative Performance of Surface-Deployed and Bottom-Mounted Echosounders in a Tidal Channel

FINAL REPORT

Dan Hasselman[1*], Louise McGarry[2], Tyler Boucher[1], Jessica Douglas[1] and Shannon MacNeil[1]

[1]Fundy Ocean Research Center for Energy, Halifax, NS
*Corresponding author: dan.hasselman@fundyforce.ca

Table of Contents

1 Executive Summary

Motivation

Scientific echosounders are the standard tool in fisheries science for investigating the abundance, distribution, behavior, and ecology of fish, and have been used for monitoring around tidal energy devices. Echosounders have been deployed on the sea floor in a stationary upward-facing orientation for monitoring around gravity-based tidal energy devices but have also been deployed at the sea surface in a downward-facing orientation, either for mobile surveys or on ships at anchor. The advent of floating tidal energy platforms provides an opportunity to deploy echosounders at the sea surface in a long-term, stationary, downward-facing orientation for monitoring. However, the strong currents that make tidal channels attractive for energy production are often dominated by turbulent hydrodynamic features and associated artefacts that can vary over the course of tidal cycles and may hinder the use of echosounders and other active acoustic technologies. Understanding the extent to which turbulent hydrodynamic features impact the use of a bottom-mounted or surface-deployed echosounder is important for designing effective monitoring systems.

In partnership with the Pathway Program, Sustainable Marine Energy (Canada) Ltd. and the Fundy Ocean Research Center for Energy, undertook a series of studies to understand whether deployment location impacted the efficacy of echosounder technology for monitoring by assessing the relative performance of surface-deployed instruments and a bottom-mounted echosounder. The bottom-mounted echosounder was the Simrad Wideband Autonomous Transceiver (WBAT: from the Simrad EK80 suite of echosounders) mounted on the Fundy Advanced Sensory Technology (FAST) autonomous underwater platform and deployed in Grand Passage, NS in the vicinity of the Sustainable Marine floating tidal energy platform (i.e., PLAT-I). The surface-deployed instruments were deployed via pole mount attached to the leading edge of the starboard pontoon of the PLAT-I platform and included a Sculpin HDC-SubC optical video camera, a Gemini 720is multibeam imaging sonar, and a downward-facing Simrad Wideband Transceiver (WBT: from the Simrad EK80 suite of echosounders).

The primary goal was to collect data to compare target detections for identifying the best placement of echosounders for monitoring in the vicinity of the PLAT-I deployed in a high flow environment. Thus, the objectives of the three studies were to i) investigate the near-surface target detection capabilities of a bottom-mounted, upward-facing, echosounder using a surface-deployed optical video camera (Study 2A), ii) address this same objective over a greater detection range using a multibeam imaging sonar (Study 2B), and iii) investigate the relative performance of a bottom-mounted upward-facing, and a surface-deployed downward-facing echosounder for target detection (Study 2C). This final goal was addressed by identifying the extent of target detection interference due to air entrained in the water by surface waves and turbulence. The PLAT-I rotors were parked during data collection for all three studies. Because of safety concerns for personnel, the PLAT-I and instruments, the FAST platform was deployed at locations in the vicinity of the PLAT-I, but at distances that precluded the possibility of

overlapping sampling volumes between the instruments mounted on the PLAT-I and the FAST platform.

Summary of Findings

No fish images were captured in the 170 hours of optical video data examined for Study 2A and Study 2B. This result was unexpected given that during Study 2A, within the water depths interrogated by the optical camera, the upward-facing echosounder recorded signals consistent with the presence of fish in 55% of the 8.3 hours of echosounder data not obfuscated by entrained air. The images captured by the video camera were of sufficiently high-resolution that the absence of fish likely reflected a lack of fish passing within the camera's field-of-view. Although the optical video data could not be used to cross-reference targets detected by the echosounder, the echosounder data collected during Study 2A contributed to our understanding of the importance of localized hydrodynamic regimes on the ability to collect useable data.

For Study 2B, the image resolution of the imaging sonar was insufficient to identify targets beyond two ambiguous categories: "single fish/debris" and "turbulence/fish/school of fish". A third category denoted instances when the PLAT-I mooring chain was within the imaging sonar field-of-view. During this study, in nominally 100% of the echosounder observation time periods, signals that could be interpreted as fish were detected at depths that coincided with the depth range interrogated by the imaging sonar (i.e., the top 11 m of the water column). However, the imaging sonar identified potential detections for only 22% of the observation periods. The source of this discrepancy likely stems from non-overlapping sample volumes due to FAST platform deployment location for this study. Although the lack of overlapping sample volumes precluded definitive cross-referencing between the two instruments, optical cameras and imaging sonars have been shown to be valuable monitoring tools elsewhere and have value for monitoring in Grand Passage. As with Study 2A, the echosounder data collected during Study 2B contributed to our understanding of the importance of localized hydrodynamics for the collection of useable data.

Analyses of signal interference due to entrained air (Study 2C) suggested a strong difference in the hydrodynamic regimes at the deployment locations of the PLAT-I and the FAST platform with consequences for the proportion of useable data at each site. Signal interference manifested in several ways: i) the presence (PLAT-I site) or absence (FAST site) of a pronounced tide-phase asymmetry in the proportion of data excluded from analyses (due to the persistence and depth penetration of entrained air), ii) the presence (PLAT-I site: flood) or absence (PLAT-I: ebb, FAST site: flood and ebb) of a pronounced negative relationship between flow-speed and the proportion of useable data, and iii) the presence (FAST site) or absence (PLAT-I site) of a reduction in the proportion of useable observation periods with increasingly restrictive minimum acceptable proportions of useable water column.

The pronounced tide-phase asymmetry at the PLAT-I site appears to be a consequence of its deployment location downstream from Peter's Island on the flood tide (upstream on the ebb tide). Consequently, the PLAT-I was deployed within the turbulent field generated by the interaction of the flood-tide with Peter's Island and its associated bathymetry. The turbulence

and associated entrained air had significant consequences for the collection of useable data on the flood tide, reducing the useable proportion of 10-minute observation periods to ≤ 30% on the flood tide; the proportion of useable observation periods on the ebb tide ranged from 85-95%. Going forward, this pronounced asymmetry indicates that useable data collected on the flood tide will be minimal at the current PLAT-I deployment location and will have important consequences for understanding the risk to fish during the flood tide phase.

Although comparative echosounder data were not available for Study 2A or Study 2B, analyses of the proportion of "useable" data collected at the FAST deployment sites for all three studies support the hypothesis that bathymetry associated with Peter's Island creates a pronounced difference in the hydrodynamic regimes associated with the flood and ebb tides at the PLAT-I site and nearby locales (Study 2A and 2B). During Study 2C, the FAST platform was deployed just outside the direct downstream flow associated with Peter's Island and the echosounder data showed little tide-phase asymmetry but did reveal a deterioration in the proportion of useable observation periods on both the flood and ebb tide when increasing the minimum proportion of the water column deemed as "useable". While the lack of a pronounced asymmetry for the FAST site in Study 2C indicated that more data was useable on the flood tide relative to the echosounder placed at the PLAT-I, it should be noted that on the ebb tide, the PLAT-I site had more "useable" data as highlighted above.

Analysis of the useable proportion of individual observations (pings) within 1-m depth bins in the depths-of-interest for the PLAT-I (i.e., 1-8 m depth) revealed the same pattern found in the data analyzed across the entire water column for the presence (FAST site: Study 2A and 2B; PLAT-I site: Study 2C) or absence (FAST site: Study 2C) of tide-phase asymmetry.

Given that the echosounders used here were from the same Simrad EK80 suite of echosounders and deployed with identical data collection parameters, the ability to detect or define the boundary of entrained air was not affected by which echosounder was used. Nor was it affected by deployment at the sea surface in a downward-facing orientation, or on the sea floor in an upward-facing orientation. The sea surface vs. sea floor positioning of the echosounders does, however, have important data collection and analytical consequences that must be considered.

The ensonification beam emitted by a transducer is cone-shaped with the apex at the transducer and the diameter of the cone increasing with distance. It follows then that the region closest to the transducer will result in a highly restricted sampling volume and leave substantial proportions of water unsampled. Therefore, to maximize the volume of sampled water, the transducer should be placed furthest from the region of interest.

As with the considerations of the hydrodynamic regime when selecting a deployment location, one must also consider the consequences in the vertical dimension. If the entrained air so common to tidal energy sites is between the transducer and the target of interest, the acoustic beam will be scattered before encountering the target and will compromise the collection of quantitative data for estimating density and abundance.

Major Take-Aways
These studies demonstrate the importance of the influence of hydrodynamics on the ability to collect useable quantitative data required for analyses and reporting on fish abundance and distribution. Deployment location of an echosounder can have a profound impact on the ability to monitor throughout the tidal cycle, such that the hydrodynamic regime will influence when and where you can observe.

To obtain quantifiable and comparable data on targets of interest, the echosounder must be deployed such that the acoustic beam encounters the targets before encountering entrained air.

Additionally, to maximize the sampling volume, and thereby the likelihood of a fish encountering the acoustic beam, the echosounder should be deployed furthest from the region of interest.

Topics for Continued Research
Because of the fast-flowing and turbulent waters found in tidal streams, the *in situ* sampling (e.g., via net tows/trawl surveys) of acoustic targets (fish) commonly done in open waters is not possible in tidal streams. Therefore, ground-truthing the identity and size of acoustic targets observed in tidal streams remains an unresolved and ongoing topic of research in the hydroacoustics community.

The presence of entrained air makes monitoring fish in tidal channels particularly problematic. Currently, there is no proven strategy to observe fish with sufficient field-of-view or resolution within a highly turbulent environment. Without the ability to observe fish throughout the entire tidal cycle, quantifying risks of turbines to fish will remain difficult. Therefore, to understand potential risks, it is important to continue to focus on developing methods to detect and observe fish, or establish means by which to infer fish presence and behavior, within turbulent tidal channels.

2   Introduction and Objectives

Scientific echosounders are the standard tool in fisheries science for quantifying the abundance and distribution of fish, and for investigating fish behaviour and ecology (Fernandes et al. 2002). They are also valuable for monitoring interactions of fish with instream tidal energy turbines. However, monitoring in tidal channels using echosounders has its own inherent challenges, as the high-flow regimes that make tidal channels desirable for tidal power development are often characterized by complex and turbulent hydrodynamic features that can entrain significant amounts of air in the water column affecting their efficacy for monitoring. Echosounders function by listening for echo returns from interfaces with densities that differ from seawater. Because the density of entrained air differs from the surrounding seawater, it returns echoes that interfere with the ability to identify those that are returned from fish and challenges the ability to collect quantitative data about fish abundance and distribution and undermining efforts to effectively monitor around tidal energy devices.

When used for monitoring around tidal energy turbines, echosounders have most often been deployed on the sea floor (either mounted on an autonomous or cabled subsea platform or integrated into the device substructure) with their ensonification cone oriented upwards for monitoring around gravity-based tidal energy turbines (Williamson et al., 2016a, 2017; Fraser et al., 2017). However, deploying and recovering bottom-mounted instruments involves considerable costs (e.g., specialized vessels and complex marine operations) and risks for monitoring (e.g., instrument malfunction and/or loss of data, loss of the instrument itself). The advent of floating tidal energy platforms provides logistical advantages (e.g., easy access to instruments and monitoring data) that can offset some of these risks, and affords new opportunities for monitoring from the surface using echosounders in a downward-facing orientation. However, the applicability of this configuration, or the more conventional bottom-mounted upward-facing orientation, for monitoring around floating tidal energy platforms have yet to be assessed.

Sustainable Marine Energy (Canada) Ltd. (hereafter Sustainable Marine) operates a floating tidal energy platform (i.e., "PLAT-I": PLATform for Inshore energy) at its tidal energy demonstration site in Grand Passage, Nova Scotia (Figure 2.1 and Figure 2.2), and conducts a series of monitoring activities using instruments deployed from the sea surface. As such, PLAT-I provides an excellent opportunity to conduct an *in situ* assessment of the performance of a bottom-mounted upward-facing echosounder for monitoring near-surface waters by comparison with data collected using surface-deployed instruments, including a downward-facing echosounder. Such an assessment is within the scope of the Pathway Program[1] – a collaborative effort between the Offshore Energy Research Association (OERA) and the Fundy Ocean Research Center for Energy (FORCE) – to establish a regulator-approved monitoring solution that can be used by tidal energy developers for monitoring the near-field (0 - 100 m) region of their tidal energy device at the FORCE demonstration site.

---

[1] https://oera.ca/research/pathway-program-towards-regulatory-certainty-instream-tidal-energy-projects

In partnership with the Pathway Program, Sustainable Marine undertook a project in Grand Passage to investigate target detection capabilities using a bottom-mounted echosounder, and to investigate the relative performance of echosounders deployed on sea floor and at the sea surface. The objectives of the project were to i) investigate the near-surface target detection capabilities of a bottom-mounted upward-facing echosounder using a surface-deployed optical video camera (Study 2A), ii) address the same objective as (i) but over a greater detection range using a multibeam imaging sonar (Study 2B), and iii) investigate the relative performance of a bottom-mounted upward-facing, and a surface-deployed downward-facing echosounder for target detection, and identify the extent of interference due to air entrained from surface waves and turbulence (Study 2C).

These studies were designed to assess the efficacy of bottom-mounted and surface-deployed echosounders for target detections and to help guide best practices for monitoring in high flow environments. These studies were <u>not</u> intended to address interactions of fish with tidal turbines and were therefore <u>not</u> designed to assess likelihood of harm to fish from encountering a tidal device, nor to assess avoidance behaviour. Similarly, these studies were <u>not</u> intended to generate data that could be used to quantify fish abundance, distribution or behaviour around tidal energy turbines. While the results of this project <u>are</u> intended to assist in identifying the best placement of echosounders for monitoring fish around tidal turbines in high flow environments, readers should consider these studies as 'proof of concept' only given the experimental nature of this work.
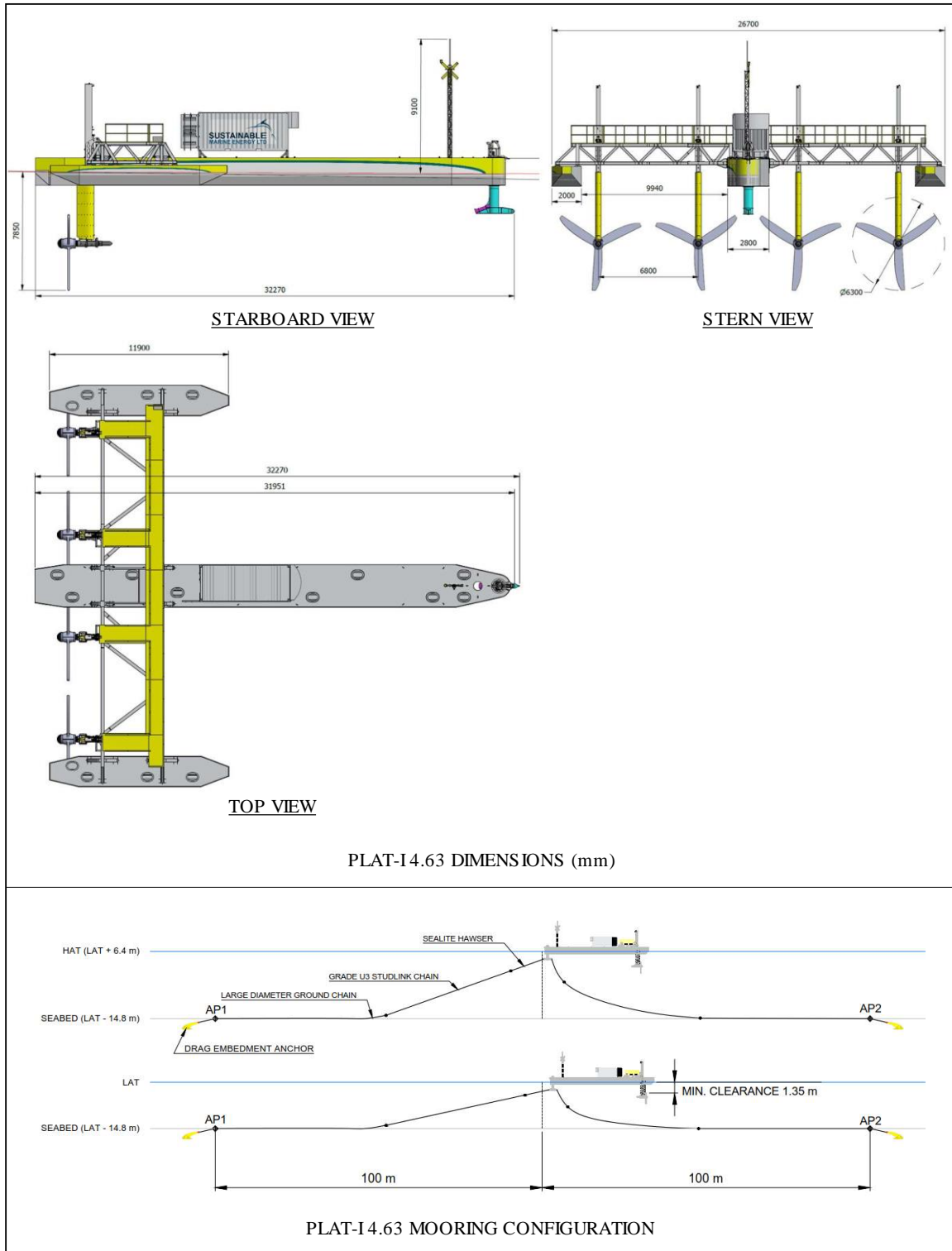
STARBOARD VIEW

STERN VIEW

TOP VIEW

PLAT-I 4.63 DIMENSIONS (mm)

PLAT-I 4.63 MOORING CONFIGURATION

Figure 2.1: Sustainable Marine PLAT-I Platform deployed in Grand Passage.

Figure 2.2: Aerial view of Grand Passage, NS. *The location of the Plat-I on flood tide and Peter's Island (bottom center of map) are shown.*

3   Methodology

All surface-deployed instruments on the PLAT-I (i.e., optical camera, imaging sonar, and echosounder) were pole-mounted at the leading edge of the starboard pontoon (Figure 3.1). The optical camera and the imaging sonar were oriented facing forward (Study 2A and 2B). Therefore, the rotation of the PLAT-I on its turret during changes in tidal phases resulted in the instruments consistently facing into the current during both ebb and flood tides. The surface-deployed echosounder was mounted in a downward-facing orientation (Study 2C). The bottom-mounted upward-facing echosounder was deployed on the seafloor on a Fundy Advanced Sensory Technology (FAST) autonomous subsea platform at locations specific to each study. The PLAT-I turbines were 'parked' for each of the three studies and were not rotating. Throughout this report when referencing locations, the terms "PLAT-I" or "PLAT-I site" and "FAST platform" or "FAST site" are used. When referencing the echosounder or its orientation, the terms "WBAT" (upward-facing) and "EK80" (downward-facing) are used.

Figure 3.1: Aerial view of PLAT-I. *The pole mount location at the leading edge of the starboard pontoon is shown as a yellow star.*

3.1   Tidal Flow Rate Data

These studies used modelled flow-rate data for Digby Neck based on the Finite-Volume Community Ocean Model (FVCOM) developed at the University of Massachusetts and the Woods Hole Oceanographic Institution (Chen and Beardsley, 2011). Modelled flow rate data was used because the flow data collected by the Valeport on the PLAT-I proved inconsistent during the studies (this issue was rectified after the studies were completed). The flow rate as modelled for Grand Passage corresponds well with the flow rate as measured by an Acoustic Doppler Current Profiler (ADCP) with the maximum flow rate overestimated by not more than 0.3 m/s. Normalized root mean squared error (NRMSE) expresses the average error between two time series. The range extends from 0.0 to 1.0. A NRMSE of 0.0 would indicate a perfect match between two time series. The NRMSE for the modelled Grand Passage flow rate versus the measured flow rate was 0.089, indicating that the average error between the two time series was 8.91% of the average ADCP-measured flow speed (Jeremy Locke, personal communication). A three-day sample of the modelled and measured flow-rate data is shown in Figure 3.1.1, and demonstrates good agreement between the data. Additional details about the model can be found elsewhere (O'Flaherty-Sproul, 2012; Guerra *et al*., 2019).
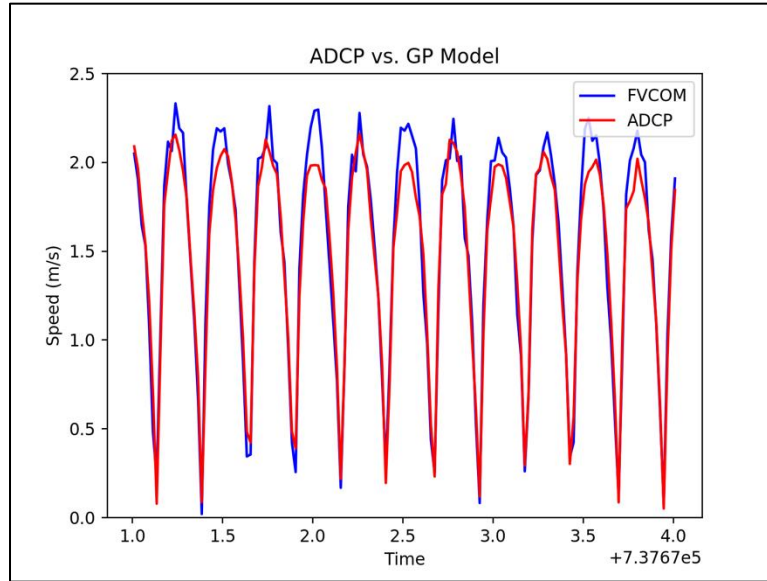
Figure 3.1.1: Measured and Modelled Tidal Flow Rate in Grand Passage. *Flow rate for three days are shown as modelled (blue: FVCOM) and measured (red: ADCP).*

Tidal flow rate for dates matching each of the studies was modelled. For studies 2A and 2B, the flow rate was modelled at the position of the PLAT-I. For Study 2C, the flow rate was modelled at the position of the PLAT-I as well as the position of the FAST platform. The model output was the depth-averaged flow rate integrated into 10-minute intervals. Time was reported in Coordinated Universal Time (UTC), and the flow-rate data reported in meters-per-second and provided in two vectors (U_x and U_v; in orthogonal directions). The model was forced solely by tides and did not include the presence of the PLAT-I.

The flow speed for each 10-minute interval, in meters per second, was calculated using the R statistical programming language (R Core Team, 2020) as follows.

$$FlowSpeed \ (^m/_S) = \ \sqrt{U_x^2 + \ U_y^2}$$ Equation 1

The direction of flow for each 10-minute interval was calculated as the 2-argument arctangent using the "atan2" function in R.

$$FlowDirection \ (radians) = atan2(U_y, U_x)$$ Equation 2

To assign tide phase (i.e., flood, ebb, slack) to each calculated flow speed, the associated calculated flow direction was compared to the online tidal predictions (www.waterlevels.gc.ca) to ensure that the correct tide phase was assigned. Calculated flow direction ≤ 0 was assigned as "ebb" and flow direction > 0 was assigned "flood". Entries for which the flow speed was less than 0.5 m/s were assigned "slack" regardless of calculated flow direction.

3.2   Study 2A – WBAT and optical camera

The purpose of *Study 2A – WBAT and optical camera* was two-fold: (i) use the images captured with an optical camera to assess the utility of an upward-facing echosounder for target detection, and ii) evaluate the applicability of an upward-facing echosounder to assess fish presence in the near-field region of floating tidal energy platforms. Figure 3.2.1 shows a conceptualization of the instrument deployment plan. Data were collected December 21-31, 2019.
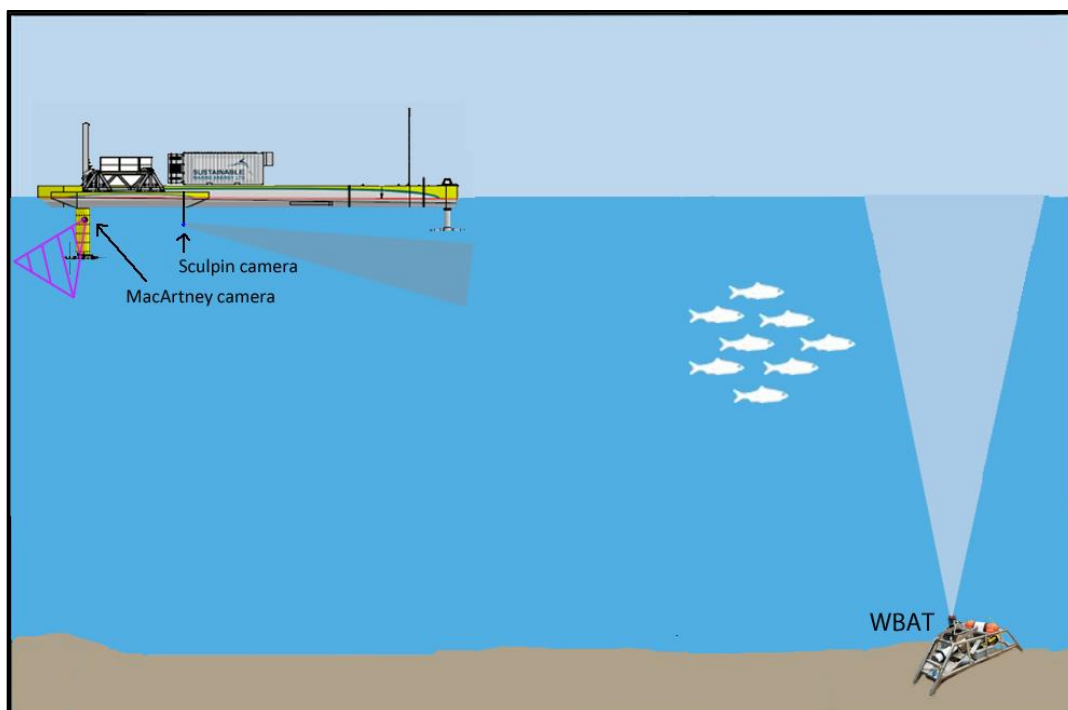

Figure 3.2.1: Study design conceptualization for Study 2A. *Shaded areas are intended for visualization purposes only, and do not accurately represent sample volumes.*

Optical Camera

An optical imaging video camera (Sculpin HDC-SubC Imaging camera; subcimaging.com) was deployed approximately one meter below the sea surface on a pole mount attached to the leading edge of the starboard pontoon of the PLAT-I (Figure 3.2.1). The camera was oriented generally horizontally such that the field-of-view encompassed the top few meters of the water column and faced forward into the tidal flow. Given that ambient light was the only source of illumination, the camera only operated during daylight hours (08:00 to 17:00 local time) for the period of December 20-31, 2019. The recorded data was stored as *.mp4 files which were examined and analyzed for the presence of fish or other large organisms by Envirosphere Consultants Ltd (see Appendix A). Examination of the video files was accomplished manually

using VLC media player software (VideoLAN: videolan.org). The results were integrated into 10-minute time bins to match the integration period of the echosounder data.

Echosounder

Hydroacoustic data were recorded using a Simrad EK80 Wideband Autonomous Transceiver (WBAT; Kongsberg Maritime, Horten, Norway) operating a 7° split-beam transducer at a frequency of 120 kHz in continuous-wave mode. WBAT data collection settings used at the tidal energy demonstration site in Minas Passage (Viehman et al., 2019) were used here (ping rate: 1 Hz; pulse length: 0.128 ms, power: 125 W). The echosounder was calibrated after the instrument was recovered following the completion of data collection for Study 2A. The resulting calibration parameters were used for all three studies in Grand Passage. The WBAT was mounted to the FAST platform in an upward-facing orientation and deployed on the seafloor approximately 30 m distant from the optical camera on the flood tide (approximately 53 m on the ebb tide as the PLAT-I rotates on its turret; Figure 3.2.2 and Table 3.2.1).
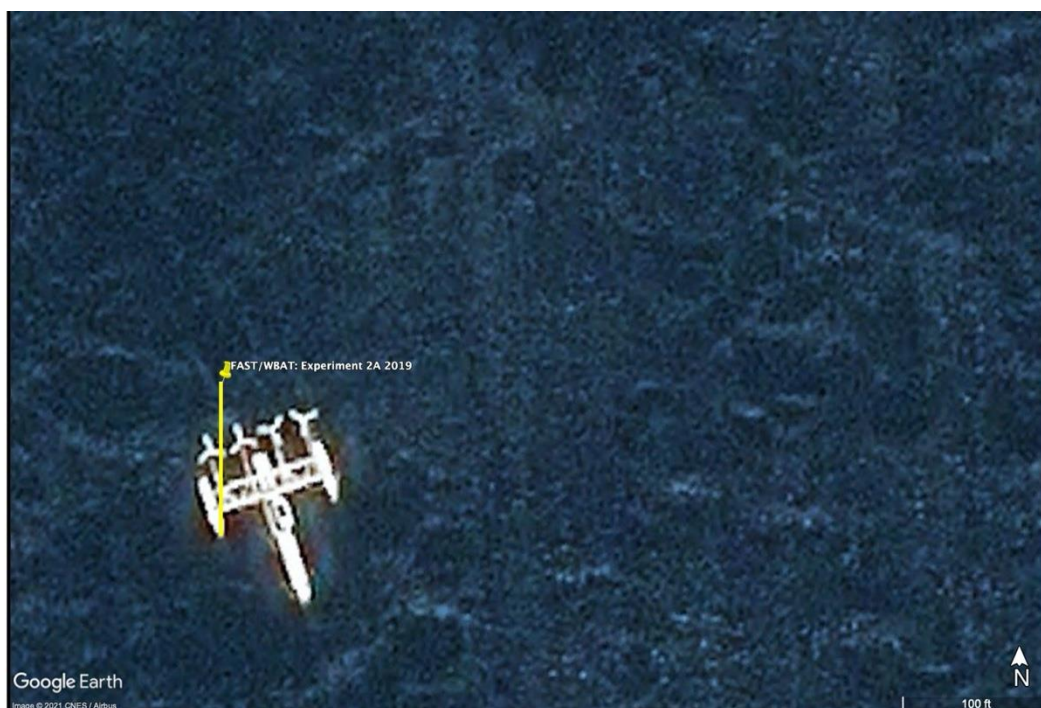

Figure 3.2.2: Deployment location of the WBAT echosounder mounted on the FAST platform, shown for Study 2A relative to the PLAT-I on a flooding tide. Length of yellow line represents the horizontal length from the optical camera deployed at the leading edge of the starboard pontoon to the position of the FAST platform: ~30 m.

Table 3.2.1: Summary of Study 2A Deployment Locations and Data Collection.

Instrument	Deployment Platform	Deployment Location	Data Collection Dates	Hours of Data Collected
Optical Camera	PLAT-I (sea surface)	45 15.830 N 66 20.210 W	Dec 20, 2019 Dec 31, 2019	150
WBAT Echosounder	FAST (sea floor)	44 15.854 N 66 20.223 W	Dec 21, 2019 Dec 31, 2019	55

Echosounder data were collected during alternating (even) hours from 08:00 to 17:00 (local time), December 21-31, 2019. Time was recorded in the data files in UTC. Each hour of data collection included 2 minutes of "passive data collection" to identify acoustical interference, followed by 53 minutes of active pinging and recording, finishing out the hour with an additional 5 minutes of passive data collection.

The echosounder data files were post-processed using Echoview version 11 (Echoview Software Pty Ltd., Hobart, Australia). Because the focus of this study was to compare target detection in the upper few meters of the water column, the data files were examined prior to post-processing. Files where interference from entrained air reached nearly to the seafloor, thereby obscuring the depths of interest for data collection, were excluded from post-processing and analyses.

The goal of post-processing activities is to prepare the raw data for analyses; apply calibration settings, set the sound speed based on the temperature and salinity of the seawater through which the acoustic beam travels to the target and back to the transducer (the proxy for estimating distance to target), and establish which recorded signals are to be included or excluded from analyses.

Sound speed applied to the echosounder data in the Echoview files was calculated using the Mackenzie (1981) sound speed equation made available in the Echoview Sonar Calculator. Temperature and salinity were determined from data collected by a Seabird Microcat 37SMP attached to the bottom-deployed FAST platform.

Signal inclusion/exclusion was established in four ways. First, for an upward-facing echosounder the following three positions for each recorded ping set the analysis boundaries: i) nearfield (i.e., the range at which the acoustic beam becomes organized and is no longer subject to constructive and destructive interference of a disorganized beam (Simmonds and MacLennan, 2005); 1.7 m for the WBAT transducer used here), ii) sea surface, including a 1-m offset to exclude the inherent acoustic deadzone that occurs due to the shape of an acoustic beam when it encounters a surface (Simmonds and MacLennan, 2005), and iii) the depth-of-penetration of air entrained by turbulence (the "turbulence" line). Second, the hydroacoustic analyst manually scrutinized each echogram to identify any additional signals that should be excluded within the analysis region (e.g., noise or echo traces not consistent with fish). Third, a minimum S_v (mean

volume backscattering strength) threshold was set. In these studies, the minimum S_v threshold was set to -66 dB re 1 m^{-1} and was chosen to exclude ambiguous signals that are returned from bubbles close to interference from entrained air. Fourth, the data were investigated for the presence of anomalously high values (> -30 dB), which may indicate the presence of transient noise within the recorded data, a gap in one of the analysis boundary lines, or acoustic backscatter returns from non-fish organisms. Subsequently, the threshold was a range of more than two orders of magnitude, from the minimum S_v threshold (-66 dB) to the maximum S_v threshold (-30 dB), that was included in the analyses of fish presence (see Section 3.6). The outcome of the post-processing work as established here defined the criteria for "fish present": S_v values between the minimum and maximum thresholds (i.e., -66 dB to -30 dB), and the manual exclusion of signals deemed 'not consistent with fish'.

Upon completion of the post-processing, the data were exported from Echoview in 10-minute time bins integrated into various depth configurations depending on analytical requirements. The exports also included the ping-by-ping depth for each of the analysis lines (nearfield, sea surface, and "turbulence"), among other things (e.g., text files documenting Echoview settings at the time of export).

For Study 2A, the depth bin configurations included (i) full water column – to assess whether fish were present somewhere in the water column for every 10-minute time bin, (ii) 1-m depth bins beginning at the sea surface (i.e., the sea surface line) - to facilitate comparison between echosounder data and data within the optical camera's field-of-view, and (iii) 1-m depth bins beginning from the sea floor (i.e., the nearfield line) – to facilitate additional analyses given that the bottom is a stable datum whereas the height of the sea surface changes with tidal phase. The exported acoustic data were merged with modelled flow-rate data in order to associate the flow rate and tide phase with recorded acoustic data. Modelled flow rates < 0.5 m/s were deemed "slack" tide. A flood tide phase was associated with a modelled northerly flow, and ebb tide phase was associated with a modelled southerly flow.

After associating the echosounder data with tide phase and flow speed, the echosounder data were analyzed for backscatter values consistent with fish within every 10-minute observation period. Data were then partitioned to summarize fish presence/absence within the depth bins overlapping the depth bins of the optical camera field-of-view.

3.3 Study 2B – WBAT, optical camera, and multibeam imaging sonar

The purpose of *Study 2B – WBAT, optical camera, and multibeam imaging sonar* was to include a multibeam imaging sonar with a greater detection range than the optical camera to assess the utility of an upward-facing echosounder for target detection. A conceptualization of the instrument deployment plan is shown in Figure 3.3.1. Data were collected January 25-February 2, 2020.
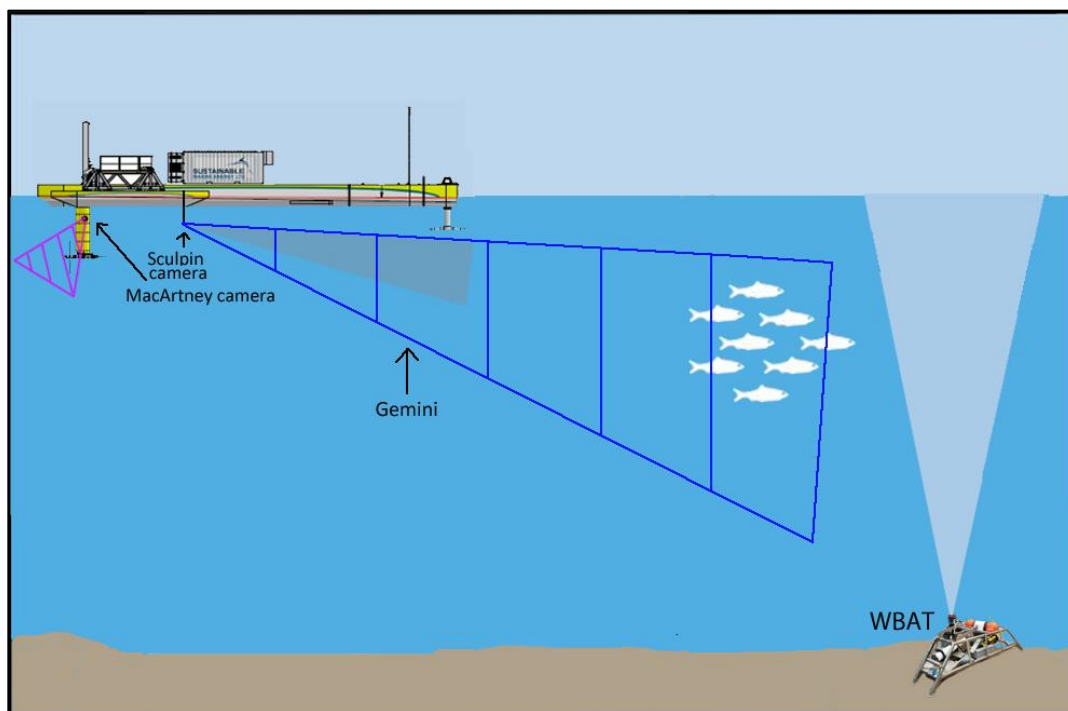
Figure 3.3.1: Study design conceptualization for Study 2B. *Shaded areas are intended for visualization purposes only, and do not accurately represent sample volumes.*

Optical Camera

The optical camera was deployed as described for Study 2A, but due to instrumentation failure only 20 hours of data were collected during this study. The data were analyzed for the presence of fish or other large organisms as described for Study 2A.

Imaging Sonar

A Gemini 720is imaging sonar (Tritech International Ltd. Westhill, Aberdeenshire, UK) was pole-mounted and deployed approximately two meters below the sea surface at the leading edge of the starboard pontoon of the PLAT-I (Figure 3.3.1). The orientation of the imaging sonar was such that the 120° field-of-view encompassed a horizontal distance of 30 meters (limited by interference beyond that distance), and a maximum depth range of 11 m (limited by the PLAT-I mooring chain in the field of view causing false positive target detections). The frame rate was 12-15 frames per second. Data were recorded on alternate (odd) hours to avoid acoustic interference between the imaging sonar and the echosounder.

The imaging sonar data were processed using SEATEC analysis software (Tritech International Ltd.) to detect targets for evaluation. Frames marked with potential detections were scrutinized for fish presence. Potential detections were classified as follows: (1) single fish/debris, (2) turbulence/fish/school of fish, and (3) mooring. Potential detections were marked by tide phase and classified into 10-minute intervals for comparison with echosounder data.

Echosounder

Echosounder setup, post-processing, and modelled flow-rate data were as described in *Section 3.2: Study 2A – WBAT and optical camera* with the following exceptions. First, the FAST platform on which the WBAT was mounted was recovered after collection of data for Study 2A and redeployed for Study 2B. Therefore, the location at which the echosounder data were collected changed between Study 2A and Study 2B (Figure 3.3.2 and Table 3.3.1). The deployment location of the FAST platform during Study 2A was in-line with the PLAT-I and very close to its mooring lines (a safety concern that was highlighted upon FAST platform recovery). Thus, for Study 2B the FAST platform was deployed approximately 30 m distant from the optical camera and Gemini (as per Study 2A), but 40 m to the northeast (heading: ~70° from the Study 2A location) for a total distance of 60 m (Figure 3.3.2). This location kept the FAST platform outside the rotation radius of the PLAT-I, and away from the mooring lines. Second, data collection for Study 2B was not restricted to daylight hours. Data were therefore collected 'round-the-clock'. Third, the Echoview exports were modified to include an export of data in cells defined by the 10-minute time bins, but with a depth interval of the top 11 m coinciding with the imaging sonar depth-range field of view. Fourth, because the depth-range of interest (11 m) for Study 2B constituted nearly the entire water column available for analyses, no data files were excluded from import into Echoview even when interference from entrained air penetrated nearly to the seafloor.

Figure 3.3.2: Deployment location of the WBAT echosounder mounted on the FAST platform, shown for Study 2B relative to the PLAT-I on a flooding tide. *Length of yellow line represents the horizontal length from the optical camera and imaging sonar deployed at the leading edge of the starboard pontoon to the position of the FAST platform: ~ 60 m.*

Table 3.3.1: Summary of Study 2B Deployment Locations and Data Collection.

Instrument	Deployment Platform	Deployment Location	Data Collection Dates	Hours of Data Collected
Optical Camera	PLAT-I (sea surface)	45 15.830 N 66 20.210 W	Jan 31, 2020 Feb 02, 2020	~ 20
Imaging Sonar	PLAT-I (sea surface)	45 15.830 N 66 20.210 W	Jan 25, 2020 Feb 02, 2020	~ 91
WBAT Echosounder	FAST (sea floor)	45 15.861 N 66 20.195 W	Jan 25, 2020 Feb 02, 2020	97

3.4 Study 2C – WBAT and EK80

The purpose of *Study 2C – WBAT and EK80* was three-fold: (i) identify the extent of signal interference by air entrained from turbulence, (ii) assess the relative performance of target detection by downward-facing *vs.* upward-facing echosounders, and (iii) provide a comparative analysis of downward-facing versus upward-facing echosounders. A conceptualization of the instrument deployment plan is shown in Figure 3.4.1. Data were collected September 3-6, 2020.
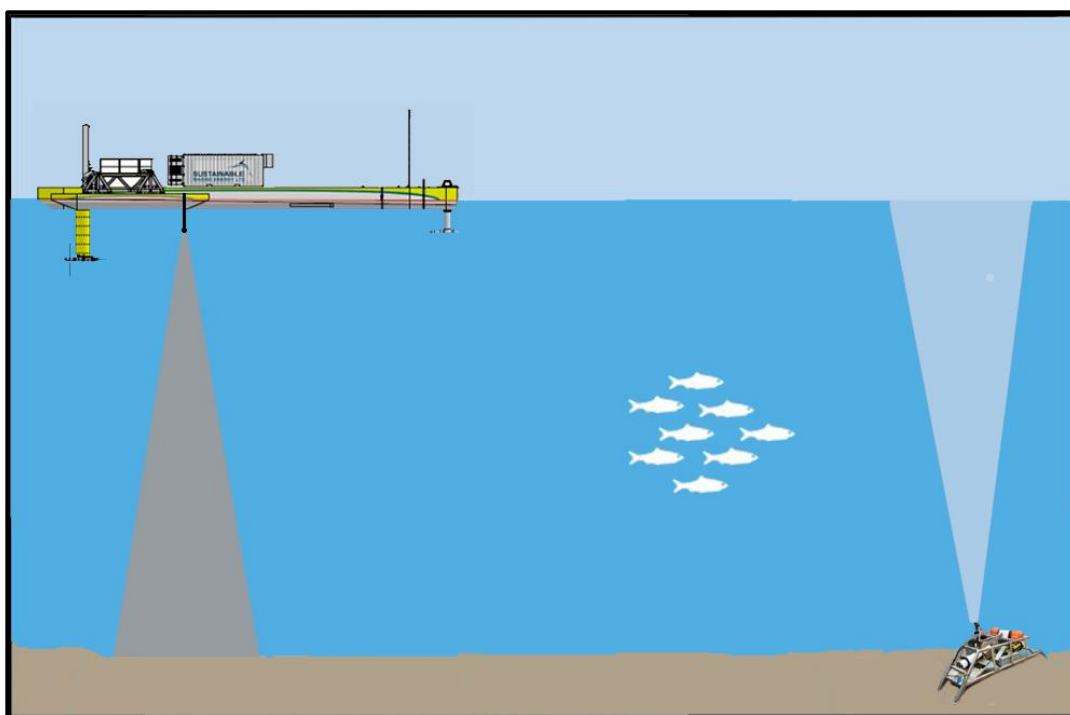

Figure 3.4.1: Study design conceptualization for Study 2C. *Shaded areas are intended for visualization purposes only, and do not accurately represent sample volumes.*

Echosounder – WBAT

Echosounder setup, data collection, and post-processing were as described in *Section 3.2: Study 2A – WBAT and optical camera*, with the following exceptions. First, the FAST platform was recovered after Study 2B and redeployed for Study 2C approximately 85 m to the north (as intended) to minimize the chance of acoustic interference between the echosounders. Therefore, the location of the WBAT data collection in Study 2C differs from that in Study 2A and Study 2B (Figure 3.4.2 and Table 3.4.1). Second, data collection for both echosounders was not restricted to daylight operations and were collected round-the-clock. Third, given that the focus of the analyses for Study 2C was to quantify the extent of signal interference by turbulence, all echosounder data files were imported into Echoview regardless of whether the acoustic returns from entrained air would preclude the use of data for analyzing for the presence of fish. Fourth, associated with importing all data to Echoview, the "turbulence line" received the same analytical scrutiny throughout the portions that would normally be block-identified as bad data to exclude them from biological analyses. This change allowed for greater precision in quantification of the presence of entrained air. And finally, due to a sensor error on the Anderaa Recording Current Meter (RCM) that was deployed on the bottom-mounted FAST platform, sound speed used in the Echoview files was estimated using the temperature and salinity measured with a thermometer and refractometer during calibration data collection in Grand Passage the week prior to Study 2C deployment. Data was integrated and exported from Echoview using the same definitions as for Study 2A.

Echosounder – EK80

A Simrad EK80 Wideband Transceiver echosounder (WBT, hereafter 'EK80'; Kongsberg Maritime, Horten, Norway) was pole-mounted in a downward-facing position, approximately one meter below the sea surface and attached to the leading edge of the starboard pontoon of the PLAT-I (Figure 3.4.1). The EK80 operated a 7° split-beam transducer at a frequency of 120 kHz in continuous-wave mode, with parameters matching the WBAT to ensure collection of comparable data (i.e., ping rate: 1 Hz; pulse length: 0.128 ms, power: 125 W). The echosounder was calibrated after completion of the data collection, with those settings applied in Echoview prior to post-processing.

Data were collected during alternating hours round-the clock from September 3-6, 2020, with time recorded in UTC. Unlike the WBAT data collection for studies 2A, 2B, and 2C, the EK80 data collection did not include a portion of the hour set to "listening" and therefore, no passive data were included in the EK80 dataset.

The echosounder data files were post-processed using Echoview version 11 as described in Section 3.2 by applying the same post-processing changes as described for the WBAT above. However, there was one change specific to the EK80 post-processing that was not applied to the WBAT post-processing. As with the WBAT post-processing, the placement of the lines that

define the boundaries of the data to be used for analyses are initially computed by software and then scrutinized by a hydroacoustics analyst. For all three studies described here, the initial placement of the lines for the WBAT data was done using the algorithms built in Echoview and available to any user. However, given the extreme dominance of interference from entrained air in the EK80 data set, the built-in Echoview algorithms failed to provide a reasonably placed turbulence line from which to start the post-processing. Instead, the initial placement of the turbulence line (and bottom line) was calculated using Echofilter – a new software developed through the Pathway Program and designed to work with Echoview (Lowe and McGarry, 2020; McGarry *et al.*, 2020). An additional change required for post-processing because of the downward-facing orientation of the EK80 transducer was that the nearfield line (1.7 m from the transducer face) defined the upper limit of the water column data available for analyses; rather than the bottom limit for the upward-facing WBAT. Likewise, the limit that defines the furthest range from the transducer to be included for analyses is the detected sea floor with a 1-m offset to remove the portion affected by the acoustic deadzone; rather than the detected sea surface with the 1-m offset for the upward-facing WBAT. Importantly, the turbulence line is equivalent in the data collected from either an upward-facing or downward-facing echosounder. As with all hydroacoustic post-processing, once the placement of the boundary lines has been estimated through an automated process, the hydroacoustic analyst inspects the line placement for each Echoview file, sets thresholds, and scrutinize for "bad data" as described for the WBAT data. As per the WBAT data for Study 2C, the placement of the turbulence line for the EK80 data was treated as though all of the recorded data would be used for analyses. Data were integrated and exported from Echoview using the same definitions as per the WBAT data.
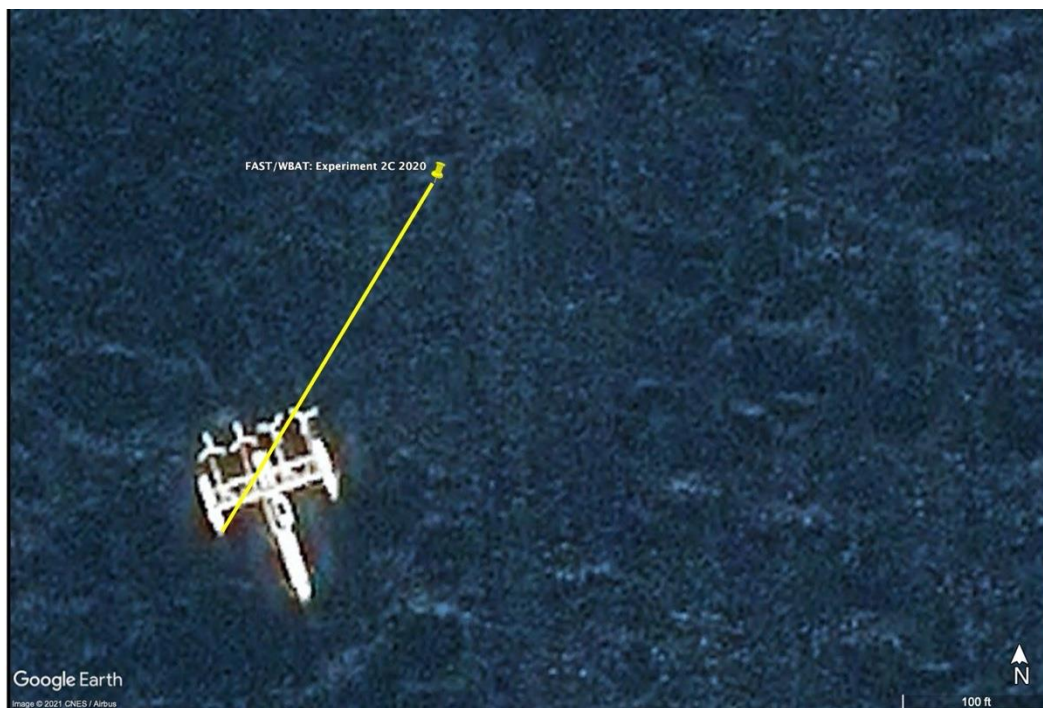

Figure 3.4.2: Deployment location of the WBAT echosounder mounted on the FAST platform, shown for Study 2C relative to the PLAT-I on a flooding tide. *Length of yellow line represents the horizontal length from the EK80 echosounder deployed at the leading edge of the starboard pontoon to the position of the FAST platform: ~85 m.*

Table 3.4.1: Summary of Study 2C Deployment Locations and Data Collection.

Instrument	Deployment Platform	Deployment Location*	Data Collection Dates	Hours of Data Collected
EK80 Echosounder	PLAT-I (sea surface)	45 15.830 N 66 20.210 W	Sep 03, 2020 Sep 06, 2020	33
WBAT Echosounder	FAST (sea floor)	45 15.876 N 66 20.190 W	Sep 03, 2020 Sep 06, 2020	36

* the deployment location noted here for the PLAT-I is the location as shown for Study 2A and 2B. However, it should be noted that prior to the data collection for Study 2C, the PLAT-I was repositioned in generally the same locale.

Modelled tidal flow rate data were as described in Section 3.1, but with the model output updated to coincide with the data collection period for this study, and produced for the location of the FAST platform and the location of the PLAT-I. Flow rate data was produced for both locations so that quantification of the associated extent of entrained air was unambiguously associated with the flow rate modelled for each site.

3.5   Data Analysis

Merge Metadata with Hydroacoustic Data

Scripts were programmed in R to merge the modelled flow rate data with the exported echosounder data. The merge associated the echosounder data, the 10-minute observation periods and the lines defining the boundaries of the analysis region, with the corresponding flow rate and tide phase.

Calculate Proportion of Useable Water Column

To quantify the extent of signal interference due to entrained air, the proportion of useable water column was calculated, first for every data point (i.e., for each "ping") included in the exported line files (surface/nearfield, turbulence, bottom/nearfield) that define the analysis region within the datasets for both the upward-facing and the downward-facing echosounders. Then the useable proportion by ping was averaged for each of the 10-minute observation periods. A visualization using data collected by an upward-facing echosounder in Minas Passage is included here (Figure 3.4.3).
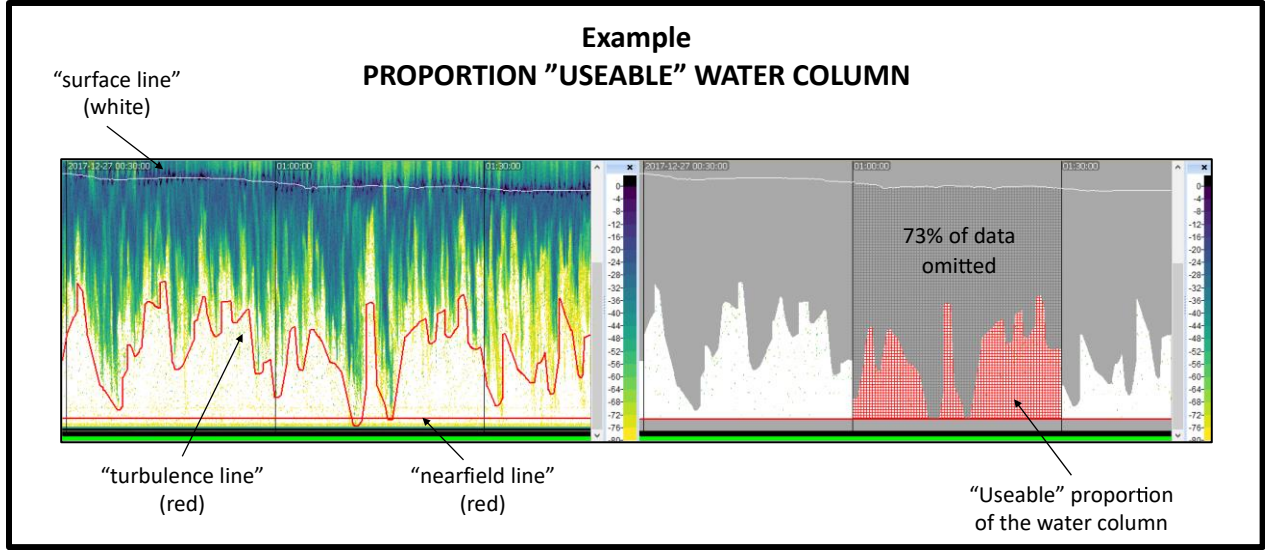
Figure 3.4.3: Example Visualization of Useable Portion of the Water Column. *The visualization was generated using data collected with an upward-facing echosounder in Minas Passage. Visualization created by Haley Viehman.*

The proportion of useable water column at each ping was calculated as follows.

1. calculate the depth range of the water column at each ping

$$R_1 = abs(D_S - D_B)$$

where, R_1 was the resulting range in meters, *abs* is the absolute value function (to avoid conflicts with upward- vs. downward-facing data), D_S was the depth position of the "surface line" ("surface with 1-m offset" or nearfield depending on echosounder orientation), D_B was the depth position of the "bottom line" (nearfield or "bottom with 1-m offset" depending on echosounder orientation)

2. calculate the depth range of the "useable" water column at each ping

$$R_2 = abs(D_T - D_B)$$

where, R_2 was the resulting range in meters, *abs* is the absolute value, D_T was the depth position of the "turbulence line" and D_B was the depth position of the "bottom line" as per above

3. calculate the fraction observable (useable portion) of the water column at each ping

$$F_O = \frac{R_2}{R_1}$$

where, F_O was the fraction observable for each ping, and R_2 and R_1 were as calculated above.

The ping-by-ping detail of useable water column was then averaged for each 10-minute observation period as follows:

4. calculate the mean of the fraction observable for each 10-minute observation period

$$F_{10,j} = \frac{\sum_{1}^{n,j} F_{O,j}}{n_j}$$

where, F_{10} is the mean fraction-observable for the 10-minute interval, j is the 10-minute interval, n_j is the number of datapoints (pings) within the 10-minute interval j, and $F_{O,j}$ are the fraction-observable values for each ping within the 10-minute interval j

5. the tidal flow rate and tide phase associated with each "useable portion" were the flow rate and tide phase from the modelled tidal flow-rate data for each 10-minute observation period.

The result of these calculations was a dataset of the mean proportion of useable water column for each 10-minute observation period associated with the corresponding modelled tidal flow rate and tide phase. To understand the relationship between tidal flow rate and the proportion of useable observations periods on the flood and ebb tide, a simple linear regression model (function: lm in R) was fit to the data.

To gain insights into the influence of tide phase on the amount of data available for analyses (i.e., whether the proportion of useable 10-minute observation periods differed between a flood and ebb tide) and the associated sensitivity to the criteria that defines "useable for analyses", the count of 10-minute observation periods meeting the criteria was calculated as a proportion of all 10-minute observation periods by tide phase (i.e., if we set criteria to include only those 10-minute observations periods for which the "useable water column" proportion met or exceeded some minimum proportion, does the count of useable 10-minute observations change?).

Calculate Proportion of Useable Data within Rotor Swept Depth for Each Data Collection Site

While assembling the results of the useable-data analyses, it became apparent that site-specific hydrodynamics, and the consequences for the extent of entrained in the water column, likely played a role in the availability of useable data. Therefore, to take advantage of the opportunity to investigate the potential influence that site-selection may have on data useability within the depths of interest, additional analyses were undertaken to document the useability of data, by site, within the swept depth of the PLAT-I rotors (1.5 to 7.8 m from surface; Sustainable Marine personal communication).

The same exported line files used for the *Proportion of Useable Water Column* analyses were analyzed on a ping-by-ping basis, rather than the 10-minute intervals above. Each ping within each 1-m depth bin, starting 1 m below the surface and ending at 8 m below the surface, was designated as "useable" or "unusable" based on whether the depth of the turbulence line was less than or greater than the depth bin, respectively. Using the same tide phase assignment as above, each ping with its designation of usable or unusable was then aggregated by tide phase. The result was that for each 1-m depth bin from 1 m to 8 m below the surface, the count of pings useable and unusable by tide phase was enumerated. From that data the proportion of useable pings was calculated by depth bin and tide phase. For Study 2A, the proportion of unusable pings needed to be estimated for the data files which were excluded from Echoview. Those files were the hour-long files for which interference from entrained air dominated nearly the entire water column. Because those files were excluded from Echoview, they were therefore not included in the line-data exports. The number of excluded pings at 1 Hz was estimated and included in the results.

3.6   Notes on Setting Minimum and Maximum S_v Thresholds for Fish

As described in Section 3.2, one of the objectives of post-processing hydroacoustic data was to establish which recorded signals of returned echo energy were to be included or excluded from analyses. Setting a minimum and a maximum threshold defines the range of signal amplitudes that are accepted for inclusion in analyses. With a dynamic range of 14 orders of magnitude (140 dB: Simrad, 2020), the EK80 suite of echosounders are capable of receiving both very weak and very strong echo returns. The dynamic range is orders of magnitude greater than the range of echo returns found for fish and fish aggregations. Setting minimum and maximum thresholds is therefore warranted. Because the amount of energy returned by fish (individuals or aggregations) is not a static characteristic, setting thresholds can be as much an art as a science.

Without *in situ* sampling to act as a guide (e.g., net tows/trawl surveys to verify species identification and fish size), the thresholds here were based on visual scrutiny of the echograms and consultation with subject-matter experts. The goal was to select a threshold sufficiently low to exclude plankton without excluding fish sizes that should reasonably be included. A minimum volume backscattering strength (S_v) threshold of -66 dB was selected, which at 120 kHz in seawater, is "equivalent" to a "generic" fish of length ~ 1 cm (Love 1971). This minimum threshold was entered into the Echoview software such that S_v values below this value were excluded from analyses, making the minimum threshold a "hard" threshold. In an effort to exclude marine mammals (lungs generate very strong echo returns) and other strong non-fish echo returns without excluding dense aggregations of fish with swim bladders, the maximum threshold was a "soft" threshold. Because this threshold was "soft", no maximum value was entered into Echoview, but after completing post-processing, the data was examined using scripts in R for S_v values ≥ -30 dB. The script output included the name of the Echoview file and the ping numbers therein which included values ≥ -30 dB. Those echograms were then examined

by an analyst to determine whether the values ≥ -30 dB were consistent with fish aggregations (included in analyses) or not (excluded from analyses).

4 Results and Discussion

4.1 Study 2A – WBAT and optical camera

Optical Camera

No fish were observed passing through the camera's field of view during the review of approximately 150 hours of video recorded December 20-31, 2019. Image resolution was sufficient to identify objects such as seaweeds, bubbles, detritus, krill, other plankton, and objects thought to be jellyfish (Appendix A).

Echosounder

Fifty-five hours of echosounder data were recorded during the study period December 21-31, 2019. Recorded data were overwhelmed by entrained air and turbulence during 18 (33%) of those hours. The tide was in its flooding phase during 17 of those 18 hours, suggesting an asymmetry in the persistence and the depth of penetration of entrained air between the flood and ebb tide phases at the deployment location of the FAST platform.

During the remaining 37 hours, there were 222 10-minute observation periods of which three were completely obscured by entrained air, turbulence, or noise, leaving 219 10-minute observation periods available for analyses. Within every useable 10-minute observation period, target detections consistent with fish passing through the echosounder beam were observed somewhere in the water column.

The echosounder data was then examined in the depth-range that corresponded to the optical camera field of view. The first position observable in the echosounder data was 1 m below the sea surface. The exclusion of data in the top-most meter of water results from the requirement to exclude potentially biased data due to the inherent deadzone associated with the interaction of the shape of the acoustic beam and sea surface (Simmonds and MacLennan, 2005). Within the 222 observation periods available in the first meter below the deadzone exclusion, recorded data for 172 (78%) of the observation periods were overwhelmed by interference from entrained air and turbulence, and "unusable". Of the remaining 50 10-minute observation periods ("useable"), signals consistent with the presence of fish were recorded for 56% of them. For comparison, within the next 1 m depth interval (i.e., 2 meters from the deadzone exclusion), 133 (60%) of the 10-minute observation periods were dominated by entrained air, leaving 89 (40%) useable periods. Within those 89 useable observation periods, 57% had return values consistent with fish presence (Table 4.1.1). In other words, the proportion of *useable*

observation periods that contained echo return values consistent with fish presence was nominally 55% within each of the first two observable meters of water.

Table 4.1.1: Summary of Study 2A Useable 10-minute Hydroacoustic Observation Periods (37 out of 55 hours of data collection). Data in this table includes only those data files which were not fully excluded due to entrained air. The remaining individual observation periods were designated as "unusable" when signals recorded from within the observation depth were dominated by entrained air and turbulence, obfuscating signals returned from fish. Each 10-minute observation period for which recorded S_v values greater than -66 dB are reported as "fish present". "Fish absent" observation periods indicate that no S_v values greater than -66 dB were observed within the useable data during the entirety of the observation period.

Of the 222 10-minute observation periods (37 hours out of 55 hours collected)…						
	Fish Present		Fish Absent		Unusable	
	(n)	(%)	(n)	(%)	(n)	(%)
At Any Depth (full water column)	219	**100 %**	0	**0 %**	3	**1 %**
Within 1-2 Meter from the Surface	28	**56 %**	22	**44 %**	172	**78 %**
Within 2-3 Meter from the Surface	51	**57 %**	38	**43 %**	133	**60 %**

Study 2A Discussion

The findings from the optical camera and echosounder starkly differ. Although no fish were observed for the 150 hours of optical camera data collected, signals consistent with the presence of fish were detected by the echosounder in depths coinciding with the cameras field-of-view for approximately 55% of the useable 10-minute time bins. Given that the camera image resolution was sufficient to identify krill, other plankton, jellyfish, seaweed, and detritus, the lack of fish being observed likely stems from fish not passing within the camera's field-of-view. Without additional sources of information, it is difficult to resolve this discrepancy, but there are several possibilities that could have contributed to the differing results.

For instance, the fields-of-view for each instrument were not co-located, nor of equal volume, and were in different deployment conditions. While co-location of the sampling volume would have been ideal, it was not feasible or safe for personnel, instruments, or the PLAT-I structure to attempt a closer deployment. Given that the diameter of the acoustic beam was approximately 1.6 m at the sea "surface" (see discussion in Section 4.3 and Figure 4.3.5) and the field-of-view of the optical camera was only a few meters, there was no opportunity to co-locate the sampling volumes. The camera was pole mounted and attached to the PLAT-I starboard pontoon, while the echosounder was deployed on a FAST platform approximately 30 m distant from the camera on the flood tide (~53 m on ebb tide due to PLAT-I rotation on turret; Figure 3.2.2 and Table 3.2.1). As such, the echosounder field-of-view was in a more "open water" setting than the optical camera. Given the distance between the position of the two instruments, we cannot rule out the possibility that the hydrodynamic conditions at these locations, or the presence of the

PLAT-I structure itself, influenced fish presence/absence. However, we have no information by which to address fish behaviour and cannot address this question.

The primary goal of this study was to investigate the near-surface target detection capabilities of a bottom-mounted upward-facing echosounder using a surface-deployed optical video camera. In this case, the echosounder recorded signals that were consistent with the presence of fish, but the camera did not. While the identity of the targets registered with the echosounder could not be discerned, this likely resulted from non-overlapping fields of view between the instruments. Nonetheless, the bottom-mounted upward-facing echosounder was shown to be effective at detecting echo returns consistent with the presence of fish in the near surface waters of Grand Passage when turbulence and entrained air did not interfere with acoustic signal transmission.

4.2 Study 2B – WBAT, optical camera, and multibeam imaging sonar

Optical Camera

No fish were observed to pass thorough the field of view of the optical camera during the review of approximately 20 hours of data collected during January 31-February 2, 2020. However, image resolution was sufficient to identify objects such as seaweeds, bubbles, detritus, krill, other plankton, and objects thought to be jellyfish (Appendix A). See *Section 4.1: Study 2A – WBAT and optical camera* for more discussion. The remainder of this section will focus on the results from the Gemini imaging sonar and echosounder data collections and results.

Imaging Sonar

Approximately 91 hours of Gemini Imaging Sonar data were collected during January 25–February 2, 2020, resulting in 546 10-minute observation periods. During 121 (22%) of the 10-minute observation periods, 336 potential targets were detected by the SEATEC software, but their identity could not be confirmed. Where direction of movement could be determined, the targets were moving in the same direction as the tidal flow. Image resolution was insufficient to definitively classify potential targets, so they were classified into three categories: "turbulence/fish/school of fish" (n = 229), "single fish/debris" (n = 97), and "mooring" (n = 10) (Table 4.2.1).

Table 4.2.1: Classification of 336 Potential Detections Using Gemini Imaging Sonar

	(n)	(%)	ebb	flood	slack
Potential Detections	336	**100 %**	94	213	29
"Mooring"	10	**3 %**	5	1	4
"Single Fish/Debris"	97	**29 %**	43	32	22
"Turbulence/Fish/School of Fish"	229	**68 %**	46	180	3

Two types of occurrences are worthy of note. First, "clouds" of potential detections moved across the Gemini field of view and appeared to be related to turbulence moving in the same direction as the tidal flow. This generally occurred during periods of higher tidal flow rates. Second, there were occurrences of the PLAT-I mooring chain moving through the field-of-view and were marked as "potential detections" by the analysis software.

Echosounder

Of the 97 hours of data recorded by the echosounder, ~70 hours (72%) were suitable for analyses. Approximately 24 hours (25%) were excluded from analyses due to entrained air penetrating all the way or nearly all the way to the seafloor. Additionally, 3 hours (3%) of data were excluded due to the presence of horizontal bands of noise from an undetermined source (Figure 4.2.1). The tide was in its flooding phase during 20 of the excluded hours, indicating a strong asymmetry in the persistence and the depth of entrained air penetration between the flood and ebb tide phases at this location.
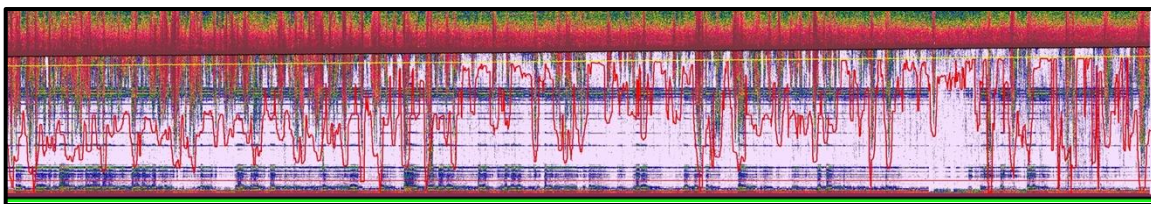

Figure 4.2.1: Example Echogram Showing Horizontal Bands of Noise. One hour of echogram data. Data was collected during a rising tide. Water depth at left is 14 meters. Water depth at right is 15 meters. Horizontal thin red line near the bottom is the nearfield exclusion line. Yellow line is the surface line inclusive of the 1-m offset for exclusion of the deadzone. Red jagged line is the unedited automated placement of the boundary of air entrained into the water column. Pink background coloring indicates that the entire hour of data was excluded from analyses. Note horizontal bands from undetermined source. Similar but not nearly so persistent bands have been noted in data collected in Minas Passage using the WBAT deployed to the seafloor attached to the FAST platform. Further investigation is required in order to determine the source of the unwanted signal.

Within the ~70 hours of useable data, there were 427 10-minute observation periods available for analyses. Echo returns consistent with the presence of fish were detected somewhere in the water column in all but one of the 427 observation periods. This remained unchanged when the echosounder data was restricted to the top 11 m of the water column to coincide with the field of view of the imaging sonar (Table 4.2.2).

The approach for handling the echosounder data within Echoview changed between the post-processing for Study 2A and Study 2B. For Study 2A, the data from the echosounder files that were dominated by acoustic returns from entrained air were excluded from Echoview (i.e., there was no useable data contained therein). When the post-processing occurred for Study 2B, all echosounder files were imported into Echoview regardless of whether each raw file contained useable data or not. For Study 2A, this meant that we could easily identify the number of observation periods that were obscured by intermittent, rather than persistent, returns from entrained air. For Study 2B, where all echosounder files were imported into Echoview, distinguishing "unusable" observations due to intermittent rather than persistent entrained air is far more complex. The analysis to distinguish the two "unusable" categories was not included in the analysis for 2B given that in the 11-m depth of interest, the number of observation periods was equivalent to that of the whole water column. See Table 4.1.1 where, for comparison, the number of unusable observation periods decreases with depth as one would expect.

Table 4.2.2: Summary of Study 2B Useable 10-minute Hydroacoustic Observation Periods. See description for Table 4.1.1 for definition of "fish present" and "fish absent".

Of the 427 10-minute observation periods (~70 hours out of 97 hours collected)…						
	Fish Present		Fish Absent		Unusable	
	(n)	(%)	(n)	(%)	(n)	(%)
At Any Depth	426	**100 %**	1	**0 %**	na	
Within 11 Meters from the Sea Surface	426	**100 %**	1	**0 %**	na	

Study 2B Discussion

Relative to the optical camera, the imaging sonar had a much larger field-of-view with a horizontal range of 30 m and a vertical range of 11 m at that distance. Therefore, the sampling volume of the imaging sonar was sufficiently large such that fish moving through the field of view would have been identifiable as fish provided that the resolution of the instrument was sufficiently high. However, the 336 potential detections could not be unambiguously resolved other than into three broad ambiguous categories and prevented adequate investigation of the target detection capability of the echosounder. The 336 potential detections made with the imaging sonar were observed across all tide phases but only within 22% of the 10-minute observation time-bins. However, echo returns consistent with fish were found within nominally 100% of the useable observation-bins.

While the difference in the proportion of observation bins with potential fish detections (22%: imaging sonar; 100%: echosounder) is notable, there are three factors that may have influenced this difference: (i) the tide phase – given that observations during ebb tide are over-represented in the echosounder data (due to the exclusion of data overwhelmed by entrained air), (ii) non-overlapping sample volumes between instruments (not co-located), and (iii) different deployment locations.

The strong asymmetry of tidal phase associated with the exclusion of hydroacoustic data due to entrained air suggests important differences in the hydrodynamic regimes at the deployment location of the FAST platform and the PLAT-I. Because of the tidal asymmetry in the persistence and extent of entrained air, flood-tide data were proportionally under-represented in the echosounder data relative to the imaging sonar data. We examined the distribution of potential detections by tide phase in order to determine whether the partial exclusion of flood tide data from the echosounder dataset affected the proportional comparison of total observation periods. In other words, if flood phase is under-represented in the echosounder data, then the ~ 100% "fish present" time bins may be overstated relative to the imaging sonar proportion of "potential detection" time bins (22%). However, the flood tide was strongly represented in the imaging sonar potential detections (Table 4.2.1), accounting for 65% of the potential detections that were categorized as "single fish/debris" or "turbulence/fish/school of fish" (i.e., excluding the "mooring" category). Therefore, the proportional difference (100% vs. 22%) of observations with potential fish detections does not appear to be a function of the difference in the proportion of tide phase observations.

The repositioning of the FAST platform for Study 2B, the diameter of the echosounder acoustic beam at the sea surface (1.6 m) and the useable horizontal range of the imaging sonar (30 m), resulted in non-overlapping sample volumes. Although the lack of overlapping sample volumes precluded definitive cross-referencing between the two instruments, optical cameras and imaging sonars have been shown to be valuable monitoring tools elsewhere (Mueller *et al.,* 2006; Hastie *et al.,* 2019a, 2019b; Williamson *et al.,* 2016b) and have value for monitoring in Grand Passage.

As a result of the repositioning of the FAST platform, the echosounder field-of-view was in a more "open water" setting than the imaging sonar mounted on the PLAT-I. Given the distance between the position of the two instruments, we cannot rule out that the possibility that hydrodynamic conditions at these locations, or the presence of the PLAT-I structure itself, influenced fish presence/absence. However, we have no information by which to address fish behaviour and cannot address this question.

The primary goal of this study was to investigate the target detection capabilities of a bottom-mounted upward-facing echosounder using a surface-deployed imaging sonar. As observed in Study 2A, the echosounder recorded signals that were consistent with the presence of fish, but the resolution of the imaging sonar was insufficient to unambiguously identify detections beyond three broad categories. Nonetheless, the bottom-mounted upward-facing echosounder

was shown to be effective at detecting echo returns consistent with the presence of fish in the depth range of the imaging sonar when turbulence and entrained air did not interfere with acoustic signal transmission.

4.3   Study 2C – WBAT and EK80

Echosounders

Hydroacoustic data were recorded at the PLAT-I site (33 hours: surface-deployed EK80) and at the FAST-platform site (36 hours: bottom-mounted WBAT) during a spring tide from September 3-6, 2020. There were 244 10-minute observation periods available for analyses from the PLAT-I site and 203 observation periods from the FAST site. Because the purpose of these data collections was to quantify the extent of signal interference from entrained air, all data were post-processed demarcating the boundary of the entrained air ("turbulence line") in Echoview without using "bad data" regions that would fully exclude data from analyses (i.e., all data were available for the analyses).

Signal Interference by Entrained Air

Hydroacoustic data from the "PLAT-I" and "FAST" sites suggests important differences in the hydrodynamic regimes at the two locations. For the PLAT-I site, the proportion of useable data decreased markedly with increasing flow speed on the flood tide (adjusted R^2 = 0.83; Figure 4.3.1 "a"); the influence of flow speed was much less pronounced on the ebb tide (adjusted R^2 = 0.00; Figure 4.3.1 "b"). This phenomenon is well illustrated in a set of echograms typical to the PLAT-I site (Figure 4.3.2 "a" and "b"). The flood tide echogram from the PLAT-I site ("a"), is dominated by persistent, strong signals of entrained air (red colors) throughout the water column, whereas the ebb tide echogram ("b") shows instances of entrained air near the sea surface but is largely dominated by echo returns from the water column not contaminated by entrained air.

The asymmetry in the proportion of useable data for analyses between flood and ebb tide phases at the PLAT-I site is particularly evident when the proportion of useable data is partitioned using a minimum "useable" threshold, regardless of flow speed (Figure 4.3.3 "a"). The proportion of useable data for each tide phase shows little change (ebb: ~100 %; flood: ~20%) regardless of how the "useable" criteria is defined. In other words, Figure 4.3.3a answers the question "how much of the data available on the flood or ebb tide are useable if we set the minimum 'useable' criteria to at least 50% of the water column (or 55%, or 60%, etc.,) regardless of flow speed?". At the PLAT-I site, the amount of useable data is strongly influenced by tide phase – useable on the ebb (~100%) but not on the flood (~20%) – and minimally influenced by tightening the criteria by which "useable" is defined.

Conversely, at the FAST deployment site for Study 2C, the amount of useable data was more influenced by how the criteria for "useable" was defined and minimally influenced by tide phase

(Figure 4.3.3 "b"). In other words, the two lines representing flood and ebb tide data track tightly together with minimal difference between the useable proportion on the flood vs. the ebb tide and show a distinct reduction in the proportion of useable data that is negatively correlated with increasing minimum criteria for "useable". When plotted relative to flow rate, there is some reduction in the proportion of "useable" data with increasing flow rate on the flood tide (adjusted R^2 = 0.51; Figure 4.3.1 "c"), but not as pronounced at the higher flow rates observed at the PLAT-I site. There is no evidence for a reduction in the proportion of useable data with increasing flow rate at the FAST deployment site on the ebb tide (adjusted R^2 = 0.02; Figure 4.3.1 "d"). The relative symmetry of useable data at the FAST site on the ebb and flood tide is illustrated in the echograms (Figure 4.3.2 "c" and "d").

These findings are consistent with the work of Hay (2017) in that the strong tidal currents in Grand Passage can be accompanied by high levels of turbulence resulting from the interaction of the currents with the channel's bathymetric features and Peter's Island (Figure 2.1). The PLAT-I is downstream from Peter's Island during the flood tide. In addition, Hay (2017) notes that spatial scales in a turbulent tidal flow can span many orders of magnitude and local seabed conditions are not sufficient from which to predict levels of turbulence with any degree of accuracy. Therefore, the presence, or absence, of turbulence capable of entraining air minimally or deeply into the water column is site-specific and dependent on the upstream conditions. A satellite image of the PLAT-I on a flood tide (Figure 4.3.4) suggests that the PLAT-I is deployed within a particularly turbulent portion of the channel; a possible consequence of its location relative to Peter's Island. If the location of the PLAT-I during a flood tide is downstream from bathymetric features generating sufficiently strong turbulence to entrain air from surface to seafloor for large portions of the flood tidal phase, but downstream from less dynamic bathymetric features on the ebb tide, the strong asymmetry in the extent of entrained air we observed would be expected. It appears that the placement of the FAST platform for Study 2C was outside the region of strong and persistent air entrainment throughout the water column. Descriptive statistics of the modelled flow rates for the two echosounder sites for Study 2C are provided in Table 4.3.1 and Table 4.3.2 and show similar flow rates at the sites.

Although comparative echosounder data were not available within Study 2A or 2B, the asymmetry in the tidal phase of the data excluded from analyses due to entrained air also suggests strong asymmetry in the extent of entrained air in the vicinity of the PLAT-I location (see Appendix B). The asymmetry suggests that the hydrodynamic regimes at the FAST site locations for Study 2A and Study 2B were more similar to that of the PLAT-I location than the FAST site for Study 2C. During Study 2A, the position of echosounder data collection was directly behind the PLAT-I on the flooding tide and during Study 2B nearby to the PLAT-I on the flooding tide. In both studies, all but one of the hours excluded due to entrained air were data collected during the flood tide. Given that the PLAT-I rotors were parked during both Study 2A and 2B, the tide-phase asymmetry of the entrained air again appears to be a function of the hydrodynamics in locations downstream from Peter's Island.
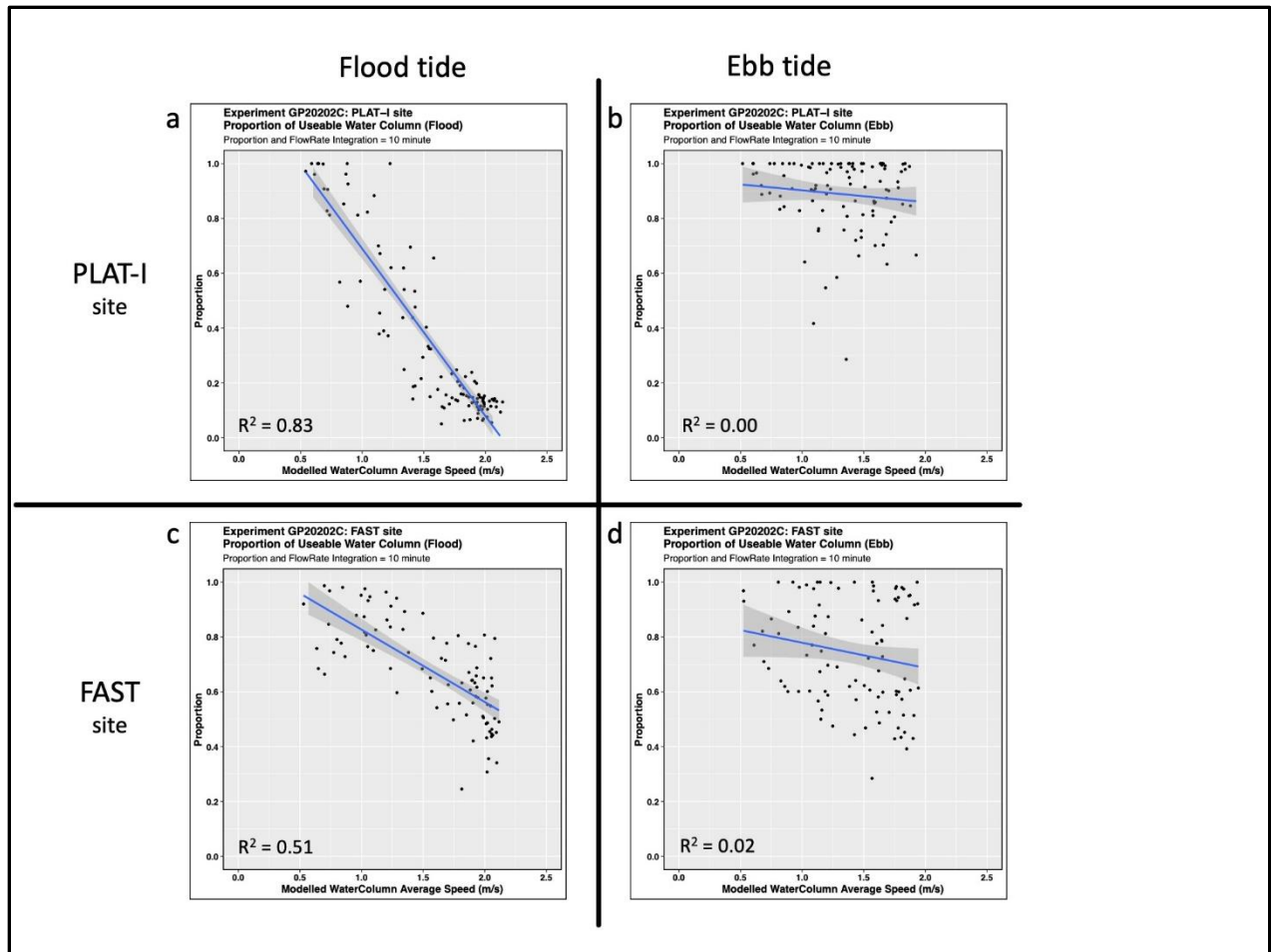
Figure 4.3.1: Proportion of Water Column Useable for Analyses as a Function of Modelled Depth-Averaged Flow Speed. *Useable proportion of water column was calculated using the depth of the top line (downward-facing: nearfield; upward-facing: surface line with 1-m offset), turbulence line (downward-facing and upward-facing), and bottom line (downward-facing: bottom line with 1-m offset; upward-facing: nearfield) integrated into 10-minute intervals and plotted as a function of depth-averaged flow speed for flood and ebb tide for data collected at the PLAT-I site (a,b) and at the FAST deployment site (c,d). Simple linear regression model fitted to the data (blue line) with 95% confidence interval (gray), and adjusted $R^2$are shown.*
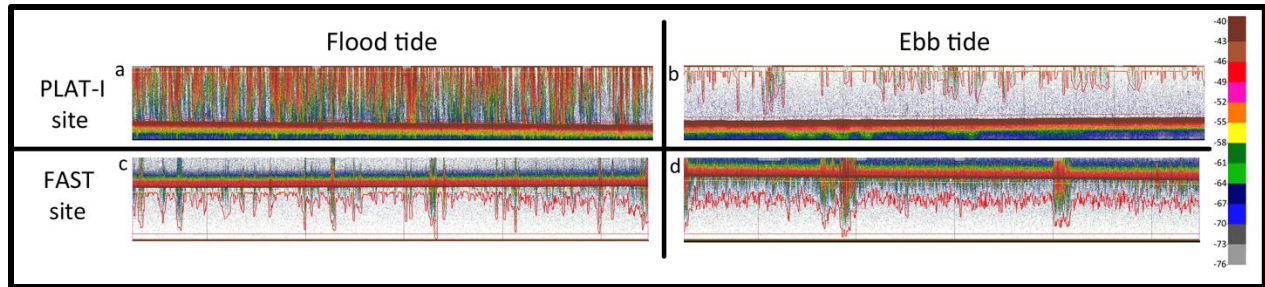
Figure 4.3.2: Study 2C Echograms at the PLAT-I site and at the FAST Site. *Typical raw echograms showing backscatter (S_v; dB re 1 m^2/m^3) values for one hour of data collection during flood and ebb tidal cycles in Grand Passage at the PLAT-I site (a, b) and at the FAST site (c,d). Jagged red line is the 'turbulence line' used to designate the extent of useable water column for analysis. Black vertical lines represent 10 min time bins used for analysis. Thin yellow horizontal line near surface is the position of the surface line (downward-facing: "nearfield" 1.7 m below transducer face; upward-facing: 1.0 m below echosounder-detected surface) and thin red horizontal line near the bottom designates the bottom of the analysis region (downward-facing: the 1-m offset from the seafloor; upward-facing: "nearfield" 1.7 m above the transducer face).*
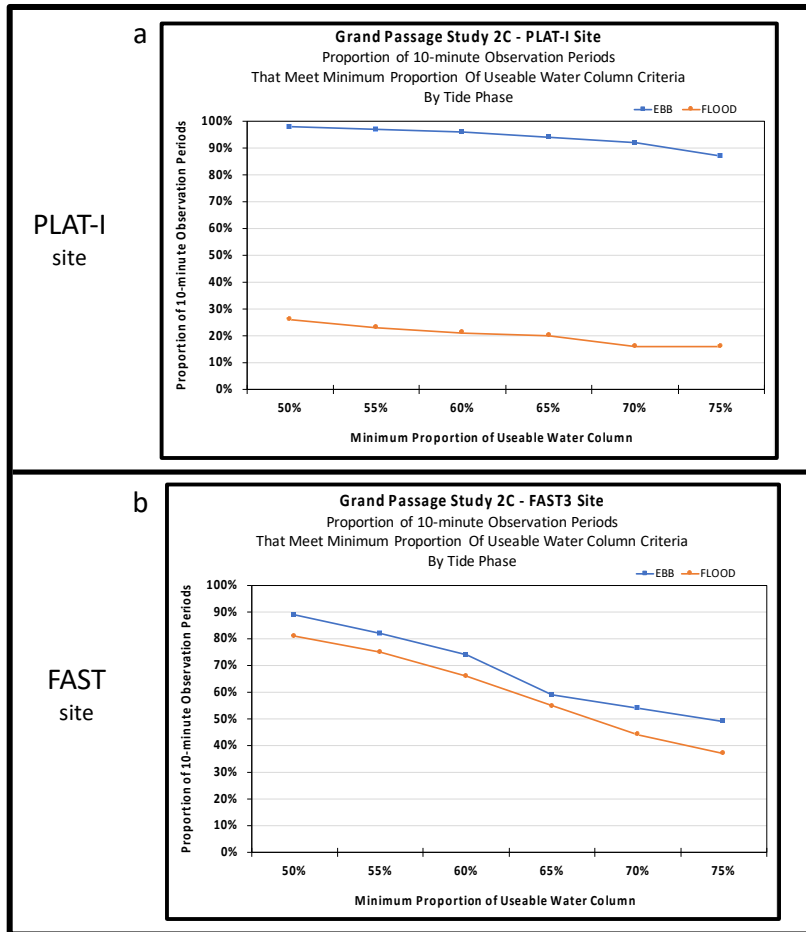
Figure 4.3.3: Proportion of Useable 10-minute Observation Periods by Tide Phase. *Dataset of 10-minute observation periods for each site was subsetted for minimum proportion of useable water column and proportion of total 10-minute observation periods by tide phase was calculated. **(a) PLAT-I site:** Tide phase strongly influences useable proportion of observations. A striking asymmetry is evident in the proportion of useable observation periods based on tide phase (~100% on ebb tide vs. 20% on flood tide). Criteria by which "useable" is defined (50% - 75%) has minimal influence on the proportion of useable observations. **(b) FAST site:** Tide phase shows minimal asymmetry in the proportion of useable observations. Criteria by which "useable" is defined (50% - 75%) has a stronger influence on the proportion of useable observations at this site.*

Figure 4.3.4: Deployment Locations of the echosounders in projects 2A, 2B and 2C. *Note the suggestion of strong turbulence in region approaching the PLAT-I.*

Table 4.3.1: Modelled Flow Rate Descriptive Statistics at Platform Locations.

DEPLOYMENT PLATFORM	LOCATION	Modelled Flow Rate (m/s)				
		Minimum	Mean	STD	Median	Maximum
PLAT-I site	45 15.830 N 66 20.210 W	0.10	1.31	0.55	1.42	2.14
FAST site	45 15.876 N 66 20.190 W	0.13	1.40	0.52	1.54	2.12

Table 4.3.2: Modelled Flow Rate Descriptive Statistics at Platform Locations by Tide Phase.

DEPLOYMENT PLATFORM	TIDE PHASE	Modelled Flow Rate (m/s)				
		Minimum	Mean	STD	Median	Maximum
PLAT-I site	ebb	0.52	1.33	0.36	1.38	1.93
	flood	0.54	1.57	0.46	1.73	2.14
	slack	0.10	0.31	0.11	0.33	0.47
FAST site	ebb	0.52	1.40	0.39	1.50	1.97
	flood	0.53	1.57	0.48	1.78	2.12
	slack	0.13	0.33	0.11	0.29	0.48

Echosounders: Downward- vs. Upward-facing

Target detection performance for a downward- vs. upward-facing echosounder is a function of i) the geometry of the opposing ensonifying cones, ii) any engineering differences inherent to the echosounders, and/or iii) the data collection parameters (e.g., pulse length, ping rate, power, acoustic frequency) being used. To empirically quantify target detections, an experiment would ideally be designed where targets with known target strength would be passed through the acoustic beam at varying speeds and depths in waters devoid of any other object (e.g., fish, zooplankton, detritus, etc.). Given the inherent challenges of such an experimental design, an empirical assessment of the target detection performance for the downward- vs. upward-facing echosounder was not possible. However, both echosounders used in this work were from the same engineering suite of echosounders (Simrad EK80) and were deployed with identical parameter settings for data collection. Thus, provided that a target passed through the acoustic beam, it would have been detected. Any differences in target detection would therefore be attributable to the opposing acoustic beam geometries of the downward- and upward-facing echosounders, and any environmental differences inherent to the PLAT-I site vs. the FAST site (e.g., differences in the extent and depth penetration of entrained air due to turbulent hydrodynamics, or differences in fish assemblages).

Because the acoustic beam is cone-shaped (Simmonds and MacLennan, 2005; Urick 1983), the probability of a target encountering the beam increases with the distance from the transducer. Thus, the implication of this fact is that to increase the likelihood of a target passing through the beam, the transducer should be placed further from the region of interest. Moreover, the implication of the cone-shaped acoustic beam means that waters closer to the transducer are under-sampled relative to the waters further away; reinforcing the conclusion that the transducer should be placed further from the region of interest to maximize the volume sampled and increase the likelihood of target detection.

Figure 4.3.5 provides an illustration of the implications for the placement of an echosounder at the sea surface (downward-facing) vs. on the sea floor (upward-facing) assuming a study site with a depth of 15 m and a flow speed of 3 m/s. The width of the blue acoustic cone denotes the volume ensonified from the transducer to the furthest extent possible against the backdrop of a yellow box denoting the 3 m of water that would pass by the transducer per second and in the interval between 1-Hz pings (i.e., 1 ping/second). The purple regions indicate areas excluded from sampling due to deployment position of the echosounder (i.e., water behind the transducer face), the transducer nearfield (1.7 m due to acoustic beam formation), and the height of the deadzone (1 m due to acoustic beam geometry).

For comparative purposes, Figure 4.3.6 provides a similar illustration as above, but with the ping rate increased to 2 Hz (i.e., 2 pings/sec). By increasing the ping rate to 2 Hz, the upward-facing echosounder provides nearly full coverage of regions near the sea surface. Within 5 m of the surface, the upward-facing echosounder samples ≥ 2/3 of the water passing by the transducer per second, whereas the downward-facing echosounder samples ≤ 1/3 of the water. Although the surface-deployed echosounder could be set to ping at a faster rate, it is still sampling a very

small volume per ping relative to an upward-facing echosounder. Therefore, when determining the orientation of an echosounder, it is important to maximize the ratio of sampled to unsampled water per ping at the depths of interest.
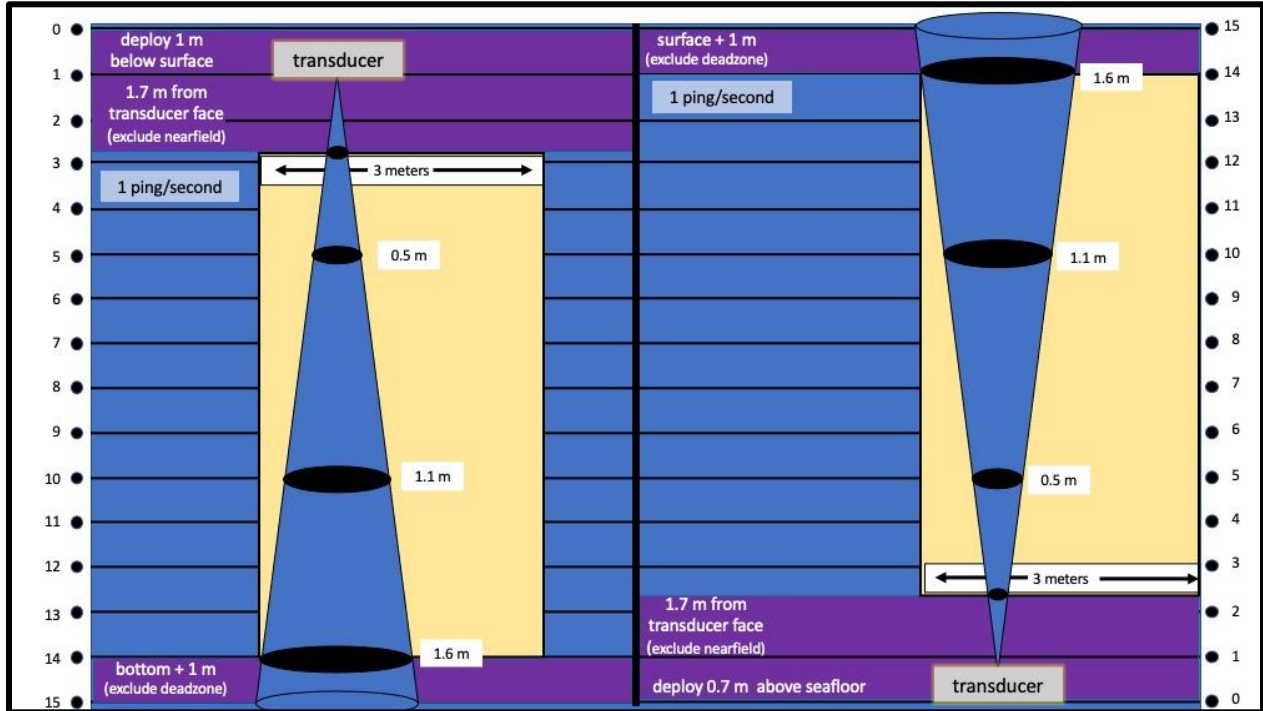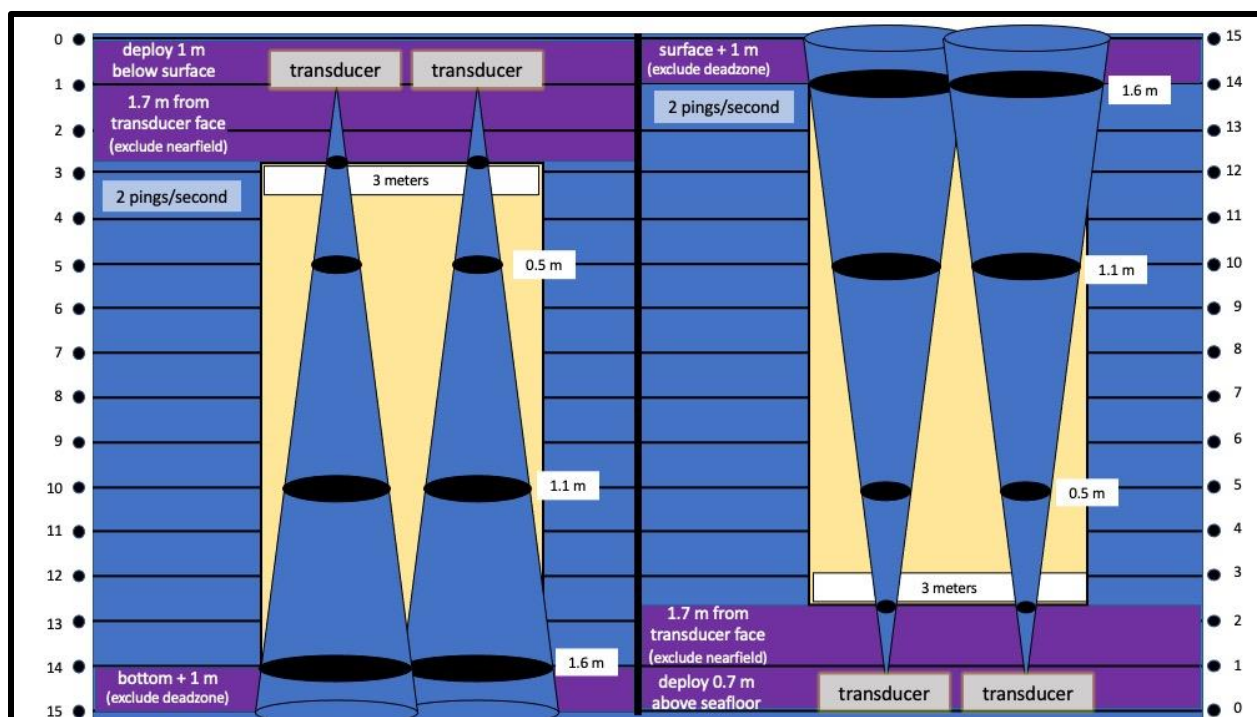

Figure 4.3.5: Echosounder Beam Diameter and Proportion of Water Ensonified at 1 Hz. *This graphic illustrates the ensonifying cone (**blue cone**) of an echosounder acoustic beam for a downward-facing transducer deployed at the surface (**left**) and an upward-facing transducer deployed at the sea floor (**right**). <u>Assumptions are as follows:</u> Water depth is 15 m (**blue background**). Transducer frequency is 120 kHz. Transducer beamwidth is 7°. Ping rate is 1 Hz. Pulse length is 1.024 ms. Water velocity is 3 m/s. Based on the transducer specifications, <u>the amount of water column excluded from observation (**purple**) is as follows:</u> Range excluded for transducer nearfield is 1.7 m from the transducer face. Height excluded for acoustic beam deadzone at sea bottom (downward-facing transducer) or at sea surface (upward-facing transducer) is 1 m. Range excluded for waters behind the transducer face: downward-facing transducer assumed to be deployed at 1 m below the surface and upward-facing transducer assumed deployed at 0.7 m above seafloor. **Black ellipses** mark the depths at which acoustic beam diameters are specified. **Yellow box** width is equivalent to 3 m at scale with the acoustic cone. The cone superimposed on the yellow box is intended to illustrate how much water would be left unsampled (visible yellow) at a ping rate of 1 ping/second (1 Hz) in a flow environment of 3 m/s.*

Figure 4.3.6: Echosounder Beam Diameter and Proportion of Water Ensonified at 2 Hz. *This graphic illustrates the ensonifying cones (**blue cone**) of an echosounder acoustic beam for a downward-facing transducer deployed at the surface (**left**) and an upward-facing transducer deployed at the sea floor (**right**). Ping rate is 2 Hz. All other assumptions are as specified in Figure 4.3.5.*

When considering target detection capabilities of a downward- vs. upward-facing echosounder, consideration must be given to the environmental characteristics of the site that will influence the ability to collect quantitative data. Tidal channels are inherently, but not uniformly, turbulent (as illustrated by the results of Study 2C) and can entrain air that will obfuscate the same portion of the water column regardless of whether an echosounder is deployed in a downward- or upward-facing orientation. However, collection of quantitative data required to estimate target abundance and distribution will be confounded if entrained air is between the echosounder and potential targets (Urick 1983, Johannesson and Mitson, 1983).

This is because acoustic energy is scattered when the acoustic beam encounters an interface with an impedance different from water (e.g., entrained air, an organism, interfaces at the sea surface and sea floor) (Simmonds and MacLennan, 2005; Urick, 1983; Johannesson and Mitson, 1983; Coates, 1989). Therefore, if the acoustic beam first encounters entrained air before reaching a target (fish), it is no longer possible to quantify the proportion of emitted energy that is returned from the target to the transducer because the amount of energy reaching the target is no longer known (Urick 1983, Johannesson and Mitson, 1983). In fact, the energy returning from the target is doubly affected, because the returning energy is scattered again as it passes back through the entrained air to the transducer. Without the ability to quantify the proportion of the transmitted energy represented by the energy returned from the target, it is not possible to produce quantitative results by which to compare changes in fish density or abundance over time (from ping to ping or from survey to survey). It is not the ability to detect or define the

boundary of entrained air that is affected by the placement of an echosounder at the sea surface or sea floor, but rather the quantification of target detections that is impacted; the comparability of any analytical results is irretrievably compromised (Urick 1983, Johannesson and Mitson, 1983). Thus, to achieve quantitative results, the orientation of a transducer needs to be such that the acoustic beam encounters a target before it encounters entrained air. For turbulent tidal channels, this means that the collection of quantitative data necessitates bottom-mounted echosounders with upward-facing transducers.

There are additional factors beyond data collection and data quality that contribute to survey-design decisions, and there are both advantages and disadvantages for surface-deployed and bottom-mounted echosounders. These trade-offs include logistical, financial and operational considerations that need to be accounted for during the development of data collection campaigns (see Table 4.3.3). For instance, surface deployments provide greater certainty about the deployment position and the location of the sampled volume of water, and access to data in (near) real-time. Surface deployments also provide logistical advantages (reduced deployment and recovery costs, instrument servicing) and reduced risks for instrument loss or damage. However, where the region of interest is near the sea surface, a downward-facing echosounder will leave most of that region unsampled due to acoustic beam geometry, and the data collected cannot be used for quantitative analyses if the acoustic beam encounters entrained air before targets of interest. Although trade-offs must be weighed when making deployment decisions, the *purpose* of investing time, money, and resources towards data collection must be the driving motivation for those decisions, because if the data is not collected in a way that supports the analytical needs, then those investments will have been wasted. The challenge is to correctly identify and weigh these trade-offs while keeping the justification and data requirements for the purpose of the data collection firmly in mind.

Additional considerations when designing echosounder data collection campaigns can be found in Appendix C.

Table 4.3.3: Advantages and Disadvantages of Surface-Deployed and Bottom-Mounted Stationary Echosounders.

Surface Deployed/downward-facing		Bottom Mounted/upward-facing	
Advantages	Disadvantages	Advantages	Disadvantages
• certainty in deployment location relative to rotor for surface deployed turbines • (near) real-time data access • (near) real-time monitoring of QA/QC for data collection • continuous data collection due to reduced need for duty-cycling (continuous access to power & data storage) • reduced costs/waste due to access to power without need for battery power • reduced marine ops costs and risks (to data, instruments, personnel)	• region between sea surface and transducer face (potential depths of interest) eliminated from data collection • narrow end of acoustic beam is near sea surface leading to a high proportion of *unsampled* water in depths of interest (near surface: upper 8 m) • entrained air between transducer and potential targets compromises ability to collect quantitative data required to estimate metrics of interest: abundance, distribution	• can sample within 1 m of sea surface • wide end of acoustic cone is near surface, increasing the proportion of water *sampled* in depths of interest (near surface: upper 8 m) • acoustic beam reaches target before encountering entrained air, providing the ability to collect quantitative data required to estimate metrics of interest: abundance, distribution	• deployment position may be imprecise relative to position of interest (i.e., turbine rotors) and limited due to subsurface infrastructure (mooring lines, inter-array cabling) • due to PLAT-I rotation on turret, if a single echosounder is deployed, the range between sampled waters and region of interest will be more advantageous on one tide phase than the other • requires highly engineered deployment platform suitable for tidal stream conditions Autonomous • data access time lag: deployment duration and delayed recovery due to weather • issues with data collection are not discovered until instrument recovery of instrument at end of deployment period • trade-off between continuous data collection and length of deployment due to requirement for onboard power source (batteries) and data storage • increased costs/waste due to requirement for battery power storage • increased marine ops costs ($$) and risks (to data, instruments, personnel) Cabled • increased marine ops costs ($$) and risks (to data, instruments, personnel) … but less than autonomous

Study 2C Discussion

The results of this study suggest that the extent of signal interference from air entrained due to turbulence is location specific, and a consequence of local hydrodynamic features in Grand Passage. This is consistent with previous work that found that the strong tidal currents in Grand Passage can be accompanied by high levels of turbulence resulting from the interaction of tidal currents with the channel's bathymetric features and Peter's Island (Hay 2017). While the extent of entrained air was strongly asymmetrical with tidal phase at the PLAT-I site, this was not observed for FAST site. Conversely, how 'useable' water column was defined did not alter the proportion of useable observation periods at the PLAT-I site, but strongly influenced the number of useable observation periods at the FAST site. Collectively, these results suggest that location-specific hydrodynamic regimes, and their influence on the collection of useable data, must be considered when selecting deployment sites for the collection of data required to meet analytical needs. Therefore, if the purpose of data collection is to document fish presence, abundance, and distribution throughout the tidal cycle (to meet regulatory expectations or satisfy ecosystem protection purposes), it is important to choose sites where the hydrodynamic regime does not preclude data collection for most or all of one tidal phase. If that is not feasible, then complementary data collection methods may be required to meet analytical requirements. However, this needs to be balanced against the possibility that a location with strong tidal phase turbulence asymmetry may be a site where data collection is suitable on the alternative tide phase (as found here). Under those circumstances, the analytical needs may require data collection at more than one location to obtain data to draw inferences when useable data cannot be obtained at the site of interest.

Results of this study, and due consideration to the fundamental principles of hydroacoustics (Simmonds and MacLennan, 2005; Urick, 1983; Johannesson and Mitson, 1983; Coates, 1989), make it clear that maximizing the sampling volume and the collection of quantitative hydroacoustic data near the sea surface requires a bottom-mounted upward-facing echosounder. However, there are substantial trade-offs (logistical, operational) relative to a surface-deployed echosounder that require consideration, including increased costs and risks associated with subsea instrument deployment and recovery in tidal channels. When weighing deployment options, the purpose of the data collection campaign should be the driving force behind the decisions that are made. Otherwise, if the data is not collected in a way that satisfies the analytical requirements, the investment of resources in the data collection effort will have been wasted. The challenge is to correctly identify and weigh the trade-offs while prioritizing the data requirements for the purpose of the data collection effort.

4.4   Findings Specific to PLAT-I Rotor Swept Depth – Across All Three Studies

The results of the by-ping analyses of the useable water in the upper 8 m of the water column are consistent with findings herein about site-specific hydrodynamic features (Table 4.4.1). The blue shaded cells highlight each tide phase and depth bin for which the proportion of useable

data was >50% of the pings collected within that tide phase. The shading intensifies in 10% increments as the proportion of useable pings increases. For the data collected at the PLAT-I site for Study 2C, there were no depth bins during the flood tide achieving 50% useable pings (shown as all white cells). However, for data collected on the ebb tide, every visible depth bin (4 - 8 m) is shaded blue with the useable proportion of pings increasing with depth (blue shading intensifies: 71% to 89% useable). The tidal asymmetry at the PLAT-I site is readily apparent and may be due to turbulence from Peter's Island. Conversely, the data collected at the FAST site for Study 2C shows a general absence of tidal asymmetry and is evident in the equivalent shading of the depth bins on the flood and ebb tides. At the FAST site for Study 2A (when the FAST platform was much closer to the PLAT-I), the tide phase asymmetry is clearly evident, although the useable data never achieved 50% on either tide phase within the top 8 m of the water column. However, readers should note that the useable proportion of pings was generally an order of magnitude greater on the ebb than on the flood tide. At the FAST site during Study 2B, the tidal asymmetry is still evident, but not as strong as the asymmetry at the site for Study 2A.

Table 4.4.1: Proportion of Useable Pings Within Each Meter of the Rotor Swept Depth Across All Three Studies. TOP Section: *The total number of data collection pings enumerated by tide phase (F = flood, E = ebb, S = slack) with proportions shown.* **BOTTOM Section:** *By depth bin, the number of useable pings in total and within each tide phase, with proportion each represents of "All Pings" by tide phase. Depth bin designation (e.g., "1 m") designates the start depth for each 1-m depth bin.* **BLACK cells:** *Echosounder exclusion ranges.* **BLUE cells:** *The cells for which number of useable pings was greater than 50% of the data collection pings available on that tide phase. Color intensity increases as the proportion of useable pings increases:* (**50%+ 60%+ 70%+ 80%+ 90%+**).

	Data Collected: Total Number of Pings															
	2A FAST site (Note[1]) (n = 175,798)				2B FAST site (n = 289,316)				2C FAST site (n = 102,000)				2C PLAT-I site (n = 127,690)			
	Total	F	E	S	Total	F	E	S	Total	F	E	S	Total	F	E	S
All Pings	175,798 100%	78,071 44%	80,819 46%	16,908 10%	289,316 100%	134,706 47%	122,439 42%	32,171 11%	102,000 100%	45,708 45%	48,727 48%	7,565 7%	127,690 100%	59,042 46%	53,074 42%	15,574 12%
	Number of USEABLE Pings with Percent of TOTAL Pings by Tide Phase															
0 m	deadzone				deadzone				deadzone				deployment depth			
1 m	3,787 2%	209 0%	2,896 4%	682 4%	14,292 5%	3,684 3%	10,121 8%	487 2%	23,868 23%	7,425 16%	14,711 30%	1,732 23%	transducer nearfield			
2 m	7,241 4%	264 0%	5,340 7%	1,637 10%	26,436 9%	5,585 4%	17,663 14%	3,188 10%	32,848 32%	11,860 26%	17,612 36%	3,376 45%	transducer nearfield			
3 m	13,730 8%	450 1%	9,438 12%	3,842 23%	44,333 15%	9,062 7%	26,187 21%	9,084 28%	45,440 45%	17,563 38%	22,406 46%	5,471 72%	63,331 50%	11,205 19%	37,567 71%	14,559 93%
4 m	21,476 12%	1,000 1%	14,564 18%	5,912 35%	67,227 23%	15,151 11%	36,675 30%	15,401 48%	57,364 56%	23,392 51%	27,097 56%	6,875 91%	66,985 52%	11,795 20%	40,316 76%	14,874 96%
5 m	29,923 17%	1,837 2%	20,750 26%	7,336 43%	93,348 32%	22,848 17%	49,397 40%	21,103 66%	68,829 67%	29,135 64%	32,331 66%	7,363 97%	70,576 55%	12,482 21%	42,881 81%	15,213 98%
6 m	39,131 22%	2,901 4%	27,223 34%	9,007 53%	120,099 42%	31,882 24%	62,424 51%	25,793 80%	79,118 78%	34,545 76%	37,009 76%	7,564 100%	73,959 58%	13,322 23%	45,282 85%	15,355 99%
7 m	49,138 28%	4,400 6%	34,564 43%	10,174 60%	146,345 51%	42,949 32%	74,982 61%	28,414 88%	86,250 85%	38,202 84%	40,483 83%	7,565 100%	76,903 60%	14,220 24%	47,233 89%	15,450 99%

Note[1]: Raw data files for which turbulence reached all the way or nearly all the way to the seafloor were excluded from Echoview (18 files). To estimate the number of pings excluded, one ping-per-second for each of the missing hours was added back in to the "All Pings" total by tide phase. Therefore, percentages as shown are reasonable estimates. Excluded files by tide phase: Flood = 17 hours. Ebb = 0 hours. Slack = 1 hour.   No raw files were excluded from Echoview for Study 2B or 2C.

Rotor Swept Depth Discussion

For the echosounder data collected during the studies reported herein, the results of the useable data analyses by 1-m depth bins within the top 8 m of the water column were consistent with the earlier results suggesting site-specific hydrodynamic regimes. The contrasts among the results demonstrate that it is not only important to understand the hydrodynamic regime among sites, but also in the depth range of interest. The implication is that none of these sites on either tide phase would have facilitated the collection of 100% useable data within the 8-m depths of interest. However, some sites are more favorable than others, and criteria for site selection, based on some minimum acceptable proportion of useable pings, should be defined by tidal phase and documented during the site selection process.

5   Conclusions

These studies were designed to assess the efficacy of bottom-mounted and surface-deployed echosounders for target detections and to help guide best practices for monitoring in high flow environments. In all three studies the bottom-mounted echosounder detected targets consistent with the presence of fish in the portion of the water column not obscured by entrained air. However, the optical camera and the imaging sonar failed to provide data by which to corroborate target identity. This may have partially resulted from non-overlapping sampling volumes between the instruments. However, the repositioning of the bottom-mounted echosounder between studies was fortuitous in the sense that it facilitated examination of how turbulence varies in space, and lead to new insights about the implications of hydrodynamics for data collection. Specifically, knowledge of local hydrodynamics is important in site selection for data collection campaigns and for meeting analytical needs to meet regulatory needs or expectations or to satisfy ecosystem protection purposes.

In addition to selecting site location for echosounder deployment, there are trade-offs inherent in selecting the positioning of the echosounder at the site (e.g., surface-deployed downward-facing versus bottom-mounted upward-facing). The trade-offs include implications for data collection (e.g., maximizing volume sampled at the depths of interest, recording echo returns that are uncontaminated by the presence of entrained air between the transducer and the targets of interest) and logistical, financial, and operational considerations. Although trade-offs must be weighed when making deployment decisions, the purpose of investing time, money, and resources towards data collection must be the driving motivation for those decisions. The challenge is to correctly identify and weigh these trade-offs while keeping the data requirements for the purpose of the data collection firmly in mind.

6 References

Chen, C., and Beardsley, R.C. (**2011**). An Unstructured Grid, Finite-Volume Coastal Ocean Model. SMAST/UMASSD-11-1101. http://fvcomo.smast.umassd.edu/fvcom/

Coates, R.F.W. (1989). *Underwater Acoustic Systems.* Wiley & Sons, Inc. New York.

Fernandes, P.G., Gerlatto, F., Holliday, D.V., Nakken, D.V., and Simmonds, E.J. (**2002**). Acoustic applications in fisheries science: the ICES contribution. ICES Marine Science Symposia **215**: 483-492.

Fisheries and Ocean Canada (**1996**). Krill on the Scotian Shelf. Stock status report 96/106E. Catalogue number Fs76-1/1996-106E-PDF.

Fraser, S., Nikora, V., Williamson, B.J., and Scott, B.E. (**2017**). Automatic active acoustic target detection in turbulent aquatic environments. Limnol. Oceanogr. Methods **15**(2): 184-199.

Guerra, M., Hay, A.E., Cheel, R.A., Trowse, G., and Karsten R. (**2019**). Turbulent flow mapping around a floating in-stream tidal energy platform, in: Proc. of the 13th European Wave and Tidal Energy Conference, Napoli, Italy.

Hastie, G.D., Bivins, M., Coram, A., Gordon, J., Jepp, P., MacAulay, J., Sparling C., and Gillespie, D. (**2019a**). Three-dimensional movements of harbour seals in a tidally energetic channel: Application of a novel sonar tracking system. Aquatic Conservation: Marine and Freshwater Ecosystems **29**(4), 564-575.

Hastie, G.D., Wu, G.-M., Moss, S., Jepp, P., MacAulay, J., Lee, A., Sparling, C.E., Evers, C., and Gillespie, D. (**2019b**). Automated detection and tracking of marine mammals: A novel sonar tool for monitoring effects of marine industry. Aquatic Conservation: Marine and Freshwater Ecosystems **29**(S1), 119-130.

Hay, A. (**2017**). Turbulence in Grand Passage, Nova Scotia: Measures of Intermittency. Report submitted to Offshore Energy Research Association.

Johannesson, K.A. and Mitson, R.B. (**1983**). Fisheries Acoustics: A practical manual for aquatic biomass estimation. FAO Fisheries Technical Paper 240. Food and Agriculture Organization of the United Nations. Rome.

Love, R.H. (**1971**). Measurements of Fish Target Strength: A Review. Fishery Bulletin 69(4): 703-715.

Lowe, S.C. and McGarry, L.P. (**2020**). Echofilter Usage Guide Release 1.0.0. Submitted to Offshore Energy Research Association and the Pathway Program.

MacKenzie, K.V. (**1981**). Nine-term equation for sound speed in the ocean. Journal of the Acoustical Society of America. **70**: 807-812. https://doi.org/10.1121/1.38690

McGarry, L.P., Douglas, J., and Lowe, S. (**2020**). Improving Automated Post-Processing of Echosounder Data with Machine Learning Models. Report submitted to Offshore Energy Research Association and the Pathway Program.

McMillan, J., Hay, A., Karsten, R., Trowse, G., Schillinger, D., and O'Flaherty-Sproul, M. (**2013**). Comprehensive tidal energy resource assessment in the lower Bay of Fundy, Canada, in: Proc. 10th European Wave and Tidal Energy Conference.

Mueller, R.P., Brown, R.S., Hop, H., and Moulton, L. **(2006)**. Video and acoustic camera techniques for studying fish under ice: a review and comparison. Reviews in Fish Biology and Fisheries **16**(2): 213-226.

O'Flaherty-Sproul, M. (**2012**). New high and low resolution numerical models of the tidal current through the Digby Neck passages, Master's thesis, Acadia University.

R Core Team (**2020**). R: A Language and Environment for Statistical Computing. R Foundation for Statistical Computing, Vienna, Austria. https://www.R-project.org.

Simmonds, J. and MacLennan, D. (**2005**). *Fisheries Acoustics Theory and Practice*, 2nd edition. Blackwell Publishing, Oxford, UK.

Simrad (**2020**). Simrad EK80 Scientific Wide Band Echo Sounder Reference Manual (395234/H). Kongsberg Maritime AS.

Urick, R.J. (**1983**). *Principles of Underwater Sound*, 3rd edition. Peninsula Publishing, Los Altos, California.

Viehman, H.A., and Zydlewski, G.B. (**2014**). Fish Interactions with a Commercial-Scale Tidal Energy Device in the Natural Environment. Estuaries and Coasts 38(Suppl 1): S241-252.

Viehman, H., Hasselman, D., Boucher, T., Douglas, J., and Bennett, L. (**2019**). Integrating Hydroacoustic Approaches to Predict Fish Interactions with In-stream Tidal Turbines. Report submitted to Fundy Ocean Research Center for Energy. Project number 300-208.

Williamson, B., Fraser, S., Blondel, P., Bell, P., Waggitt, J., and Scott B. (**2016a**). Integrating a multibeam and multifrequency echosounder on the FLOWBEC seabed platform to track fish and seabird behavior around tidal turbine structures. In 4th Marine Energy Technology Symposium (METS). Washington, D.C. p.5.

Williamson, B., Blondel, P., Armstrong, E., Bell, P.S., Hall, C., Waggitt, J.J., and Scott, B.E. (**2016b**). A Self-Contained Subsea Platform for Acoustic Monitoring of the Environment Around Marine Renewable Energy Devices – Field Deployment at Wave and Tidal Energy Sites in Orkney, Scotland. IEEE Journal of Oceanic Engineering **41**(1): 67-81.

Williamson, B., Fraser, S., Blondel, P., Bell, P.S., Waggitt, J.J., and Scott, B.E. (**2017**). Multisensor Acoustic Tracking of Fish and Seabird Behavior Around Tidal Turbine Structures in Scotland. IEEE Journal of Oceanic Engineering **42**(4): 948-965.

Appendix A.   Envirosphere Consultants Limited: Review of Underwater Video

Envirosphere CONSULTANTS LIMITED

Review of Underwater Videos from Grand Passage, Nova Scotia—

Test Videos December 2019-January 2020

March 12, 2020

Prepared for:

Fundy Ocean Research Center for Energy
1690 Hollis Street, Unit 1001
Halifax, Nova Scotia B3J 1V7

Prepared by:

Envirosphere Consultants Limited
120 Morison Drive, Windsor Nova Scotia Unit 5 B0N 2T0
902 798 4022 | enviroco@ns.sympatico.ca | www.envirosphere.ca

EXECUTIVE SUMMARY

As part of a test program for an underwater acoustic imaging sonar, the Fundy Ocean Research Centre for Energy (FORCE) recorded underwater video from a camera co-located and coincident with the sonar equipment. Envirosphere Consultants Limited screened the approximately 170 hours of video for the occurrence of fish and other large marine organisms. No fish were observed. Videos were clear enough to determine occurrence of fish (if present), tidal state, and presence of detritus and detritus as well as occasional marine invertebrate organisms.

INTRODUCTION AND BACKGROUND

The Fundy Ocean Research Centre for Energy (FORCE) has been participating in tests of acoustic imaging equipment intended for monitoring movements and behaviour of fish around instream tidal energy devices. Its participation has included use of underwater video equipment (a Deep Blue surface-connected underwater camera system) deployed in the vicinity of an experimental acoustic imaging sonar, in Grand Passage, Digby Neck, Nova Scotia. The project was intended to provide information to identify targets potentially occurring in the vicinity, to assist in interpreting the sonar record. Video records were obtained in experiments in December 2019 (primary data collection period) and for a short period in February 2020. Videos obtained were submitted to Envirosphere Consultants Limited, a marine environmental consultant located in Windsor, Nova Scotia, which has experience in underwater video interpretation, for review and documentation.

METHODOLOGY

Videos for both periods (December 2019 and February 2020) were provided on portable hard drives. Videos were typically fifteen minutes long but occasionally longer (up to 30 minutes) or shorter (1-2 minutes), a period presumably set by the video capture system. The majority were recorded in daylight; however some night periods were captured but were disregarded in the analysis. The camera had a 'normal' perspective and field of view, so that targets at some distance would be detected (FORCE personal communication).

Video was viewed in the VLC video viewer (VLC is an open-source media player made by the VideoLAN organization—www.videolan.org) on personal computers with the MicroSoft Windows 10 operating system. VLC allows viewing to be speeded up without loss of frames and a speed of 2x was typically used in viewing. Initially the video was viewed at normal speed, but it was almost immediately decided to use a faster speed, particularly since it was discovered that there was little in the videos, to ensure the project could be completed within timelines required. Also initially, image captures were made of miscellaneous objects (e.g. seaweed, objects thought to be jellyfish, detritus etc.), but the practice was excessively time-consuming and was dropped after approximately the second day. Occasionally videos were examined by another member of the team, with a view to locating and capturing images to illustrate miscellaneous objects seen in the videos.

For each video viewed, the viewer recorded the file name on paper, and any observations. FORCE had provided an Excel spreadsheet listing the file names, the times and durations of the videos. The data logging system had an intrinsic start date and time, which was translated to actual dates and times using a conversion factor provided by FORCE. The list of videos also indicated the video clips obtained at night

---

and therefore which were to be omitted. Videos were in MP4 video format. The video record was continuous over the times analyzed.

RESULTS

Occurrence of Fish

Video coverage consisted of approximately 150 hours of video in 755 separate clips, typically 15-minutes in duration, as well as 152 clips taken overnight (the latter were not examined). None of the videos detected fish or other large organisms.

Occurrence of Miscellaneous Objects

Miscellaneous objects seen included seaweeds, bubbles, objects thought to be jellyfish, detritus, krill, and other plankton (Figures 1-20).

General Quality of Video

Typically the video captured the movements of particles, bubbles and other objects suspended in the water in the camera's field of view. Tidal motion could be observed by the movement towards or away from the camera of particles, or periods of slack tide. Images were mostly grey although changes in colour could be observed in individual video clips, including brief shifts to 'warmer' tones (yellowish or orange) thought to be changes in sunlight reaching the water surface. In most videos, due to the absence of reference points, it was not possible to assess the field of view. However several of the objects captured in images were estimated to be at several metres distance (e.g. see Figure 15 & 16), indicating that the camera was adequately covering the required field of view. At times, objects passing through appeared to be coloured due to the incident light, while some objects, for example those thought to be jellyfish, were naturally reddish. Ctenophores were bright reflective white. A red seaweed, as well as an euphausiid (krill) caught in one of the images were their natural colour.

Conclusions and Recommendations

The video was of sufficient quality to detect fish and larger organisms in the field of view. It did not, however, include reference points or scales (for example part of a physical device or a ruler) to assist in determining size of objects if observed, and it is suggested that this be attempted in future.

Positioning of the camera, which appears to have a horizontal field of view, may not be ideal for detecting fish furthest from it, due to overall turbidity and presence of particles in the water. Orienting the camera towards the water surface, which would appear bright from below, may improve the detection of distant occurrences of fish.

The frame rate and compression used in producing MP4 files from the video excessively blurs objects occurring near the camera, although more distant objects were clear. Occurrence of large objects including fish can probably readily be detected both near and at some distance from the camera.

Figures

Figure 1. Piece of seaweed near camera. Three shaded circles near object arise from the camera system and are in all videos.
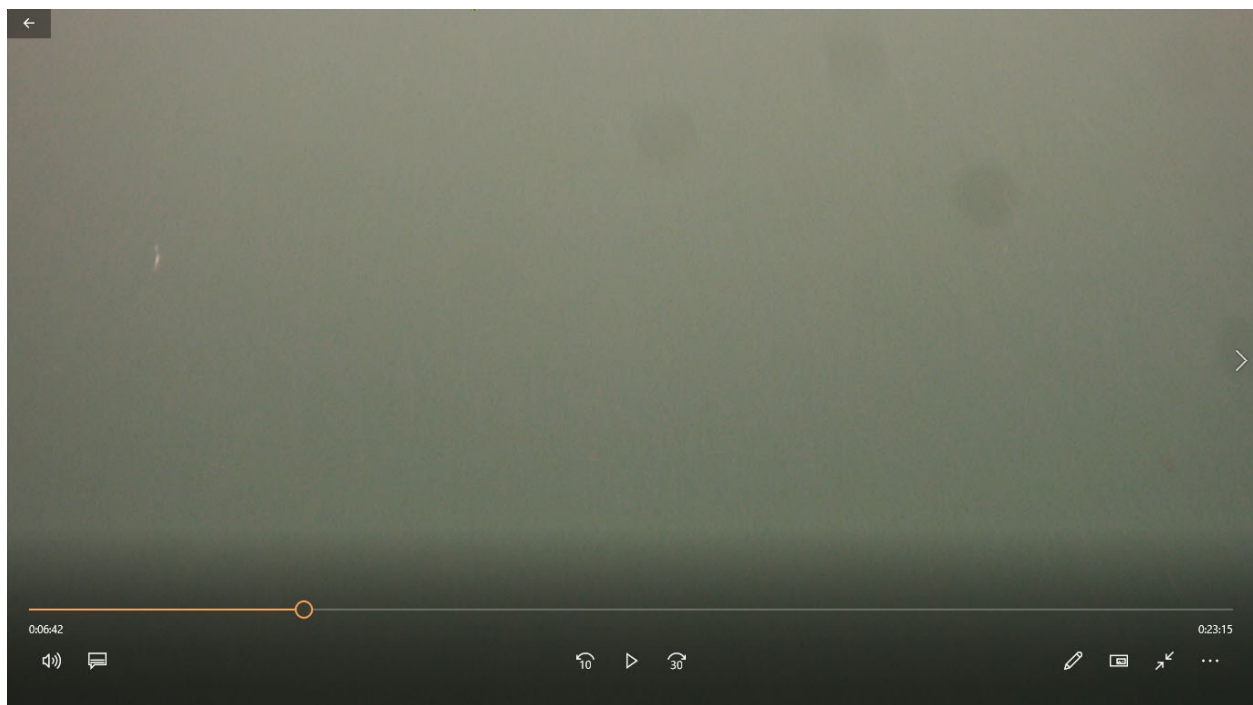
Figure 2. Unidentified particle.

Figure 3. Unidentified particle.
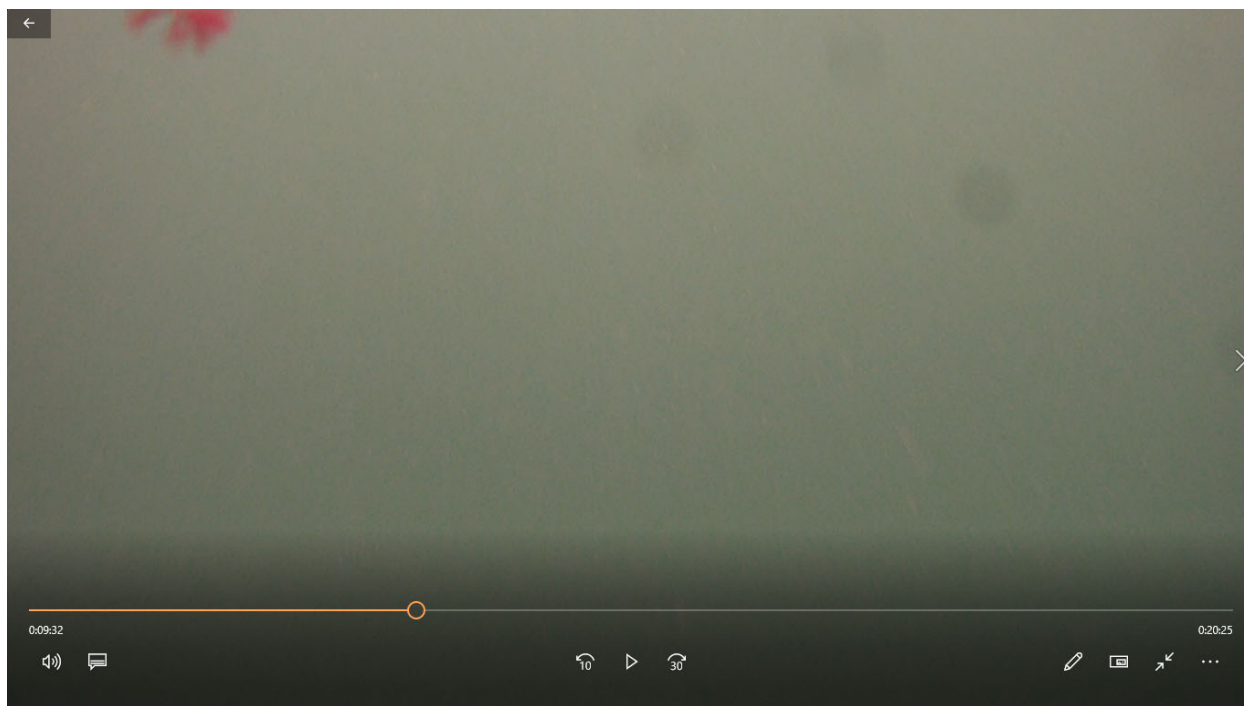
Figure 4. Red seaweed on edge of field.

Figure 5. Small algae piece.
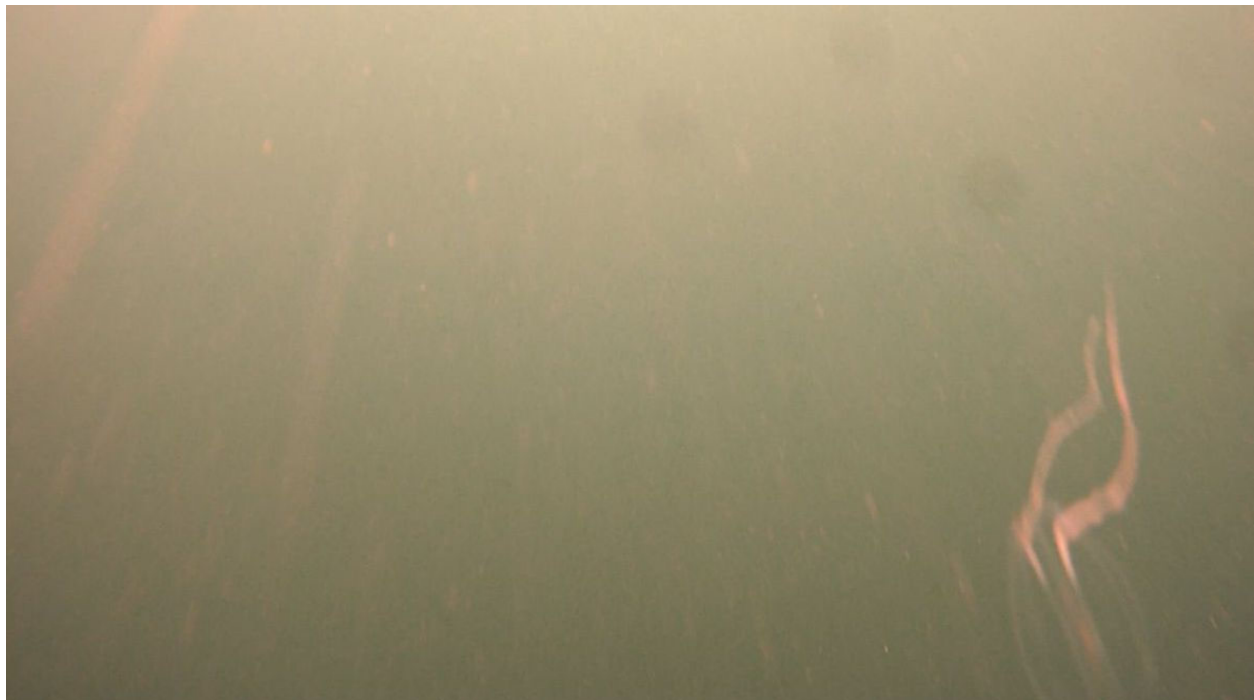
Figure 6. Plankton organism (probably a Ctenophore) and typical streaking of particles passing near the camera.

Figure 7. Plankton organism (upper left), probably Ctenophore) passing near camera.

Figure 8. Piece of seaweed.
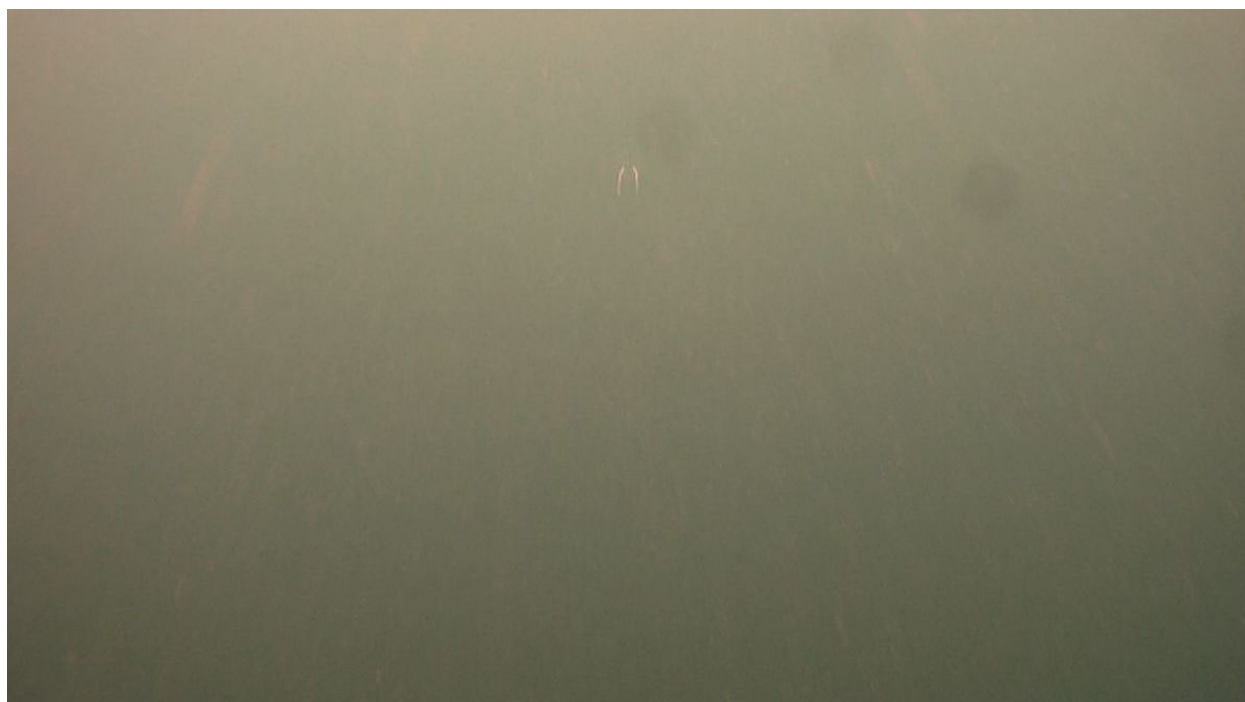
Figure 9. Small plankton object.

Figure 10. Orange blur probably seaweed passing near camera at high tidal current speed.
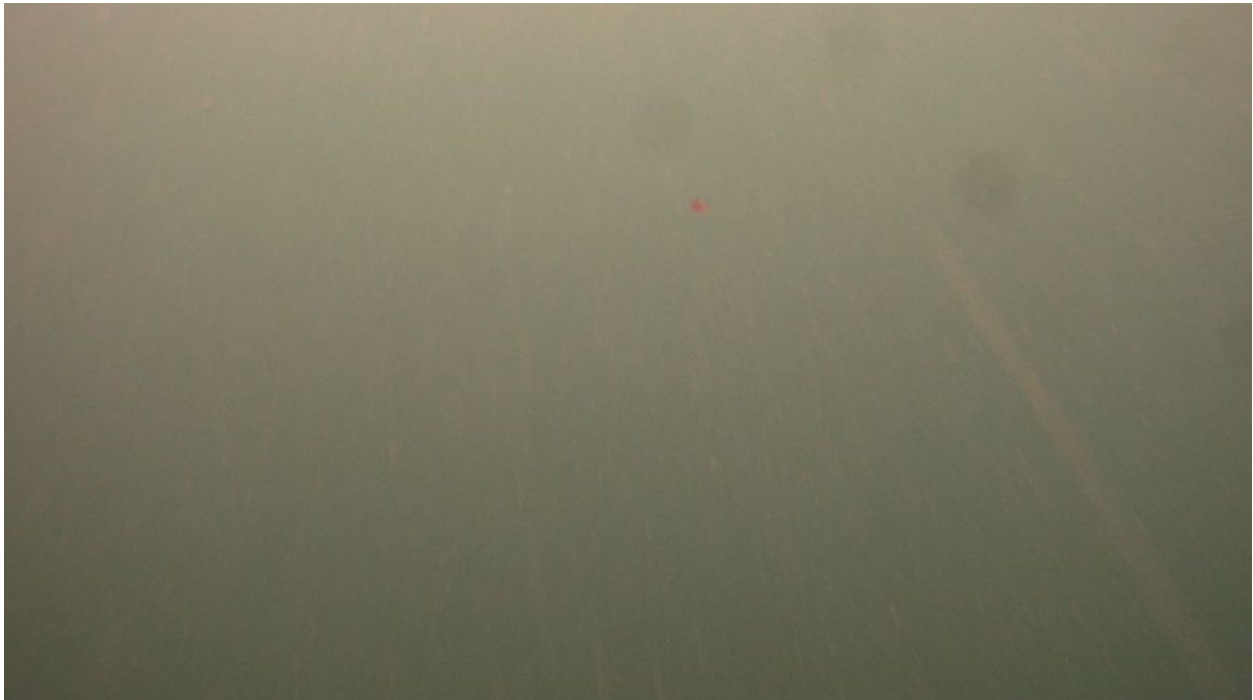
Figure 11. Small algae piece and typical streaks of particles passing near the camera lens.

Figure 12. Red seaweed fragment.

Figure 13. Plankton organism (Ctenophore)
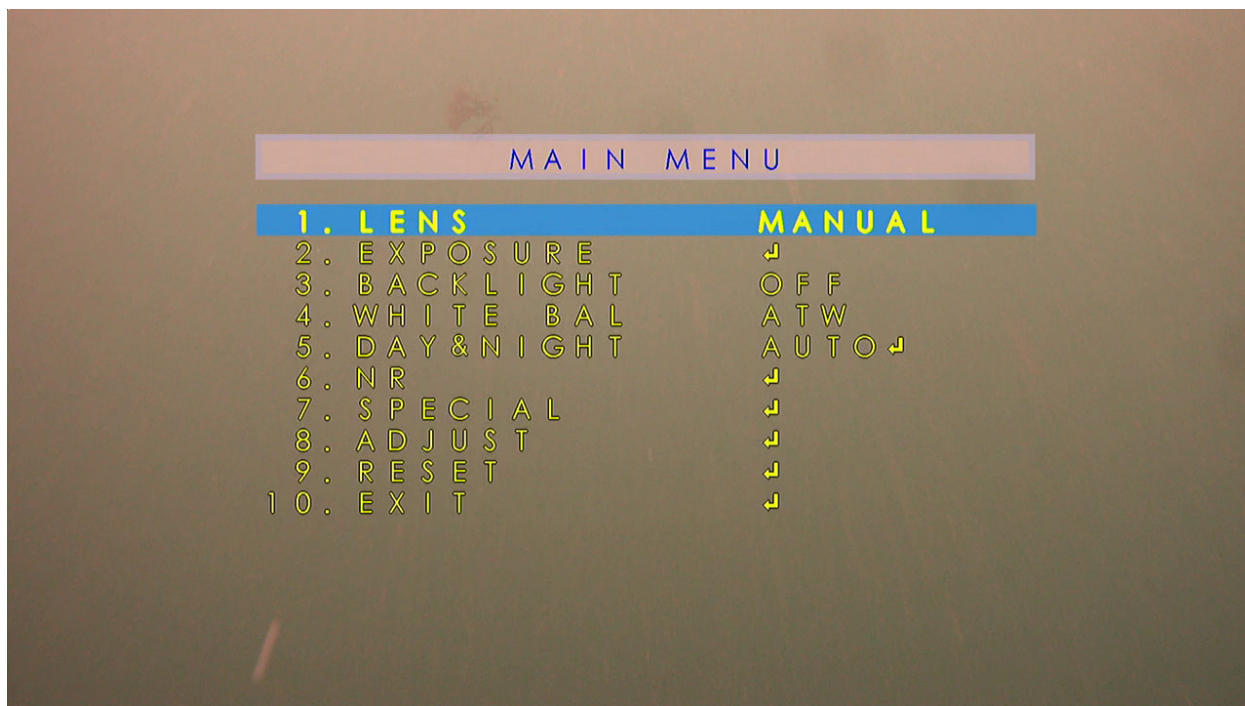
Figure 14. Clump of rockweed (*Fucus* sp) estimated to be 15-20 cm in height (top of frame above main menu).
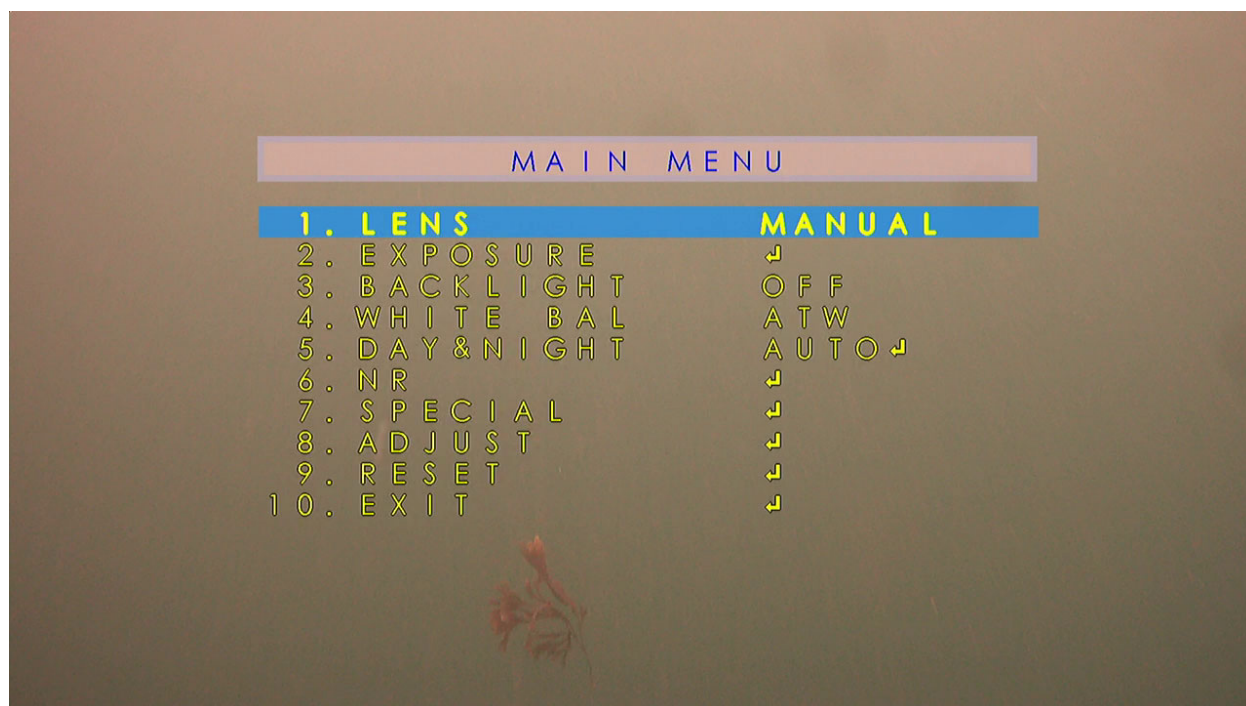
Figure 15. Same clump of rockweed (Fucus sp) as in Figure 14 passing by camera.
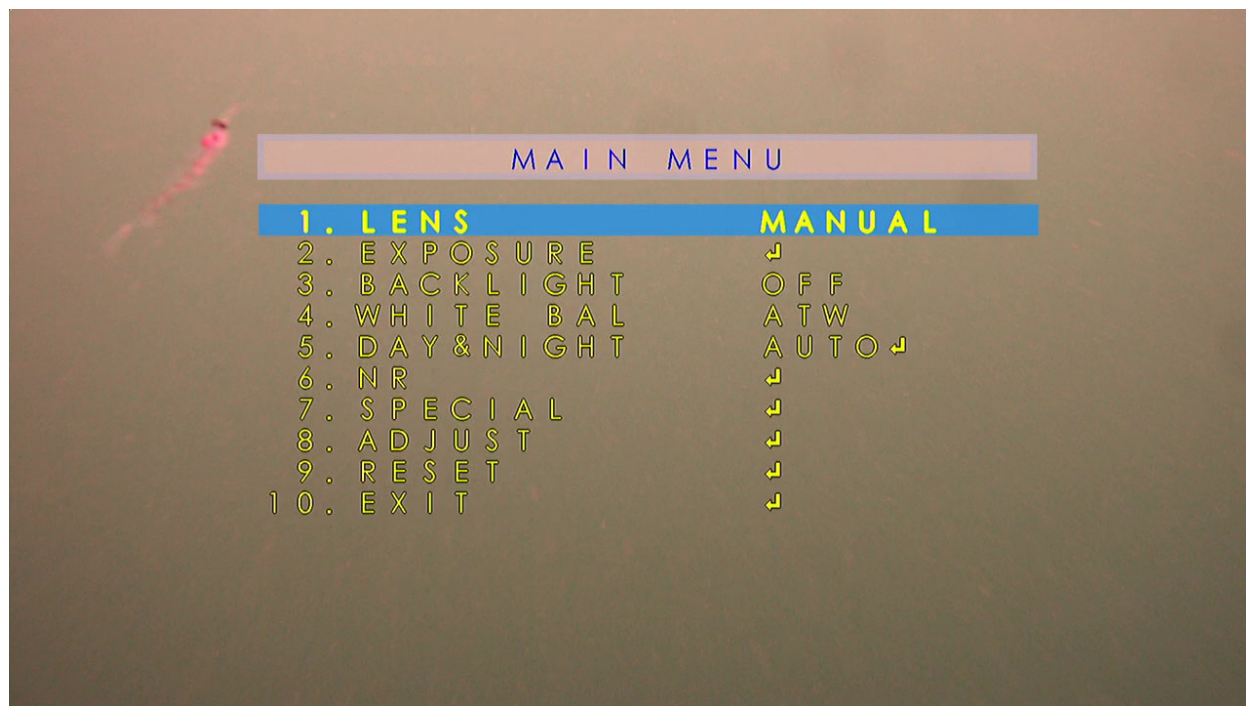
Figure 16. Plankton (euphausiid (krill) (upper left).

Figure 17. Algae piece and typical camera view.

Figure 18. Unidentified particle.

Figure 19. Typical image, fine particulates passing by camera in foreground.

Figure 20. Typical image, fine particulates passing by camera in foreground.

Appendix B.   Study Period Post-Processed Echogram Images

Study 2B Echograms

The following echograms are the processed data files from Study 2B illustrating the amount of data lost to entrained air. Black regions are excluded from analyses. Yellow line is the line at the sea surface. Red line is the software-determined turbulence line refined by the analyst in the useable portions of the echogram.
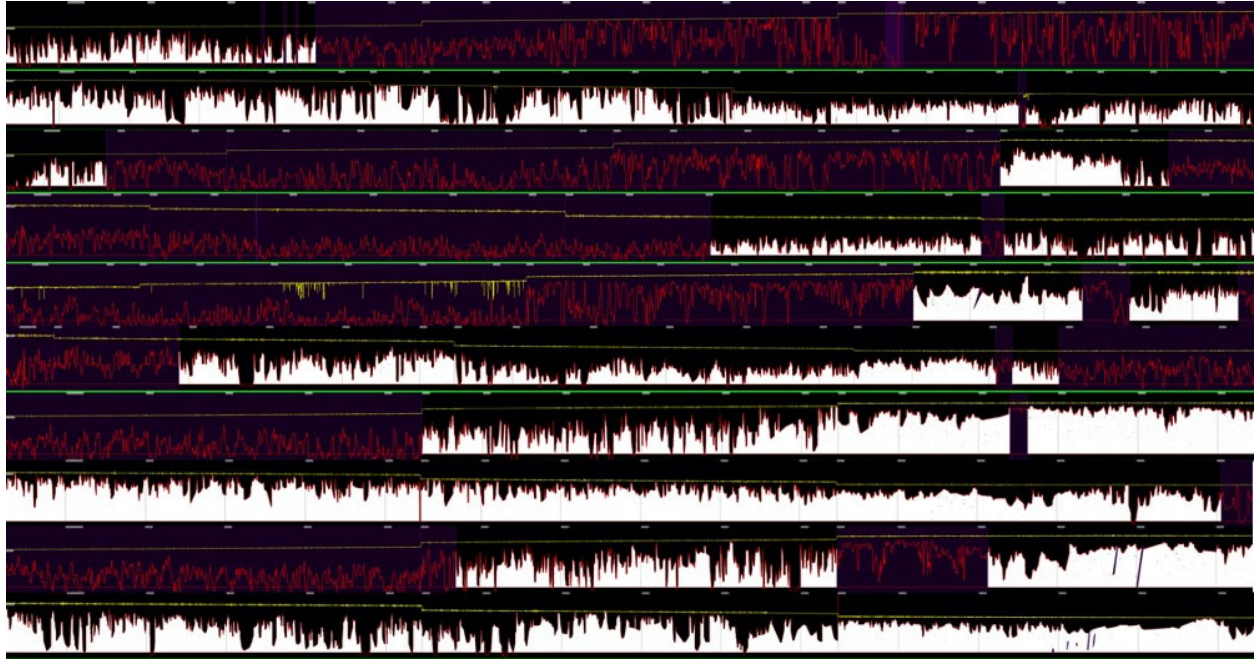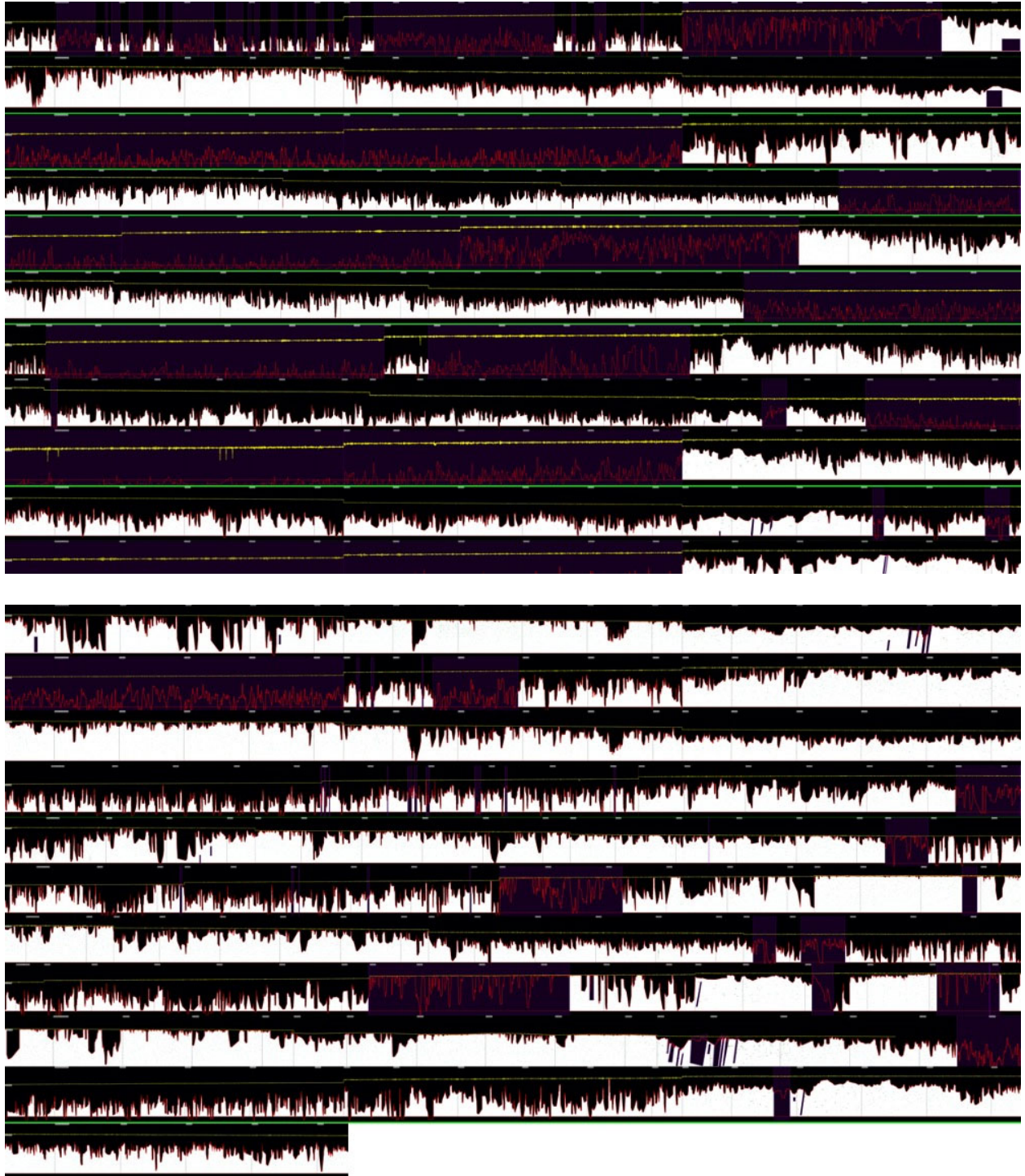
Study 2C Example Echograms

Provided here are four sequential hours of data collected during Study 2C illustrating the difference in the persistence and penetration of entrained air at the two sites. (WBAT = FAST site; EK80 = PLAT-I site).
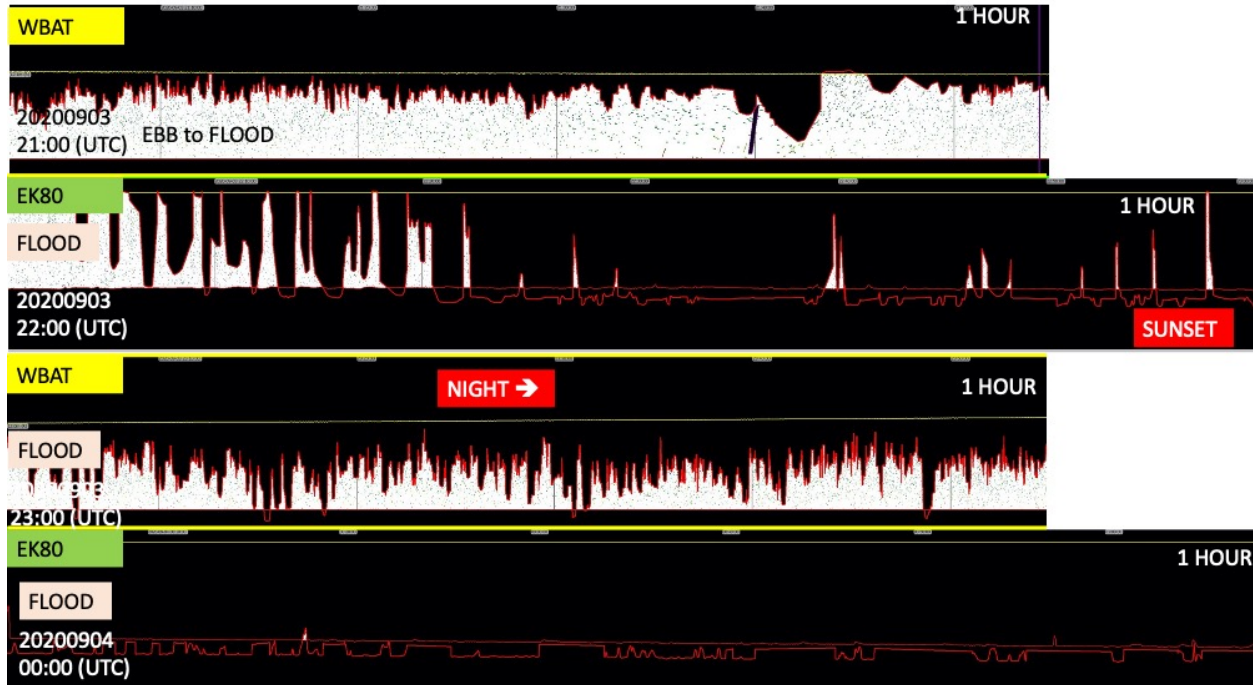
Appendix C.　　Future Considerations

The information provided in this section is intended to provide the reader with a list of general hydroacoustic topics that require consideration when making decisions regarding hydroacoustic study design. This section is <u>not</u> intended to address any of the specific findings or recommendations stemming from Study 2A, 2B, or 2C – those findings and recommendations are specific to those studies and are discussed above. As such, recommendations are not included here because the implications of the trade-offs inherent in hydroacoustic study design will be site- and study-specific. Rather, this section serves as a reference to the topics that are inherent to hydroacoustic study design; it stands alone from the remainder of the report – it is not exhaustive, but rather a starting point. Simmonds and MacLennan (2005) is a good reference for additional information on these topics.

While weighing the trade-offs during the decision-making process inherent to any hydroacoustic study, it is imperative to consider that the explicit goal of all hydroacoustic surveys is to collect good quality data that meets the requirements of the study. Without protecting data integrity and quality, all other decisions are moot, and the resources invested in the project will be wasted. Therefore, the comparative information presented below is organized by the order of consideration, beginning with a little background information.

Characteristics of the acoustic beam of scientific echosounders
The acoustic beam of scientific echosounders are highly engineered to produce a directed beam with the energy highly focused. Once the acoustic pulse is released into the water, the beam spreads (much like an inflating balloon). The end result is that the acoustic pulse takes on a cone shape with the apex of the cone at the transducer and the beam-swath (diameter) widening with distance from the transducer.
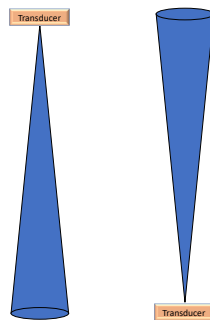
Implication: To sample the maximum volume of water, the transducer should be placed furthest from the area of interest. For reference, the diameter of the acoustic beam at a few distances from the transducer are presented below.

Acoustic	Diameter at select distances from the transducer		
Beamwidth	15 m	30 m	45 m
7°	1.8 m	3.7 m	5.5 m

Limitations to the useable portion of the acoustic beam (addressed in Section 4.3 above)
The full length of the beam (from transducer to sea floor or sea surface) is not analytically available. The engineering of transducers is such that when the acoustic pulse first enters the water, the acoustic wave is not yet organized. As such, there is a range near the transducer (the "nearfield") in which there is constructive and destructive interference, and in this region the amount of energy reaching a target is unknown. Therefore, the <u>proportion</u> of energy returned ("backscattered") to the transducer cannot be quantified and all acoustic returns from within the nearfield range are excluded from analyses. The nearfield is a function of the transducer beamwidth and frequency. For a transducer with a 7° beamwidth operating at 120 kHz, the nearfield range is 1.7 m. Therefore, all data within the first 1.7 m from the transducer face must be excluded from analyses.

Likewise, at the far end of the acoustic beam we need to consider physics in order to understand that there is a portion of the data that must be excluded. As the acoustic beam travels through the water the front of the beam is curved. Therefore, when encountering a planar surface, such as the sea surface or the seabed, the transducer will first receive returns from only that portion of the beam that first encounters the surface, rather than returns from the full diameter of the beam. Therefore, we are again faced with a phenomenon where the amount of energy reaching the target (the sea surface or the sea floor) cannot be known, and therefore the <u>proportion</u> of the energy returned cannot be quantified. As such, the data will be biased because energy will not be returned from the volume under the beam where the curved beam has not yet reached the surface. This unsampled volume is called the "deadzone". Like the nearfield range, the deadzone height must be calculated and all data within that range excluded from analyses. The deadzone height is a function of the transducer beamwidth, sound speed, acoustic pulse length, and water depth (i.e., range from transducer to the sea floor or the sea surface). For a transducer with a 7° beamwidth operating in the waters of Grand Passage and Minas Passage at typical survey pulse lengths, the deadzone exclusion is 1 m.

When designating the nearfield distance and the deadzone height, a small buffer is added to the calculation results. The values reported here (1.7 m nearfield range and 1 m deadzone height) include the buffer and therefore are the portions of the recorded data excluded from analyses: all acoustic returns within the first 1.7 m from the transducer face and all acoustic returns within the 1 m deadzone height at the sea floor or sea surface.

Implication: When considering a downward- vs. upward-facing echosounder, it is important to recognize that all data within the nearfield range will be excluded. Further, the water behind

the transducer will not be available for sampling. Therefore, if a transducer is deployed 1 m below the sea surface, the first 2.7 m nearest the sea surface will not be sampled, whereas if the echosounder is deployed upward-facing it is only the first 1 meter nearest the sea surface that will not be sampled.
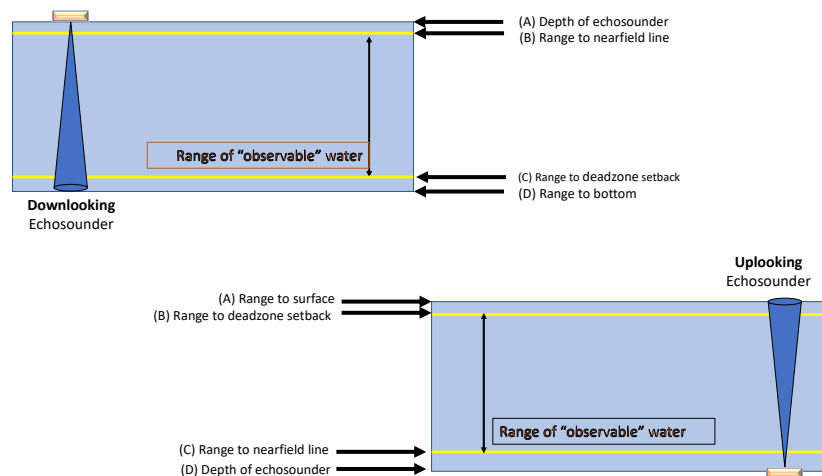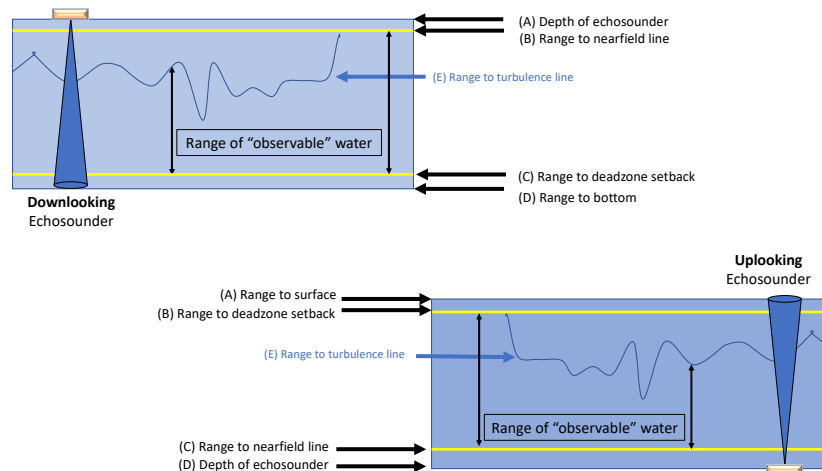

With that understanding of the acoustic beam, we can now address the questions specific to applying hydroacoustic technology to a project.

Questions to consider:
- Echosounder placement: What portion of the water column is the target for data collection? (near sea surface? midwater? near seafloor?)
  - Implication: Select echosounder placement (e.g., upward-facing, downward-facing, side-looking) so as to maximize the diameter of the beam, and therefore volume sampled, at the area of interest.
- Echosounder placement: Are there features specific to the placement options that need to be considered?
  - Example: If it is desirable to deploy the transducer at the sea surface in a downward-facing mode, are there features of the deployment site (e.g., obstructions, presence of a wake, etc.) such that data will be compromised? Likewise, for the deployment of an upward-facing transducer at the sea floor (e.g., obstruction of the acoustic beam by other instruments deployed on the same platform as the echosounder or structural and anchoring components of tidal turbines).

- o Implication: In order to ensure the highest quality data, avoidance of obstructions within the beam path is imperative and wakes, with their inherent entrained air, must be avoided.
- Echosounder placement: Given the presence of persistent and deeply penetrating entrained air in tidal energy sites, the effect of entrained air on data quality must be considered when selecting the placement of a transducer (e.g., upward- or downward-facing). The implications of the presence of the entrained air cannot be overstated.
  - o Background: Echosounders record time from ping transmission to the return of the backscattered energy, and record the intensity of the energy returning to the transducer. The work of the hydroacoustician is to interpret the recorded time and intensity into something biologically meaningful. With a known sound speed, time is converted into the range from the transducer to the target. The backscattered energy is used as our proxy for fish density and abundance. This is a simplified explanation, but the take-away is that highly accurate measurements are important. The challenge presented by air entrained into the water is that the amount of energy reaching the target (fish) is unknown and therefore the proportion of emitted sound pulse returned by the target is unknown. The presence of the entrained air is doubly problematic for a surface-deployed transducer in that the sound pulse is twice affected; once on the way down through the layer of entrained air, and then again on the way back to the transducer.
  - o Implication: If the question at hand is whether there are fish in the water column, a simple presence/absence question, then the quantity of energy returned is not the important measure. However, if the question concerns a comparative study of the density or abundance of fish over time, then it is imperative to avoid transmission of the acoustic beam through the entrained air to the target of interest.
  - o Caveat: While the placement of an echosounder at the sea floor will provide an unobstructed path for the acoustic beam between the transducer and the target of interest, the target strengths of fish when ensonified from below are less well-studied than the target strengths of fish when ensonified from above. However, the implications for quantitative interpretation of hydroacoustic data are far greater if the acoustic beam must pass through entrained air.

(A) Depth of echosounder
(B) Range to nearfield line
(E) Range to turbulence line
Range of "observable" water
(C) Range to deadzone setback
(D) Range to bottom
Downlooking Echosounder

Uplooking Echosounder
(A) Range to surface
(B) Range to deadzone setback
(E) Range to turbulence line
Range of "observable" water
(C) Range to nearfield line
(D) Depth of echosounder

- <u>Data requirements:</u> To support the data needs of the project, in which domain is it more important to measure backscatter? Time? Space?
  - o <u>Implication:</u> A stationary echosounder can measure data in high resolution in time, whether surface- or bottom-mounted, whereas high resolution in the spatial domain requires a mobile deployment of a transducer.
- <u>Data requirements:</u> In order to support the data needs of the project, how frequently should sampling occur? (e.g., 1 ping per second? 2 pings per second? 4 pings per second?)
  - o <u>Consideration:</u> Even within the same family of echosounders, such as the Simrad EK80 series, the maximum ping rate achievable is not identical. The WBAT is limited to 1 or 2 pings per second whereas the surface deployed EK80 (WBT) is capable of at least 4 pings per second. If not restricted by the technology, the maximum ping rate achievable is restricted by water depth, although the maximum ping rate may not be suitable for a given study when considering the oversampling that occurs when the same volume is ensonified by more than one ping.
  - o <u>Implication:</u> Using Grand Passage as an example, at a range of 15 m, nominally the water depth nearby to the position of the PLAT-I, the beam diameter is ~1.8 at the sea surface. At a ping rate of 1 ping per second, approximately 1/3 of the surface waters will not be sampled. The proportion of unsampled volume of water increases for the depth ranges sampled by the narrowing beam closer to the transducer.
  - o <u>Note:</u> The other operational echosounder settings, such as pulse length and transmitted power are equivalent for the WBAT and the EK80 for the needs in Minas Passage or Grand Passage. There are restrictions to the maximum transmitted power for the WBAT, that would impact the usefulness of the WBAT in deep waters but do not impact in water depths found in Minas Passage or Grand Passage.

- Data requirements: To support the data needs of the project, will the restrictions imposed by data storage and power needs of an autonomous echosounder deployed on the sea floor be acceptable? If unacceptable, is a cabled solution an option?
  - Note: Technological solutions in addition to a cabled solution exist but are costly and the robustness of the systems for operation in the vigorous environment of a tidal energy site would need to be investigated.
- Analysis requirements: Given that the data can be readily retrieved, processed, analyzed for a surface-deployed echosounder, will the lag in data processing and analyses inherent with bottom-mounted echosounders be acceptable?
  - Note: Technology exists by which to relay data from autonomous echosounders to the surface for transmission over the internet. However, substantial upfront investment is required, and their robustness for operation in the vigorous environments of tidal energy sites would need to be investigated.
- Deployment considerations: A sea floor deployment of an echosounder system requires a substantial investment in procuring a suitable deployment platform and the logistical needs and expense with each deployment and retrieval.

The above is a list of the initial factors that need to be considered when selecting the placement (surface or sea floor) for deployment of a scientific echosounder. They are interrelated and need to be prioritized and evaluated given the resources (financial, logistical, etc.) that are available. It needs to be stressed that the data and analytical needs of any project must be identified so that inherent trade-offs can be evaluated in terms of consequence to the project success.

Appendix V

Study 1 – Relative Performance of Surface vs. Bottom-Mounted Hydrophones in a Tidal Channel

FINAL REPORT

Daniel J. Hasselman[1*], Tyler Boucher[1], Jessica Douglas[1] and Shannon MacNeil[1]

[1]Fundy Ocean Research Center for Energy, Halifax, NS
*Corresponding author: dan.hasselman@fundyforce.ca

Contents

Executive Summary

Passive Acoustic Monitoring (PAM) technologies are commonly used to monitor echolocating marine mammals around tidal energy devices. However, the detection efficiency of PAM instruments can be hindered by a variety of factors (e.g., signal attenuation, flow noise, ambient noise) inherent to high flow environments that can vary with deployment depth, and can impede monitoring efforts. While previous work indicated that conventional hydrophones that record raw pressure time series data may be preferrable for monitoring harbour porpoise in tidal channels, where these technologies should be deployed for effective monitoring (i.e., at the sea surface or on the sea floor) remains an unresolved issue.

In partnership with the Pathway Program, Sustainable Marine Energy Canada Ltd. and the Fundy Ocean Research Center for Energy assessed the relative performance of a surface deployed and bottom-mounted conventional hydrophone to understand whether deployment location impacted the detection range of the instrument. An icListen HF hydrophone was deployed about 2 m below the surface from a floating tidal energy platform (i.e., PLAT-I) and bottom-mounted on an autonomous subsea platform 65 m from the PLAT-I in Grand Passage, NS. A series of passive drifts were then conducted from a vessel over the platform and in the vicinity of the PLAT-I across a range of tidal flow conditions while playing synthetic harbour porpoise clicks ('pseudo clicks') emitted from an icTalk. The drifts measured by the surface deployed hydrophone occurred in August 2020; the drifts measured from the bottom-mounted hydrophone occurred in January 2020.

We found that it was possible to detect pseudo-clicks and real harbour porpoise clicks from both hydrophone locations. However, data from the surface deployed hydrophone contained audible interference from waves and the broadband, impulsive, bursting of bubbles associated with wave action that is difficult to differentiate from echolocation clicks. This ambient noise will negatively affect automated porpoise click detectors and could lead to increased rates of false-positive detections. The surface-deployed hydrophone also had substantial electrical noise in the data which could affect automated detectors. The drifting vessel had to stay clear of the PLAT-I whereas it could pass directly over the bottom-mounted hydrophone. These differences in drift geometry made the comparison of detection ranges challenging. Pseudo clicks were detected at greater distances from the bottom-mounted than the surface deployed hydrophone. However, it is important to bear in mind that these results were generated using synthetic clicks generated by an icTalk (nearly omnidirectional), and that real harbour porpoise emit a stronger echolocation click using a directional beam. Further, understanding the effects of current velocity on the quality of the icTalk signal could help with interpretation of results.

The choice of which PAM instrument to use and where to deploy it depends on the scientific question being asked. A primary objective of the Pathway Program is to define, test and validate an environmental effects monitoring solution that can be used by tidal energy developers for monitoring the near-field (0 - 100m) region of their tidal energy device at the FORCE demonstration site. Both hydrophone mounting locations were able to detect low-

power pseudo-clicks close to or longer than 100 m, and thus satisfy the near-field monitoring requirement. While it is possible to detect harbour porpoise clicks using a surface deployed hydrophone, the detection range for automated detectors may be smaller than a bottom-mounted hydrophone due to impulsive ambient noise associated with wave action at the surface. Moreover, harbour porpoise clicks are directional and are typically produced while diving and foraging at depth and are less likely to be detected by a surface deployed hydrophone. However, for a surface-deployed turbine, such as the PLAT-I, having the monitoring hydrophone close to the turbine depth may provide more relevant data than a bottom mounted hydrophone. An important consideration in selecting a monitoring technology is whether near-real-time data are required or if archival results provided several months after collection is sufficient. For real-time data, a hydrophone mounted on the turbine platform is much more economically sustainable than a separate monitoring platform with its own power and data cable. For archival data analysis and reporting, especially for bottom mounted turbines and for prototyping programs, a separate bottom mooring for the monitoring equipment may be a better solution based on cost and performance.

Given these considerations, the results of these measurements did not provide sufficient evidence to strongly prefer one hydrophone position over another. Rather, developers are encouraged to demonstrate that they are able to detect pseudo-clicks in the turbine's near-field using a drifting projector. When cabled hydrophones are to be used, developers need to safeguard against acoustic and electronic contamination from equipment on their tidal energy devices.

Introduction and Objectives

Passive Acoustic Monitoring (PAM) technologies are frequently used to monitor echolocating marine mammals (primarily porpoise and dolphin) in high flow environments that are the focus of instream tidal power development (Adams et al., 2019; Malinka et al., 2018). However, the detection efficiency of PAM instruments for monitoring vocalizing marine mammals in tidal channels is impacted by several factors, including the vocalizing bandwidth for the target species and the potential masking of these sounds by flow noise and ambient sound (e.g., sediment transport on the seafloor), as well as the propagating environment, reverberation, sensor placement and sensor deployment methodology (Hasselman et al., 2020a). A recent comparative study of PAM technologies revealed that conventional hydrophones (i.e., those that record raw pressure time series data) may be preferable to 'stand alone' click detectors for monitoring harbour porpoise in tidal channels; particularly if appropriate sensitivity settings for the instrument are coupled with a suitable click detector and classifier (Hasselman et al., 2020b). However, where conventional hydrophones should be deployed (i.e., surface deployed or bottom-mounted) for effective monitoring of harbour porpoise remains an unresolved issue.

Although monitoring of instream tidal turbines (typically bottom-mounted devices) has frequently involved the deployment of instruments on the seafloor (either mounted on an autonomous or cabled subsea platform, or integrated into the device substructure), deploying and recovering such instruments involves considerable costs (i.e., specialized vessels and complex marine operations) and risks for monitoring (e.g., instrument malfunction and loss of data, loss of the instrument itself). While floating tidal energy platforms provide several advantages for monitoring (i.e., easy access to instruments and monitoring data) that may offset some of these aforementioned risks, monitoring from the sea surface in tidal channels has its own inherent challenges. For instance, the acoustic detection range of PAM instruments is known to vary with deployment depth (Sostres Alonso & Nuuttila, 2015), and their ability to detect harbour porpoise echolocation clicks may be impacted by signal attenuation and interference from waves and turbulence near the sea surface in tidal channels (Hasselman et al., 2020a).

Sustainable Marine Energy Canada Ltd. ('Sustainable Marine') operates a floating tidal energy platform (i.e., 'PLAT-I' – PLATform for Inshore Energy; Figures 1 and 2) at its tidal demonstration site in Grand Passage, Bay of Fundy. Sustainable Marine conducts a series of monitoring activities using surface deployed instruments, including the use of a conventional hydrophone (OceanSonics icListenHF) for monitoring harbour porpoise (*Phocoena phocoena*) activity. Thus, the PLAT-I provides an excellent opportunity to conduct an *in-situ* assessment of the relative performance of a surface deployed and bottom-mounted conventional hydrophone for detecting harbour porpoise in a tidal channel. To that end, the primary objective of this study was to evaluate the relative performance of a surface deployed and bottom-mounted conventional hydrophone to understand whether deployment location impacts the detection range of synthetic harbour porpoise clicks.

5

Figure 1: a)The PLAT-I moored in Grand Passage (photo credit: www.oceannews.com/news/energy/sustainable-marine-energy-reveals-plans-for-tidal-energy-project); b)a

This study constitutes the final component of comparative tests for PAM technologies under Phase 3 ('Technology Validation') of The Pathway Program[1]. A primary objective of the Pathway Program is to define, test and validate an environmental effects monitoring solution that can be used by tidal energy developers for monitoring the near-field (0 – 100m) region of their tidal energy devices at the FORCE tidal demonstration site in the Minas Passage. This work serves to determine whether the relative performance of a PAM device used for detecting harbour porpoise vocalizations is impacted by the deployment location (i.e., surface vs. bottom) so that an informed decision can be made about the deployment location for PAM devices for future monitoring efforts.

Sea Mammal Research Unit Consulting North America Ltd. (SMRU) conducted the data analyses component of this work, and their final report is included herein as an Appendix. The body of this report outlines the field components of this project, and only reflects the main points of the results contained in the SMRU report. For a more thorough understanding of the results and interpretation of the data, readers are encouraged to review the Appendix.

Methodology

Although collaborative in spirit, this project was conducted under contract between Sustainable Marine and the Offshore Energy Research Association (OERA) under the Pathway Program and

---

[1] https://oera.ca/research/pathway-program-towards-regulatory-certainty-instream-tidal-energy-projects

6
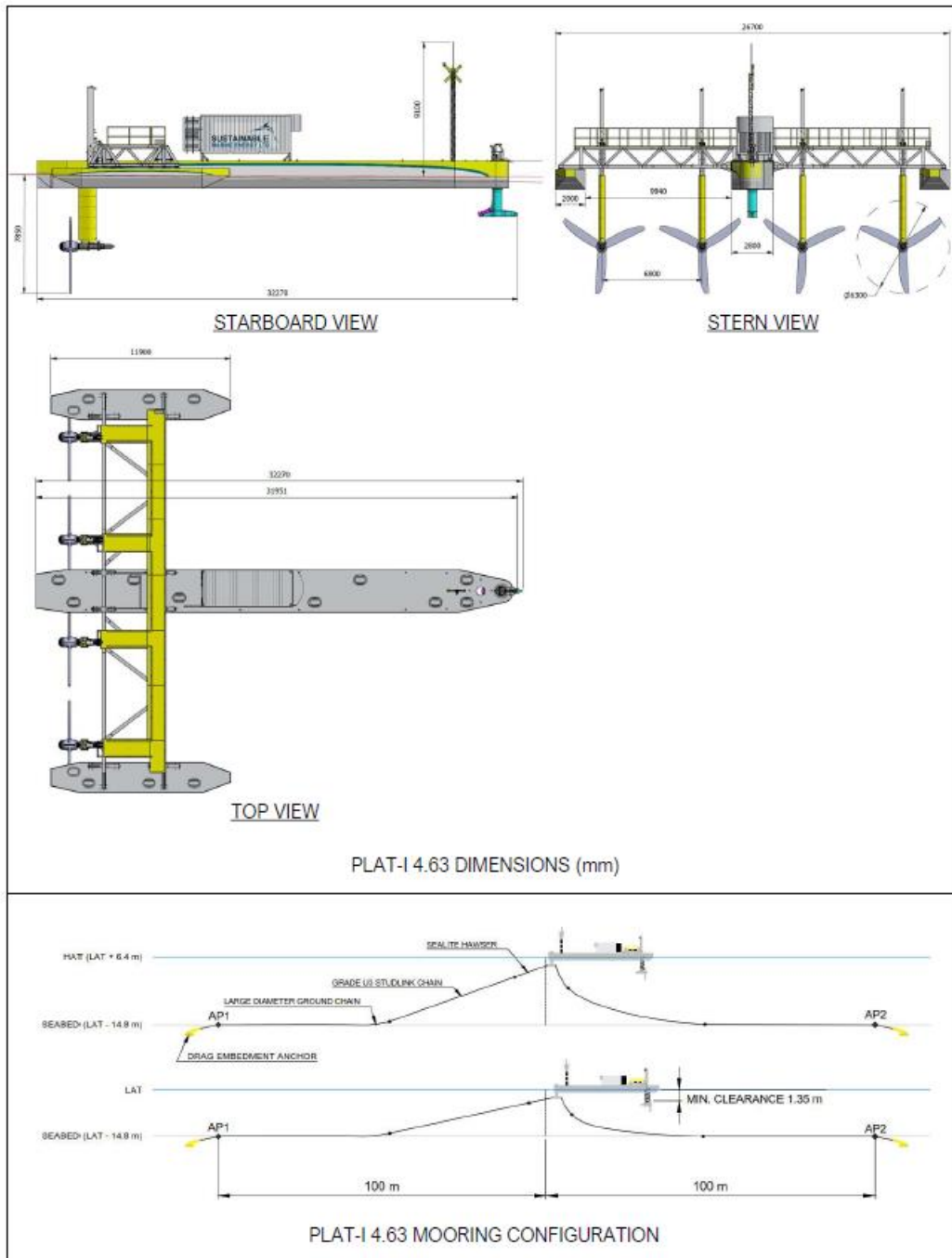
Figure 2: Schematic of the PLAT-I 4.63 showing starboard, stern and top views along with mooring configuration.

utilized the PLAT-I deployed in Grand Passage, NS. Sustainable Marine sub-contracted the Fundy Ocean Research Center for Energy (FORCE) to conduct the field trials and data collection,

and FORCE sub-contracted SMRU to conduct the data analyses and reporting aspects of the project. The relative performance of a PAM instrument deployed at the surface vs. on the seabed was assessed across a range of tidal flow conditions experienced in Grand Passage by playing synthetic harbour porpoise clicks (hereafter 'pseudo clicks') emitted by an Ocean Sonics Ltd. icTalk (a positive control for signal detections) during a series of passive drifts from a vessel (i.e., 'SMEagol') in the vicinity of the PAM instruments (Figure 3).

For the purposes of this study, the icListen HF served as a surrogate for PAM devices and was justified on the grounds that this project was not designed to address questions about the performance of any given hydrophone *per se* (a topic previously addressed; Hasselman et al. 2020b), but rather the potential effects of signal interference inherent to the deployment location on the performance of PAM technologies in general. Thus, we make the assumption that any potential signal interference associated with waves and turbulence near the surface has an approximately equal effect on hydrophone performance across the suite of conventional PAM technologies that are available, and that might be used for monitoring harbour porpoise in tidal channels.

Field trials

The surface deployed icListen HF was pole-mounted 2m below the surface near the bow of the port outer hull of the PLAT-I and was cabled to provide power supply and data storage to an external hard drive connected to a laptop. The bottom-mounted icListen HF was connected to an Ocean Sonics SmartRecorder that extended the data storage capacity of the hydrophone as required for the duration of the deployment. Both the bottom-mounted hydrophone and SmartRecorder were integrated into one of FORCE's FAST (Fundy Advanced Senor Technology) subsea platforms and deployed in Grand Passage approximately 65m (from center spread) north of the PLAT-I at 17m depth (high water) (Figure 4).

Both the surface and bottom-mounted hydrophones were deployed over two periods (January 7-17, and August 12-21, 2020) to record pseudo clicks during the passive drift trials and real harbour porpoise in the area over a range of tidal flow conditions. Passive drifts were

conducted on January 14 and August 19 over the FAST platform and near the PLAT-I from the SMEagol, with the icTalk deployed over the side of the vessel at approximately 5 m depth (water depth was 15-30 meters in the drift area). During the August 19th drifts, the orientation of the icTalk was alternated between an upward and downward facing orientation to ensure both hydrophones could adequately detect pseudo clicks. These drifts were conducted over an entire tidal cycle (i.e., ebb and flood tide) to determine the ability of the surface deployed and bottom-mounted hydrophones to detect this positive control signal across a range of flow conditions experienced in Grand Passage. The center frequency of the pseudo clicks from the icTalk was 130 kHz, with pseudo clicks produced every 0.3 seconds at peak-to-peak sound pressure levels of 130 dB re 1μPa at 1 m from the projector. A handheld GPS (Garmin Oregon

600) recorded the vessel tracks during the passive drifts. Tidal current velocity data for Grand Passage was obtained using open source software based on the FVCOM model (Chen & Beardsley, 2011) and provided to SMRU for analysis.
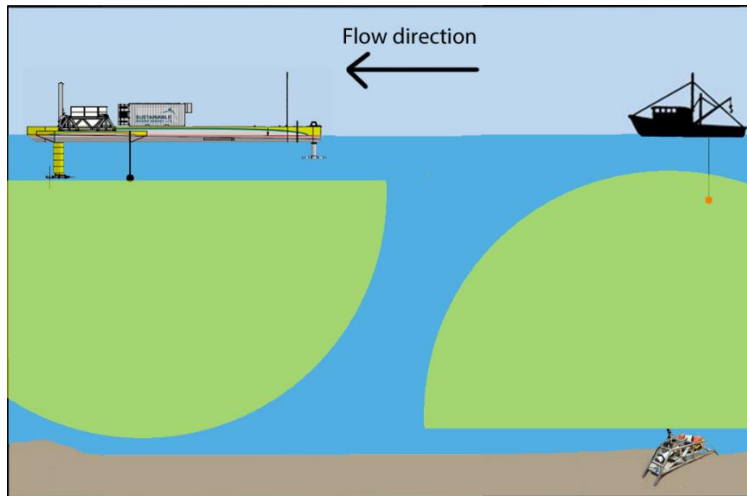
Figure 3: Schematic of the study design in Grand Passage, showing the icTalk (red dot) suspended from a vessel, and the icListen hydrophones deployed on the seabed and near the surface from the PLAT-I (not to scale).
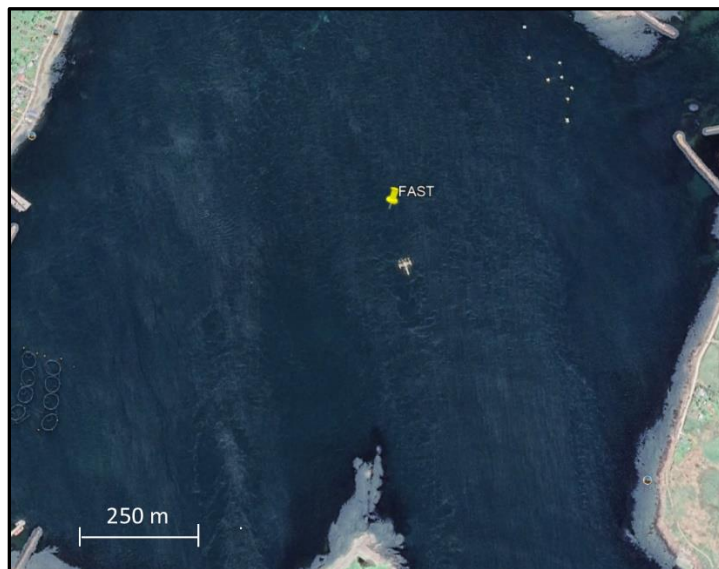
Figure 4: Satellite image of Grand Passage showing the location of the PLAT-I (center) on flood tide and the approximate position of the bottom-mounted hydrophone deployed on the FAST platform (image credit: Google Earth).

Upon completion of the data collection in January, it was discovered that electrical interference from a power inverter on the PLAT-I had contaminated the data from the surface deployed hydrophone, making it unusable. However, the data from the bottom-mounted hydrophone was suitable for analyses (Figure 5). Conversely, upon completion of the data collection in August, it was discovered that the Smart Recorder on the bottom-mounted hydrophone failed to store data, whereas the PLAT-I mounted data was suitable for analyses. Following discussions with SMRU, the decision was made to proceed with analyses using the bottom-mounted hydrophone data collected in January with the surface deployed hydrophone data collected in August. Although not ideal, analyses of detection range and the development of detection functions to understand relative performance of surface deployed and bottom mounted hydrophones can still be accomplished using this approach.
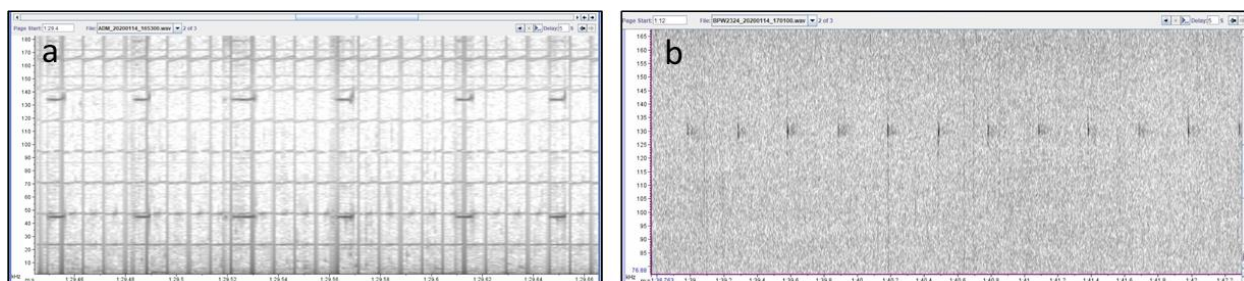
Figure 5: Spectrograms showing a) electrical interference for the surface deployed icListen hydrophone mounted on the PLAT-I in January 2020, and b) pseudo clicks from the bottom-deployed icListen hydrophone.

Data analysis

Upon platform recovery, data from both hydrophones were downloaded and provided to SMRU for standard QA/QC procedures and analyses. The project plan called for the use of automated detectors to identify the pseudo-clicks. Automated detectors differentiate signals (in this case pseudo-clicks) from noise in the data. To improve signal detectability, processing can be applied to remove noise or enhance the signal before comparing to a threshold value. For harbour porpoise clicks, the signal is very short but relatively narrowband, and in this instance the only good enhancement is to filter out energy at frequencies above and below those of the echolocation click, followed by summing the energy over a short period of time. Once processed, a click can be identified when the short-time energy exceeds the average energy. However, if the signal-to-noise ratio (SNR) remains low despite these measures, then a detection cannot be made (B. Martin, pers. comm. 2021). In this case, processing to improve signal detectability was not applied to the data. A low signal to noise ratio (SNR) for the surface deployed hydrophone (due to either ambient noise, or range between the icTalk and the PLAT-I mounted hydrophone during drifts) prevented the use of automated click detectors to find pseudo clicks in the data. Thus, all detections were made manually by trained analysts, and only

drifts where at least one pseudo click was detected were included in analyses. The relative performance of the surface deployed and bottom-mounted hydrophone was assessed by constructing detection functions that describe the probability of detecting pseudo clicks by each hydrophone and evaluating the detection range for the surface deployed and bottom-mounted hydrophone. Details are provided in the Appendix.

Results

A total of 9,098 pseudo clicks were annotated from the bottom-mounted hydrophone across the 58 passive drifts conducted during the January 2020 deployment. The potential for collision between the drifting vessel and the PLAT-I prevented close approaches to the surface deployed hydrophone except during high-water and low-water slack periods when current and vessel movement were low. As such, only four of the 35 passive drifts during the August 2020 deployment approached within 100m of the PLAT-I, and 368 pseudo clicks were annotated in the dataset collected by the surface deployed hydrophone. Instances where pseudo clicks were not recorded during some passive drifts were likely due to the low source level of the icTalk, flow noise, ambient noise, and the passive drift not passing close enough to the hydrophones, or some combination thereof.

Pseudo clicks were generally detected during drifts over the bottom-mounted hydrophone, with pseudo clicks at the beginning and end of the drifts (when the icTalk was furthest away) being less detectable. This is consistent with the findings of previous drifting experiments using bottom-mounted hydrophones (Hasselman et al., 2020b). However, this pattern was not observed for the surface deployed hydrophone, as pseudo clicks were sporadically detected throughout the drifts in no definitive pattern. The median and 3rd quartile sound pressure levels of the surface-deployed data were ~2 dB lower than for the bottom mounted data (Figure 6), however, the surface mounted data contained substantially more short impulsive noise (comparing Figures 6 and 7), which could have made detecting the clicks more difficult for the analysts.
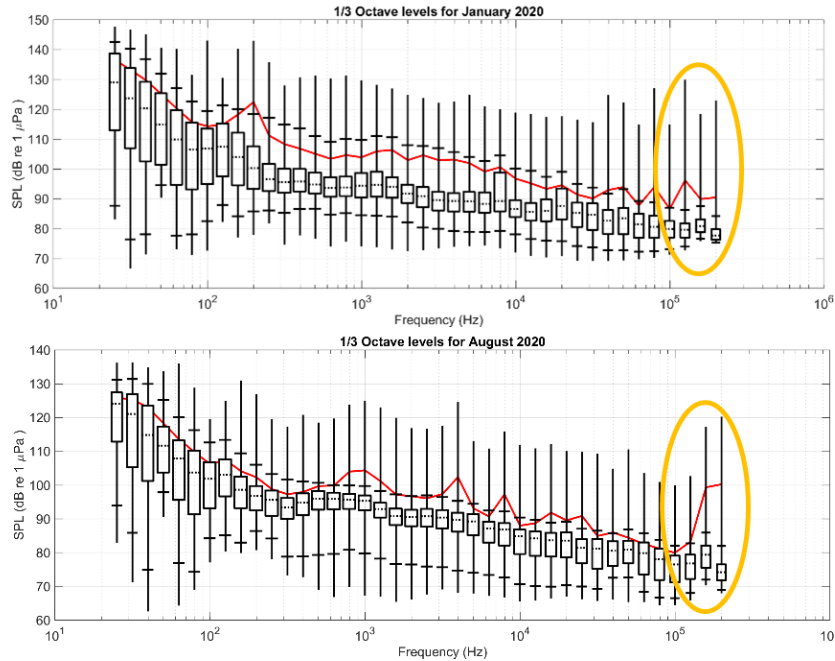
Figure 6: Decidecade sound pressure levels recorded for the bottom-mounted hydrophone (top panel) and the surface deployed hydrophone (bottom panel). Data is represented by box and whisker plots (minimum, Q1, median, Q3, maximum) and mean values are represented by a solid red line. Orange circles highlight the frequency range of harbour porpoise clicks and pseudo clicks generated by the icTalk.

The data collected from the PLAT-I mounted hydrophone contained interference from wave action and the broadband, impulsive, bursting of bubbles associated with waves that is particularly challenging to differentiate from echolocation clicks (Figure 7). Impulsive noise like that detected in this study for surface deployed hydrophones will negatively affect automated porpoise click detectors and may lead to an increased rate of false-positive detections. In contrast to the surface deployed hydrophone, interference in the bottom-mounted hydrophone dataset was predominantly characterized by occasional boat noise (from the drifting vessel re-positioning itself for the next pass), which was comparatively easy to differentiate from pseudo clicks (Figure 8) and does not impede the use of porpoise click detectors.
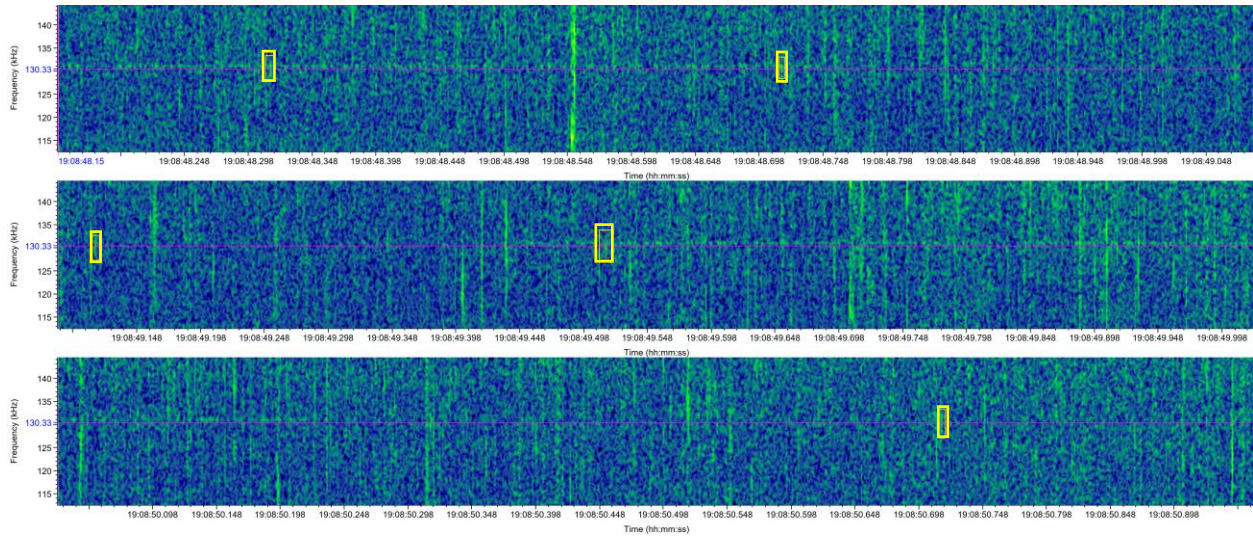
Figure 7: Spectrogram (FFT = 2048, 50% overlap, 512 kHz sample rate) from the PLAT-I mounted hydrophone during passive drifts showing received pseudo clicks (yellow boxes), and a 130 kHz reference line (purple) used for aiding in the click detection process. Vertical lines throughout the spectrogram indicate noise likely generated by bubbles near the surface.
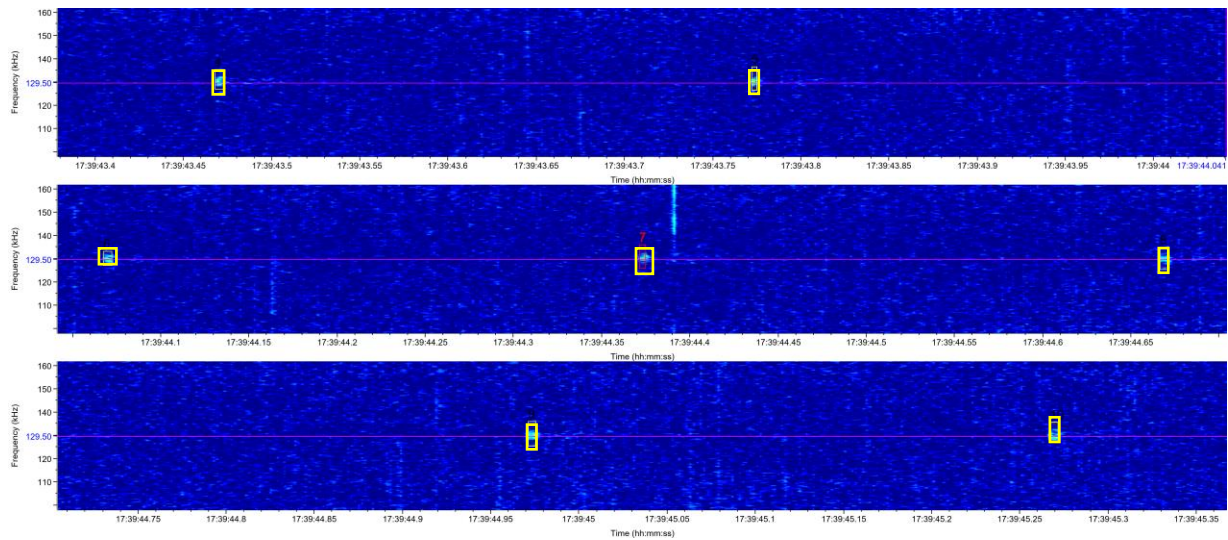
Figure 8: Spectrogram (FFT = 2048, 50% overlap, 512 kHz sample rate) from the bottom-mounted hydrophone during passive drifts showing received pseudo clicks (yellow boxes), and a 130 kHz reference line (purple) used for aiding in the click detection process. Lack of impulsive sounds facilitated easier detection of pseudo clicks.

The generation of detection functions from the drift data revealed that the proportion of pseudo clicks detected by the surface deployed hydrophone was considerably lower than that

13

detected by the bottom-mounted hydrophone (Figure 9). The maximum detection range for pseudo clicks from the surface deployed hydrophone was 88m compared to 135m for the bottom-mounted hydrophone. Assuming the source level of real harbour porpoise clicks is ~60dB greater than the icTalk (Villadsgaard et al., 2007), but with a penalty of 30 dB for off-axis clicks, the 50% detection range for the surface deployed and bottom-mounted hydrophones is approximately 170m and 310m, respectively. These values are based on manual annotations of the spectrograms and represent over-estimates of the detection range for automated detectors, especially for the surface deployed hydrophone where interference made the use of the available automated click detectors of little value. However, it is important to recognize that more data was collected by the bottom mounted hydrophone than that mounted on the PLAT-I (i.e., pseudo clicks detected during 58 and 4 drifts, respectively). Data compatibility issues between the surface deployed and bottom mounted hydrophone made the comparison of detection ranges challenging, and these results should be considered preliminary.

The modelled tidal current velocity for both the surface deployed and bottom-mounted hydrophone ranged from 0-2 m/s. Maximum flow values were higher at surface than at the sea bottom. When taking flow rate into consideration, these preliminary analyses suggest that even under similar current velocities, the detection probability range may be greater for the bottom-mounted hydrophone than the surface deployed hydrophone. Additional work is required to explore this further.
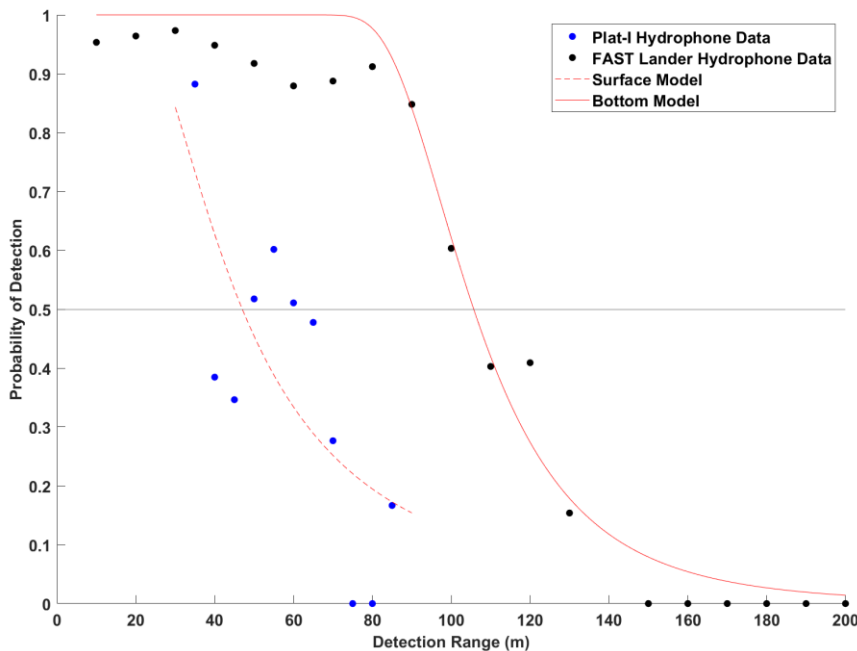
Figure 9: Detection functions for surface deployed and bottom-mounted hydrophones showing reduced detection range for the hydrophone mounted on the PLAT-I. The 50% detection probability is shown by the horizontal line.

Conclusions and Recommendations

Using PAM technologies to monitoring echolocating marine mammals in tidal channels dominated by high current velocities is inherently challenging. The choice of which instrument to use and where it should be deployed depends on the scientific questions being asked; particularly those by regulatory agencies if the monitoring is related to industry. A primary objective of the Pathway Program is to define, test and validate an environmental effects monitoring solution that can be used by tidal energy developers for monitoring the near-field (0 – 100m) region of their tidal energy devices at the FORCE tidal demonstration site in the Minas Passage.

Previous work under the Pathway Program evaluated multiple PAM technologies and revealed that conventional hydrophones that record raw pressure time series data may be preferable for monitoring harbour porpoise in Minas Passage (Hasselman et al., 2020b). This study sought to evaluate the relative performance of a surface deployed and bottom-mounted conventional hydrophone to understand whether deployment location impacts instrument detection range.

While it is possible to detect harbour porpoise clicks from a surface deployed hydrophone, the detection range appears smaller than bottom-mounted hydrophones and sufficient care must be taken to avoid acoustic and electrical contamination from other equipment on floating tidal energy platforms. However, it is important to bear in mind that the results of this study are based on a relatively small number of pseudo clicks collected from the PLAT-I mounted hydrophone in Grand Passage. Conditions may differ at the FORCE site and additional data would help to further refine expectations about the utility of a surface deployed hydrophone for monitoring harbour porpoise. These preliminary results suggests that the reduced detection range for the surface deployed hydrophone was not attributed to differences in flow velocities (flow noise) over the surface of the hydrophones, but rather short impulsive noise at the surface from wave action and air bubbles that is similar to porpoise clicks. These impulsive sounds masked many of the pseudo clicks generated by the icTalk during the passive drift trials and interfered with the click detection process. These factors influenced the data collected using the specific configuration and mounting of the surface deployed hydrophone, and it is possible that these issues could be partially addressed through an alternative mounting configuration.

It is important to note that harbour porpoise clicks are directional, and are typically produced while diving and foraging at depth (Sørensen et al., 2018). As such, harbour porpoise are less likely to produce clicks while directed at the surface, and are less likely to be detected by surface deployed hydrophones. However, porpoise also employ clicks to image their environment, and for surface deployed turbines having a hydrophone at the same depth as the turbine may provide more relevant detection information than would be provided by a bottom mounted hydrophone offset from the turbine location. For foraging porpoise, the directionality of clicks will have a negative effect on the median detection range, as an elevated proportion of the clicks reaching the surface hydrophone will be off-axis. While the inclusion of additional
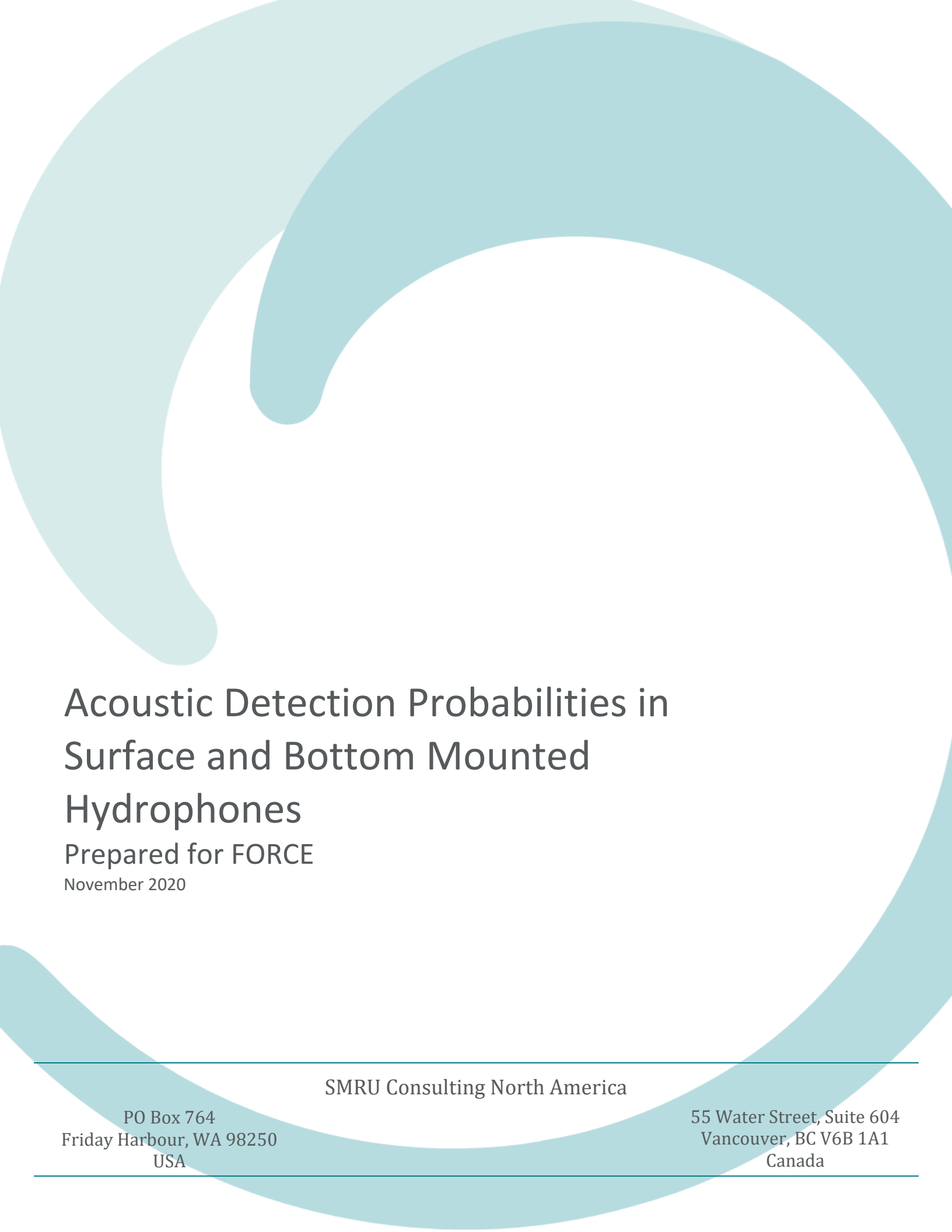
covariates (variation in drift speed, tidal current, sound profiles) may help to refine the detection model, the large disparity in the impulsive noises suggest they would be unlikely to result in a different interpretation of the data collected in this program.

Given the various considerations listed above, the results of this work suggests that PAM monitoring for harbour porpoise in high flow environments can be conducted using surface mounted hydrophones, but more work is required to refine detection ranges in tidal channels. While surface deployed hydrophones may be used, developers need to implement safeguards against acoustic and electrical contamination from equipment on their tidal every devices, and need to be aware of the potentially smaller detection range that a surface deployed hydrophone might provide. Measurement of in-situ detection ranges using a drifting projector, similar to the drifts performed in this program, should be considered to verify that hydrophones are able to detect porpoise in the turbine's near-field (100 m).

References

Adams, M., Sanderson, B., Porskamp, P., & Redden, A. (2019). Comparison of co-deployed drifting passive acoustic monitoring tools at a high low tidal site: C-PODs and icListen HF hydrophones. *The Journal of Ocean Technology*, *14*, 61–83.

Chen, C., & Beardsley, R. C. (2011). *An Unstructured Grid, Finite-Volume Coastal Ocean Model*. SMAST/UMASSD-11-1101. http://fvcom.smast.umassd.edu/fvcom/

Hasselman, D. J., Barclay, D. R., Cavagnaro, R., Chandler, C., Cotter, E., Gillespie, D. M., Hastie, G. D., Horne, J. K., Joslin, J., Long, C., McGarry, L. P., Mueller, R. P., Sparling, C. E., Williamson, B. J., & Staines, G. J. (2020). Environmental monitoring technologies and techniques for detecting interactions of marine animals with turbines. In *Report for Ocean Energy Systems (OES)*.

Hasselman, D. J., Boucher, T., & Douglas, J. (2020). *Data Analysis Component of Comparative Passive Acoustic Monitoring (PAM) Technology Assessment*.

Malinka, C. E., Gillespie, D. M., Macaulay, J. D. J., Joy, R., & Sparling, C. E. (2018). First in situ passive acoustic monitoring for marine mammals during operation of a tidal turbine in Ramsey Sound, Wales. *Marine Ecology Progress Series*, *590*, 247–266. https://doi.org/10.3354/meps12467

Sørensen, P. M., Wisniewska, D. M., Jensen, F. H., Johnson, M., Teilmann, J., & Madsen, P. T. (2018). Click communication in wild harbour porpoises (Phocoena phocoena). *Scientific Reports*, *8*(1), 1–11. https://doi.org/10.1038/s41598-018-28022-8

Sostres Alonso, M., & Nuuttila, H. K. (2015). Detection rates of wild harbour porpoises and bottlenose dolphins using static acoustic click loggers vary with depth. *Bioacoustics*, *24*(2), 101–110. https://doi.org/10.1080/09524622.2014.980319

Villadsgaard, A., Wahlberg, M., & Tougaard, J. (2007). Echolocation signals of wild harbour porpoises, Phocoena phocoena. *Journal of Experimental Biology*, *210*(1), 56–64. https://doi.org/10.1242/jeb.02618

Appendix – SMRU Final Report

Acoustic Detection Probabilities in Surface and Bottom Mounted Hydrophones

Prepared for FORCE

November 2020

SMRU Consulting North America

PO Box 764
Friday Harbour, WA 98250
USA

55 Water Street, Suite 604
Vancouver, BC V6B 1A1
Canada

Acoustic Detection Probabilities in Surface and Bottom Mounted Hydrophones

25 November 2020

Prepared by SMRU Consulting

Authors:

Kaitlin Palmer, PhD
Senior Research Scientist

Jessica Thompson, BS
Junior Scientist

Jason Wood, PhD
Senior Research Scientist

1   Executive Summary

In support of the Pathways program an assessment of the relative acoustic detection range of harbour porpoise was undertaken. The primary goal of this study is to determine whether the relative performance of a PAM device used for detecting harbour porpoise vocalizations is impacted by the deployment location (i.e., surface vs. bottom) so that an informed decision can be made about the deployment location for PAM devices for future monitoring efforts. Two hydrophones were deployed during this study. One was affixed to the Sustainable Marine Energy (SME) Plat-I floating platform in Grand Passage, NS and suspended 4 m below the surface. The second was deployed on a Fundy Advanced Sensor Technology (FAST) bottom lander 17 m below the surface. An icTalk projected porpoise-like clicks (pseudo-clicks) while drifting freely in the current past the two hydrophones. Due to technical difficulties, data from drifts were not collected simultaneously on both surface and bottom hydrophones. Therefore, data from January 14, 2020 were used for the bottom hydrophone analyses and data from August 19, 2020 for the surface hydrophone analyses.

Pseudo clicks recorded from both hydrophones were manually annotated (N = 9,098 in bottom recordings, N=368 in surface recordings) and we estimated the proportion of clicks missed by the analyst based on known inter-click-intervals of the icTalk.

Our key findings are as follows:
1) Pseudo-clicks could be detected by instruments in both locations.
2) The maximum detection range for pseudo-clicks recorded by the surface-mounted hydrophone was 88 m and 135 m for the bottom mounted hydrophone. Similarly, the range at which the detection probability dropped to 50% was 46 m for data collected by the surface mounted recordings and 104 m for the bottom mounted recordings.
3) The difference in detection range between the surface and bottom could primarily be attributed to elevated high-frequency noise at the surface hydrophone.
4) Despite the lower detection range at the surface, the surface-mounted hydrophone did opportunistically record wild harbour porpoise.

Given these findings we recommend the use of bottom-moored hydrophones where economically feasible.

Table of Contents

List of Figures

List of Tables

2   Introduction

To meet Canadian and Nova Scotian regulations, Tidal Instream Energy Converters (TISECs) installed in Nova Scotian waters have been required to institute marine mammal Environmental Effects Monitoring Plans (EEMPs). Much of this effort has focused on using echolocation click detectors to detect the presence of harbour porpoise (*Phocoena phocoena*). Early TISEC projects in Nova Scotian waters were bottom mounted devices and testing sites lacked surface infrastructure from which to mount click detectors. As a result, harbour porpoise monitoring has mostly been done by deploying click detectors on the seafloor. However, SME's TISEC technology is a floating platform (Plat-I) with attached Schottel turbines. This provides the option of mounting click detectors from the Plat-I instead of on the seafloor.

Deploying and recovering instruments from the seafloor (bottom) represents considerable cost and risk for monitoring activities. Deployment and recovery typically require vessels equipped with davits and loss of bottom mounted instruments does occur. As such, deploying instruments from the floating Plat-I could represent cost savings if successful. However, changing the deployment depth of an acoustic recorder is known to have large impacts on acoustic detection range (Sostres *et al.* 2015). Any successful surface deployment would need to prove the ability to detect harbor porpoise in the near field.

Here we seek to determine first if it possible to detect harbor porpoise from the Plat-I and second if the detection range is similar to detection ranges obtained from bottom mounted instruments. To achieve this, we measure how the detection ranges of simulated harbour porpoise clicks are impacted by the deployment location (i.e., surface vs. bottom). This information will allow managers to make informed decisions about the utility and limitations of various deployment options.

3 Methods

3.1 Data Collection

This project is a collaborative effort between FORCE, OERA and SMEC and utilized the Plat-I floating tidal energy platform deployed in Grand Passage, NS. The relative performance of a Passive Acoustic Monitoring (PAM) device deployed at the surface and on the bottom was assessed across the range of tidal flows experienced in Grand Passage using synthetic harbour porpoise click-trains emitted from an Ocean Sonics icTalk. Here we investigate whether it is possible to detect harbor porpoise clicks in the near field range (>100 m) of the Plat-I as well as the mid-field range (100-1000 m) of the Plat-I.

 For the purposes of this project, Ocean Sonics icListen hydrophones served as a surrogate for PAM devices in general. This can be justified on the grounds that this study is not designed to address questions pertaining to the performance of any given hydrophone per se (a topic already addressed in a prior study), but rather the potential effects of signal interference inherent to the deployment location(i.e., near the surface or bottom) on the performance of PAM devices in this application. Thus, we make the assumption that any potential signal interference associated with waves and turbulence near the surface has an approximately equal effect on hydrophone performance across the suite of PAM technologies that are available and might be used in EEMP monitoring.

3.1.1 Hardware

An icListen HF hydrophone was mounted on a FAST lander at a depth of 17m during high water (i.e., 'bottom-mounted'), approximately 65m North of the Plat-I. The Plat-I (i.e., 'surface-deployed') had a pole-mounted icListen HF near the bow of the platform at a depth of 4m. Upon completion of the passive drift tracks, the icListen hydrophones remained deployed for a few days to gather opportunistic data from harbour porpoise transiting the area. Upon completion of the study, the icListen hydrophones were recovered and the data were downloaded and sent to a SMRU Consulting for analysis.

3.1.2 Drift Experiments

Passive drifts in the vicinity of the FAST lander and Plat-I platform were made from a vessel while playing synthetic click trains using the icTalk. These passive drifts occurred on January 14, 2020, and again on August 19, 2020 over the course an entire tidal cycle (ebb and flood stages) to determine the ability of the icListen hydrophones to detect this signal across the range of flow conditions. Lightbulb implosions were used to validate the ability of the systems to detect loud implosive sounds and a SoundTrap was deployed with the intent to synchronize recordings across Plat-I and FAST lander. However, since data were ultimately derived from different time periods, synchronization was not possible.

The icTalk transducer is reported to be nearly omni-directional, however marginal beam patterns can result in large variations in detection ranges. To account for the downward, and more on-axis, orientation of icTalk with respect to the bottom-mounted hydrophones, we changed the orientation of the projector during the summer drifts. For these experiments we

implemented two orientations of the icTalk. For half of the drifts, the hydrophone was oriented downward and for the other half the icTalk was inverted on the cable such that the element was facing upward. The passive drift tracks were recorded using a handheld GPS unit and used later for analyses.
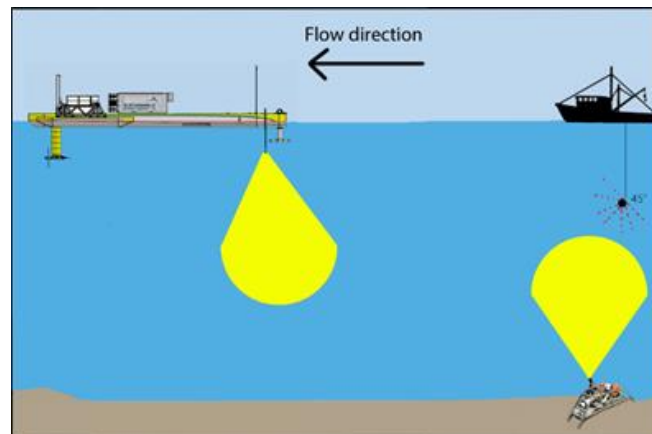

Figure 1: Schematic of study design for Grand Passage indicating the locations of the two hydrophones on the Plat-I floating platform and the FAST bottom lander as well as the icTalk suspended from the vessel.

Technical challenges prevented data collected from the Plat-I from being used during the winter drifts. These issues were resolved during the intervening months before August when the trial was re-run. However, data from the FAST lander could not be recovered from the summer drifts. As such, we were limited in our analysis to comparing the bottom mounted hydrophone data collected in the winter to the surface monitored hydrophone data collected in the summer.

3.2   Detecting Pseudo-Clicks

Because of the low signal to noise ratio (SNR) for the pseudo-clicks detected by instruments attached to the Plat-I, it was not possible to use automated-detectors to find pseudo-clicks. Thus, all annotations were made by trained analysts using Raven Lite software. For both surface and bottom data, analysts identified the start and end time of each passive drift and manually searched for pseudo-clicks matching the 130 kHz center frequency, 5 kHz bandwidth and .01 s duration and 0.3 s inter-pulse-interval. When SNR values were low either because of the range between the vessel and the sensors or high ambient noise levels the inter-pulse-interval was used to estimate the expected arrival time for the pseudo-clicks. The section of the spectrogram including the expected arrival time was then searched for potential pseudo-clicks. Only drifts where at least one pseudo-click could be manually detected in the data were included in the range analysis.

3.3 Range Estimates

The start time of each drift was estimated by using the first GPS position provided for each of the drifts. The continuous range between the vessel GPS and the bottom lander was obtained by interpolating the GPS coordinates from each drift. For the surface comparison, the distance between the drifting vessel and the position of the Plat-I were continuously monitored and the range between the two were again interpolated.

3.4 Comparing Detection Ranges

3.4.1 Signal Measurements

We calculated the signal to noise ratio (SNR) of each signal using (Equation 1) where peak is the peak pressure of the pseudo-click within the detection window and rms is the root-mean squared pressure of the 0.78 ms surrounding each peak.

$$SNR = 20 * log10\left(\frac{Peak}{RMS}\right)$$

Equation 1

It is not possible to perfectly center manual annotations around each pseudo-click. Therefore, custom Matlab scripts were used to calculate SNR from the region of the annotation. To estimate the exact arrival time of the pseudo-click, a 0.04 s selection of the raw sound recordings was extracted from the data based on the midpoint of each annotation. This section of data contained both the click and a sample of the background noise.

The exact arrival time of the click was obtained by first bandpass filtering the signal between 128 and 132 kHz (i.e. the 1/3 octave band centered on 130 kHz). The peak time of the filtered signal was used to estimate the exact arrival time of each pseudo-click.

This same process was repeated for 'missed clicks'. Here we estimated the arrival time of the missed annotation based on the inter-pulse-interval of the received clicks. For example, if received pseudo-clicks were observed at 0.0s, 0.3s, 0.6s and 0.12s, we assumed a missed pseudo-click at 0.9 s.

Following Miller and Whalberg (2013), data for noise level metrics were filtered using a band filter centered on 130kHz for noise and received level measurements. This resulted in a bandpass filter between approximately 115 and 145 kHz.

Ambient noise levels in all cases were measured in rms over the 115-145 one third octave band measured over 1.6µs.

3.4.2 Detection Functions

Detection functions describe the probability of detecting an animal as a function of range between the source and the 'observer' (Equation 2). Distance sampling methods are typically used to estimate the proportion of data missed as a function of range. However, in this study the ranges between the sound source and observer were known for both detected and missed clicks.

$$Detection\ Probability \propto g(SNR)$$ Equation 2

In acoustics, the observers are hydrophones, and the acoustic detection represents the source. Factors affecting the detection probability are characterized by the sonar equation (Equation 3). Equation 3 where SL is the source level of the signal of interest (here pseudo-clicks), NL is the ambient noise level at the arrival time of the signal and TL is the transmission loss over the range between the source and receiver. All values are measured in decibels (dB) and measured across the same bandwidth.

$$SNR = SL - TL - NL$$ Equation 3

Here we assume that the detection function is described by a hazard rate function (Equation 4) where σ and b are the unknown parameters describing the shape of the function, r is the range between the source and receiver (in meters), and SNR is the signal to noise ratio of each detection as measured from the data.

$$P(r) = 1 - exp^{(-(r/\sigma)^{-b}))}$$ Equation 4

To estimate σ and b, the proportion of pseudo-clicks detected was calculated for 10m bins. Initial values of σ and b were chosen at random and an optimization function (mean squared error) was used to refine the values. Parameters σ and b were obtained for both surface and bottom experiments.

Finally, using the sonar equations we extrapolated our findings of the detection range of pseudo-clicks estimate the 50% detection range for wild harbour porpoise (Equation 5). Here we assumed consistent noise regimes, source levels of 130 dB re 1μPa for the icTalk (SL1) and 160 dB re 1μPa²s for the porpoise (SL2; Teilmann et al., 2002). Transmission loss is the sum of spherical spreading ($20 \cdot log_{10}(r)$) and molecular absorption ($38 \cdot log_{10}(r)$), and r1 is the observed 50% detection range, and r is the estimated 50% detection range given the new source levels.

The system of equations was used to estimate the range at which real harbour porpoise would be detected under similar conditions where *r1* is the observed range and estimate range for wild porpoise clicks and ranges are measured in kilometers.

$$SNR = SL1 - TL - NL = 130 - NL - 20 * log_{10}(r1) - 38 * log_{10}\left(\frac{r1}{1000}\right)$$

$$SNR = SL2 - TL - NL = 160 - NL - 20 * log_{10}(r) - 38 * log_{10}\left(\frac{r}{1000}\right)$$

3.5 Current Effects

Tidal current velocity data were obtained using open source software (Chen and Beardsley 2011) and provided to FORCE and SMRU Consulting for analysis. The current model estimated the tri-axial current velocity on a 10 min scale for the seabed and surface and the magnitude of the tri-axial current velocity was used for each experiment. For the FAST lander experiment we used the current velocity modelled for the seabed and surface models for the Plat-I.

Modelled current velocity were matched with each pseudo-click arrival. Because drifts typically lasted less than 5 minutes, the maximum being 9 min, this resulted in each drift being associated with one velocity estimate.

To determine what, if any, effect tidal current had on the analysis, a subset of the drifts for the surface and bottom mounted recorders were selected and the detection functions were compared to each other. Here we sought to identify whether differences in the observed detection function for the entire data sets could be attributed to flow noise. If so, we would expect that the surface and bottom detection functions would be nearly identical for the data subset.

4 Results

4.1 Drift Data

The Plat-I hydrophone data from the January drifts was contaminated by electronic noise which was traced to a power supply issue and these data could not be used. During the August drifts, the FORCE lander hydrophone did not collect data. As such, we did not have simultaneous acoustic data from both the platform and lander and had to analyze the two data set separately.

The FORCE crew undertook a total of 58 drifts on January 14, 2020 and 35 drifts on August 19th 2020. The Plat-I rotates freely in the current creating a navigational hazard which precluded

close approaches to the hydrophone mounted on the Plat-I except when current and vessel movement was extremely low. Because of this, only three of the 35 drifts on August 19th approached within 100m of the Plat-I mounted hydrophone. Pseudo-clicks from the icTalk were observable in data from these drifts.
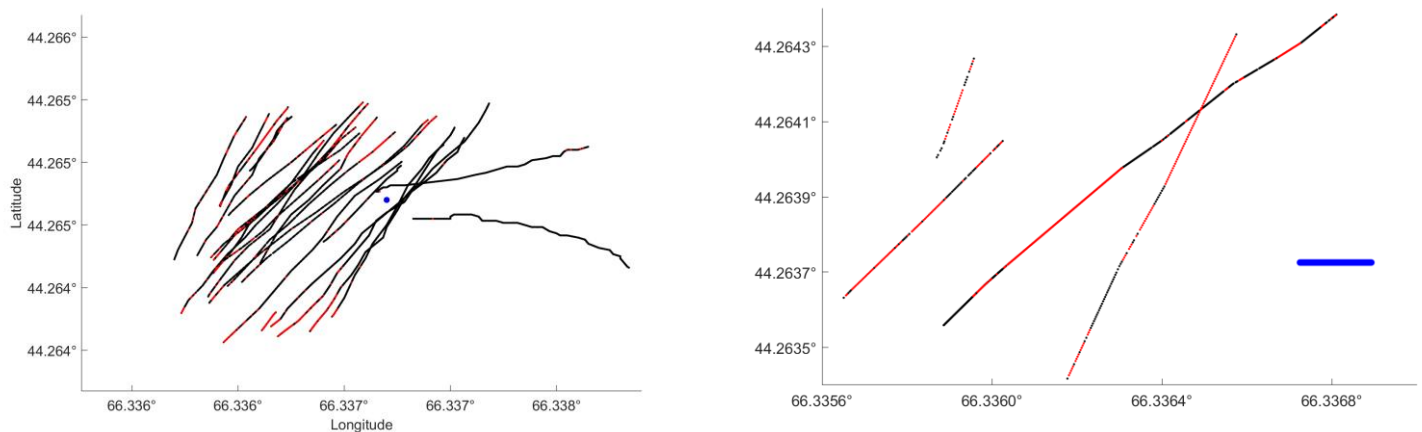

Figure 2 Survey data included in the analysis. Overhead view of the vessel drifts with respect to the bottom lander in January (left panel) and Plat-I surface platform in August (right panel). Black points represent pseudo-click annotations and red points indicate detections missed by the analyst. Blue point represents the hydrophone location on the FAST Lander or mobile Plat-I.

For each drift past the bottom lander, pseudo-clicks were generally detected throughout the drift with pseudo-clicks at the beginning and end of the drift (when the icTalk was furthest away) being less detectable. This pattern was not as obvious in the few observable drifts past the surface platform. In these later drifts, pseudo-clicks were masked by ambient noise within ranges where the clicks would otherwise be detectable.

Table 1 Summary table for drift, annotations, noise levels and detection ranges at the two study sites. Values in parentheses represent 95% confidence intervals.

	Surface Plat-I	Bottom FAST Lander
Total Drifts	35	58
Drifts Annotated	4	27
Number of Annotations	368	9,098
Median Noise Level (dB re 1uPa) in the 130 kHz octave band	76.4 (70.8-83.6)	73.9 (71.1-78.5)
SNR (dB)	5.3 (3.3-10.3)	3.8 (1.8-14.1)
Maximum Detection Range (m)	88	135

4.2 Noise Levels

One third octave, also known as decidecade bands, noise levels throughout the recording survey periods were measured (Figure 3). Surface recordings had lower low frequency noise than recordings from the bottom lander. However, above 100 kHz, noise levels were considerably higher in data collected by the hydrophone mounted to the Plat-I (Figure 3).
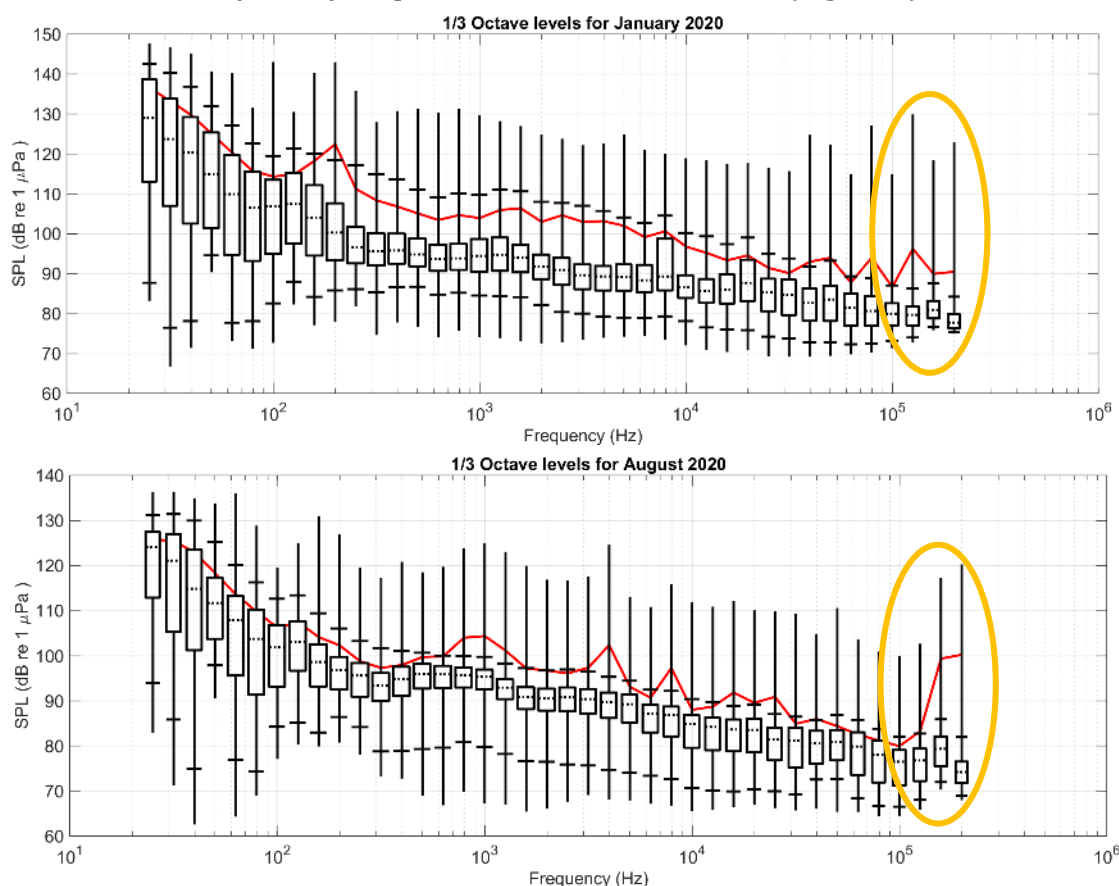

Figure 3 One third octave sound pressure levels recorded at the bottom lander site (winter, top panel) and at the Plat-I (surface, bottom panel). Orange circles indicate frequency range of harbour porpoise clicks and icTalk pseudo-clicks.

The rms noise level in the one third octave band including the130 kHz pseudo-clicks was measured during all drifts, regardless of whether they were included in the detection analysis. The median band during the drifts at the bottom platform was 73.9 dB and 76.4 re 1µPa at the surface location. Noise levels associated with the bottom lander were normally distributed ranging from 70-80 dB$_{rms}$ re 1µPa across the 115-145 kHz band.

However, noise levels recorded at the surface platform were multi-modally distributed with peaks at 72, 79, and 83 dB$_{rms}$ re 1µPa measured over 1.6 µs (Figure 4). Transient increases in ambient noise levels during the drifts resulted in considerable interference in our ability to

detect pseudo-clicks and depressed the maximum detection range. Increased noise levels, necessarily, result in a reduction of the detection range of clicks produced at a constant amplitude.
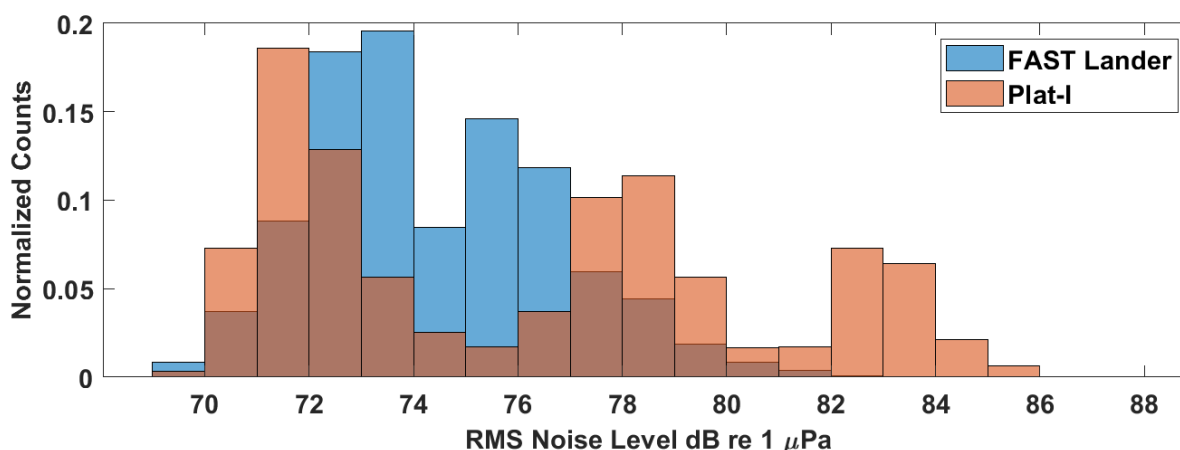

Figure 4 Noise level rms SPL distribution in the 130 kHz octave band associated with the drifts.

The quality of the noise regime in the 130 kHz band also differed significantly between the two surveys. Data collected at the surface contained audible interference from wave action and the broadband, impulsive, bursting of bubbles associated with waves. This type of noise is particularly challenging to differentiate from the impulsive nature of echolocation clicks (Figure 5). Impulsive noise also adversely affects porpoise detectors through the same mechanism, confounding impulses from noise increase the number of false positive detections. Identifying pseudo-clicks in these data required a significant amount of time and near continuous spectrogram parameter tuning.
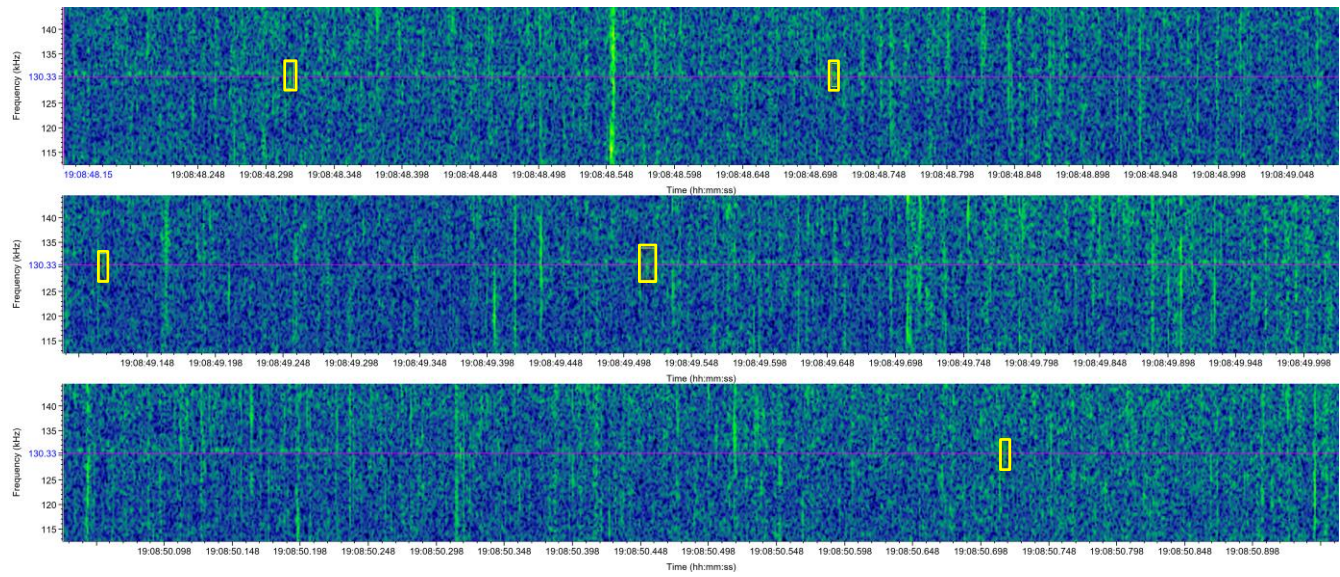
Figure 5 Spectrogram (FFT = 2048, 50% overlap, 512 kHz sample rate) of surface drift showing received pseudo-clicks (yellow boxes) a 130kHz reference line (purple line) used for aiding in the detection process. Vertical lines throughout indicate likely bubble action.

In contrast to the surface recordings, the interference in the recordings from the bottom mounted hydrophone was predominantly characterized by occasional boat noise (Figure 6). There was considerably less energy in the higher frequency data. In these data, the scope of the analysis (e.g., number of drifts annotated) was limited not by the ability to detect pseudo-clicks but by time. Noise in the data collected by the bottom mounted hydrophone was characterized by continuous gaussian noise in which it was easy to identify pseudo-clicks. Figure 6 shows a representative sample of data containing pseudo-clicks collected by the bottom mounted hydrophone.
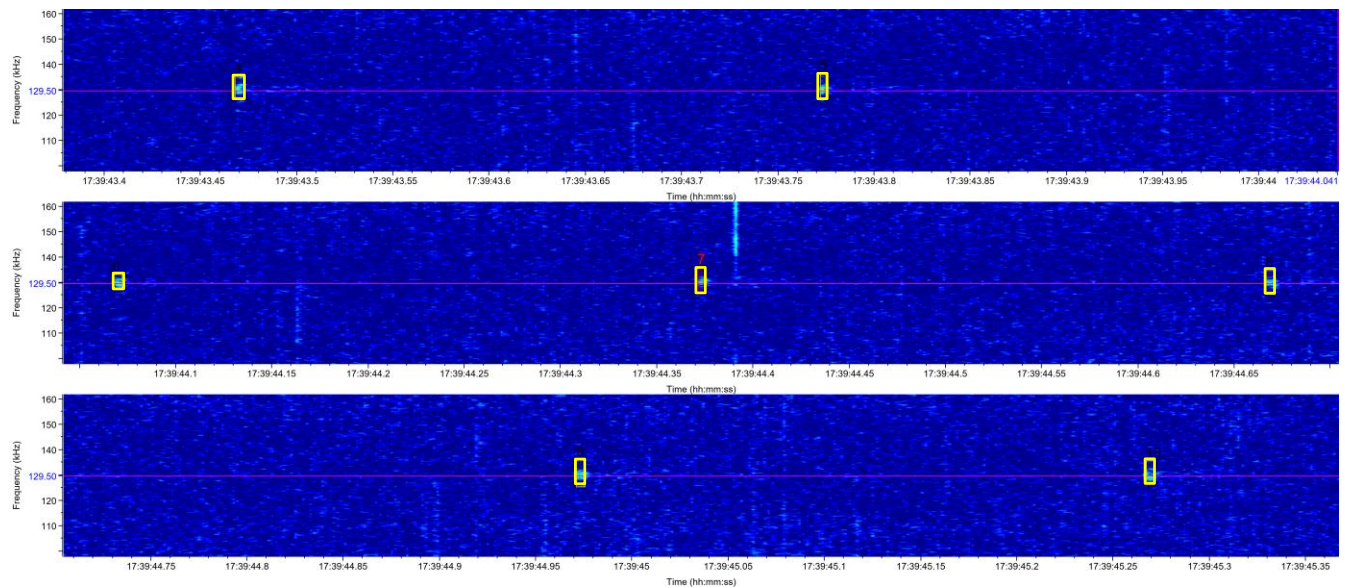
Figure 6 Spectrogram (FFT = 2048, 50% overlap, 512 kHz sample rate) of FAST lander data showing received pseudo-clicks (yellow boxes) a 130kHz reference line (purple line) used for aiding in the detection process. Lack of impulsive sounds allowed for easier detection of pseudo-clicks and will facilitate automated detection.

4.3   Detection Functions

The proportion of pseudo-clicks detected at the surfaces was markedly lower than pseudo-clicks detected by the bottom-mounted hydrophone (Figure 7). The maximum pseudo-click detection range at the surface deployment was 88 m as compared to 135 m for the bottom lander. The 50% detection range for the surface hydrophone was 46 m and 104 m for the bottom mounted hydrophone. Assuming the harbor porpoise source levels are ~30 dB higher than the icTalk, Equation 5 is used to solve for the expected detection range of 'real' harbor porpoise clicks. Using these values, we estimate 50% detection range of 144 m at the surface and 342 m at the bottom. Again, these values were calculated using human observers, and as such represent over-estimates of the detection range especially at the surface where interference made the use of automated detectors impossible.
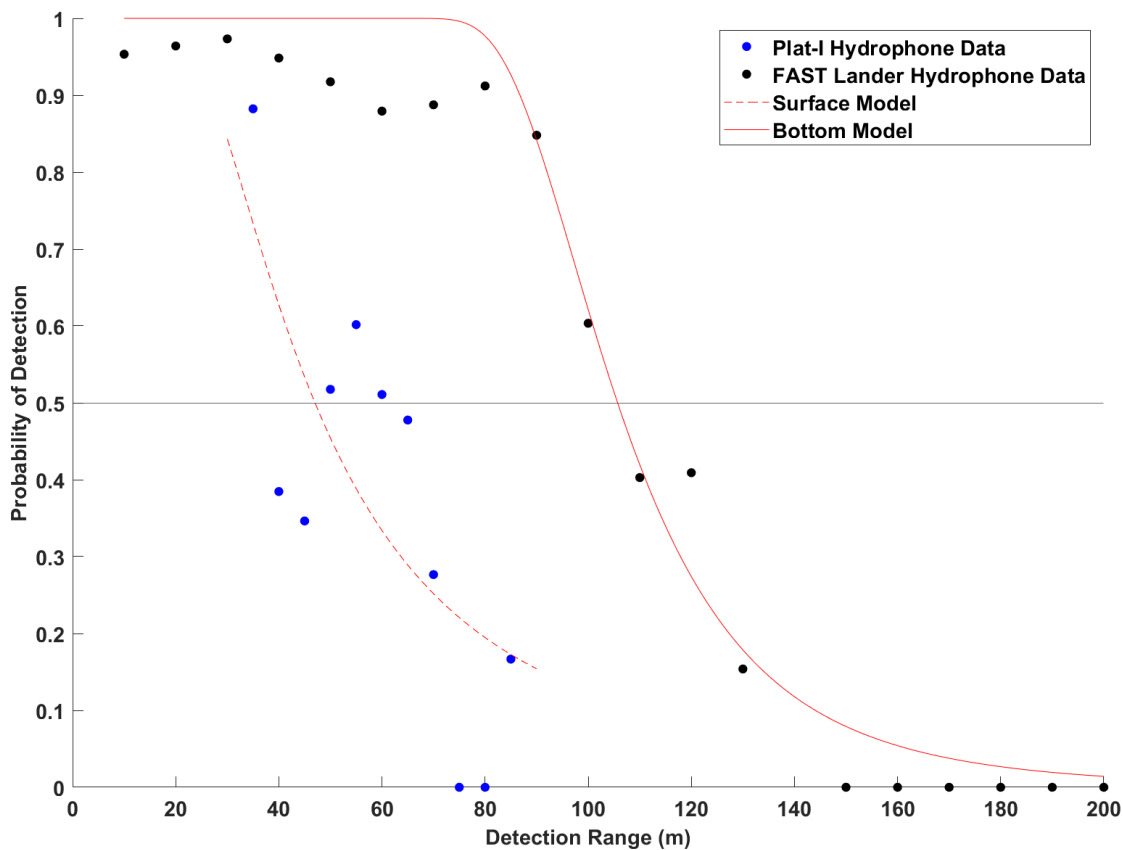
Figure 7 Proportion of pseudo-clicks detected and modeled detection function for data collected by bottom mounted instruments (black points) and instruments deployed at the surface (blue points). Horizontal line indicates 50% detection probability.

4.4 Current Effects

For both Plat-I and FAST Lander the modelled current velocity ranged from 0 to 2 m/s (Figure 8). Maximum flow velocities were higher at the Plat-I location and minimum flow velocities (<1 m/s) were observed at the FAST Lander. Data associated with current velocities between 0.5 and 1.25 m/s were selected for the flow analysis. This resulted in two drifts from each experiment being included with a total of 637 pseudo-click arrivals at the FAST Lander and 635 at the Plat-I.
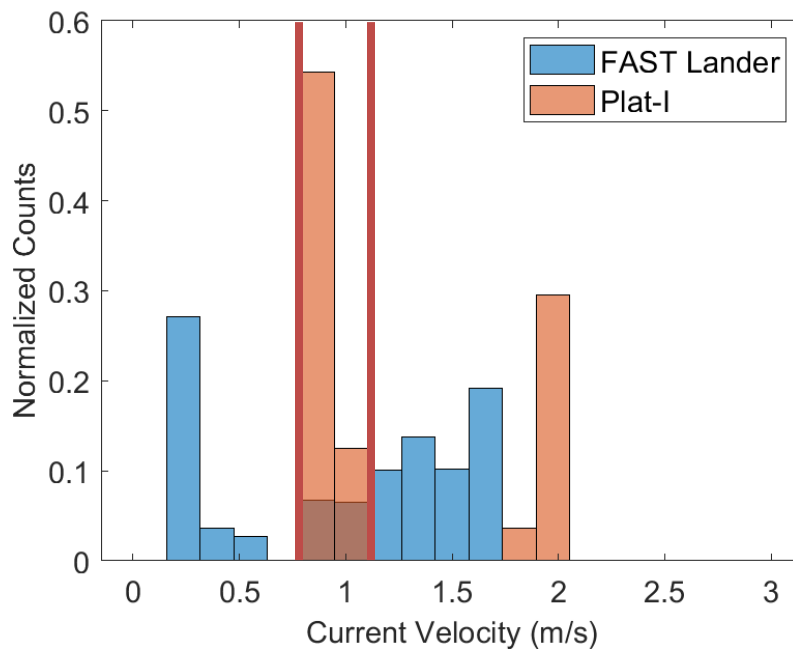
Figure 8 Normalized histogram of the modelled current velocities associated with all drift trials included in the analysis. Modeled values for the FAST lander were derived from the seabed models and surface model for the Plat-I. Red lines indicate data collected from periods with similar flow velocities and selected for the flow analysis.

With two drifts from the each of the Plat-I and FAST lander data sets included in the flow analysis, there were insufficient data to create meaningful detection functions. However, the pattern in the proportion of pseudo clicks detected vs. range were consistent with the observations from the whole dataset. This indicates that under similar current velocities, the detection probability range is still considerably greater at the FAST lander location than from a hydrophone mounted at on the Plat-I (Figure 9).
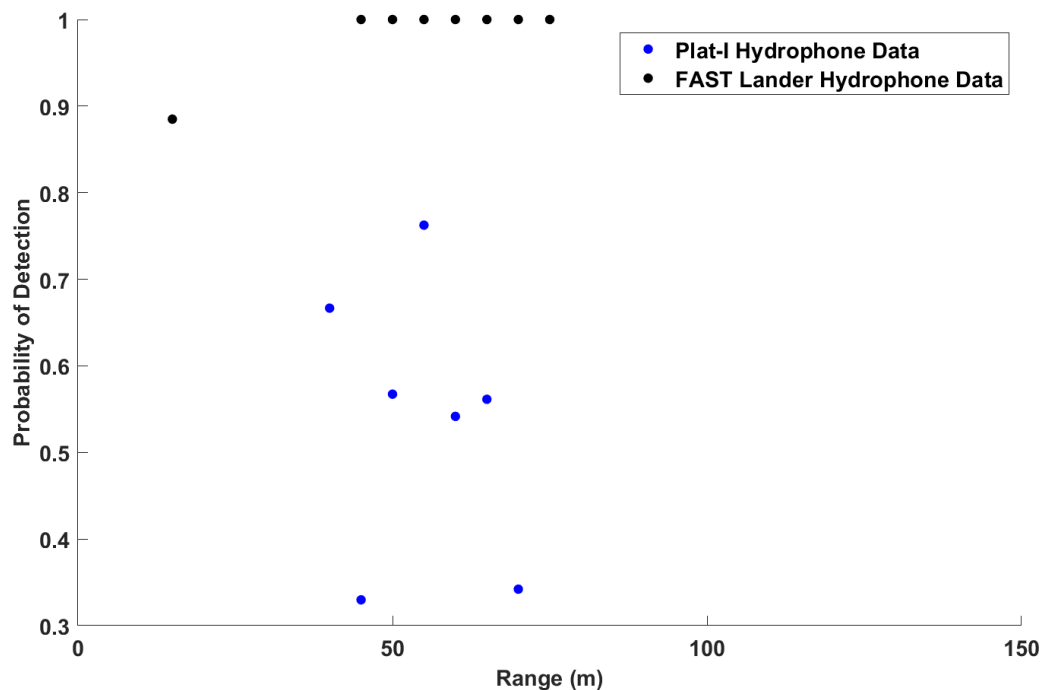
Figure 9 Observed detection probabilities for the flow experiment (modelled flow velocity greater than 0.5 m/s and less than 1.25 m/s). As with the full data set, the detection probability was consistently higher for recordings made at the FAST lander.

4.5   Opportunistic Sightings

FORCE staff noted the presence of harbour porpoise in the waters surrounding the Plat-I during the August 19th drift experiments. Staff removed the icTalk from the water during this time and noted the approximate range between the wild porpoise and the surface hydrophone. SMRU Consulting staff investigated data from the Plat-I and were able to confirm the presence of echolocation clicks in the acoustic recordings consistent with staff observation (Figure 10).
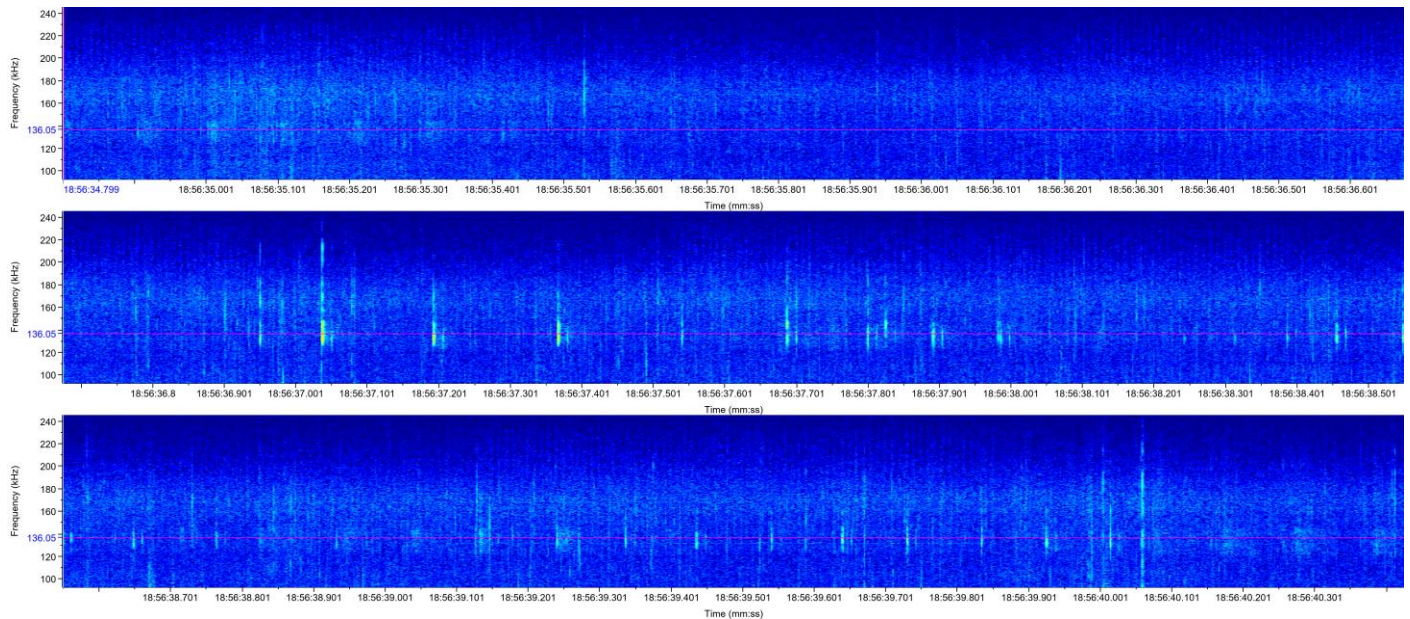
Figure 10 Spectrogram (FFT = 2048, 50% overlap, 512 kHz sample rate) of wild harbour porpoise clicks recorded by the surface-mounted hydrophone.

5 Discussion

This study demonstrates that it is possible to detect harbour porpoise clicks from hydrophones mounted on either bottom moored landers or the Plat-I floating platform *if* sufficient care is taken to avoid acoustic contamination from other equipment on the Plat-I platform. Pseudo-clicks produced by the icTalk were observed in both data sets and wild harbour porpoise echolocation clicks were detected in both data sets.

The estimated detection range at the surface hydrophone was considerably smaller than that for the bottom hydrophone. The difference in detection ranges could be attributable to any aspect of the sonar equation (SL, TL, NL). While the source level of the icTalk was fixed throughout the study, high frequency sounds are necessarily directional and the beam pattern of icTalk is not completely uniform. We also investigated whether current speed between the two disparate experiments could drive the difference in detection ranges. For a small subset of data consisting of limited current velocities we found similar detection ranges as the full data set. This suggests noise induced by current flow over the hydrophones did not drive the differences we found in detection range between the bottom and surface mounted hydrophones.

Transmission loss characteristic also varies between the two sets of drifts. Clicks, or pseudo-clicks arriving at the surface mounted hydrophone are subjected to interference from wave action under normal conditions. The presence of thermoclines can also 'trap' sounds in shallow or deep water depending on the direction of the thermocline. However, we do not expect this to have had a major impact on the current study given the extensive tidal mixing in the area.

The biggest contributor to the variation in detection range between the two hydrophone locations was ambient noise. The increased noise at the surface masked many pseudo-clicks and interfered with the detection process.

Potential covariates that we did not directly account for included water depth, wind speed, direction relative to the instrument, and vessel speed. Windspeed is a major contributor to ambient noise levels in moderate to high frequencies and could contribute to disparities in the noise regime between the two sites. However, historical records indicate similar windspeeds (1-14 km/hr; < Beaufort 2) during the winter and summer drift experiments (https://climate.weather.gc.ca/). While windspeed is not typically thought to impart noise in high frequencies that assumption is limited to deep water deployments. Hydrophones are not typically placed near the surface because the impulsive nature of wave action and bubbles bursting is necessarily broadband. The nature of high frequency noise is not well characterized for surface deployed hydrophones, but bubble and spray action caused by breaking waves can induce broadband noise and interference into the high frequency components of the noise regime, regardless of the source (Macaulay et al., 2017).

It is also important to note that harbour porpoise clicks are directional, and animals preferentially produce them while diving and foraging at depth (Sørensen *et al.* 2018). This is not the case with the icTalk which more closely resembles and omni-directional transducer. In doing so, animals are on, average, less likely to produce clicks while directed at the surface. The directionality of the clicks will have limited effects on the maximum detection range as that is determined by clicks received on-axis of the porpoise. However, the median detection range will decrease as a greater proportion of the clicks reaching the surface hydrophone will be off-axis.

Ideally the data from this study would have been derived from a single day of drifts which would have provided consistency across the covariates of interest including tidal flow, wind speed, depth etc. This would limit some of the confounding factors that are not easily addressed in the present study. These include variation in drift speed, tidal currents, sound speed profiles etc. Regardless, the large disparity in noise levels in the 130 kHz band suggests that additional covariates would help refine the detection models but are unlikely to result in different interpretations of the data.

With the considerations above, we recommend that EEMPs focused on harbour porpoise around TISECs use bottom mounted-hydrophones wherever possible. Where there is a need for real-time or near-real time monitoring surface mounted hydrophones can be used, but only with careful design and monitoring to avoid acoustic contamination from other equipment and consideration of a smaller detection range.

6 Conclusions

This report sought to 1) determine whether it is possible to detect harbor porpoise in the near field with hydrophones deployed at or near the surface and 2) compare the detection range of a hydrophone deployed at the surface with one deployed on the seafloor.

We found that it was possible to detect both pseudo-clicks and real harbor porpoise clicks from a surface mounted hydrophone. Therefore, maintaining a hydrophone from the Plat-I can provide some insight into the presence of harbor porpoise very near the platform, assuming the mechanical and electrical noise emanating from the machinery is limited as it was in the latter part of the summer. Platform mounted hydrophones provide potential for real time monitoring of harbor porpoise and expeditious knowledge of instrument malfunction issues whereas this is not possible for bottom-moored archival instruments.

In comparing detection ranges there were considerable issues with data compatibility between the surface and bottom drifts. With the data that were collected, we found that the detection range for pseudo-clicks was considerably greater for the hydrophone moored to the seafloor than the one at the surface. Though the discrepancy in data collection limits the generalization of this finding, for the converse to be true and average detection range to be as large or larger at the surface than at the bottom, it would require one or both of the following conditions to be true. Harbor porpoise would need to produce clicks while on-axis with the surface hydrophone more often than while they were on-axis with the bottom mounted hydrophone. This would require that click production be greater at the surface or when oriented upward than at depth or oriented towards the seafloor. Second, noise levels and interference the surface would need to be lower than those at the bottom. We do not believe these hypotheses are likely. Thus, while acknowledging the considerable limitations of these data, we believe that under similar environmental conditions, the detection range for hydrophones mounted at the surface will likely be smaller than bottom mounted hydrophones in nearly all instances.

Acknowledgements

References

Chen, C. and Beardsley R.C., 2011. An Unstructured Grid, Finite-Volume Coastal Ocean Model. SMAST/UMASSD-11-1101. http://fvcom.smast.umassd.edu/fvcom/

Macaulay, J., Gordon, J., Gillespie, D., Malinka, C., & Northridge, S. (2017). Passive acoustic methods for fine-scale tracking of harbour porpoises in tidal rapids. *The Journal of the Acoustical Society of America*, 141(2), 1120-1132.

Miller, L.A., and Wahlberg, M., 2013. Echolocation by the harbour porpoise: Life in coastal waters. *Frontiers in Physiology,* 4, pp.52.

Sørensen, P.M., Wisniewska, D.M., Jensen, F.H., Johnson, M., Teilmann, J. and Madsen, P.T., 2018. Click communication in wild harbour porpoises (*Phocoena phocoena*). *Scientific Reports*, 8(1), pp.1-11.

Sostres Alonso, M. and Nuuttila, H.K., 2015. Detection rates of wild harbour porpoises and bottlenose dolphins using static acoustic click loggers vary with depth. *Bioacoustics*, 24(2), pp.101-110.

Teilmann, J., Miller, L. A., Kirketerp, T., Kastelein, R. A., Madsen, P. T., Nielsen, B. K.,Au, W. W. (2002). Characteristics of echolocation signals used by a harbour porpoise (*Phocoena phocoena*) in a target detection experiment.*Aquatic Mammals*,28(3), 275-284.